이학박사 학위논문

Statistical Process Control in Count Time Series Models

계수 시계열 모형에서 통계적 공정 관리

2018년 8월

서울대학교 대학원

통계학과

김 한 울

Statistical Process Control in Count Time Series Models

by

Hanwool Kim

A Thesis
submitted in fulfillment of the requirement
for the degree of
Doctor of Philosophy
in Statistics

The Department of Statistics
College of Natural Sciences
Seoul National University
August, 2018

Abstract

This thesis consider cumulative sum (CUSUM) charts based statistical process control (SPC) in count time series. Time series of counts have gained much attention in recent years in diverse fields such as manufacturing process, communication, queueing systems, medical science, crime and insurance. First, we considers the first-order integer-valued autoregressive (INAR) process with Katz family innovations to include a broad class of INAR(1) processes featuring equi-, over-, and under-dispersion. Its probabilistic properties such as ergodicity and stationarity are investigated. Further, a SPC procedure based on the CUSUM control chart is considered to monitor autocorrelated count processes. The CUSUM-type test statistic with conditional least square (CLS) and squared difference (SD) estimator for the PINAR(1) model and its application to the diagnostic of control chart are also investigated. Also, we propose an upper one-sided CUSUM-type chart based on the considered CUSUM statistic for an effective detection and a change point estimation. For enhanced monitoring Markov counting process with excessive zeros. we consider three control charts, namely cumulative sum (CUSUM) chart with a delay rule (CUSUM-DR), conforming run length (CRL)-CUSUM chart, and the combined Shewhart CRL-CUSUM chart. Moreover, for an easy implementation of the attribute fixed sampling interval (FSI) and variable sampling internal (VSI) CUSUM control charts, an R package, attrCUSUM, is developed.

Keywords: INAR model, CUSUM chart, Statistical process control, R, Software.

Student number: 2010-20220

Contents

List of Tables

List of Figures

Chapter 1

Introduction

This thesis consider modeling and statistical process control (SPC) in count time series. Time series of counts have gained much attention in recent years from the researchers and practitioners in diverse fields such as manufacturing process, communication, medical science, insurance, and queueing systems. Al-Osh and Alzaid (1987) and McKenzie (1985); McKenzie (1988) introduced the first-order integer-valued autoregressive (INAR) process based on a binomial thinning, and later, Alzaid and Al-Osh (1990) and Jin-Guan and Yuan (1991) extended it to higher order INAR processes. Al-Osh and Aly (1992) considered iterated thinning operator for modeling autoregressive processes with negative binomial marginal distribution and innovations (NBIINAR(1)), whereas Alzaid and Al-Osh (1993) studied INAR(1) processes with generalized Poisson marginal distribution based on quasi-binomial thinning operator (GPQINAR(1)). Franke and Seligmann (1993) considered the existence of conditional maximum likelihood (CML) estimator. Park and Oh (1997) studied the asymptotic properties of INAR(1) processes and the distributional relation to $M/M/\infty$ queueing systems. Meanwhile, Zheng et al. (2007) studied random coeffi-

cient INAR(1) processes (RCINAR(1)) and Kang and Lee (2009) considered the parameter change test for RCINAR(1) models based on the cumulative sum (CUSUM) test. Weiß (2008) provided a comprehensive review of existing thinning operators and related INAR(1) processes. Later, Ristić et al. (2009) introduced a new first order autoregressive process for modeling autocorrelated geometric marginals based on negative binomial thinning operator (NGINAR(1)). Jazi et al. (2012a) recently considered INAR(1) processes with zero inflated Poisson innovations to analyze count data with excessive zeros. Further, Ristić et al. (2013) introduced INAR(1) process with geometric marginals based on generalized binomial thinning operator (DCGINAR(1)) and Li et al. (2015) studied mixed INAR(1) processes with zero inflated generalized power series innovations. Further, Bourguignon et al. (2015) considered the INAR(1) with power series innovations and Bourguignon and Vasconcellos (2015) examined an improved estimator in terms of bias based on the squared difference (SD) estimator originally considered by Weiß (2012). Although there exist many models to analyze autocorrelated count data as mentioned earlier, practitioners often encounter a problem in selecting correct models among the candidates. In some situations, this task may be difficult and there must be a justification in applying the chosen model to data: for example, either a model-check test or goodness-of-fit test are requited. To avoid this difficulty, instead of using a specific model, one can consider using a model family that can accommodate a broad class of integer-valued time series models. Motivated by this, we consider the INAR(1) process with the Katz family (KF) innovations, abbreviated as INARKF(1) as our the first subject. We investigates its probabilistic properties such as the ergodicity, stationarity and moments. Also, we apply the CUSUM chart, mentioned below, for detecting a mean increase with numerical experiments and real data analysis for illustration of the

superiority of our considered method.

Control chart has long been playing a central role as a statistical process control (SPC) method for detecting an abnormal change in manufacturing processes. It is well known that the traditional Shewhart $\bar{X}$ control chart reacts slowly to small shifts of the process mean. Page (1954) introduced the cumulative sum (CUSUM) control chart to improve the performance when monitoring small to moderate shifts. For more details on control charts, we refer to Montgomery (2009). Although sampling is usually conducted with a fixed sampling interval (FSI) to maintain control charts, the variable sampling interval (VSI) is also adopted to improve the efficiency of monitoring: see Reynolds et al. (1988); Reynolds et al. (1990) and Saccucci et al. (1992). Epprecht et al. (2010) recently applied the VSI control scheme to the exponential weighted moving average (EWMA) chart, which is an alternative to the Shewhart control chart designed for faster monitoring. In the VSI control scheme, sampling intervals are planned to be varying according to the information obtained from the precedent control statistic and the performance is usually evaluated by the average time to signal (ATS) triggering an out-of-control condition. For more details, we refer to Reynolds et al. (1990). When dealing with the rare events such as the infection rate of rare diseases or the number of non-conforming units in a high-quality manufacturing process, traditional control charts for attribute often lose their efficiency owing to the excessive number of zeros in count data. Those zeros cause an over-dispersion for the data, and thereby, underestimating the target values in the monitoring process: see Woodall (2006). In order to overcome this defect, several authors considered control charts adopting zero-inflated models for count data. Sim and Lim (2008) considered Shewhart-type control charts for zero-inflated Poisson (ZIP) and binomial (ZIB) distributions based on the Jeffrey's prior intervals and

Blyth-Still intervals. Wang (2009) introduced an improved control chart using adjusted confidence intervals to cope with the case of small non-conforming rates. He et al. (2012) and Rakitzis et al. (2016) recently studied the CUSUM control chart for zero-inflated Poisson and binomial distributions. Conventionally, the detection of an increase, rather than a decrease, in model parameters has been a core issue, because the increase is mainly due to the process deterioration induced by an assignable cause.

Meanwhile, He et al. (2014) considered a combination of CUSUM charts based on zero-truncated Poisson CUSUM chart (ZTP-CUSUM) and conforming run length (CRL)-based CUSUM (CRL-CUSUM) chart. It is well known that in the monitoring process exhibiting zero-inflation, the CRL-type control charts are particularly effective than other existing control schemes, see Goh (1987); Wu et al. (2000); Wu et al. (2001); Ohta et al. (2001). But as far as we know, CRL-type charts for the monitoring of Markov counting processes, which are our main focus, have not been developed in the literature so far. Due to the automation and advancement of quality in production process, the existence of serial dependence becomes increasingly common phenomenon in the modern manufacturing industry. For this reason, monitoring such processes has received a great deal of attention by many authors in recent years. For example, several control charts to monitor the first-order integer-valued autoregressive (INAR(1)) model are studied by Weiß (2007). Weiss and Testik (2009) applied upper one-sided CUSUM charts to monitoring Poisson INAR(1) (PINAR(1)) model and Li et al. (2016) considered several charts for the new geometric INAR(1) (NGINAR(1)) model. Recently, Rakitzis et al. (2017) considered Shewhart-type and CUSUM charts based on the zero-inflated Poisson INAR(1) (ZIPINAR(1)) model and the first-order zero-inflated Poisson autoregres-

sive conditional heteroskedasticity (ZIPINARCH(1)) model for monitoring processes with serial dependence and zero-inflation. In Chapter 4, we consider improved monitoring of Markov counting process with zero-inflation, based on the ZIPINAR(1) and ZIPINARCH(1) model, which are suitable candidate models to capture serial dependence and zero-inflation. To this end, we consider three kinds of control charts. The first one is a new CUSUM-type chart based on a delay rule (CUSUM-DR) which is a generalization of the ZTP-CUSUM chart considered by He et al. (2014). The remainders are the CRL-CUSUM chart and the combined Shewhart CRL-CUSUM chart.

The change point problem has been a popular topic in time series analysis since the parameter change in the underlying time series model is observed at times in actual practice as a result of changes in, for instance, the policy of government, the quality of health care and the performance of machine in manufacturing process. It is well known that inferences without knowing a parameter change can lead to incorrect conclusions. For this reason, the change point detection problem has been investigated by many authors such as Csörgö and Horváth (1997), Lee et al. (2003), Hušková et al. (2007), Franke et al. (2012), Pap and Szabó (2013), Kang and Lee (2014), Lee et al. (2016) and Huh et al. (2017). Among the existing methods of change point test, the cumulative sum (CUSUM) test has long been popular because its ease of understanding and implementation in practice. In Chapter 5 and 6, we consider the usage of conditional least squares (CLS) estimator and SD estimator-based CUSUM test statistic, respectively. We propose control schemes based on virtual in-control sample and illustrate the performances of the proposed charts. Also, real data examples are employed to provide the applicability of our proposed charts.

In this study, we also consider the VSI CUSUM control chart considered by Reynolds et al. (1990), focusing on the ZIB distribution proposed by Hall (2000). We particularly deal with the task of monitoring an increase of the propor-tion parameter in ZIB processes using the VSI CUSUM chart and compare its performance with that of the FSI CUSUM chart considered by Rakitzis et al. (2016) via measuring their ATS triggering an out-of-control condition. Moreover, we put our efforts to develop an R package, attrCUSUM, for an easy implementation of the attribute VSI CUSUM control chart, which is available from the comprehensive R archive network (CRAN).

This thesis is organized as follows. Chapter 2 reviews the INAR process and CUSUM control charts. Chapter 3 considers the INARKF(1) process and its application to SPC based on the CUSUM control chart. Chapter 4 investigate the CRL-CUSUM and CUSUM-DR chart for monitoring Markovian processes with frequent zeros. Chapter 5 and 6 apply the CLS and SD estimator-based CUSUM test statistic to monitoring autocorrelated count process. Finally, the usage of the R package attrCUSUM developed for statistical design of FSI and VSI CUSUM chart is given in 7.

Chapter 2

Reviews

2.1 Integer-valued autoregressive (INAR) models

Since Al-Osh and Alzaid (1987) introduced the INAR (1) model using a random sum-type operator, the binomial thinning operator, it has become a popular process for modeling count data with serial dependence. The binomial thinning operator, '$\circ$', designated by Steutel and van Harn (1979) is defined as

$$\alpha \circ X = \sum_{i=1}^{X} B_i(\alpha), \tag{2.1.1}$$

where X is a non-negative integer-valued random variable and $B_i(\alpha)$'s are independent and identically distributed (i.i.d.) Bernoulli random variables with success probability $\alpha \in [0, 1]$, independent of X. The process $\{X_t\}_{t\in\mathbf{N_0}}$ is an INAR(1) model if

$$X_t = \alpha \circ X_{t-1} + \epsilon_t, \qquad t \in \mathbf{N}, \tag{2.1.2}$$

where $\alpha \in [0,1)$, '$\circ$' is the binomial operator in (4.2.1) and ϵ_t's are i.i.d. random variables defined on the non-negative integer values with a finite second moment, independent of X_{t-s}, $s \in \mathbf{N}$. The INAR(1) model forms a homogeneous Markov chain and there is a strictly stationary process satisfying the relation in (4.2.2).

For a strictly stationary process PINAR(1) model with $\theta^\top = (\alpha, \lambda) \in [0,1) \times (0,\infty)$, its marginal density follows a Poisson distribution with mean $\mu = \frac{\lambda}{1-\alpha}$ and the transition probabilities are given as

$$\begin{aligned} P\left(X_t = j | X_{t-1} = i\right) &= \sum_{k=0}^{\min(i,j)} P\left(\alpha \circ X_{t-1} = k | X_{t-1} = i\right) P\left(\epsilon_t = j-k\right) \\ &= \mathrm{e}^{-\lambda} \sum_{k=0}^{\min(i,j)} \binom{i}{k} \alpha^k (1-\alpha)^{i-k} \frac{\lambda^{j-k}}{(j-k)!}, \qquad i,j \in \mathbf{N_0}. \end{aligned}$$

Also, the h-step conditional expectation and variance of a stationary PINAR(1) model, see Kim and Lee (2017), are calculated as

$$\begin{aligned} \mathbb{E}\left(X_{t+h} | X_t\right) &= \alpha^h (X_t - \mu) + \mu, \\ \mathrm{Var}\left(X_{t+h} | X_t\right) &= \alpha^h (1-\alpha^h) X_t + (1-\alpha^h)\mu, \qquad h \in \mathbf{N}. \end{aligned}$$

where $\mu = \frac{\lambda}{1-\alpha}$. For additional properties of a stationary PINAR(1) model such as higher moments, refer to as Eduarda Da Silva and Oliveira (2004) and Bourguignon and Vasconcellos (2015).

Consider the residual process $\{u_t = X_t - \alpha X_{t-1} - \lambda\}_{t \geq 1}$ of the PINAR(1) model, which does not necessarily need to be stationary. we can express $X_t = \alpha X_{t-1} + u_t + \lambda$. Using Proposition 1 in Weiß (2012) and Theorem 14.0.1 in Meyn and Tweedie (2012), the fact that $\lim_{t\to\infty} \mathbb{E}u_t = 0$ and $\lim_{t\to\infty} \mathrm{Var}(u_t) = \lambda(1+\alpha)$ can be easily checked

and we obtain the results as follows:

Lemma 2.1.1. *Suppose* $\{X_t\}_{t\geq 0}$ *is a PINAR(1) model with parameter vector* $\theta^\top = (\alpha, \lambda) \in (0,1) \times (0,\infty)$ *and* $\mathbb{E}X_0^4 \in (0,\infty)$. *Then, for* $k = 1,2,3,4$, *and* $1 \leq i < j$, *we obtain*

$(a)\ |\mathbb{E}X_t^k - \mathbb{E}Y_0^k| = O(\alpha^t)$,

$(b)\ |\mathrm{Cov}(X_i, X_j) - \mathrm{Cov}(Y_i, Y_j)| = O(\alpha^{j-i})$,

$(c)\ |\mathrm{Cov}(D_{X,i}^2, D_{X,j}^2) - \mathrm{Cov}(D_{Y,i}^2, D_{Y,j}^2)| = O(\alpha^{j-i})$,

where $\{Y_t\}_{t\geq 0}$ *is a stationary PINAR(1) model with parameter vector* $\theta^\top = (\alpha, \lambda) \in (0,1) \times (0,\infty)$, $D_{X,i} = \frac{X_i - X_{i-1}}{2}$ *and* $D_{Y,i} = \frac{Y_i - Y_{i-1}}{2}$.

Because the true values of parameter vector θ cannot be known in practice, it must be estimated from a given sample path. There are conventional estimators to estimate the parameter of PINAR(1) model such as the Yule-Walker (YW), conditional least squares (CLS) and CML estimator which, in general, has the best performance among those in terms of bias and mean squared error (MSE), see Al-Osh and Alzaid (1987) for the details. In addition to conventional estimators, Weiß (2012) considered a simple estimator called a SD estimator based on an unbiased estimator of λ and fact that $\mu = \frac{\lambda}{1-\alpha}$ as follows:

$$\hat{\theta}^{sd} = \begin{pmatrix} \hat{\alpha}^{sd} \\ \hat{\lambda}^{sd} \end{pmatrix} = \begin{pmatrix} 1 - \frac{\hat{\lambda}^{sd}}{\bar{X}_n} \\ \frac{\sum_{t=1}^{n}(X_t - X_{t-1})^2}{2n} \end{pmatrix}, \tag{2.1.3}$$

where $\bar{X}_n = \frac{\sum_{t=0}^{n} X_t}{n+1}$. Bourguignon and Vasconcellos (2015) show that the asymptotic

joint distribution of $\sqrt{n}(\hat{\theta}^{sd} - \theta)$ is $\mathrm{N}(0, \Sigma)$ with

$$\Sigma = \begin{pmatrix} \frac{\alpha(1-\alpha^2)}{\lambda} + (1-\alpha)^2 \frac{3+\alpha}{1+\alpha} & -\lambda(1-\alpha)\frac{3+\alpha}{1+\alpha} \\ -\lambda(1-\alpha)\frac{3+\alpha}{1+\alpha} & \lambda\left(1 + \lambda\frac{3+\alpha}{1+\alpha}\right) \end{pmatrix}.$$

From numerical experiments in Weiß (2012) and Bourguignon and Vasconcellos (2015), it is admissible that the SD estimator can be a good alternative with closed form to CML estimator in terms of bias and MSE.

2.2 CUSUM control chart

Control chart is one of the most useful tools in statistical process control (SPC). Among control charts, the cumulative sum (CUSUM) control scheme, introduced by Page (1954), is well known as a standard tool for detecting small to moderate abnormal changes in the process of interest: see Montgomery (2012) for a general review. A conventional upper one-sided CUSUM control statistic for detecting a mean increase is expressed as:

$$C_0 = c_0, \tag{2.2.4}$$

$$C_t = \max\left(0, X_t - k + C_{t-1}\right), \quad t \in \mathbf{N}, \tag{2.2.5}$$

where $c_0 (\geq 0)$ is called the 'starting value', usually set to be 0, $k (\geq \mathbb{E}X_t)$ is called the 'reference value', and $h (> 0)$ is the 'control limit'. When $C_t \geq h$ occurs, the process of interest is regarded as 'out-of-control'. The reference value k acts as a tuning parameter for the sensitive detection of a mean increase, preventing the statistic from drifting towards the control limit h.

The performance of control charts is commonly measured by the average run length (ARL), which stands for the expected number of points plotted on a chart until an out-of-control signal is triggered. There are two types of ARL. First, ARL_0 (in-control ARL) is the expected number of points until a false alarm occurs, that is, the control chart mistakenly triggers an out-of-control signal from the start of monitoring. Second, ARL_1 (out-of-control ARL) is the expected number of points until the control chart alarms a shift from the start of the shift.

Although sampling is usually conducted with a fixed sampling interval (FSI) to maintain control charts, the variable sampling interval (VSI) is also adopted to improve the efficiency of monitoring: see Reynolds et al. (1988); Reynolds et al. (1990) and Saccucci et al. (1992). Epprecht et al. (2010) recently applied the VSI control scheme to the exponential weighted moving average (EWMA) chart, which is an alternative to the Shewhart control chart designed for faster monitoring. In the VSI control scheme, sampling intervals are planned to be varying according to the information obtained from the precedent control statistic and the performance is usually evaluated by the average time to signal (ATS) triggering an out-of-control condition. For more details, we refer to Reynolds et al. (1990).

In below we illustrate the merits (M) and shortcomings (S) of traditional control schemes.

- Shewhart-type
  - M: easy to implement; sensitive in detecting large mean shifts.
  - S: Not good at detecting small to moderate mean shifts and at detecting dynamic changes.
- CUSUM, EWMA
  - M: sensitive in detecting small mean shifts.

  - S: Not good at detecting large mean shifts and at detecting dynamic changes; need to set tuning parameter.

- Combined Shewhart and CUSUM/EWMA
  - M: Detect a wide range of mean shifts and dynamic patterns.
  - S: Need to set multiple parameter; can not detect dynamic patterns.
- GLR-type
  - M: Detect a wide range of mean shifts and dynamic patterns; can estimate directly change point.
  - S: Poor performance when the change is small of the change pattern is decaying.

Chapter 3

On First-order Integer-valued Autoregressive Process with Katz Family Innovations

3.1 Introduction

This chapter considers the first-order INAR process with Katz family innovations. This family of INAR processes includes a broad class of INAR(1) processes with Poisson, negative binomial, and binomial innovations, respectively featuring equi-, over-, and under-dispersion. Its probabilistic properties such as ergodicity and stationarity are investigated and the formula of the marginal mean and variance is provided. Further, a statistical process control (SPC) procedure based on the cumulative (CUSUM) control chart is considered to monitor autocorrelated count processes. A simulation and real data analysis are conducted for illustration.

This chapter is organized as follows. Section 3.2 introduces the INARKF(1) pro-

cess and investigates the probabilistic properties such as its existence, stationarity, ergodicity, and other probabilistic properties. Section 3.3 discusses the conditional maximum likelihood estimator and compares the fitness of the INARKF(1) to a real data set with that of other existing models. Section 3.4 considers the SPC procedure for INARKF(1) processes, wherein the CUSUM approach is taken to detect a mean increase. Section 3.5 provides the proofs for the theorems presented in Section 3.2. Finally, Section 3.6 provides concluding remarks.

3.2 INAR(1) process with Katz innovations

The distribution of non-negative integer-valued random variables can be uniquely expressed recursively in the following manner:

$$p_{j+1} = f(j, \Theta)p_j, \qquad j = 0, 1 \ldots, \tag{3.2.1}$$

where Θ is a vector of parameters and p_j denotes the probability mass function. Katz (1965) designated a simple system to generate (3.2.1) with two parameters $\Theta = (\theta_1, \theta_2)$, such as

$$f(j, \Theta) = \max\left(\frac{\theta_1 + \theta_2 j}{1 + j}, 0\right), \qquad j = 0, 1, \ldots, \tag{3.2.2}$$

where $\theta_1 > 0$, $\theta_2 < 1$. It can be easily seen that $\theta_2 \geq 0$ implies $p_j > 0$ for all $j \in \mathbf{N_0}$ and $\theta_2 < 0$ implies $p_{\lceil -\theta_1/\theta_2 \rceil + k} = 0$ for all $k \in \mathbf{N}$, wherein $\lceil x \rceil$ denotes the smallest integer not less than x.

Remark 1. It is well known (cf. Johnson et al. (1992)) that

[i] If $\theta_2 < 0$ and $-\theta_1/\theta_2 \in \mathbf{N}$, the KF distribution coincides with $Bin(-\theta_1/\theta_2,$

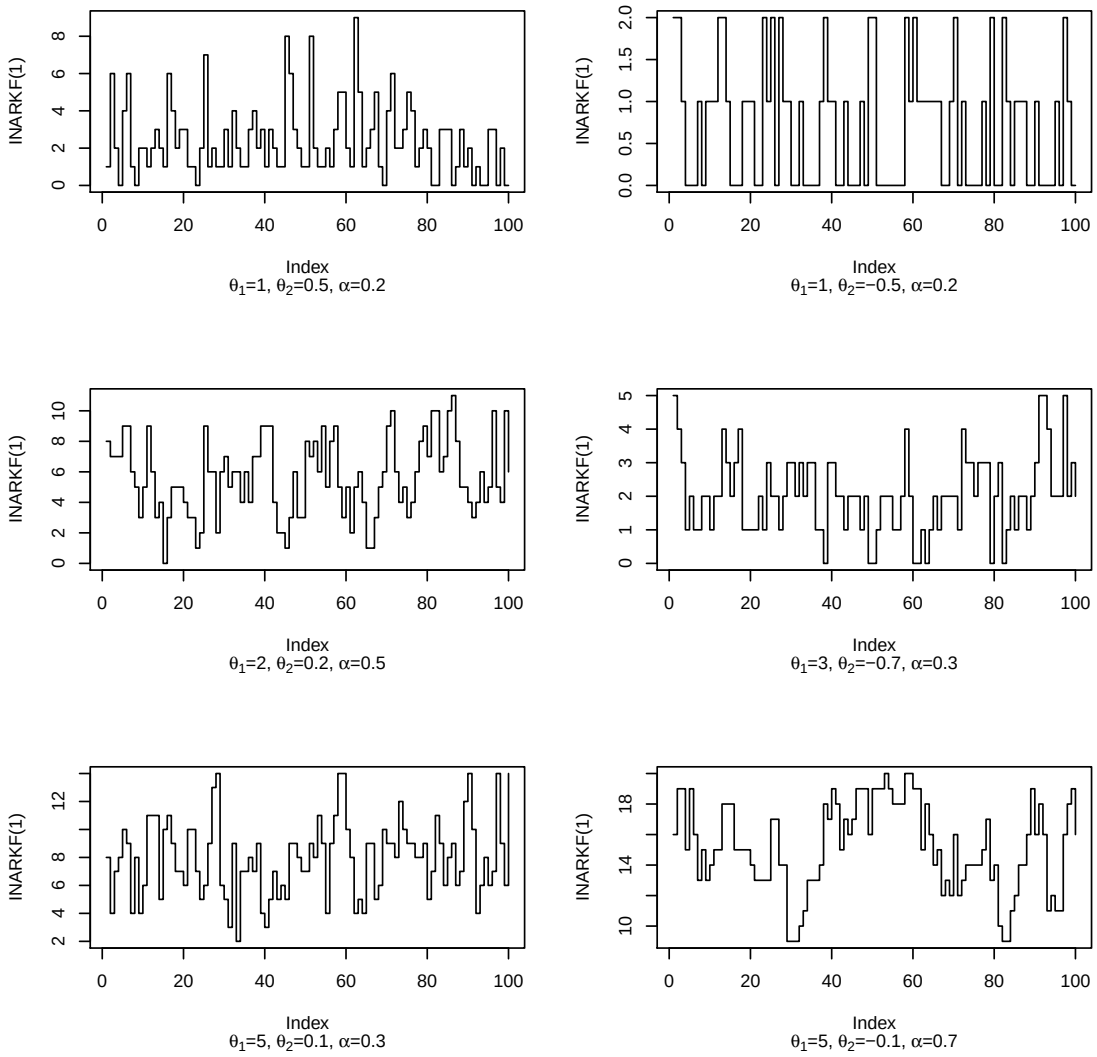

Figure 3.1: The sample paths of INARKF(1) processes with length 100

$\theta_2/(\theta_2 - 1)$).

[ii] If $0 < \theta_2 < 1$, the KF distribution coincides with $NB\,(\theta_1/\theta_2, 1 - \theta_2)$.

[iii] If $\theta_2 = 0$, the KF distribution coincides with $Poisson\,(\theta_1)$.

Although the probabilistic structure of the Katz family is quite simple, it covers a wide spectrum of distributions. According to Fang (2003), under the assumption that $-\theta_1/\theta_2 \in \mathbf{N}$ when $\theta_2 < 0$, the ratio of the variance to the mean of the KF distribution is obtained as $r = (1-\theta_2)^{-1}$. When $r = 1$, the KF distribution can be interpreted as the Poisson distribution (equi-dispersion); when $r < 1$, the binomial distribution (under-dispersion); when $r > 1$, the negative binomial distribution (over-dispersion).

Definition 3.2.1. The INARKF(1) process is the INAR(1) process defined by

$$X_t = \alpha \circ X_{t-1} + \epsilon_t, \quad t \in \mathbf{N}, \tag{3.2.3}$$

where ϵ_t are i.i.d. KF random variables with parameter (θ_1, θ_2): see (3.2.1) and (3.2.2), independent of $X_s, s \le t-1$, and $B_i(\alpha)$'s are the ones in (4.2.1).

Figure 3.1 shows a simulated sample path of an INARKF(1) process with length 100. A negative θ_2 shows a relatively under-dispersed process, whereas a positive θ_2 shows an over-dispersion. Below, we verify that the INARKF(1) process exists and is stationary and ergodic, the proof of which is deferred to Section 3.5.

Theorem 3.2.1. *The process $\{X_t\}_{t\in\mathbf{Z}}$ is an irreducible, aperiodic and positive recurrent (and thus ergodic) Markov chain. Hence, there exists a strictly stationary process satisfying (3.2.3).*

Remark 2. It can be easily seen that $EX_t^k \le C < \infty$, $k = 1, 2, 3, 4$, for some $C > 0$. Moreover, by Theorem 3.2.1, X_t converges to X in distribution, where X follows the stationary marginal distribution. Thus, from the portmanteau lemma (cf. Theorem 29 of Billingsley (1979)), we obtain $EX^k \le \lim_{t\to\infty} EX_t^k < \infty$, $k = 1, 2, 3, 4$.

Below, we investigate the probabilistic properties of the INARKF(1) process such as the transition probabilities and k-step prediction. For convenience, in what follows

of Section 2, we impose a condition that the KF distribution satisfies $-\theta_1/\theta_2 \in \mathbf{N}$ when $\theta_2 < 0$. Then, the transition probability and stationary marginal density can be expressed as follows: for $i, j \geq 0$,

$$\begin{aligned} p_{ij} &:= P\left(X_t = j | X_{t-1} = i\right) \\ &= \sum_{k=0}^{\min(i,j)} P\left(\alpha \circ X_{t-1} = k | X_{t-1} = i\right) P\left(\epsilon_t = j - k\right) \\ &= \sum_{k=0}^{\min(i,j)} \binom{i}{k} \alpha^k \left(1-\alpha\right)^{i-k} \left[\binom{\theta_1/\theta_2 + j - k - 1}{j-k} \left(1-\theta_2\right)^{\theta_1/\theta_2} \theta_2^{j-k} \right]; \end{aligned}$$

$$\begin{aligned} p_j &:= P\left(X_t = j\right) \\ &= \sum_{i=0}^{\infty} p_{ij} P\left(X_{t-1} = i\right) \\ &= \sum_{i=0}^{\infty} \sum_{k=0}^{\min(i,j)} \binom{i}{k} \alpha^k \left(1-\alpha\right)^{i-k} \left[\binom{\theta_1/\theta_2 + j - k - 1}{j-k} \left(1-\theta_2\right)^{\theta_1/\theta_2} \theta_2^{j-k} \right] p_i, \end{aligned} \tag{3.2.4}$$

wherein $\frac{1}{0}$ is interpreted as $\lim_{x \to 0} \frac{1}{x}$.

Moreover, the k-step prediction can be conducted based on the fact as follows:

Theorem 3.2.2. *Let $\{X_t\}_{t \in \mathbf{Z}}$ be an INARKF(1) process. Then, the k-step conditional mean and variance are given as*

$$\begin{aligned} \mathbb{E}\left(X_{t+k} | X_t\right) &= \alpha^k X_t + \frac{\left(1-\alpha^k\right)}{1-\alpha} \frac{\theta_1}{1-\theta_2}, \\ \mathrm{Var}\left(X_{t+k} | X_t\right) &= \alpha^k (1-\alpha^k) X_t + \frac{\alpha\left(1-\alpha^{k-1}\right)\left(1-\alpha^k\right)}{1-\alpha^2} \frac{\theta_1}{1-\theta_2} + \frac{1-\alpha^{2k}}{1-\alpha^2} \frac{\theta_1}{\left(1-\theta_2\right)^2}. \end{aligned}$$

Remark 3. It can be easily seen that $\lim_{k\to\infty} E\left(X_{t+k}|X_t\right) = \frac{\theta_1}{(1-\alpha)(1-\theta_2)}$ and $\lim_{k\to\infty} Var\left(X_{t+k}|X_t\right) = \frac{\theta_1(1+\alpha(1-\theta_2))}{(1-\alpha^2)(1-\theta_2)^2}$.

Moreover, we can see that the self-decomposability (cf. Steutel and van Harn, 1979) holds for of the INARKF(1) process, the proof of which is given in Section 3.5:

Theorem 3.2.3. *If $\{X_t\}_{t\in\mathbf{Z}}$ is a stationary INARKF(1) process, X_t is a discrete self-decomposable (DSD) random variable.*

The following can be obtained via using the Theorem 2.1 of Zhang and Wang (2015).

Proposition 3.2.1. *Let $\{X_t\}_{t\in\mathbf{Z}}$ be a stationary INARKF(1) process with $(\theta_1, \theta_2, \alpha)$. Then, for $s, \tau \in \mathbf{N}$ with $s < \tau$, we have*

(i) $\mu_X = \mathbb{E}X_t = \frac{1}{1-\alpha}\frac{\theta_1}{1-\theta_2}$;

(ii) $\mathbb{E}X_t^2 = \frac{\theta_1(1+\alpha(1-\theta_2))}{(1-\alpha^2)(1-\theta_2)^2} + \frac{\theta_1^2}{(1-\alpha^i)(1-\theta_2)^2}$;

(iii) $\mathbb{E}\left(X_tX_{t+s}\right) = \alpha\mathbb{E}\left(X_tX_{t+s-1}\right) + \frac{\theta_1^2}{(1-\alpha)(1-\theta_2)^2}$;

(iv) $\mathbb{E}X_t^3 = (1-\alpha^3)^{-1}\Big[3\alpha^2\mathbb{E}X_t^2(1-\alpha+\mu_\epsilon)$
$+ \alpha\mu_X\left((1-\alpha)(1-2\alpha) + 3(1-\alpha)\mu_\epsilon + 3\mu_{\epsilon,2}\right) + \mu_{\epsilon,3}\Big]$;

(v) $\mathbb{E}\left(X_t^2X_{t+s}\right) = \alpha\mathbb{E}\left(X_t^2X_{t+s-1}\right) + \mathbb{E}X_t^2\mu_\epsilon$.

(vi) $\mathbb{E}\left(X_tX_{t+s}^2\right) = \alpha^2\mathbb{E}\left(X_tX_{t+s-1}^2\right) + \left(\alpha(1-\alpha) + 2\alpha\mu_\epsilon\right)\mathbb{E}\left(X_tX_{t+s-1}\right) + \mu_X\mu_{\epsilon,2}$;

(vii) $\mathbb{E}\left(X_tX_{t+s}X_{t+\tau}\right) = \alpha\mathbb{E}\left(X_tX_{t+s}X_{t+\tau-1}\right) + \mu_\epsilon\mathbb{E}\left(X_tX_{t+s}\right)$,

where $\mu_\epsilon = \mathbb{E}\epsilon_t = \frac{\theta_1}{1-\theta_2}$, $\mu_{\epsilon,2} = \mathbb{E}\epsilon_t^2 = \frac{\theta_1(1+\theta_1)}{(1-\theta_2)^2}$ *and* $\mu_{\epsilon,3} = \mathbb{E}\epsilon_t^3 = \frac{\theta_1\left(\theta_1^2+3\theta_1+1+\theta_2\right)}{(1-\theta_2)^3}$.

Remark 4. The variance-to-mean ratio of a stationary INARKF(1) process is given by

$$\frac{\sigma_X^2}{\mu_X} = \frac{\sigma_\epsilon^2/\mu_\epsilon + \alpha}{1+\alpha} = \frac{(1-\theta_2)^{-1} + \alpha}{1+\alpha} = \frac{r+\alpha}{1+\alpha}.$$

Thus, $r = 1$ implies the equi-dispersion and $r > 1$ and $r < 1$ imply the over- and under-dispersion, respectively.

3.3 Parameter estimation and real example

Given observations $x_1, \ldots, x_n$, the log-likelihood function is defined by

$$\begin{aligned} l(\theta_1, \theta_2, \alpha) &= \log \left[P(X_1 = x_1) \prod_{t=2}^{n} P\left(X_t = x_t | X_{t-1} = x_{t-1}\right) \right] \\ &= \log P(X_1 = x_1) + \sum_{t=2}^{n} \log P(X_t = x_t | X_{t-1} = x_{t-1}), \end{aligned}$$

$$P(X_t = x_t | X_{t-1} = x_{t-1}) = \sum_{k=0}^{\min(x_{t-1}, x_t)} \binom{x_{t-1}}{k} \alpha^k (1-\alpha)^{x_{t-1}-k} P\left(\epsilon_t = x_t - k\right).$$

Here, the probability mass function of innovations can be obtained as follows:

$$\begin{aligned} P\left(\epsilon_t = x_t - k\right) &= \left[\prod_{i=0}^{x_t - k - 1} \max\left(\frac{\theta_1 + \theta_2 i}{1+i}, 0 \right) \right] P\left(\epsilon_t = 0\right), \\ P\left(\epsilon_t = 0\right) &= \frac{1}{1 + \sum_{j=1}^{\infty} \left[\prod_{i=0}^{j-1} \max\left(\frac{\theta_1 + \theta_2 i}{1+i}, 0 \right) \right]} \\ &= \begin{cases} (1-\theta_2)^{\theta_1/\theta_2} & \text{if } \theta_2 > 0 \\ e^{-\theta_1} & \text{if } \theta_2 = 0 \\ \left(\frac{1}{1-\theta_2} \right)^{-\theta_1/\theta_2} & \text{if } \theta_2 < 0 \text{ and } -\theta_1/\theta_2 \in \mathbf{N} \\ \frac{1}{1 + \sum_{j=1}^{\lceil -\theta_1/\theta_2 \rceil} \left[\prod_{i=0}^{j-1} \max\left(\frac{\theta_1 + \theta_2 i}{1+i}, 0 \right) \right]} & \text{if } \theta_2 < 0 \text{ and } -\theta_1/\theta_2 \notin \mathbf{N}, \end{cases} \end{aligned}$$

wherein $\prod_{i=0}^{-1} \max\left(\frac{\theta_1 + \theta_2 i}{1+i}, 0 \right) = 1$.

Table 3.1: The mean and MSE (in parentheses) of (C)MLE

θ_1	θ_2	α	n	$\hat{\theta_1}^{cml}$	$\hat{\theta_2}^{cml}$	$\hat{\alpha}^{cml}$	$\hat{\theta_1}^{ml}$	$\hat{\theta_2}^{ml}$	$\hat{\alpha}^{ml}$
5	-0.1	0.2	100	5.0573	-0.1589	0.1763	5.0549	-0.1711	0.1731
				(0.1814)	(0.0476)	(0.0091)	(0.1891)	(0.0495)	(0.0092)
			200	5.0328	-0.1398	0.1864	5.0377	-0.1459	0.1832
				(0.0888)	(0.0223)	(0.0046)	(0.0884)	(0.0227)	(0.0049)
			500	5.0171	-0.1156	0.1943	5.0194	-0.1177	0.1927
				(0.0306)	(0.0068)	(0.0018)	(0.0316)	(0.0072)	(0.0020)
			1000	5.0111	-0.1073	0.1977	5.0129	-0.1087	0.1967
				(0.0160)	(0.0031)	(0.0009)	(0.0163)	(0.0032)	(0.0010)
5	0.1	0.2	100	5.0403	0.0532	0.1816	5.0494	0.0430	0.1768
				(0.1925)	(0.0344)	(0.0098)	(0.2019)	(0.0354)	(0.0100)
			200	5.0228	0.0725	0.1911	5.0298	0.0640	0.1876
				(0.0835)	(0.0138)	(0.0050)	(0.0879)	(0.0145)	(0.0052)
			500	5.0433	0.0942	0.1979	5.0796	0.0902	0.1980
				(0.0324)	(0.0053)	(0.0019)	(0.0333)	(0.0054)	(0.0019)
			1000	5.0035	0.0964	0.1994	5.0052	0.0940	0.1998
				(0.0143)	(0.0027)	(0.0009)	(0.0154)	(0.0028)	(0.0009)
5	-0.3	0.5	100	5.0958	-0.4464	0.4736	5.0982	-0.4593	0.4689
				(0.3716)	(0.2071)	(0.0083)	(0.3724)	(0.2084)	(0.0089)
			200	5.0448	-0.3570	0.4843	5.0538	-0.3705	0.4809
				(0.2553)	(0.0722)	(0.0040)	(0.2588)	(0.0756)	(0.0042)
			500	5.0221	-0.3365	0.4946	5.0272	-0.3444	0.4925
				(0.0881)	(0.0266)	(0.0016)	(0.0898)	(0.0272)	(0.0016)
			1000	5.0022	-0.3072	0.5014	5.0058	-0.3130	0.4999
				(0.0377)	(0.0121)	(0.0007)	(0.0384)	(0.0123)	(0.0007)
2	-0.5	0.2	100	2.0074	-0.5162	0.1821	2.0082	-0.5162	0.1821
				(0.0219)	(0.0472)	(0.0094)	(0.0218)	(0.0472)	(0.0093)
			200	2.0034	-0.5124	0.1903	2.0035	-0.5125	0.1909
				(0.0102)	(0.0202)	(0.0057)	(0.0102)	(0.0196)	(0.0056)
			500	2.0003	-0.5065	0.1967	2.0002	-0.5068	0.1975
				(0.0036)	(0.0077)	(0.0020)	(0.0036)	(0.0079)	(0.0021)
			1000	2.0001	-0.5027	0.1987	2.0001	-0.5028	0.1987
				(0.0016)	(0.0038)	(0.0010)	(0.0017)	(0.0039)	(0.0010)
2	-0.5	0.5	100	2.0333	-0.6021	0.4747	2.0356	-0.6113	0.4730
				(0.0901)	(0.1392)	(0.0087)	(0.0922)	(0.1398)	(0.0087)
			200	2.0106	-0.5142	0.4873	2.0116	-0.5177	0.4862
				(0.0254)	(0.0409)	(0.0043)	(0.0258)	(0.0402)	(0.0043)
			500	2.0015	-0.5079	0.4977	2.0015	-0.5089	0.4983
				(0.0072)	(0.0121)	(0.0014)	(0.0074)	(0.0121)	(0.0014)
			1000	2.0003	-0.5032	0.4994	2.0004	-0.5069	0.4999
				(0.0028)	(0.0053)	(0.0006)	(0.0030)	(0.0054)	(0.0006)
2	0.5	0.2	100	2.0166	0.4729	0.1814	2.0210	0.4658	0.1765
				(0.0347)	(0.0112)	(0.0082)	(0.0365)	(0.0117)	(0.0084)
			200	2.0062	0.4907	0.1950	2.0097	0.4848	0.1906
				(0.0148)	(0.0046)	(0.0047)	(0.0157)	(0.0049)	(0.0047)
			500	2.0016	0.4970	0.1959	2.0037	0.4938	0.1940
				(0.0055)	(0.0018)	(0.0017)	(0.0058)	(0.0019)	(0.0017)
			1000	2.0013	0.4988	0.1991	2.0022	0.4976	0.1979
				(0.0026)	(0.0009)	(0.0008)	(0.0027)	(0.0009)	(0.0008)

Table 3.2: ML estimates, AIC, BIC and RMS of burglary data

model	parameters	MLE	AIC	BIC	RMS
PINAR(1)	λ	4.9021	846.27	852.21	4.081
	α	0.1794			
NBINAR(1)	n	4.0768	757.52	766.43	4.067
	p	0.4058			
	ρ	0.2560			
GPQINAR(1)	λ	3.7243	755.12	764.03	4.085
	θ	0.3944			
	ρ	0.3448			
NBRCINAR(1)	n	3.7878	757.51	766.41	4.081
	p	0.3825			
	ρ	0.3339			
NBIINAR(1)	n	3.9045	757.88	766.72	4.071
	α	0.9346			
	ρ	0.3024			
NGINAR(1)	μ	5.3233	788.55	794.49	4.343
	α	0.6165			
GINAR(1)	p	0.1787	810.37	816.31	4.178
	α	0.3605			
DCGINAR(1)	μ	4.9605	804.59	813.50	4.177
	α	0.4447			
	θ	0.4360			
ZINAR(1)	λ	4.9610	829.81	838.72	4.091
	ρ	0.2276			
	α	0.3628			
INARG(1)	π	0.2040	762.49	768.43	4.092
	α	0.3629			
INARKF(1)	θ_1	1.4834	754.90	763.81	4.067
	θ_2	0.6634			
	α	0.2585			

Then, the maximum likelihood estimator (MLE) $(\hat{\theta_1}, \hat{\theta_2}, \hat{\alpha})$ of $(\theta_1, \theta_2, \alpha)$ is given as the $(\theta_1, \theta_2, \alpha)$ that maximizes the log-likelihood function. It can be performed by using numerical maximization procedures found easily in most of statistical programming languages. One can also obtain a conditional MLE (CMLE) via conditioning on the first observation.

Table 3.1 lists a simulated result about the mean and mean squared errors (MSEs) of the MLE and CMLE for different values of $(\theta_1, \theta_2, \alpha)$ and n =100, 200, 500, 1000. The Monte Carlo simulation experiments are performed via using the R programming language: see the R project for statistical computing (http://www.r-

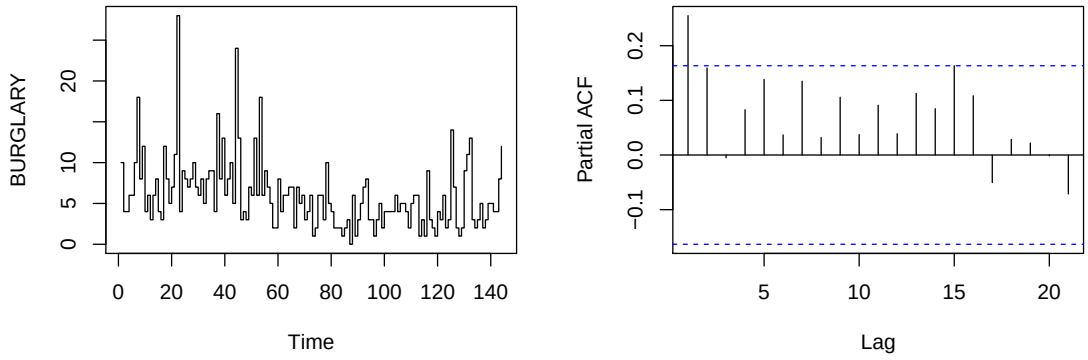

Figure 3.2: The sample path and PACF plot of the burglary data

project.org). The number of Monte Carlo replications for each case is 500. The (conditional) MLE of $(\theta_1, \theta_2, \alpha)$ is obtained by maximizing the (conditional) log-likelihood function using the Nelder-Mead method. Here, due to the complex seen in (3.2.4), the marginal density of X_1 is empirically obtained through a simulated process of size $20,000$ at given $(\theta_1, \theta_2, \alpha)$. Table 3.1 shows that for all cases, $\hat{\theta}_1$ is overestimated whereas $\hat{\theta}_2$ and α are underestimated. Both the magnitude of bias and MSE of $\hat{\theta}_1$ increase as θ_1 and α increase, mainly affected by the former rather than the latter. Similarly, those of $\hat{\theta}_2$ increase as θ_1 and α increase. Moreover, it can be observed that the bias and MSE decay to zero and the CMLE and MLE have a similar performance. It is also revealed that the estimation of θ_1 is slightly worsened when either (mainly) θ_1 or α becomes larger.

Below, we illustrate an example to fit the INARKF(1) process to a real data set. To this task, we use the burglary data series reported in the 65th police car beat in Pittsburgh: see the Forecasting Principles site (http://www.forecastingprinciples.com). The data set comprises 144 observations, monthly observed from 1990 to 2001.

The sample path plot and partial autocorrelation function are shown in Figure 3.2. The sample mean, variance, dispersion and autocorrelation are obtained as 5.9583, 17.8304, 2.9925 and 0.2551, respectively. Here, we compare the fitness of the INARKF(1) process with that of PINAR(1), INAR(1) process with Poisson marginals (Al-Osh and Alzaid, 1987), NBINAR(1), INAR(1) process with negative binomial marginals (McKenzie, 1986; Weiß, 2008), GPQINAR(1), quasi-binomial INAR(1) process with generalized Poisson marginals (Alzaid and Al-Osh, 1993), NBRCINAR(1), random coefficient INAR(1) process with negative binomial marginals (Weiß, 2008), NBIINAR(1), iterated INAR(1) process with negative binomial marginals and innovations (Al-Osh and Aly, 1992), NGINAR(1), negative binomial thinning based INAR(1) process with geometric marginals and innovations (Ristić et al., 2009), GINAR(1), INAR(1) process with geometric marginals (Alzaid and Al-Osh, 1988), DCGINAR(1), dependent counting INAR(1) process with geometric marginals (Ristić et al., 2013), ZINAR(1), INAR(1) process with zero inflated Poisson innovations (Jazi et al., 2012a), and INARG(1), INAR(1) process with geometric innovations (Jazi et al., 2012b).

For each process, we calculate the MLE, AIC, BIC, and root mean square (RMS) of predicted values. Table 3.2 shows that the INARKF(1) has the smallest AIC, BIC, RMS values, which suggests to adopt the INARKF(1) process among the models under consideration. The MLE in this case is obtained as $(\hat{\theta}_1, \hat{\theta}_2, \hat{\alpha}) = (1.4834, 0.6634, 0.2585)$.

3.4 CUSUM chart to monitor a mean increase

In this section, we consider the CUSUM control chart for INARKF(1) processes to monitor an increase of θ_1 when θ_2 and α are fixed. We do this because the mean increases as θ_1 increases when the dispersion of the INARKF(1) process is fixed. For a review of the CUSUM control chart, we refer to Weiss and Testik (2009) and Chao-Wen and Reynolds Jr (2001).

Let $\{X_t\}$, $t \in \mathbf{N}$, be a stationary INARKF(1) process with parameter $(\theta_{1_0}, \theta_2, \alpha)$ and marginal mean μ_X. A one-sided CUSUM control chart for detecting the mean increase is then expressed as a plot of the CUSUM statistic as follows:

$$\begin{aligned} C_0 &= c_0, \\ C_t &= \max\left(0, X_t - k + C_{t-1}\right), \quad t \in \mathbf{N}, \end{aligned}$$

where c_0 is a non-negative starting value, commonly set to be 0, $k \geq \mu_X$ is the reference value, and $h > 0$ is the limit value.

Note that the bivariate process $(X_t, C_t)_{t\in\mathbf{N}}$ has the Markov property with following transition probabilities:

$$\begin{aligned} p(x, y|w, z) :&= P\left(X_t = x, C_t = y | X_{t-1} = w, C_{t-1} = z\right) \\ &= p_{wx}\mathbf{I}_y\left(\max(0, x - k + z)\right); \\ p_1(x, y|w) :&= P\left(X_1 = x, C_1 = y | C_0 = w\right) \\ &= p_x\mathbf{I}_y\left(\max(0, x - k + w)\right), \end{aligned} \tag{3.4.5}$$

where $\mathbf{I}_y(\cdot)$ denote the indicator function. To conduct the calculation for ARLs of the designed CUSUM chart, here we employ the Markov chain approach of Brook

and Evans (1972): see Weiss and Testik (2009) for a review of this approach used for autocorrelated count processes. The marginal probabilities in (3.4.5) can be empirically obtained based on the generated process of size 20,000, as done in Section 3.4.

For exploring the CUSUM control chart to detect a small increase, we design a chart with its in-control ARL being near 200. Since it is difficult to obtain a closed form to optimize the CUSUM control chart for a specified increase, we choose k such

Table 3.3: The ARL of INARKF(1) CUSUM control chart with $\theta_{1_0} = 1.5$

θ_{1_0}	θ_2	α	μ_X	k	h	θ_1:	1.5	1.6	1.7	2	2.5	3	5	10
1.5	-0.5	0.25	1.33	2	5		233.7	155.4	108.8	38.6	14.2	7.8	2.7	1.2
				3	2		279.9	198.6	146.9	50.7	17.6	8.6	2.1	1.0
		0.50	2.00	3	7		216.0	147.0	105.2	40.6	15.4	8.4	2.7	1.1
				4	3		259.3	180.6	131.7	49.7	17.7	8.7	2.0	1.0
		0.75	4.00	5	19		203.7	133.0	92.7	36.3	14.7	8.4	3.0	1.3
				6	9		225.6	150.1	105.5	39.8	14.2	7.1	1.9	1.0
	-0.8	0.25	1.14	2	3		205.4	158.9	126.8	74.1	15.3	7.6	2.3	1.1
				3	1		201.6	162.8	135.2	87.1	16.0	7.4	1.9	1.0
		0.50	1.71	2	13		208.9	145.3	107.1	55.3	17.2	10.5	4.3	2.0
				3	4		207.4	158.6	125.4	72.2	17.1	8.4	2.3	1.0
		0.75	3.43	4	23		201.4	141.8	105.6	55.7	17.2	10.1	3.9	1.8
				5	10		232.8	168.5	127.3	67.2	16.3	8.0	2.3	1.0
	-0.9	0.25	0.80	1	5		202.9	176.7	155.8	13.2	9.2	5.3	2.6	1.2
				2	1		235.8	219.5	205.4	12.0	8.2	3.4	1.4	1.0
		0.50	1.20	2	4		204.4	184.1	167.6	15.8	10.2	4.9	1.9	1.0
				3	1		236.6	215.8	198.8	14.1	9.0	3.7	1.3	1.0
		0.75	2.40	3	15		202.7	176.1	155.3	17.0	11.3	6.1	2.7	1.2
				4	5		230.1	203.1	181.5	15.6	9.4	4.0	1.3	1.0
	0.1	0.25	2.22	3	10		254.2	154.9	100.1	36.5	13.6	7.9	3.0	1.3
				4	5		212.6	145.7	103.2	43.3	15.5	7.9	2.2	1.0
		0.50	3.33	4	19		213.1	128.1	83.1	32.7	13.9	8.5	3.4	1.5
				5	10		231.9	149.9	101.5	39.8	14.3	7.6	2.4	1.0
		0.75	6.67	7	57		203.2	118.2	77.4	33.8	16.2	10.5	4.4	2.1
				8	31		210.6	126.7	82.5	32.0	12.8	7.5	2.8	1.2
	0.2	0.25	2.67	3	18		201.6	114.6	72.5	29.1	13.5	8.7	3.7	1.8
				4	9		232.8	151.4	102.6	39.5	14.0	7.6	2.6	1.1
		0.50	4.00	5	19		209.0	127.8	83.5	32.3	13.1	7.8	3.0	1.3
				6	11		211.4	138.1	94.3	37.4	13.5	7.1	2.2	1.0
		0.75	8.00	9	46		200.3	117.5	75.6	30.3	13.1	8.1	3.3	1.6
				10	29		210.6	127.2	82.4	31.0	11.7	6.5	2.4	1.0
	0.5	0.25	4.00	5	19		202.5	123.4	80.0	30.3	12.3	7.4	3.0	1.4
				6	13		228.9	151.4	103.6	40.2	14.1	7.5	2.5	1.1
		0.50	6.00	7	33		205.5	120.3	76.7	29.8	12.8	8.0	3.2	1.5
				8	22		218.8	136.5	89.8	33.7	12.6	7.1	2.6	1.1
		0.75	12.00	13	76		201.4	113.5	71.9	28.9	13.0	8.2	3.5	1.8
				14	53		205.1	118.9	75.4	28.2	11.3	6.7	2.7	1.1

as $\lfloor \mu_X + 1 \rfloor$ and $\lfloor \mu_X + 2 \rfloor$, and find the smallest integer h such that the ARL_0 is greater than 200 with $c_0 = 0$, where $\lfloor x \rfloor$ stands for the largest integer not exceeding x.

Tables 3.3 and 3.4 demonstrate the adequacy of the CUSUM control chart for INARKF(1) processes, showing a reasonable performance for all over-, equi-, or under-dispersed autocorrelated count processes. Table 3.5 illustrates an example to compare the CUSUM control chart with the c-chart for several different parameters.

Table 3.4: The ARL of INARKF(1) CUSUM control chart with $\theta_{1_0} = 3$

θ_{1_0}	θ_2	α	μ_X	k	h	θ_1:	3	3.25	3.5	4	5	7	10	15
3	-0.5	0.25	2.67	3	12		203.3	85.4	45.3	20.4	9.2	4.4	2.6	1.7
				4	5		256.8	127.8	69.9	27.5	8.7	3.0	1.6	1.1
		0.50	4.00	5	13		233.3	110.2	59.8	24.8	9.3	3.9	2.2	1.3
				6	6		205.3	107.7	61.9	26.1	8.5	2.8	1.3	1.0
		0.65	5.71	6	38		202.1	90.6	51.9	25.9	12.4	6.0	3.5	2.2
				7	18		218.2	104.2	57.3	24.3	9.1	3.7	2.1	1.2
	-0.8	0.25	2.29	3	7		299.0	142.2	78.4	26.3	9.1	3.7	2.1	1.3
				4	3		326.1	181.0	111.4	36.2	10.3	3.0	1.4	1.0
		0.50	3.43	4	15		211.1	103.3	60.0	24.5	10.3	4.6	2.6	1.7
				5	7		266.0	142.1	85.3	31.1	10.0	3.3	1.6	1.1
		0.65	4.90	5	41		205.6	97.4	59.7	29.3	14.6	7.2	4.2	2.6
				6	16		200.7	103.7	61.7	24.8	9.5	3.8	2.2	1.2
	-0.9	0.25	2.07	3	5		357.1	213.3	139.4	29.6	9.2	3.3	1.8	1.1
				4	2		353.1	237.8	171.9	35.4	9.9	2.7	1.3	1.0
		0.50	3.11	4	10		233.6	138.1	90.6	25.9	9.6	3.9	2.2	1.3
				5	4		212.8	138.0	96.8	27.4	8.8	2.7	1.3	1.0
		0.65	4.44	5	23		213.6	118.9	76.3	25.4	11.1	5.0	2.9	1.9
				6	10		215.7	131.0	87.7	25.8	8.9	3.2	1.6	1.0
	0.1	0.25	4.44	5	19		226.1	89.3	45.8	20.0	8.9	4.2	2.5	1.6
				6	10		226.6	108.4	58.3	22.8	7.8	3.1	1.7	1.1
		0.50	7.00	8	21		217.9	96.8	51.2	21.1	8.3	3.6	2.1	1.2
				9	13		221.9	107.1	58.4	23.2	7.7	2.9	1.5	1.0
		0.65	9.52	10	55		203.9	84.5	46.9	22.8	10.8	5.3	3.1	2.0
				11	32		206.6	90.5	48.2	20.5	8.2	3.6	2.1	1.2
	0.2	0.25	5.33	6	22		218.8	87.0	44.6	19.5	8.6	4.1	2.5	1.6
				7	13		238.5	110.7	58.3	22.4	7.8	3.2	1.8	1.1
		0.50	8.00	9	32		212.2	88.2	46.3	20.3	8.8	4.1	2.4	1.5
				10	20		211.9	97.2	51.7	20.8	7.6	3.1	1.8	1.1
		0.65	11.43	12	63		202.5	82.3	45.2	21.9	10.3	5.0	3.0	2.0
				13	39		201.3	86.3	45.6	19.6	8.0	3.6	2.1	1.2
	0.5	0.25	8.00	9	31		206.1	83.1	42.7	18.6	8.2	3.9	2.4	1.5
				10	21		208.8	95.7	50.3	19.9	7.4	3.2	1.9	1.1
		0.50	12.00	13	53		200.1	79.7	42.2	19.4	8.9	4.3	2.5	1.7
				14	37		206.6	88.1	45.7	18.9	7.6	3.4	2.0	1.2
		0.65	17.14	18	87		200.6	78.7	42.6	20.3	9.5	4.7	2.8	1.9
				19	62		203.0	82.3	42.8	18.5	7.9	3.7	2.2	1.3

A conventional one-sided c-chart for detecting a mean increase is the plot of the c statistic as follows:

$$c_0 = 0,$$
$$c_t = X_t, \quad t \in \mathbf{N}.$$

The process is regarded out-of-control when the signal, $c_t \geq h$, is triggered where $h > 0$ is the upper control limit. For comparison, we choose the upper control limit of c-chart such that its in-control ARL is near 500. On the other hand, we design a CUSUM control chart with $\lfloor \mu_X + 1 \rfloor$, $c_0 = 0$ and h such that its in-control ARL is grater than that of the c-chart. As expected, the CUSUM control chart appears to detect a small increase better than the c-control chart. However, a large increase is not so well-detected as the small case: the performance in this case is slightly worsened.

To illustrate the applicability of CUSUM control chart, we use the disorderly conduct data series reported in the 44th police car beat in Pittsburgh. This data set

Table 3.5: Comparison of the c-chart and CUSUM control chart

θ_{1_0}	θ_2	α	μ_X								
3.2	-0.2	0.27	3.65	θ_1:	3.2	3.4	3.8	4.2	5	7	10
				CUSUM(k=4, h=24)	543.42	194.56	56.67	29.88	15.01	6.74	3.83
				c-Chart(h=10)	512.09	310.69	197.89	64.67	21.73	4.25	1.45
5.4	-0.1	0.25	6.55	θ_1:	5.4	5.6	6	6.4	8	10	15
				CUSUM(k=7, h=32)	508.30	223.97	74.27	39.24	12.80	6.97	3.43
				c-Chart(h=15)	492.06	409.93	179.15	100.88	18.18	4.93	1.26
3.1	0	0.65	9	θ_1:	3.15	3.35	3.75	4.15	5	7	10
				CUSUM(k=10, h=56)	551.31	214.32	63.55	32.34	14.90	6.47	3.63
				c-Chart(h=19)	529.01	289.98	105.90	47.40	13.35	2.20	1.03
2	0.1	0.54	4.83	θ_1:	2	2.2	2.6	3	4	5	8
				CUSUM(k=5, h=63)	510.16	148.70	50.64	29.83	14.61	9.73	5.00
				c-Chart(h=13)	503.17	252.80	82.94	35.29	8.16	3.18	1.08
5.5	0.4	0.16	10.91	θ_1:	5.5	5.7	6.1	6.5	8	10	15
				CUSUM(k=11, h=90)	505.24	198.33	77.88	47.63	19.34	10.88	5.36
				c-Chart(h=25)	489.64	269.31	156.42	95.44	19.99	5.51	1.36

Table 3.6: ML estimates, AIC, BIC and RMS of disorderly conduct data (From 1990 to 1996)

model	parameters	MLE	AIC	BIC	RMS
PINAR(1)	λ	3.1333	366.73	371.59	2.120
	α	0.2154			
NBINAR(1)	n	11.6397	364.66	371.95	2.123
	p	0.7443			
	ρ	0.2828			
GPQINAR(1)	λ	3.5073	365.63	372.93	2.121
	θ	0.1258			
	ρ	0.2629			
NBRCINAR(1)	n	13.3209	365.69	372.98	2.121
	p	0.7686			
	ρ	0.2624			
NBIINAR(1)	n	5.2047	524.51	531.80	6.154
	α	0.5403			
	ρ	2.3e-06			
NGINAR(1)	μ	4.3067	388.39	393.25	2.497
	α	0.7995			
GINAR(1)	p	0.2571	396.10	400.96	2.264
	α	0.5177			
DCGINAR(1)	μ	3.0627	396.87	404.16	2.256
	α	0.5291			
	θ	0.2992			
ZINAR(1)	λ	3.1875	368.30	375.59	2.122
	ρ	6.4e-08			
	α	0.2109			
INARG(1)	π	0.3236	370.05	374.91	2.215
	α	0.5001			
INARKF(1)	θ_1	2.2080	364.29	371.58	2.119
	θ_2	0.2537			
	α	0.2511			

Table 3.7: ARL_0 of CUSUM control chart for disorderly conduct data with $k = 4$

model		ARL_0							
	h:	19	20	21	22	23	24	25	26
INARKF(1)		72.4	79.0	85.9	93.0	100.6	108.4	116.6	125.0
PINAR(1)		84.3	91.9	99.9	108.3	116.9	126.0	135.3	145.0
	h:	27	28	29	30	31	32	33	34
INARKF(1)		133.9	143.0	152.6	162.4	172.6	183.2	194.1	205.4
PINAR(1)		155.1	165.5	176.2	187.3	198.8	210.5	222.7	235.1
	h:	35	36	37	38	39	40	41	42
INARKF(1)		217.1	229.1	241.5	254.3	267.5	281.0	295.0	309.4
PINAR(1)		248.0	261.1	274.7	288.6	302.8	317.4	332.3	347.6

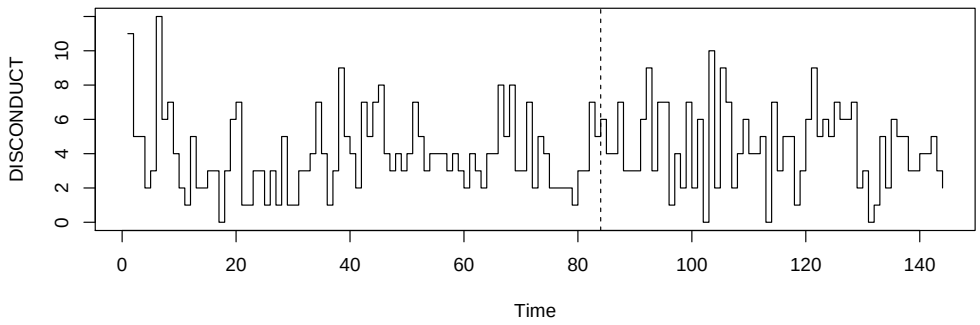

Figure 3.3: The sample path of disorderly conduct data

is monthly data observed from 1990 to 2001. We first use the data from 1990 to 1996 to fit the INARKF(1) process, and then apply the CUSUM control chart to the data from 1997 to check whether the mean increase occurs or not. The sample plot and the ACF and PACF plots are given in Figure 3.3 (the dashed line denotes December 1996) and Figure 3.4, respectively. The sample path plot shows that one cannot easily detect a mean increase after the dashed line. For disorderly conduct data from 1990 to 1996, the sample mean, variance, dispersion, and autocorrelation are given as 3.9643, 5.3602, 1.3521 and 0.2261, respectively. As in Section 3, the INARKF(1) model and others are fitted to the data before the dashed line. Because Table 3.6 demonstrates that the INARKF(1) process is the most adequate, we consider the CUSUM statistic with reference value $k = 4$ based on the selected INARKF(1) process with parameters $(\theta_1 = 2.2080, \theta_2 = 0.2537, \alpha = 0.2511)$ and choose a suitable limit value h. For the reference value $k = 4$, the ARL_0 of the CUSUM control chart with limit value $h = 23$ and $h = 34$ are obtained as 100.6 and 205.4, respectively: see Table 3.7. Here, because the number 205.4 is greater than the length of data and is also large enough, we conclude that $h = 34$ is more suitable as a predetermined limit

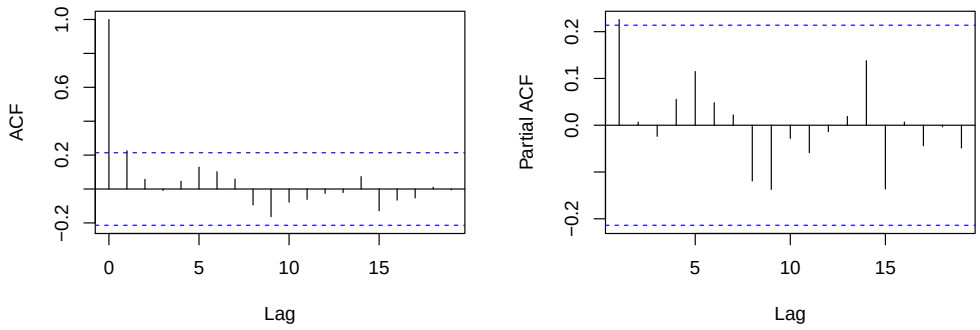

Figure 3.4: The ACF and PACF plot of disorderly conduct data (From 1990 to 1996)

value of the CUSUM control chart with reference value $k = 4$. The plot of CUSUM statistic for disorderly conduct data is given in Figure 3.5, wherein the dashed and dot-dash lines respectively stand for $h = 23$ and $h = 34$. Meanwhile, the $C_{1,t}$ and $C_{2,t}$ respectively stand for the CUSUM statistic with reference value $k = 4$ of the disorderly conduct data from 1990 to 1996 and from 1997 to 2001, respectively. In both cases, the initial state of the CUSUM statistic, $C_{1,0}$ and $C_{2,0}$, is set to be 0. Since the maximum value of the CUSUM statistic $C_{1,t}$ is 19, we conclude that the process is in-control. However, surprisingly, the plot of $C_{2,t}$ has an increasing trend and $C_{2,t} \geq h$ occurs at $t = 44$ (August 2000). In fact, the sample mean of the data from $t = 1$ (January 1997) to $t = 44$ (August 2000) is 4.818 which is grater than that of the past observations. This phenomenon is hard to catch unless the CUSUM control scheme has been applied. We also apply the CUSUM control chart based on a PINAR(1) process (Weiss and Testik, 2009) to this data. From the results in Table 3.6, a PINAR(1) process with parameters ($\lambda = 3.1333$, $\alpha = 0.2151$) is fitted. In this case, the corresponding limit value h for the $\text{ARL}_0 \approx 100, 200$ are given as 21 and 31, respectively, which are less than the corresponding limit values under the assumption

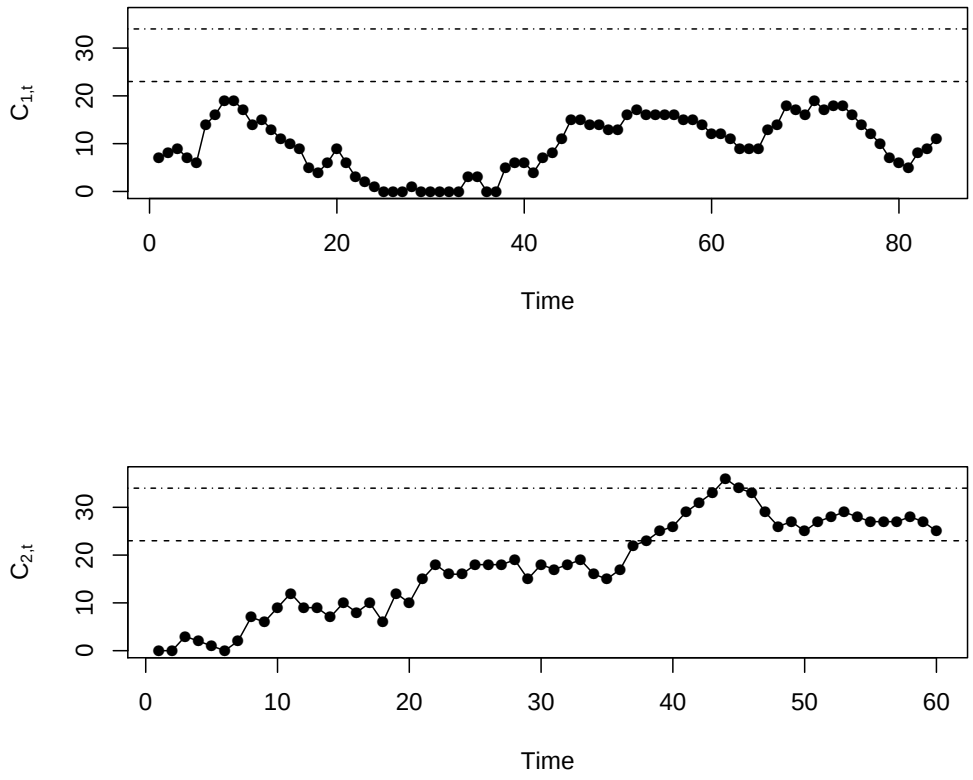

Figure 3.5: The plot of CUSUM statistic for disorderly conduct data

of INARKF(1) process. In this case, unexpected false alarm occurs frequently in its in-control state, which is an undesirable situation to practitioners. This shows that the CUSUM control chart based on INARKF(1) processes outperforms that based on PINAR(1) processes.

3.5 Proofs

Proof of Theorem 3.2.1. We follow the lines of the proof of Proposition 2 of Bourguignon et al. (2015). We first consider the case of $\theta_2 > 0$. It can be easily seen that $\{X_t\}$ is an irreducible and aperiodic Markov chain. Let $P^t(i,j) = P\left(X_t = j | X_0 = i\right)$. Then, either $\{X_t\}$ is positive recurrent or $\lim_{t\to\infty} P^t(i,j) = 0$ owing to Theorem 4.3.3 of Ross (1996). Since $\{X_t\}$ is irreducible, it suffice to show that $\lim_{t\to\infty} P^t(0,0)$ exists and is positive. Note that Katz family distribution is reduced to an NB distribution when $\theta_2 > 0$.

Since X_t has the same distribution as $\alpha^t \circ X_0 + \sum_{j=0}^{t-1} \alpha^j \circ \epsilon_{t-j}$ (Al-Osh and Alzaid (1987)),

$$\begin{aligned}
P^t(x,0) &= P\left(X_t = 0 | X_0 = x\right) \\
&= P\left(\alpha^t \circ X_0 = 0 | X_0 = x\right) P\left(\epsilon_t = 0\right) \prod_{i=1}^{t-1} P\left(\alpha^i \circ \epsilon_{t-i} = 0\right) \\
&= \left(1-\alpha^t\right)^x \left(1-\theta_2\right)^{\theta_1/\theta_2} \prod_{i=1}^{t-1} \left(\frac{1-\theta_2}{1-\theta_2(1-\alpha^i)}\right)^{\theta_1/\theta_2} \\
&= \left(1-\theta_2\right)^{t\theta_1/\theta_2} \left(1-\alpha^t\right)^x \prod_{i=1}^{t-1} \left(1-\theta_2\left(1-\alpha^i\right)\right)^{-\theta_1/\theta_2}.
\end{aligned}$$

We claim that that

$$P^t\left(x,0\right) = \left(1-\theta_2\right)^{t\theta_1/\theta_2} \left(1-\alpha^t\right) \prod_{i=1}^{t-1} \left(1-\theta_2\left(1-\alpha^i\right)\right)^{-\theta_1/\theta_2}.$$

For $t = 1$, we get

$$\begin{aligned} P^1(x,0) &= P(X_1 = 0 | X_0 = x) \\ &= P(\alpha \circ X_0 = 0 | X_0 = x) P(\epsilon_1 = 0) \\ &= (1-\theta_2)^{\theta_1/\theta_2} (1-\alpha)^x \end{aligned}$$

Next, if the above is valid for t, we get

$$\begin{aligned} P^{t+1}(x,0) &= P(X_{t+1} = 0 | X_0 = x) \\ &= \sum_{y=0}^{\infty} (1-\theta_2)^{t\theta_1\theta_2} \left(1-\alpha^t\right)^y \prod_{i=1}^{t-1} \left(1-\theta_2\left(1-\alpha^i\right)\right)^{-\theta_1/\theta_2} \\ &\quad \times \sum_{k=0}^{\min(x,y)} \binom{x}{k} \alpha^k (1-\alpha)^{x-k} \binom{\theta_1/\theta_2 + y - k - 1}{y-k} (1-\theta_2)^{\theta_1/\theta_2} \theta_2^{y-k} \\ &= (1-\theta_2)^{(t+1)\theta_1\theta_2} \prod_{i=1}^{t-1} \left(1-\theta_2\left(1-\alpha^i\right)\right)^{-\theta_1/\theta_2} \\ &\quad \times \sum_{y=0}^{\infty} \sum_{k=0}^{\min(x,y)} \left(1-\alpha^t\right)^y \binom{x}{k} \alpha^k (1-\alpha)^{x-k} \binom{\theta_1/\theta_2 + y - k - 1}{y-k} \theta_2^{y-k}, \end{aligned}$$

which equals

$$
\begin{aligned}
&= (1-\theta_2)^{(t+1)\theta_1\theta_2} \prod_{i=1}^{t-1} \left(1-\theta_2\left(1-\alpha^i\right)\right)^{-\theta_1/\theta_2} \\
&\quad \times \sum_{k=0}^{x} \sum_{y=k}^{\infty} \left(1-\alpha^t\right)^y \binom{x}{k} \alpha^k (1-\alpha)^{x-k} \binom{\theta_1/\theta_2+y-k-1}{y-k} \theta_2^{y-k} \\
&= (1-\theta_2)^{(t+1)\theta_1\theta_2} \prod_{i=1}^{t-1} \left(1-\theta_2\left(1-\alpha^i\right)\right)^{-\theta_1/\theta_2} \\
&\quad \times \sum_{k=0}^{x} \left(1-\alpha^t\right)^k \binom{x}{k} \alpha^k (1-\alpha)^{x-k} \sum_{y=k}^{\infty} \left(\theta_2\left(1-\alpha^t\right)\right)^{y-k} \binom{\theta_1/\theta_2+y-k-1}{y-k}, \\
&= (1-\theta_2)^{(t+1)\theta_1\theta_2} \prod_{i=1}^{t-1} \left(1-\theta_2\left(1-\alpha^i\right)\right)^{-\theta_1/\theta_2} \\
&\quad \times \sum_{k=0}^{x} \left(1-\alpha^t\right)^k \binom{x}{k} \alpha^k (1-\alpha)^{x-k} \sum_{z=0}^{\infty} \left(\theta_2\left(1-\alpha^t\right)\right)^{z} \binom{\theta_1/\theta_2+z-1}{z}.
\end{aligned}
$$

Then, owing to Newton's generalized binomial theorem, we can have

$$
\begin{aligned}
&P^{t+1}(x,0) \\
&= (1-\theta_2)^{(t+1)\theta_1\theta_2} \prod_{i=1}^{t} \left(1-\theta_2\left(1-\alpha^i\right)\right)^{-\theta_1/\theta_2} \sum_{k=0}^{x} \left(1-\alpha^t\right)^k \binom{x}{k} \alpha^k (1-\alpha)^{x-k} \\
&= (1-\theta_2)^{(t+1)\theta_1\theta_2} \prod_{i=1}^{t} \left(1-\theta_2\left(1-\alpha^i\right)\right)^{-\theta_1/\theta_2} \sum_{k=0}^{x} \left(\frac{1-\alpha^t}{1-\alpha}\right)^k \binom{x}{k} \alpha^k (1-\alpha)^{x} \\
&= (1-\theta_2)^{(t+1)\theta_1\theta_2} (1-\alpha)^x \prod_{i=1}^{t} \left(1-\theta_2\left(1-\alpha^i\right)\right)^{-\theta_1/\theta_2} \sum_{k=0}^{x} \binom{x}{k} \left(\alpha+\alpha^2+\cdots+\alpha^t\right)^k \\
&= (1-\theta_2)^{(t+1)\theta_1\theta_2} (1-\alpha)^x \left(1+\alpha+\alpha^2+\cdots+\alpha^t\right)^x \prod_{i=1}^{t} \left(1-\theta_2\left(1-\alpha^i\right)\right)^{-\theta_1/\theta_2} \\
&= (1-\theta_2)^{(t+1)\theta_1/\theta_2} \left(1-\alpha^{t+1}\right)^x \prod_{i=1}^{t} \left(1-\theta_2\left(1-\alpha^i\right)\right)^{-\theta_1/\theta_2},
\end{aligned}
$$

and therefore,

$$\begin{aligned}
&P^{t+1}(0,0) \\
&= \sum_{x=0}^{\infty} P^1(0,x)\, P^t(x,0) \\
&= (1-\theta_2)^{(t+1)\theta_1/\theta_2} \left(1-\theta_2(1-\alpha^t)\right)^{-\theta_1/\theta_2} \prod_{i=1}^{t-1} \left(1-\theta_2(1-\alpha^i)\right)^{-\theta_1/\theta_2} \\
&= (1-\theta_2)^{\theta_1/\theta_2} \prod_{i=1}^{t} \left(\frac{1-\theta_2}{1-\theta_2\left(1-\alpha^i\right)}\right)^{\theta_1/\theta_2}.
\end{aligned}$$

This validates our conjecture.

Note that

$$\log P^t(0,0) = \frac{\theta_1}{\theta_2}\log(1-\theta_2) + \frac{\theta_1}{\theta_2}\sum_{i=1}^{t-1}\left[\log(1-\theta_2) - \log\left(1-\theta_2\left(1-\alpha^i\right)\right)\right],$$

and set $f(\theta) = \log(1-\theta)$. Then, by the mean value theorem, we can write $f(\theta_2) - f\left(\theta_2\left(1-\alpha^i\right)\right) = f'(\theta_i)\alpha^i\theta_2$ for some $\theta_i \in \left(\min\left(\theta_2, \theta_2\left(1-\alpha^i\right)\right), \max\left(\theta_2, \theta_2\left(1-\alpha^i\right)\right)\right)$, so that

$$\log P^t(0,0) = \frac{\theta_1}{\theta_2} f(\theta_2) + \theta_1 \sum_{i=1}^{t-1} f'(\theta_i)\alpha^i.$$

Since $|f'|$ has a finite maximum $M(\theta)$ on $[\min\left(\theta_2, \theta_2\left(1-\alpha^i\right)\right), \max\left(\theta_2, \theta_2\left(1-\alpha^i\right)\right)]$, we see $\sum_{i=1}^{\infty} |f'(\theta_i)\alpha^i| \le M(\theta)\sum_{i=1}^{\infty}\alpha^i < \infty$, which implies that $\lim_{t\to\infty}\log P^{t+1}(0,0)$ exists and is finite, so that $\lim_{t\to\infty} P^t(0,0) > 0$.

Since the case of $\theta_2 < 0$ can be similarly handled and the case of $\theta_2 = 0$ is reduced to the Poisson distribution case, the theorem is validated. □

Proof of Theorem 3.2.3. Since the proof for the case of $\theta_2 = 0$ is manifest owing to Alzaid and Al-Osh (1988), we only provide the proof for the case of $\theta_2 \neq 0$. Note that X_t has the same distribution as $\sum_{i=0}^{\infty} \alpha^i \circ \epsilon_{t-i}$, where ϵ_t are i.i.d. $KF(\theta_1, \theta_2)$ random variables with the probability generating function (PGF):

$$G_\epsilon(z) = (1-\theta_2)^{\theta_1/\theta_2} (1-\theta_2 z)^{-\theta_1/\theta_2}.$$

Then, the PGF of X_t is given by

$$G_X(z) = \prod_{i=0}^{\infty} \left[(1-\theta_2)^{\theta_1/\theta_2} \left(1-\theta_2+\alpha^i\theta_2(1-z)\right)^{-\theta_1/\theta_2} \right], \tag{3.5.6}$$

which implies that X_t has the same distribution as $Y_0 + \sum_{i=1}^{\infty} Y_i$, where Y_i are independent random variables with PGF:

$$G_{Y_i}(z) = \left[(1-\theta_2)^{\theta_1/\theta_2} \left(1-\theta_2+\alpha^i\theta_2(1-z)\right)^{-\theta_1/\theta_2} \right].$$

Since Y_0 has the same distribution as ϵ_t and $\alpha \circ X_{t-1}$ has the same distribution as $\sum_{i=1}^{\infty} Y_i$, owing to (3.5.6), the PGF of $\alpha \circ X_{t-1}$ is obtained as

$$\begin{aligned} G_X(\alpha z + 1 - \alpha) &= \prod_{i=0}^{\infty} \left[(1-\theta_2)^{\theta_1/\theta_2} \left(1-\theta_2+\alpha^{i+1}\theta_2(1-z)\right)^{-\theta_1/\theta_2} \right] \\ &= \prod_{i=1}^{\infty} G_{Y_i}(z). \end{aligned}$$

This asserts the theorem. □

3.6 Concluding remarks

In this chapter, we considered the INAR(1) process with the Katz family innovations and investigated its probabilistic properties such as the ergodicity and stationarity. A numerical experiment is conducted to examine the performance of the (conditional) MLE and a real example is provided to demonstrate the validity of the INARKF(1) process. Further, the INARKF(1) process is applied to a SPC problem and the CUSUM control chart is considered to detect a small mean increase of autocorrelated count processes. All the obtained results confirmed the validity of the INARKF(1) process. In practice, the Katz distribution family has merit to overcome the weakness that the conventional Poisson INAR(1) process has, that is, the equi-dispersion. Because the INARKF(1) process inherits great flexibility of the Katz family, it has a high potential to extend to diverse applications. Concerning the SPC, it would be worth study to compare the CUSUM control chart with other charts such as the residual-based CUSUM chart and the exponential weighted moving average (EWMA) chart.

Chapter 4

Improved CUSUM monitoring of Markov counting process with frequent zeros

4.1 Introduction

Control chart originally introduced by Shewhart (1924) has become one of the most commonly used tools of statistical process control (SPC) for process monitoring. When the quality characteristics of considered processes are hard to express numerically, each inspected unit is classified as either conforming or nonconforming in compliance with its specification. Zero-inflated Poisson (ZIP) distributions are frequently used for modeling near-zero defect processes. Xie and Goh (1993) considered a control scheme based on ZIP distributions for monitoring zero-inflated processes subject to random shocks, and He et al. (2012) proposed log-likelihood ratios-based cumulative sum (CUSUM)-type charts. Meanwhile, He et al. (2014)

considered a combination of the CUSUM charts based on zero-truncated Poisson CUSUM (ZTP-CUSUM) and 'conforming run length' (CRL)-based CUSUM (CRL-CUSUM) charts. It is well known that in monitoring process with zero-inflation, the CRL-type control chart is more effective than other existing control schemes, see Goh (1987); Wu et al. (2000); Wu et al. (2001); Ohta et al. (2001). However, the CRL-type chart for monitoring Markov counting processes is not yet fully developed in the literature.

Due to the automation and advancement of quality in production process, serially correlated processes have become increasingly common in the modern manufacturing industry, and monitoring on those processes has received considerable attention from many researchers. For example, we can refer to Weiß (2007) who study various control charts in first-order integer-valued autoregressive (INAR(1)) models, Weiss and Testik (2009) who apply upper one-sided CUSUM charts for Poisson INAR(1) (PINAR(1)) models, Li et al. (2016) who consider control charts for geometric INAR(1) (NGINAR(1)) models, and Kim and Lee (2017) who propose the INAR(1) models with Katz family innovations (INARKF(1)) for modeling serially dependent processes exhibiting under-, equi- and over-dispersion in a unified manner and apply the CUSUM charts to monitoring mean increase. Rakitzis et al. (2017) recently considered the Shewhart-type and CUSUM charts based on zero-inflated Poisson INAR(1) (ZIPINAR(1)) models and first-order zero-inflated Poisson autoregressive conditional heteroskedasticity (ZIPINARCH(1)) models for monitoring processes with serial dependence and zero-inflation.

This study aims to improve the capability of monitoring Markov counting processes with zero-inflation based on ZIPINAR(1) and ZIPINARCH(1) models. To this end, we consider three types of control charts, that is, a new CUSUM-type

chart with delay rule (CUSUM-DR), which is a generalization of the ZTP-CUSUM chart considered by He et al. (2014), and CRL-CUSUM and combined Shewhart CRL-CUSUM charts.

This paper is organized as follows. Section 4.2 briefly reviews ZIPINAR(1) and ZIPINARCH(1) models with their statistical properties and investigates some Markov chain properties required for statistical design and performance evaluation. Section 4.3 describes the control schemes considered in this study. Section 4.4 conducts numerical experiments and Section 4.5 provides a real data example to showcase the proposed charts. Concluding remarks are given in Section 4.6. Finally, a Markov chain method for calculating the ARL of the CUSUM-DR chart is described in Appendix.

4.2 Modeling zero-inflated Markov counting process

In this section, we introduce ZIPINAR(1) and ZIPINARCH(1) models and state some probabilistic properties and estimating method. We also investigate a commonly used approximation method used for the statistical design and performance evaluation of control charts.

4.2.1 Zero-inflated Poisson INAR(1) model

Since Al-Osh and Alzaid (1987) introduced the INAR(1) model with the binomial thinning operator (Steutel and van Harn, 1979), it has become a popular process for modeling count data with serial dependence. The binomial thinning operator '$\circ$'

designated by Steutel and van Harn (1979) is defined as

$$\alpha \circ X = \sum_{i=1}^{X} B_i(\alpha), \tag{4.2.1}$$

where X is a non-negative integer-valued random variable and $B_i(\alpha)$'s are independent and identically distributed (i.i.d.) Bernoulli random variables with success probability $\alpha \in [0,1]$, independent of X. A process $\{X_t\}_{t\in\mathbf{N_0}}$ is said to follow an INAR(1) model if

$$X_t = \alpha \circ X_{t-1} + \epsilon_t, \qquad t \in \mathbf{N}, \tag{4.2.2}$$

where $\alpha \in [0,1)$, '$\circ$' is the binomial operator in (4.2.1) and ϵ_t's are i.i.d. random variables, defined on non-negative integer values, with a finite second moment, independent of X_{t-s} for $s \in \mathbf{N}$. The INAR(1) process in (4.2.2) is a homogeneous Markov chain and strictly stationary.

INAR(1) models have been extensively studied by many authors, see Scotto et al. (2015) for a review. Among these, Jazi et al. (2012a) considered the zero-inflated Poisson INAR(1) (ZIPINAR(1)) model with parameter $(\alpha, \lambda, \rho)^\top$ and innovations ϵ_t, which are zero-inflated Poisson distributed with rate parameter $\lambda > 0$ and zero-inflation parameter $\rho \in [0,1)$ as below:

$$\begin{aligned} P(\epsilon_t = l) &= \begin{cases} 0 & \text{with probability } \rho \\ \frac{\lambda^l \mathrm{e}^{-\lambda}}{l!} & \text{with probability } 1-\rho \end{cases} \\ &= \mathbb{1}(l=0)\rho + (1-\rho)\frac{\lambda^l \mathrm{e}^{-\lambda}}{l!}, \qquad l \in \mathbf{N_0}, \end{aligned}$$

where $\mathbb{1}(\cdot)$ is the indicator function. It is easy to check that the ZIPINAR(1) model

reduces to a PINAR(1) model when $\rho = 0$. The mean and variance of innovations are obtained as $\mathbb{E}(\epsilon_t) = \lambda(1-\rho)$ and $\mathrm{Var}(\epsilon_t) = \lambda(1-\rho)(1+\rho\lambda)$, respectively.

Transition probabilities $p_{ij} \equiv P(X_{t+1} = j | X_t = i)$ of the ZIPINAR(1) model are given as

$$p_{ij} = \sum_{k=0}^{\min(i,j)} \binom{i}{k} \alpha^k (1-\alpha)^{i-k} \left(\mathbb{1}(j-k=0)\rho + (1-\rho)\frac{\lambda^{j-k}\mathrm{e}^{-\lambda}}{(j-k)!} \right), \qquad i, j \in \mathbf{N_0}.$$

Further, marginal probabilities $p_j \equiv P(X_t = j)$ are given as

$$p_j = \sum_{i=0}^{\infty} \sum_{k=0}^{\min(i,j)} \binom{i}{k} \alpha^k (1-\alpha)^{i-k} \left(\mathbb{1}(j-k=0)\rho + (1-\rho)\frac{\lambda^{j-k}\mathrm{e}^{-\lambda}}{(j-k)!} \right) p_i, \qquad j \in \mathbf{N_0}, \tag{4.2.3}$$

which is importantly used when evaluating the performance of control charts. Because the infinite sum representation in Equation (4.2.3) is not analytically tractable, we take the Markov chain-based approximation approach as in Subsection 4.2.3. to numerically calculate the marginal probabilities of ZIPINAR(1) models.

The 1-ahead conditional mean $\mathbb{E}(X_{t+1}|X_t)$ and variance $\mathrm{Var}(X_{t+1}|X_t)$ are given as

$$\mathbb{E}(X_{t+1}|X_t) = \alpha X_t + \lambda(1-\rho), \quad \mathrm{Var}(X_{t+1}|X_t) = \alpha(1-\alpha)X_t + \lambda(1-\rho)(1+\rho\lambda).$$

Based on these, marginal mean $\mu \equiv \mathbb{E}(X_t)$, variance $\sigma^2 \equiv \mathrm{Var}(X_t)$ and ratio of variance-to-expectation are calculated as

$$\mu = \frac{\lambda(1-\rho)}{1-\alpha}, \quad \sigma^2 = \frac{\lambda(1-\rho)(1+\alpha+\rho\lambda)}{1-\alpha^2}, \quad \sigma^2/\mu = 1 + \frac{\rho\lambda}{1+\alpha}. \tag{4.2.4}$$

This particularly shows that the ZIPINAR(1) model is a suitable candidate for modeling autocorrelated counting processes with over-dispersion.

The autocovariance and autocorrelation functions are given by

$$\mathrm{Cov}(X_{t+h}, X_t) = \alpha^h \sigma^2, \quad \mathrm{Corr}(X_{t+h}, X_t) = \alpha^h, \quad h \in \mathbf{N_0}. \tag{4.2.5}$$

which coincide with those of conventional AR(1) models. More details regarding ZIPINAR(1) models, such as k-ahead conditional expectation and discrete self decomposability, can be found in Jazi et al. (2012a).

4.2.2 Zero-inflated Poisson INARCH(1) model

Here we consider another Markov counting process with frequent zeros. A process $\{X_t\}_{t\in\mathbf{N_0}}$ is said to follow a ZIPINARCH(1) model with parameter $(\alpha, \omega, \rho)^\top$ when X_{t+1}, conditioned on $X_t, X_{t-1}, \ldots$, is zero-inflated Poisson distributed according to $Poi(\omega + \alpha X_t)$, where $\alpha \in [0, 1)$ and $\omega > 0$ and $\rho \in [0, 1)$. Transition probabilities $p_{ij} = P(X_{t+1} = j | X_t = i)$ are given as

$$p_{ij} = \mathbb{1}(j = 0)\rho + (1 - \rho)\frac{(\omega + \alpha i)^j \mathrm{e}^{-(\omega+\alpha i)}}{j!}, \qquad i, j \in \mathbf{N_0},$$

where ω, α and ρ are ARCH parameters and zero-inflation parameter, respectively. If $\rho = 0$, the ZIPINARCH(1) model reduces to a PINARCH(1) model, see Ferland et al. (2006); Weiß (2010). Lee et al. (2016) showed that $\{X_t\}_{t\in\mathbf{N_0}}$ forms a stationary process.

As with ZIPINAR(1) models, marginal probabilities can be obtained approximately based on the Markov chain approach as in Subsection 4.2.3. The 1-ahead

conditional mean $\mathbb{E}(X_{t+1}|X_t)$ and variance $\mathrm{Var}(X_{t+1}|X_t)$ are

$$\mathbb{E}(X_{t+1}|X_t) = (1-\rho)(\omega + \alpha X_t), \quad \mathrm{Var}(X_{t+1}|X_t) = (1-\rho)(\omega + \alpha X_t)(1 + \rho\omega + \rho\alpha X_t).$$

Based on these, marginal mean $\mu = \mathbb{E}(X_t)$, variance $\sigma^2 = \mathrm{Var}(X_t)$ and ratio of variance-to-expectation are obtained as

$$\mu = \frac{(1-\rho)\omega}{1-(1-\rho)\alpha}, \quad \sigma^2 = \frac{(1-\rho)\omega(1+\rho\omega-(1-\rho)\alpha)}{(1-(1-\rho)\alpha^2)(1-(1-\rho)\alpha)^2}, \quad \sigma^2/\mu = \frac{1-\alpha(1-\rho)+\rho\omega}{(1-\alpha(1-\rho))(1-\alpha^2(1-\rho))}. \tag{4.2.6}$$

It is easy to check $\sigma^2/\mu > 1$, indicating that the ZIPINARCH(1) model is suitable for modeling over-dispersed Markov counting processes. The autocovariance and autocorrelation functions are given as

$$\mathrm{Cov}(X_{t+h}, X_t) = ((1-\rho)\alpha)^h \sigma^2, \quad \mathrm{Corr}(X_{t+h}, X_t) = ((1-\rho)\alpha)^h, \quad h \in \mathbf{N_0}. \tag{4.2.7}$$

For more details regarding ZIPINARCH models, see Lee et al. (2016), Zhu (2012) and Huh et al. (2017).

4.2.3 Some commonly required properties

In this subsection, we investigate some properties required for the statistical design and performance evaluation of our proposed control schemes when the given process is either ZIPINAR(1) or ZIPINARCH(1). For a reference regarding more general Markov processes, we refer to Meyn and Tweedie (2012).

Let $\{X_t\}_{t\in\mathbf{N_0}}$ be either a stationary ZIPINAR(1) or ZIPINARCH(1) process. Then, marginal probabilities $p_j = P(X_t = j)$ can be approximately calculated with

a large $M \in \mathbf{N}$ as the solution of equation:

$$\mathbf{P}^*\mathbf{p} = \mathbf{p}, \tag{4.2.8}$$

where

$$\mathbf{P}^* = \text{diag}\left(\frac{1}{\sum_{j=0}^{M} p_{0j}}, \ldots, \frac{1}{\sum_{j=0}^{M} p_{Mj}}\right)\mathbf{P},\ \mathbf{P} = \begin{pmatrix} p_{00} & p_{01} & \cdots & p_{0M} \\ p_{10} & p_{11} & \cdots & p_{1M} \\ \vdots & \vdots & \ddots & \vdots \\ p_{M0} & p_{M1} & \cdots & p_{MM} \end{pmatrix} \text{ and } \mathbf{p} = \begin{pmatrix} p_0 \\ p_1 \\ \vdots \\ p_M \end{pmatrix}.$$

This numerical approximation method in Equation (4.2.8) is useful when an analytic form of the stationary marginal distribution is hard to attain. Because $\{n \in \mathbf{N_0} : p_n > 0\}$ has infinitely many elements, we use the approximation in Equation (4.2.8) with $M = \lfloor \mu + 20\sigma \rfloor + 1$. This method can also be used to calculate the approximate truncated expectation as follows:

$$\mu_r^* \equiv \mathbb{E}(X_t | X_t \geq r) = \frac{\mu - \sum_{j=0}^{r-1} j p_j}{1 - P(X < r)}, \qquad r \in \mathbf{N}, \tag{4.2.9}$$

which is importantly used in the design of CUSUM-DR charts introduced in Section 4.3.

Consider

$$T = \min\{t \in \mathbf{N} : X_t \geq 1\}, \tag{4.2.10}$$

where T stands for the first-hitting time to touch or across 1. We can easily check

that the distributions of T and $T|X_0 = l$ for $l \in \mathbf{N_0}$ are given as

$$P(T = n) = \begin{cases} 1 - p_0 & \text{if } n = 1 \\ p_0(1 - p_{00})p_{00}^{n-2} & \text{if } n \geq 2, \end{cases} \tag{4.2.11}$$

$$P(T = n|X_0 = l) = \begin{cases} 1 - p_{l0} & \text{if } n = 1 \\ p_{l0}(1 - p_{00})p_{00}^{n-2} & \text{if } n \geq 2. \end{cases} \tag{4.2.12}$$

Then, using the fact that $\mathbb{E}(T) = \sum_{n=0}^{\infty} P(T > n)$ and $\mathbb{E}(T|X_0 = l) = \sum_{n=0}^{\infty} P(T > n|X_0 = l)$, we obtain

$$\mathbb{E}(T) = 1 + \frac{p_0}{1 - p_{00}}, \tag{4.2.13}$$

$$\mathbb{E}(T|X_0 = l) = 1 + \frac{p_{l0}}{1 - p_{00}}, \tag{4.2.14}$$

$$\mathbb{E}(T|X_0 \geq 1) = \frac{1}{1 - p_0} \tag{4.2.15}$$

for $l \in \mathbf{N_0}$. These play an important role in the statistical design and performance evaluation of CRL-CUSUM and combined Shewhart CRL-CUSUM charts considered in Section 4.3.

In what follows, θ denotes the model parameter of $\{X_t\}_{t\in\mathbf{N}}$. For ZIPINAR(1) models, $\theta = (\alpha, \lambda, \rho)^\top$, and for ZIPINARCH(1) models, $\theta = (\alpha, \omega, \rho)^\top$. The θ can be estimated numerically using the maximum likelihood (ML) method. Given observations $x_1, x_2, \ldots, x_n$ generated from $\{X_t\}_{t\in\mathbf{N}}$, the log-likelihood function is given as

$$l(\theta|x_1, x_2, \ldots, x_n) = p_{x_1} + \sum_{i=1}^{n-1} \log p_{x_i x_{i+1}}. \tag{4.2.16}$$

The ML estimator $\hat{\theta}$ of θ is obtained as the value that maximizes the log-likelihood function in Equation (4.2.16). In actual calculation, we use the R programming language (R Core Team, 2017). One can also get a conditional ML estimator conditioning on the first observation x_1.

4.3 Control chart for zero-inflated Markov counting process

In this section, we consider several control schemes for monitoring mean increase, namely, a change from $\mu = \mu_0$ to $\mu = \mu_0 + \delta$ with $\delta > 0$. The detection of mean increase has been of great importance in practice because this case is mainly related to process deterioration such as aggravation of production quality due to machine wear. We only consider the case that design parameters are positive integers, since this is common in monitoring Markov counting processes, see Weiss and Testik (2009), Kim and Lee (2017), Rakitzis et al. (2017) and Yontay et al. (2013).

In practice, the upper one-sided Shewhart-type chart (Shewhart, 1924) is the most natural for monitoring mean increase because it is easy to implement and can quickly detect an abnormal change. However, it is well known that in general, the Shewhart-type chart has low detection sensitivity to relatively small shifts.

Scheme 1. Upper one-sided Shewhart-type chart (Shewhart(u))
Given design parameter $u \in \mathbf{N}$ (upper control limit), observations $\{X_t\}_{t\in\mathbf{N}}$ are plotted on the Shewhart-type chart with the in-control (IC) region $[0, u)$. The process is regarded out-of-control (OoC) when $X_t \geq u$ occurs.

Due to its sensitivity to small to moderate shifts, the CUSUM control chart proposed by Page (1954) has received considerable attention from many authors,

see He et al. (2012); Weiss and Testik (2009); Kim and Lee (2017); Rakitzis et al. (2017); Yontay et al. (2013); Lucas (1985); Reynolds et al. (1990); Chao-Wen and Reynolds Jr (2001); Rakitzis et al. (2016). A conventional upper one-sided CUSUM statistic is expressed as follows:

$$\begin{aligned} C_0 &= c_0, \\ C_t &= \max(C_{t-1} + X_t - k, 0), \qquad t \in \mathbf{N}, \end{aligned}$$

where reference value $k \in \mathbf{N}$ is selected based on μ. The k affects the detection sensitivity of CUSUM charts and also has a role to prevent CUSUM statistics from being absorbed into OoC region. To properly choose this value, we adopt an empirical rule provided by Weiss and Testik (2009), namely, $k = \lfloor \mu \rfloor + 1$ or $\lfloor \mu \rfloor + 2$. The initial value c_0 is set to 0, which is common in the design of CUSUM charts, see Weiss and Testik (2009), Kim and Lee (2017), Yontay et al. (2013) and Lucas (1985).

Scheme 2. CUSUM chart (CUSUM(k,h))
Given reference value $k \in \mathbf{N}$ and control limit $h \in \mathbf{N}$, statistics $\{C_t\}_{t \in \mathbf{N}}$ are plotted on the CUSUM chart with IC region $[0, h)$. An OoC signal is triggered if $C_t \geq h$.

In general, the CUSUM chart outperforms the Shewhart-type chart when monitoring small to moderate shifts. However, Rakitzis et al. (2017) found that when monitoring autocorrelated counting processes with excessive zeros, the CUSUM chart does not perform well and is less sensitive to small to moderate shifts than the Shewhart-type chart.

To handle zero-inflated Poisson counts with serial independence, He et al. (2014) considered zero-truncated CUSUM charts. Here, we consider a modified CUSUM chart with delay rule (CUSUM-DR), which is a generalization of the zero-truncated

CUSUM chart:

$$\begin{aligned} C_0^d &= c_0^d, \\ C_t^d &= \mathbb{1}(X_t \geq r)\max(C_{t-1}^d + X_t - k^d, 0) + \mathbb{1}(X_t < r)C_{t-1}^d, \end{aligned} \tag{4.3.17}$$

where $c_0^d \in \mathbf{N_0}$, $r \in \mathbf{N}$, and reference value $k^d \in \mathbf{N}$ is chosen based on the truncated expectation μ_r^* in Equation (4.2.9), that is, $k^d = \lfloor \mu_r^* \rfloor + 1$ or $\lfloor \mu_r^* \rfloor + 2$. We call r 'delay rule parameter'. The initial value c_0^d is set to 0 in performance evaluation.

Scheme 3. CUSUM-DR chart (CUSUM-DR(r,k^d,h^d))
Given delay rule parameter $r \in \mathbf{N}$, reference value $k^d \in \mathbf{N}$, and control limit $h^d \in \mathbf{N}$, CUSUM-DR statistics $\{C_t^d\}_{t\in\mathbf{N}}$ are plotted with IC region $[0, h^d)$. The CUSUM-DR chart triggers an OoC signal if $C_t^d \geq h^d$.

The CUSUM-DR chart is basically designed to selectively update CUSUM statistics and to avoid a bad influence of relatively lower values on the CUSUM chart. When $r = 1$, the CUSUM-DR chart coincides with the zero-truncated CUSUM chart (He et al., 2014). Because a too large delay rule parameter r gives rise to a relative low update frequency of CUSUM-DR charts and worsens overall chart performance, r should be carefully determined. Since our numerical experiments indicate a poor performance of CUSUM-DR charts with $r > \lceil \mu \rceil + 1$, r is selected within range $r \leq \lceil \mu \rceil + 1$.

In addition to the aforementioned schemes, we consider a CUSUM-type chart based on CRL values. A random variable CRL_i, $i \in \mathbf{N}$, is defined as the number of observation between the $(i-1)$th and ith nonconforming observations, inclusive of the nonconforming observation at the end, see Wu et al. (2000). Consider a Bernoulli process $\{B_t\}_{t\in\mathbf{N}}$ defined as $B_t = \mathbb{1}(X_t \geq 1)$, where $(B_t = 1)$ means that

we observe nonconforming observation at time t. CRL_i values can be obtained by taking a transformation of $\{B_t\}$. For instance, suppose that we have observations $\{0,0,3,0,5,2,0,0,0,1\}$. Then, the corresponding Bernoulli process values are given as $\{0,0,1,0,1,1,0,0,0,1\}$ and CRL values are obtained as $\{3,2,1,4\}$. It is easy to see that

$$\mathbb{E}(\mathrm{CRL}_1) = \mathbb{E}(T) = 1 + \frac{p_0}{1-p_{00}}, \tag{4.3.18}$$

$$\mathbb{E}(\mathrm{CRL}_i) = \mathbb{E}(T|X_0 \geq 1) = \frac{1}{1-p_0}, \quad i \in \mathbf{N}\backslash\{1\}, \tag{4.3.19}$$

where $\mathbb{E}(T)$ and $\mathbb{E}(T|X_0 \geq 1)$ are the ones in Equations (4.2.13) and (4.2.15), respectively. This fact is importantly used in the statistical design of CRL-CUSUM charts. It is obvious that the mean increase, induced by a decrease in zero-proportion, leads to a decrease in the mean of CRL values. For this reason, we naturally consider the lower-sided CRL-CUSUM chart whose control statistic based on the CRL values is given as follows:

$$\begin{aligned} C_0^c &= c_0^c, \\ C_i^c &= \max(C_{i-1}^c + k^c - \mathrm{CRL}_i, 0), \end{aligned} \tag{4.3.20}$$

where $i \in \mathbf{N}$, $c_0^c \in \mathbf{N_0}$, set to 0, and reference value $k^c \in \mathbf{N}\backslash\{1\}$ is chosen from $\mathbb{E}(\mathrm{CRL}_2)$ in Equation (4.3.19), namely, $k^c = \lceil \mathbb{E}(\mathrm{CRL}_2) \rceil - 1$ or $\lceil \mathbb{E}(\mathrm{CRL}_2) \rceil - 2$ as in the conventional lower one-sided CUSUM chart (Yontay et al., 2013). Notice that since $\mathrm{CRL}_i \geq 1$, the CRL-CUSUM chart can be applied only to the case of $\mathbb{E}(\mathrm{CRL}_2) > 2$, or equivalently, $p_0 > \frac{1}{2}$, which is not a stringent condition in high-quality processes with zero-inflation.

Scheme 4. CRL-CUSUM chart (CRL-CUSUM(k^c,h^c))
Given reference value $k^c \in \mathbf{N}\backslash\{\mathbf{1}\}$ and control limit $h^c \in \mathbf{N}$, $\{C_i^c\}_{t\in\mathbf{N}}$ values are plotted on the CRL-CUSUM chart with IC region $[0, h^c)$. An OoC signal is triggered if $C_i^c \geq h^c$.

Because the CRL-CUSUM chart does not perform well when zero proportion is nearly constant, we consider its combination with a Shewhart chart.

Scheme 5. Combined Shewhart CRL-CUSUM chart (S CRL-CUSUM(u,k^c,h^c))
Given upper control limit $u \in \mathbf{N}$ in the Shewhart-type chart, reference value $k^c \in \mathbf{N}\backslash\{\mathbf{1}\}$, and control limit $h^c \in \mathbf{N}$ of the CRL-CUSUM chart, observations $\{X_t\}_{t\in\mathbf{N}}$ are plotted on the Shewhart chart with IC region $[0, u)$. Moreover, CRL-CUSUM statistics $\{C_i^c\}_{t\in\mathbf{N}}$ are plotted on the CRL-CUSUM chart with IC region $[0, h^c)$. An OoC signal is triggered if either $X_t \geq u$ or $C_i^c \geq h^c$.

A common measure for evaluating the detection effectiveness of control charts is the average time to signal (ATS). The ATS is defined as the average amount of time from the start of process monitoring until a signal is alarmed by control chart. When the process is IC, the corresponding ATS is denoted as ATS_0, which is interpreted as the average time until a false alarm occurs. Meanwhile, when the process is OoC, ATS_1 denotes the corresponding ATS value. When the process of interest is IC, the larger the ATS_0 is, the less frequently the false alarms occurs, whereas the smaller the ATS_1 is, the more effectively the detection of change can be made. For fair comparison, the values of ATS_0 of considered charts should be set to a predetermined value. Because of the discrete nature of design parameters, ATS_0 values cannot be exactly the same as the predetermined value, and they are only made as close as possible in our numerical experiments.

The ATS value in Shewhart-type, CUSUM, and CUSUM-DR charts coincides

with the average run length (ARL), defined as the average number of points plotted on a chart until an OoC signal occurs. To evaluate the ATS performance of control charts, we take the Markov chain approach proposed by Brook and Evans (1972). In Appendix 4.7 and 4.8, we provide a Markov chain method for computing the ARL values of CUSUM-DR and the ATS values of CRL-CUSUM charts. For a reference as to the Shewhart-type and CUSUM charts, we refer to Weiss and Testik (2009); Weiß and Testik (2012).

Figure 4.1 illustrates a path example of control statistics with mean increase in Phase II for the ZIPINAR(1) model. The path is obtained from Phase I data ($t = 1, 2, \ldots, 100$) generated from the ZIPINAR(1) model with $\lambda = 4.2$, $\alpha = 0.3$ and $\rho = 0.8$, wherein the corresponding μ, μ_1^* and $\mathbb{E}(\mathrm{CRL}_2)$ are calculated as 1.2, 3.198, 2.665, respectively. Meanwhile, the parameters of Phase II process ($t = 101, 102, \ldots, 120$) are set to $\lambda = 4.8$, $\alpha = 0.4$ and $\rho = 0.7$, wherein the corresponding μ, μ_1^* and $\mathbb{E}(\mathrm{CRL}_2)$ are obtained as 2.4, 3.874 and 1.614, respectively. We consider the CUSUM-type control charts such as the conventional CUSUM chart with $k = 2$, the CUSUM-DR chart with $r = 1$, $k^d = 4$, and the CRL-CUSUM chart with $k^c = 2$. Notice that in Figure 4.1(d), $\{t_i\}_{i\in\mathbf{N}}$ denotes a subsequence of $\{t\}_{t\in\mathbf{N}}$ such that $C_{t_i}^c = C_i^c$. The result shows that the CUSUM-type control chart sensitively reacts to an abnormal change. The performance of aforementioned control charts is compared in Section 4.4.

4.4 Performance evaluation

We evaluate the chart performance in terms of ATS value for stationary ZIPINAR(1) and ZIPINARCH(1) models. As mentioned earlier, we focus on monitoring mean

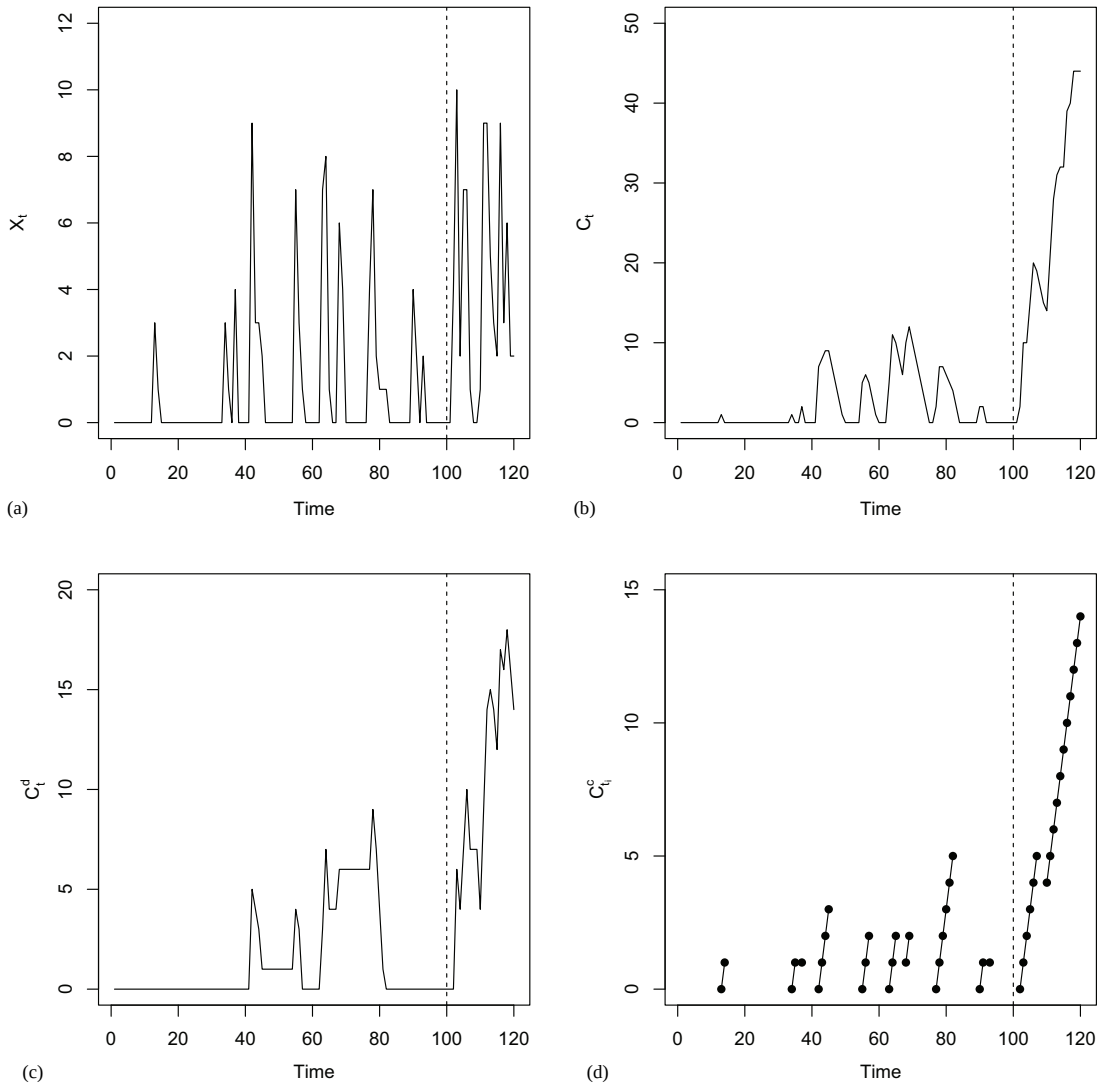

Figure 4.1: An example of control statistics: (a) sample path; (b) CUSUM statistic with $k = 2$; (c) CUSUM-DR statistic with $r = 1$ and $k^d = 4$; (d) CRL-CUSUM statistic with $k^c = 2$

increase, that is, a shift from IC mean $\mu = \mu_0$ to OoC mean $\mu = \mu_0 + \delta$, $\delta > 0$. For this, we introduce $(\gamma, \mu, \rho)^\top$, where $\gamma = \text{Corr}(X_{t+1}, X_t)$ and μ and ρ are marginal mean and zero-inflation parameter.

Consider the ZIPINAR(1) model with parameter $\theta = (\alpha, \lambda, \rho)^\top$. Given IC parameters $(\gamma, \mu, \rho)^\top = (\alpha, \lambda/(1-\alpha), \rho)^\top = (\gamma_0, \mu_0, \rho_0)^\top$, we consider the following three OoC scenarios:

- Mean increase by up-shift in dependence parameter α.
  Namely, $(\gamma_0, \mu_0, \rho_0)^\top \longrightarrow (\gamma_0 + \eta_\gamma, \mu_0 + \delta, \rho_0)^\top$.
- Mean increase by up-shift in rate parameter of innovation λ.
  Namely, $(\gamma_0, \mu_0, \rho_0)^\top \longrightarrow (\gamma_0, \mu_0 + \delta, \rho_0)^\top$.
- Mean increase by down-shift in zero-inflation parameter of innovation ρ.
  Namely, $(\gamma_0, \mu_0, \rho_0)^\top \longrightarrow (\gamma_0, \mu_0 + \delta, \rho_0 - \eta_\rho)^\top$.

Here, the corresponding values of α, λ, ρ, η_γ and η_ρ can be obtained using the relationships in (4.2.4) and (4.2.5).

Following the approach of Rakitzis et al. (2017), given IC parameters $(\gamma, \mu, \rho)^\top = (\gamma_0, \mu_0, \rho_0)^\top$ of the ZIPINAR(1) model, the corresponding IC parameters of the ZIPINARCH(1) model are set to $(\gamma, \mu, \rho)^\top = (\gamma_0, \mu_0, \rho_{0,arch})^\top$, wherein $\rho_{0,arch}$ gives rise to the same IC mean, autocorrelation and zero-proportion in both ZIPINAR(1) and ZIPINARCH(1) models.

For the ZIPINARCH(1) model with IC parameters $(\gamma, \mu, \rho)^\top = ((1-\rho)\alpha, (1-\rho)\omega/(1-(1-\omega)\alpha), \rho)^\top = (\gamma_0, \mu_0, \rho_{0,arch})^\top$, we consider the following two OoC scenarios:

- Mean increase by up-shift in constant parameter ω.
  Namely, $(\gamma_0, \mu_0, \rho_{0,arch})^\top \longrightarrow (\gamma_0, \mu_0 + \delta, \rho_{0,arch})^\top$.
- Mean increase by down-shift in zero-inflation parameter ρ.
  Namely, $(\gamma_0, \mu_0, \rho_{0,arch})^\top \longrightarrow (\gamma_0, \mu_0 + \delta, \rho_{0,arch} - \eta_\rho)^\top$.

Using relationships (4.2.6) and (4.2.7), we can calculate the corresponding values of α, ω, ρ and η_ρ. Notice that the presence of zero-inflation parameter ρ reduces the influence of ARCH parameter α on the process mean, and thus, the case of ARCH parameter change is omitted in this study.

The results on the ATS performance of the considered charts are reported in Tables 4.1-4.5, wherein the corresponding zero proportions (denoted by 'zp'), truncated expectations, and expected CRL values are provided. The lowest OoC ATS value is highlighted in bold face. The choice of reference value in each CUSUM-type chart is made in the manner mentioned in Section 4.3. For the CUSUM-DR chart, the results for the case of $r \leq \lceil \mu_0 \rceil + 1$ are only provided because detection performance for $r > \lceil \mu_0 \rceil + 1$ is unsatisfactory according to our numerical experiments. Moreover, only the case of zero-proportion > 0.5 is considered since such situation is better suited to the process with excessive zeros.

In Table 4.1, we provide the ATS profiles with mean increase by a shift in α when the data follows a ZIPINAR(1) model. The results show that the CRL-CUSUM chart has the best performance in the detection of small and moderate shifts (about $\delta \leq 1.0$) excepting the case of $(\gamma_0,\mu_0,\rho_0) = (0.5,1.2,0.8)$. When there are large shifts (about $\delta \geq 1.0$), the conventional CUSUM chart is superior to the others. For $(\gamma_0, \mu_0, \rho_0) = (0.5,1.2,0.8)$, the conventional CUSUM chart performs slightly better than the CRL-CUSUM chart when $\delta = 0.4, 0.5$. However, the difference is not significant. For most cases, the CUSUM-DR chart performs better than the Shewhart-type chart. However, these charts are significantly worse than the CUSUM and CRL-CUSUM charts. Meanwhile, the combined Shewhart CRL-CUSUM chart shows the performance in between the CUSUM and CRL-CUSUM charts. It could be reasoned that the CRL-CUSUM chart outperforms other charts because an increase

Table 4.1: ATS profiles when the data follows ZIPINAR(1) model with mean increases by up-shifts in α

Information	Control Chart Design	ATS								
		δ								
		0.0	0.1	0.2	0.3	0.4	0.5	1.0	1.5	2.0
(γ_0,μ_0,ρ_0): (0.2,1.2,0.7)	Shewhart(9)	343.7	276.7	226.3	188.3	159.2	136.7	75.7	50.4	37.2
zp: 0.584	CUSUM(2,15)	350.3	205.9	136.7	98.9	76.1	61.3	30.6	**20.7**	**15.8**
μ_1^*: 2.882	CUSUM-DR(1,3,16)	363.1	326.1	265.3	210.3	167.6	135.7	61.4	37.5	26.6
μ_2^*: 3.707	CUSUM-DR(2,5,5)	374.4	293.2	231.6	185.7	151.6	126.0	62.3	39.1	27.9
$\mathbb{E}(\text{CRL}_1)$: 3.028	CRL-CUSUM(2,12)	349.7	**162.9**	**100.8**	**72.4**	**56.7**	**47.0**	**27.2**	**20.7**	17.6
$\mathbb{E}(\text{CRL}_2)$: 2.402	S CRL-CUSUM(10,2,14)	370.8	184.7	114.6	81.8	63.6	52.3	29.4	21.8	17.9
(γ_0,μ_0,ρ_0): (0.2,1.2,0.8)	Shewhart(11)	318.4	266.5	225.4	193.1	167.7	147.4	89.2	63.0	48.5
zp: 0.672	CUSUM(2,21)	321.3	202.4	140.9	105.5	83.3	68.4	**36.1**	**25.1**	**19.6**
μ_1^*: 3.656	CUSUM-DR(1,4,14)	316.8	308.5	265.5	219.7	181.0	150.5	73.1	45.9	33.2
μ_2^*: 4.679	CUSUM-DR(1,5,8)	308.2	260.0	211.9	173.3	143.6	121.0	63.2	41.5	30.8
$\mathbb{E}(\text{CRL}_1)$: 4.387	CRL-CUSUM(3,30)	314.0	**164.6**	**111.7**	**85.6**	**70.2**	**60.0**	37.2	28.8	24.4
$\mathbb{E}(\text{CRL}_2)$: 3.047	S CRL-CUSUM(12,3,37)	314.8	178.7	123.6	95.2	78.1	66.6	40.7	30.8	25.5
(γ_0,μ_0,ρ_0): (0.2,2.0,0.7)	Shewhart(13)	453.1	375.2	313.7	265.2	226.7	195.9	108.2	70.6	51.1
zp: 0.523	CUSUM(3,27)	477.8	318.4	226.6	169.9	132.9	107.5	**51.6**	**33.4**	**24.8**
μ_1^*: 4.190	CUSUM-DR(1,5,16)	467.0	391.1	318.2	258.3	211.4	175.2	83.1	50.2	35.0
μ_2^*: 5.193	CUSUM-DR(2,7,8)	444.0	363.7	298.0	246.2	205.7	174.1	89.2	55.7	39.2
$\mathbb{E}(\text{CRL}_1)$: 2.751	CRL-CUSUM(2,22)	456.4	**253.4**	**171.6**	**129.8**	**105.1**	**88.9**	53.6	41.1	34.8
$\mathbb{E}(\text{CRL}_2)$: 2.095	S CRL-CUSUM(14,2,27)	466.0	275.7	189.3	143.4	115.8	97.5	56.8	41.7	33.7
(γ_0,μ_0,ρ_0): (0.3,0.4,0.8)	Shewhart(6)	959.1	658.2	480.7	369.6	295.5	243.5	122.3	78.3	56.1
zp: 0.764	CUSUM(1,10)	1023.0	290.5	143.8	91.8	67.0	53.0	27.1	18.7	**14.2**
μ_1^*: 1.696	CUSUM-DR(1,2,7)	970.6	480.8	274.7	180.5	130.7	101.1	46.4	30.0	21.8
μ_2^*: 2.593	CUSUM-DR(2,3,4)	982.9	582.5	368.7	254.8	189.0	147.7	66.8	42.1	30.1
$\mathbb{E}(\text{CRL}_1)$: 6.071	CRL-CUSUM(3,22)	1035.9	**207.4**	**101.5**	**67.1**	**50.9**	**41.6**	**24.0**	**18.3**	15.5
$\mathbb{E}(\text{CRL}_2)$: 4.240	CRL-CUSUM(4,56)	968.1	229.8	128.8	91.8	72.7	61.1	37.4	29.3	25.4
	S CRL-CUSUM(7,3,23)	964.8	214.2	105.3	69.7	52.9	43.2	24.9	18.8	15.5
	S CRL-CUSUM(7,4,61)	955.9	242.1	136.0	96.8	76.5	64.1	38.6	29.5	24.5
(γ_0,μ_0,ρ_0): (0.3,0.8,0.8)	Shewhart(8)	349.0	280.2	230.5	193.8	166.0	144.6	85.6	59.8	45.5
zp: 0.673	CUSUM(1,22)	330.7	177.1	115.8	85.1	67.2	55.7	31.2	22.5	17.8
μ_1^*: 2.450	CUSUM-DR(1,3,8)	348.1	252.1	185.7	142.1	112.9	92.7	47.0	31.2	23.4
μ_2^*: 3.347	CUSUM-DR(2,4,6)	475.0	358.5	270.5	209.1	166.4	136.1	66.6	42.8	31.3
$\mathbb{E}(\text{CRL}_1)$: 4.585	CRL-CUSUM(2,9)	326.9	**145.5**	**87.5**	**61.6**	**47.6**	**39.1**	**22.1**	**16.6**	**13.9**
$\mathbb{E}(\text{CRL}_2)$: 3.062	CRL-CUSUM(3,33)	350.8	169.0	110.9	83.7	68.0	57.9	36.0	28.2	24.3
	S CRL-CUSUM(9,2,10)	329.7	158.8	96.6	68.0	52.3	42.7	23.7	17.5	14.3
	S CRL-CUSUM(9,3,39)	351.2	180.8	120.3	91.0	73.9	62.8	38.3	29.2	24.2
(γ_0,μ_0,ρ_0): (0.3,1.2,0.8)	Shewhart(12)	1327.4	1014.6	795.3	638.5	523.8	437.9	220.1	137.5	96.9
zp: 0.625	CUSUM(2,30)	1375.2	681.0	397.2	260.4	185.8	141.2	60.3	38.3	**28.6**
μ_1^*: 3.198	CUSUM-DR(1,4,16)	1324.5	896.8	619.4	444.4	331.6	256.3	103.3	59.9	41.4
μ_2^*: 4.174	CUSUM-DR(2,5,12)	1272.3	935.1	682.6	508.4	389.1	306.0	126.7	72.9	49.8
$\mathbb{E}(\text{CRL}_1)$: 4.171	CRL-CUSUM(2,18)	1427.2	**546.1**	**289.4**	**185.7**	**134.0**	**104.5**	**51.7**	**36.9**	30.1
$\mathbb{E}(\text{CRL}_2)$: 2.665	S CRL-CUSUM(13,2,20)	1385.9	598.4	322.0	205.5	147.2	113.9	55.0	38.5	30.8
(γ_0,μ_0,ρ_0): (0.4,1.2,0.8)	Shewhart(10)	396.5	326.7	274.5	234.7	203.7	179.1	108.1	75.5	57.3
zp: 0.580	CUSUM(2,22)	400.3	252.7	175.8	131.3	103.3	84.5	43.7	**29.9**	**23.0**
μ_1^*: 2.854	CUSUM-DR(1,3,20)	392.5	304.7	239.2	191.6	156.9	131.1	67.7	44.3	32.8
μ_2^*: 3.789	CUSUM-DR(1,4,10)	429.2	310.0	234.1	183.6	148.5	123.3	63.2	41.5	30.7
$\mathbb{E}(\text{CRL}_1)$: 3.979	CUSUM-DR(2,4,13)	388.6	311.9	251.3	205.3	170.5	144.0	75.7	49.4	36.2
$\mathbb{E}(\text{CRL}_2)$: 2.378	CRL-CUSUM(2,18)	406.6	**229.8**	**153.9**	**114.5**	**91.1**	**76.0**	**43.9**	33.1	27.8
	S CRL-CUSUM(11,2,21)	400.6	242.2	165.5	123.7	98.5	82.0	46.6	34.3	28.0
(γ_0,μ_0,ρ_0): (0.5,1.2,0.8)	Shewhart(9)	304.1	256.1	219.4	190.9	168.2	149.8	94.6	67.7	52.1
zp: 0.534	CUSUM(2,20)	288.5	196.4	144.3	112.2	**91.0**	**76.2**	**41.8**	**29.1**	**22.5**
μ_1^*: 2.576	CUSUM-DR(1,3,14)	301.6	224.2	173.9	139.7	115.5	97.7	53.5	36.4	27.4
μ_2^*: 3.481	CUSUM-DR(1,4,8)	314.5	236.0	184.6	149.4	124.2	105.5	58.2	39.5	29.6
$\mathbb{E}(\text{CRL}_1)$: 3.811	CUSUM-DR(2,4,9)	317.5	244.4	194.3	158.8	132.8	113.3	62.8	42.4	31.7
$\mathbb{E}(\text{CRL}_2)$: 2.147	CRL-CUSUM(2,23)	300.8	**194.4**	**141.9**	**111.7**	92.6	79.6	49.7	38.7	33.2
	S CRL-CUSUM(10,2,28)	306.3	206.4	152.8	120.9	100.3	86.0	52.5	39.6	32.6

Table 4.2: ATS profiles when the data follows ZIPINAR(1) model with mean increases by up-shifts in λ

Information	Control Chart Design	ATS								
		δ								
		0.0	0.1	0.2	0.3	0.4	0.5	1.0	1.5	2.0
(γ_0,μ_0,ρ_0): (0.2,1.2,0.7)	Shewhart(9)	343.7	217.6	145.2	101.3	73.4	55.0	18.8	9.7	**6.4**
zp: 0.584	CUSUM(2,15)	350.3	211.3	139.1	98.2	73.2	57.1	24.9	15.6	11.4
μ_1^*: 2.882	CUSUM-DR(1,3,16)	363.1	**183.3**	**112.3**	**78.1**	**59.1**	47.2	23.3	15.5	11.8
μ_2^*: 3.707	CUSUM-DR(2,5,5)	374.4	218.0	136.3	90.8	63.9	**47.1**	**16.9**	**9.6**	6.7
$\mathbb{E}(CRL_1)$: 3.028	CRL-CUSUM(2,12)	349.7	289.5	246.3	214.1	189.5	170.1	114.4	88.6	74.0
$\mathbb{E}(CRL_2)$: 2.402	S CRL-CUSUM(10,2,14)	370.8	266.9	196.8	147.9	113.1	87.8	30.2	14.0	8.3
(γ_0,μ_0,ρ_0): (0.2,1.2,0.8)	Shewhart(11)	318.4	194.5	126.4	86.7	62.2	46.3	**16.4**	**9.2**	**6.7**
zp: 0.672	CUSUM(2,21)	321.3	202.0	138.2	100.9	77.5	62.0	29.2	18.9	14.2
μ_1^*: 3.656	CUSUM-DR(1,4,14)	316.8	**172.0**	**108.1**	**75.6**	**56.9**	**45.2**	22.0	14.7	11.3
μ_2^*: 4.679	CUSUM-DR(1,5,8)	308.2	180.6	115.5	79.4	57.9	44.3	18.3	11.1	8.1
$\mathbb{E}(CRL_1)$: 4.387	CRL-CUSUM(3,30)	314.0	272.1	241.0	217.0	198.0	182.6	136.1	112.8	99.0
$\mathbb{E}(CRL_2)$: 3.047	S CRL-CUSUM(12,3,37)	314.8	231.3	171.4	127.8	96.1	73.1	23.5	11.6	7.7
(γ_0,μ_0,ρ_0): (0.2,2.0,0.7)	Shewhart(13)	453.1	316.2	227.0	167.2	126.1	97.2	34.2	16.6	**10.0**
zp: 0.523	CUSUM(3,27)	477.8	321.0	227.5	168.7	130.0	103.4	46.0	28.0	20.0
μ_1^*: 4.190	CUSUM-DR(1,5,16)	467.0	290.1	**192.6**	**135.4**	**100.1**	**77.2**	32.0	19.4	13.9
μ_2^*: 5.193	CUSUM-DR(2,7,8)	444.0	**288.9**	196.3	138.9	101.9	77.3	**28.5**	**15.6**	10.5
$\mathbb{E}(CRL_1)$: 2.751	CRL-CUSUM(2,22)	456.4	404.3	362.6	328.7	300.8	277.5	202.7	163.4	139.7
$\mathbb{E}(CRL_2)$: 2.095	S CRL-CUSUM(14,2,27)	466.0	365.6	289.2	230.3	184.4	148.4	54.8	24.6	13.5
(γ_0,μ_0,ρ_0): (0.3,0.4,0.8)	Shewhart(6)	959.1	355.5	167.6	93.0	58.0	39.5	**12.4**	**7.4**	**5.8**
zp: 0.764	CUSUM(1,10)	1023.0	351.8	165.0	94.9	62.7	45.4	18.1	11.5	8.6
μ_1^*: 1.696	CUSUM-DR(1,2,7)	970.6	**271.6**	**118.2**	**67.6**	**45.5**	**33.8**	14.7	9.7	7.4
μ_2^*: 2.593	CUSUM-DR(2,3,4)	982.9	310.8	136.9	75.3	48.1	34.0	12.8	8.1	6.3
$\mathbb{E}(CRL_1)$: 6.071	CRL-CUSUM(3,22)	1035.9	501.9	307.5	217.6	168.7	138.8	80.4	61.8	52.6
$\mathbb{E}(CRL_2)$: 4.240	CRL-CUSUM(4,56)	968.1	421.1	266.8	200.6	164.9	142.6	95.8	78.8	69.8
	S CRL-CUSUM(7,3,23)	964.8	412.2	221.7	136.5	91.3	64.5	18.5	9.4	6.6
	S CRL-CUSUM(7,4,61)	955.9	379.6	216.1	141.4	98.0	69.9	18.9	9.4	6.6
(γ_0,μ_0,ρ_0): (0.3,0.8,0.8)	Shewhart(8)	349.0	194.3	118.9	78.5	55.0	40.5	**14.5**	**8.5**	**6.4**
zp: 0.673	CUSUM(1,22)	330.7	182.4	117.8	84.5	65.0	52.5	26.8	18.3	14.2
μ_1^*: 2.450	CUSUM-DR(1,3,8)	348.1	**177.4**	**104.7**	**69.2**	**49.8**	**38.1**	16.8	10.9	8.3
μ_2^*: 3.347	CUSUM-DR(2,4,6)	475.0	229.1	128.0	80.5	55.5	41.0	16.5	10.3	7.7
$\mathbb{E}(CRL_1)$: 4.585	CRL-CUSUM(2,9)	326.9	259.5	214.3	182.5	159.0	141.2	93.0	72.1	60.6
$\mathbb{E}(CRL_2)$: 3.062	CRL-CUSUM(3,33)	350.8	269.3	220.1	187.8	165.1	148.3	104.6	85.8	75.2
	S CRL-CUSUM(9,2,10)	329.7	221.8	154.1	110.2	81.0	61.1	20.8	10.8	7.4
	S CRL-CUSUM(9,3,39)	351.2	233.5	163.8	118.7	87.9	66.3	21.4	10.9	7.4
(γ_0,μ_0,ρ_0): (0.3,1.2,0.8)	Shewhart(12)	1327.4	746.2	449.1	286.5	192.1	134.5	36.5	**16.5**	**10.1**
zp: 0.625	CUSUM(2,30)	1375.2	714.5	419.2	270.8	188.8	139.8	53.4	31.6	22.5
μ_1^*: 3.198	CUSUM-DR(1,4,16)	1324.5	624.3	335.6	202.2	134.0	95.8	34.8	20.7	14.9
μ_2^*: 4.174	CUSUM-DR(2,5,12)	1272.3	**590.2**	**311.2**	**184.2**	**120.4**	**85.2**	**30.4**	18.1	13.0
$\mathbb{E}(CRL_1)$: 4.171	CRL-CUSUM(2,18)	1427.2	1117.1	904.0	751.8	639.3	553.9	328.0	235.4	187.0
$\mathbb{E}(CRL_2)$: 2.665	S CRL-CUSUM(13,2,20)	1385.9	903.4	604.4	414.6	291.4	209.8	55.9	22.8	12.7
(γ_0,μ_0,ρ_0): (0.4,1.2,0.8)	Shewhart(10)	396.5	253.4	171.0	120.9	88.9	67.6	**24.7**	**13.3**	**9.0**
zp: 0.580	CUSUM(2,22)	400.3	256.4	176.9	129.5	99.4	79.2	36.7	23.3	17.2
μ_1^*: 2.854	CUSUM-DR(1,3,20)	392.5	223.4	145.2	103.9	79.6	64.0	31.7	21.1	16.0
μ_2^*: 3.789	CUSUM-DR(1,4,10)	429.2	268.4	179.2	126.5	93.6	72.0	29.1	17.2	12.2
$\mathbb{E}(CRL_1)$: 3.979	CUSUM-DR(2,4,13)	388.6	**220.1**	**140.4**	**98.2**	**73.6**	**58.0**	27.1	17.6	13.2
$\mathbb{E}(CRL_2)$: 2.378	CRL-CUSUM(2,18)	406.6	338.4	289.4	252.9	224.9	202.8	139.7	110.6	94.0
	S CRL-CUSUM(11,2,21)	400.6	289.4	214.5	162.5	125.4	98.4	36.2	18.0	11.2
(γ_0,μ_0,ρ_0): (0.5,1.2,0.8)	Shewhart(9)	304.1	204.7	144.6	106.4	80.9	63.4	**25.6**	**14.4**	**9.8**
zp: 0.534	CUSUM(2,20)	288.5	197.6	143.5	109.2	86.4	70.5	34.6	22.5	16.7
μ_1^*: 2.576	CUSUM-DR(1,3,14)	301.6	**196.4**	**136.8**	**100.8**	**77.8**	**62.3**	29.4	19.0	14.1
μ_2^*: 3.481	CUSUM-DR(1,4,8)	314.5	213.7	152.6	113.6	87.6	69.6	30.2	17.9	12.5
$\mathbb{E}(CRL_1)$: 3.811	CUSUM-DR(2,4,9)	317.5	206.6	142.9	104.0	79.0	**62.3**	27.4	17.0	12.3
$\mathbb{E}(CRL_2)$: 2.147	CRL-CUSUM(2,23)	300.8	252.6	218.1	192.5	172.9	157.5	113.4	92.7	80.7
	S CRL-CUSUM(10,2,28)	306.3	229.2	176.5	138.9	111.2	90.3	37.6	19.8	12.5

Table 4.3: ATS profiles when the data follows ZIPINAR(1) model with mean increases by down-shifts in ρ

Information	Control Chart Design	ATS								
		δ								
		0.0	0.1	0.2	0.3	0.4	0.5	1.0	1.5	2.0
(γ_0,μ_0,ρ_0): (0.2,1.2,0.7)	Shewhart(9)	343.7	306.4	275.0	248.3	225.4	205.6	137.3	98.1	73.4
zp: 0.584	CUSUM(2,15)	350.3	255.2	190.5	145.3	113.1	89.8	36.2	**19.9**	**13.1**
μ_1^*: 2.882	CUSUM-DR(1,3,16)	363.1	290.8	236.6	195.3	163.2	138.1	68.7	40.6	26.8
μ_2^*: 3.707	CUSUM-DR(2,5,5)	374.4	324.7	283.9	250.0	221.4	197.3	118.3	77.0	53.0
$\mathbb{E}(CRL_1)$: 3.028	CRL-CUSUM(2,12)	349.7	**224.3**	**153.5**	**111.2**	**84.7**	**67.2**	**31.5**	20.9	16.1
$\mathbb{E}(CRL_2)$: 2.402	S CRL-CUSUM(10,2,14)	370.8	250.1	174.1	126.6	96.1	76.0	35.4	23.4	18.0
(γ_0,μ_0,ρ_0): (0.2,1.2,0.8)	Shewhart(11)	318.4	285.7	258.1	234.4	214.1	196.3	134.4	98.1	74.8
zp: 0.672	CUSUM(2,21)	321.3	240.0	183.7	143.9	114.9	93.6	**41.9**	**24.4**	**16.7**
μ_1^*: 3.656	CUSUM-DR(1,4,14)	316.8	264.9	224.0	191.2	164.7	143.0	77.8	47.8	32.0
μ_2^*: 4.679	CUSUM-DR(1,5,8)	308.2	263.6	227.5	197.9	173.4	152.9	88.0	55.6	37.6
$\mathbb{E}(CRL_1)$: 4.387	CRL-CUSUM(3,30)	314.0	**212.7**	**155.9**	**121.2**	**98.6**	**82.9**	46.6	33.1	26.3
$\mathbb{E}(CRL_2)$: 3.047	S CRL-CUSUM(12,3,37)	314.8	224.8	169.1	133.5	109.6	92.7	52.7	37.5	29.6
(γ_0,μ_0,ρ_0): (0.2,2.0,0.7)	Shewhart(13)	453.1	419.7	390.0	363.2	339.2	317.4	234.6	180.1	142.3
zp: 0.523	CUSUM(3,27)	477.8	371.0	292.1	233.2	188.7	154.6	68.0	**37.9**	**24.9**
μ_1^*: 4.190	CUSUM-DR(1,5,16)	467.0	398.9	342.8	296.4	257.7	225.1	122.7	73.5	47.5
μ_2^*: 5.193	CUSUM-DR(2,7,8)	444.0	398.5	359.0	324.6	294.4	267.9	173.7	118.7	84.4
$\mathbb{E}(CRL_1)$: 2.751	CRL-CUSUM(2,22)	456.4	**320.1**	**237.5**	**184.8**	**149.5**	**124.8**	**67.9**	47.7	37.6
$\mathbb{E}(CRL_2)$: 2.095	S CRL-CUSUM(14,2,27)	466.0	344.9	262.8	207.3	169.0	141.8	78.1	54.9	43.2
(γ_0,μ_0,ρ_0): (0.3,0.4,0.8)	Shewhart(6)	959.1	696.5	530.5	418.0	338.0	278.8	129.9	73.6	$*$
zp: 0.764	CUSUM(1,10)	1023.0	515.7	288.8	175.7	114.5	79.1	23.3	**12.2**	$*$
μ_1^*: 1.696	CUSUM-DR(1,2,7)	970.6	610.1	409.6	288.7	211.5	159.7	54.2	25.6	$*$
μ_2^*: 2.593	CUSUM-DR(2,3,4)	982.9	676.7	491.2	370.5	287.7	228.8	91.8	46.7	$*$
$\mathbb{E}(CRL_1)$: 6.071	CRL-CUSUM(3,22)	1035.9	342.2	156.8	**91.3**	**62.2**	**46.8**	**21.5**	14.9	$*$
$\mathbb{E}(CRL_2)$: 4.240	CRL-CUSUM(4,56)	968.1	**274.2**	**145.6**	98.8	75.2	61.0	33.1	24.2	$*$
	S CRL-CUSUM(7,3,23)	964.8	345.7	160.8	93.8	63.9	48.1	22.1	15.2	$*$
	S CRL-CUSUM(7,4,61)	955.9	287.4	153.8	104.6	79.6	64.6	34.8	25.2	$*$
(γ_0,μ_0,ρ_0): (0.3,0.8,0.8)	Shewhart(8)	349.0	293.7	250.8	216.8	189.3	166.8	97.6	63.8	44.6
zp: 0.673	CUSUM(1,22)	330.7	204.0	136.9	**98.6**	**75.0**	**59.7**	**28.2**	18.2	13.3
μ_1^*: 2.450	CUSUM-DR(1,3,8)	348.1	271.3	216.0	175.1	144.2	120.3	56.5	31.6	19.8
μ_2^*: 3.347	CUSUM-DR(2,4,6)	475.0	379.7	309.2	255.7	214.2	181.5	90.2	51.9	32.8
$\mathbb{E}(CRL_1)$: 4.585	CRL-CUSUM(2,9)	326.9	215.4	149.8	109.1	82.8	65.0	**28.2**	**17.6**	**13.2**
$\mathbb{E}(CRL_2)$: 3.062	CRL-CUSUM(3,33)	350.8	**203.3**	**136.8**	101.7	80.7	67.0	37.4	27.2	22.2
	S CRL-CUSUM(9,2,10)	329.7	225.6	159.9	117.4	89.2	70.0	30.1	18.7	13.9
	S CRL-CUSUM(9,3,39)	351.2	214.2	147.0	110.3	88.0	73.3	40.8	29.3	23.4
(γ_0,μ_0,ρ_0): (0.3,1.2,0.8)	Shewhart(12)	1327.4	1157.4	1017.5	900.9	802.9	719.5	445.2	299.0	212.5
zp: 0.625	CUSUM(2,30)	1375.2	894.3	603.0	420.8	303.3	225.5	75.3	**39.0**	**25.5**
μ_1^*: 3.198	CUSUM-DR(1,4,16)	1324.5	1023.5	803.8	640.3	516.7	421.9	176.9	89.4	51.7
μ_2^*: 4.174	CUSUM-DR(2,5,12)	1272.3	1024.4	835.5	689.3	574.6	483.3	227.7	123.5	74.1
$\mathbb{E}(CRL_1)$: 4.171	CRL-CUSUM(2,18)	1427.2	**838.0**	**526.0**	**351.4**	**248.4**	**184.7**	**71.0**	43.4	32.2
$\mathbb{E}(CRL_2)$: 2.665	S CRL-CUSUM(13,2,20)	1385.9	888.4	579.9	392.3	277.3	205.1	77.3	47.0	34.7
(γ_0,μ_0,ρ_0): (0.4,1.2,0.8)	Shewhart(10)	396.5	344.2	301.4	265.9	236.2	211.1	129.0	85.9	60.7
zp: 0.580	CUSUM(2,22)	400.3	297.5	226.6	176.5	140.3	113.7	**49.8**	**28.6**	**19.3**
μ_1^*: 2.854	CUSUM-DR(1,3,20)	392.5	309.1	248.3	202.9	168.4	141.7	70.3	42.0	28.2
μ_2^*: 3.789	CUSUM-DR(1,4,10)	429.2	350.3	289.6	242.2	204.6	174.4	87.6	50.4	31.9
$\mathbb{E}(CRL_1)$: 3.979	CUSUM-DR(2,4,13)	388.6	317.6	263.2	220.8	187.3	160.5	83.4	50.0	33.0
$\mathbb{E}(CRL_2)$: 2.378	CRL-CUSUM(2,18)	406.6	**280.5**	**203.9**	**155.2**	**122.8**	**100.5**	51.3	35.3	27.9
	S CRL-CUSUM(11,2,21)	400.6	289.0	215.0	165.4	131.5	107.8	54.9	37.4	29.1
(γ_0,μ_0,ρ_0): (0.5,1.2,0.8)	Shewhart(9)	304.1	261.3	226.7	198.3	174.7	155.0	91.8	59.8	41.4
zp: 0.534	CUSUM(2,20)	288.5	222.3	175.1	140.5	114.7	95.1	**45.1**	**26.8**	**18.3**
μ_1^*: 2.576	CUSUM-DR(1,3,14)	301.6	242.3	197.8	163.8	137.3	116.5	58.5	34.7	22.9
μ_2^*: 3.481	CUSUM-DR(1,4,8)	314.5	259.8	217.2	183.6	156.7	134.9	70.7	42.0	27.2
$\mathbb{E}(CRL_1)$: 3.811	CUSUM-DR(2,4,9)	317.5	261.4	218.0	183.9	156.7	134.8	70.6	42.3	27.7
$\mathbb{E}(CRL_2)$: 2.147	CRL-CUSUM(2,23)	300.8	**216.7**	**164.7**	**130.8**	**107.7**	**91.3**	52.7	38.8	32.1
	S CRL-CUSUM(10,2,28)	306.3	226.6	174.4	139.3	115.0	97.5	55.6	39.8	31.5

Table 4.4: ATS profiles when the data follows ZIPINARCH(1) model with mean increases by up-shifts in ω

Information	Control Chart Design	ATS								
		δ								
		0.0	0.1	0.2	0.3	0.4	0.5	1.0	1.5	2.0
(γ_0,μ_0): (0.2,1.2)	Shewhart(9)	401.5	276.5	197.2	145.0	109.6	84.8	31.0	15.5	9.4
(α,ω,ρ): (0.437,2.100,0.543)	CUSUM(2,17)	444.5	289.8	199.1	143.3	107.4	83.3	34.1	20.1	14.1
zp: 0.584	CUSUM-DR(1,3,19)	424.7	**215.9**	**130.3**	**89.4**	**66.8**	**53.0**	25.5	16.8	12.6
μ_1^*: 2.882	CUSUM-DR(1,4,9)	464.8	325.1	233.8	172.5	130.3	100.6	36.2	18.6	11.9
μ_2^*: 3.423	CUSUM-DR(2,4,9)	403.2	248.1	161.2	110.3	79.2	59.3	**22.4**	**12.9**	**9.1**
$\mathbb{E}(CRL_1)$: 2.455	CRL-CUSUM(2,9)	430.1	378.3	341.4	314.4	294.1	278.7	239.7	226.7	221.9
$\mathbb{E}(CRL_2)$: 2.402	S CRL-CUSUM(10,2,10)	392.4	306.3	242.8	194.5	157.1	127.7	50.1	23.7	13.4
(γ_0,μ_0): (0.2,1.2)	Shewhart(12)	671.6	454.1	319.0	231.6	173.2	132.9	47.5	23.6	14.2
(α,ω,ρ): (0.582,2.792,0.656)	CUSUM(2,26)	679.5	446.0	307.4	221.4	165.7	128.4	52.0	30.4	21.3
zp: 0.672	CUSUM-DR(1,4,22)	677.7	**335.7**	**190.4**	**123.2**	**88.3**	**68.0**	31.1	20.3	15.3
μ_1^*: 3.656	CUSUM-DR(2,5,13)	654.1	400.2	255.4	170.2	118.6	86.5	**30.4**	**17.5**	12.4
μ_2^*: 4.079	CUSUM-DR(2,6,9)	688.7	454.0	310.3	218.8	158.7	118.1	37.7	18.7	**12.1**
$\mathbb{E}(CRL_1)$: 3.081	CRL-CUSUM(3,32)	701.8	624.7	572.8	536.6	510.7	491.7	447.7	435.6	432.1
$\mathbb{E}(CRL_2)$: 3.047	S CRL-CUSUM(13,3,41)	672.4	513.8	399.3	313.0	246.7	195.4	69.0	32.1	18.5
(γ_0,μ_0): (0.2,2.0)	Shewhart(11)	214.3	165.9	130.7	104.7	85.1	70.1	31.3	17.2	10.9
(α,ω,ρ): (0.409, 3.270, 0.511)	CUSUM(3,20)	226.2	172.3	134.8	107.9	88.2	73.4	36.4	22.8	16.3
zp: 0.523	CUSUM-DR(1,5,12)	226.5	**159.6**	**116.0**	**86.8**	**67.0**	**53.1**	**23.1**	**14.2**	10.2
μ_1^*: 4.190	CUSUM-DR(2,5,13)	232.6	161.6	116.5	87.0	67.2	53.5	24.1	15.0	10.9
μ_2^*: 4.494	CUSUM-DR(3,6,8)	232.4	171.3	129.2	99.6	78.4	62.8	26.5	15.0	10.1
μ_3^*: 5.003	CUSUM-DR(3,7,5)	219.1	166.6	129.1	101.8	81.7	66.5	28.6	15.6	**10.0**
$\mathbb{E}(CRL_1)$: 2.110	CRL-CUSUM(2,11)	225.5	218.3	212.5	207.8	204.1	201.0	192.0	188.5	187.0
$\mathbb{E}(CRL_2)$: 2.095	S CRL-CUSUM(12,2,14)	227.8	196.0	168.2	144.1	123.2	105.3	49.3	25.8	15.4
(γ_0,μ_0): (0.3,0.4)	Shewhart(6)	433.9	247.8	156.0	105.5	75.3	56.2	19.8	10.4	**6.7**
(α,ω,ρ): (0.722, 0.674, 0.584)	CUSUM(1,10)	477.6	266.0	163.9	109.3	77.6	58.0	22.4	13.3	9.6
zp: 0.764	CUSUM-DR(1,2,7)	427.7	**217.9**	**125.1**	**79.6**	**55.1**	**40.8**	**16.2**	10.0	7.4
μ_1^*: 1.696	CUSUM-DR(1,3,4)	491.9	276.2	170.7	113.2	79.4	58.2	19.4	10.2	6.9
μ_2^*: 2.665	CUSUM-DR(2,3,4)	420.8	233.8	143.7	95.4	67.2	49.8	17.8	**9.9**	6.8
$\mathbb{E}(CRL_1)$: 4.751	CRL-CUSUM(3,12)	421.5	238.3	157.9	116.9	93.5	79.0	51.9	45.1	42.8
$\mathbb{E}(CRL_2)$: 4.240	CRL-CUSUM(4,30)	435.4	205.9	133.1	101.1	83.9	73.5	53.7	48.6	46.8
	S CRL-CUSUM(7,3,14)	435.2	234.2	147.2	103.2	77.9	61.8	27.3	14.9	9.3
	S CRL-CUSUM(7,4,36)	425.6	203.1	128.2	93.6	73.8	60.6	28.3	15.1	9.3
(γ_0,μ_0): (0.3,0.8)	Shewhart(9)	401.4	275.1	196.8	146.0	111.6	87.6	34.6	18.5	11.8
(α,ω,ρ): (0.746,1.393,0.598)	CUSUM(2,14)	400.7	279.5	203.3	153.2	118.9	94.8	40.5	23.4	16.0
zp: 0.673	CUSUM-DR(1,3,12)	404.0	**253.8**	**167.1**	**115.3**	**83.4**	**63.1**	**25.3**	**15.4**	11.2
μ_1^*: 2.450	CUSUM-DR(2,4,8)	403.8	270.4	188.9	136.9	102.4	78.8	29.7	16.3	**11.0**
μ_2^*: 3.231	CRL-CUSUM(2,6)	461.2	392.1	344.5	310.5	285.6	267.0	220.9	205.8	200.3
$\mathbb{E}(CRL_1)$: 3.228	CRL-CUSUM(3,25)	397.3	290.3	231.9	196.7	173.9	158.3	124.3	114.3	110.7
$\mathbb{E}(CRL_2)$: 3.062	S CRL-CUSUM(10,2,7)	423.4	312.3	237.4	184.7	146.4	117.9	48.3	25.1	15.4
	S CRL-CUSUM(10,3,33)	398.1	273.8	204.4	160.7	130.5	108.1	48.1	25.2	15.5
(γ_0,μ_0): (0.3,1.2)	Shewhart(12)	544.3	397.3	297.9	228.8	179.5	143.4	58.4	30.8	19.2
(α,ω,ρ): (0.727,2.034,0.587)	CUSUM(2,27)	546.3	391.0	288.5	219.0	170.6	136.1	58.4	34.2	23.8
zp: 0.625	CUSUM-DR(1,4,18)	542.4	365.1	252.2	179.1	131.2	99.3	**38.0**	**22.4**	**15.9**
μ_1^*: 3.198	CUSUM-DR(2,4,22)	527.0	**335.9**	**226.3**	**161.1**	**120.7**	**94.4**	41.4	25.6	18.4
μ_2^*: 3.808	CUSUM-DR(2,5,13)	552.2	394.4	288.8	216.3	165.4	128.9	47.9	25.2	16.5
$\mathbb{E}(CRL_1)$: 2.741	CRL-CUSUM(2,8)	672.1	609.5	562.8	527.3	499.8	478.3	420.8	400.1	392.0
$\mathbb{E}(CRL_2)$: 2.665	S CRL-CUSUM(13,2,9)	529.9	420.0	337.0	273.1	223.4	184.2	79.0	40.8	24.5
(γ_0,μ_0): (0.4,1.2)	Shewhart(14)	1289.3	961.4	732.4	568.8	449.3	360.5	144.4	72.7	42.6
(α,ω,ρ): (0.801,1.442,0.501)	CUSUM(2,41)	1293.9	914.3	660.4	487.6	367.9	283.6	104.5	56.2	37.4
zp: 0.580	CUSUM-DR(1,3,50)	1283.0	**701.9**	**425.7**	**286.4**	**209.6**	**162.9**	**73.7**	46.7	34.1
μ_1^*: 2.854	CUSUM-DR(1,4,27)	1287.4	916.1	662.3	485.9	361.8	273.5	88.5	**44.2**	**28.6**
μ_2^*: 3.646	CUSUM-DR(2,4,33)	1275.8	838.4	568.5	399.2	290.9	219.8	83.3	47.2	32.1
$\mathbb{E}(CRL_1)$: 2.520	CRL-CUSUM(2,14)	1294.5	1014.2	825.5	693.7	598.8	528.6	355.3	294.6	268.4
$\mathbb{E}(CRL_2)$: 2.378	S CRL-CUSUM(15,2,7)	1250.9	927.6	711.4	561.2	453.4	373.5	170.8	92.0	54.4
(γ_0,μ_0): (0.5,1.2)	Shewhart(12)	662.5	523.0	419.5	341.4	281.4	234.6	108.9	60.1	37.4
(α,ω,ρ): (0.813,0.976,0.385)	CUSUM(2,35)	669.3	510.3	395.6	311.7	249.3	202.5	87.6	49.7	33.6
zp: 0.534	CUSUM-DR(1,3,31)	664.5	**483.7**	**358.8**	**271.6**	**210.1**	**166.1**	**69.5**	**40.8**	**28.4**
μ_1^*: 2.576	CUSUM-DR(1,4,20)	650.6	508.8	404.0	325.2	265.1	218.4	95.7	50.9	31.7
μ_2^*: 3.515	CUSUM-DR(2,4,23)	667.1	507.8	393.4	309.9	247.9	201.3	86.6	48.2	31.7
$\mathbb{E}(CRL_1)$: 2.394	CRL-CUSUM(2,20)	699.2	497.3	376.7	300.5	249.8	214.6	135.7	109.7	97.9
$\mathbb{E}(CRL_2)$: 2.147	S CRL-CUSUM(13,2,27)	688.7	498.9	377.0	296.9	242.3	203.5	109.4	69.8	46.7

Table 4.5: ATS profiles when the data follows ZIPINARCH(1) model with mean increases by down-shifts in ρ

Information	Control Chart Design	ATS								
		δ								
		0.0	0.1	0.2	0.3	0.4	0.5	1.0	1.5	2.0
(γ_0,μ_0): (0.2,1.2)	Shewhart(9)	401.5	344.4	298.8	261.9	231.5	206.2	126.6	86.3	63.1
(α,ω,ρ): (0.437,2.100,0.543)	CUSUM(2,17)	444.5	319.7	236.0	178.4	137.9	108.8	43.2	23.7	15.7
zp: 0.584	CUSUM-DR(1,3,19)	424.7	330.5	263.8	215.0	178.6	150.7	77.0	47.7	33.0
μ_1^*: 2.882	CUSUM-DR(1,4,9)	464.8	372.0	303.4	251.6	211.5	180.1	93.0	56.7	38.4
μ_2^*: 3.423	CUSUM-DR(2,4,9)	403.2	326.7	269.2	225.2	190.8	163.5	86.3	53.2	36.3
$\mathbb{E}(CRL_1)$: 2.455	CRL-CUSUM(2,9)	430.1	**239.8**	**148.4**	**100.3**	**72.9**	**56.0**	**24.7**	**16.0**	**12.0**
$\mathbb{E}(CRL_2)$: 2.402	S CRL-CUSUM(10,2,10)	392.4	241.2	155.5	106.8	78.0	60.0	26.5	17.1	12.8
(γ_0,μ_0): (0.2,1.2)	Shewhart(12)	671.6	565.2	481.9	415.6	362.0	318.1	184.6	121.0	85.8
(α,ω,ρ): (0.582,2.792,0.656)	CUSUM(2,26)	679.5	481.7	351.3	263.1	201.9	158.5	63.0	**35.0**	**23.5**
zp: 0.672	CUSUM-DR(1,4,22)	677.7	515.6	402.8	322.1	262.8	218.1	104.8	62.5	42.4
μ_1^*: 3.656	CUSUM-DR(2,5,13)	654.1	516.4	415.8	340.5	283.1	238.5	118.1	70.0	46.5
μ_2^*: 4.079	CUSUM-DR(2,6,9)	688.7	555.0	455.0	378.5	319.1	272.1	140.3	84.6	56.5
$\mathbb{E}(CRL_1)$: 3.081	CRL-CUSUM(3,32)	701.8	**354.0**	**223.5**	**161.2**	**126.0**	**103.7**	**56.6**	40.3	32.1
$\mathbb{E}(CRL_2)$: 3.047	S CRL-CUSUM(13,3,41)	672.4	384.1	252.3	185.1	145.9	120.6	65.8	46.3	36.2
(γ_0,μ_0): (0.2,2.0)	Shewhart(11)	214.3	195.3	178.7	164.2	151.4	140.1	99.1	74.1	57.7
(α,ω,ρ): (0.409,3.270,0.511)	CUSUM(3,20)	226.2	185.8	154.2	129.2	109.3	93.3	47.7	28.7	19.5
zp: 0.523	CUSUM-DR(1,5,12)	226.5	197.8	173.9	153.9	137.0	122.7	75.5	50.7	36.4
μ_1^*: 4.190	CUSUM-DR(2,5,13)	232.6	202.8	178.1	157.5	140.1	125.3	77.2	52.1	37.6
μ_2^*: 4.494	CUSUM-DR(3,6,8)	232.4	205.9	183.6	164.5	148.2	134.1	86.2	59.8	43.9
μ_3^*: 5.003	CUSUM-DR(3,7,5)	219.1	196.8	177.5	161.0	146.5	134.0	89.9	64.3	48.3
$\mathbb{E}(CRL_1)$: 2.110	CRL-CUSUM(2,11)	225.5	**158.8**	**118.2**	**92.1**	**74.6**	**62.2**	**33.6**	**23.2**	**17.9**
$\mathbb{E}(CRL_2)$: 2.095	S CRL-CUSUM(12,2,14)	227.8	170.9	131.4	104.3	85.3	71.7	39.2	27.1	20.9
(γ_0,μ_0): (0.3,0.4)	Shewhart(6)	433.9	285.6	204.8	155.9	123.9	101.6	50.7	32.6	23.6
(α,ω,ρ): (0.722,0.674,0.584)	CUSUM(1,10)	477.6	260.8	162.5	111.0	81.1	62.4	26.5	16.3	11.6
zp: 0.764	CUSUM-DR(1,2,7)	427.7	255.7	171.5	124.4	95.4	76.3	35.7	22.5	16.1
μ_1^*: 1.696	CUSUM-DR(1,3,4)	491.9	305.2	209.5	154.1	119.2	95.7	44.8	27.9	19.8
μ_2^*: 2.665	CUSUM-DR(2,3,4)	420.8	264.3	183.5	136.5	106.6	86.3	41.7	26.5	19.1
$\mathbb{E}(CRL_1)$: 4.751	CRL-CUSUM(3,12)	421.5	163.9	**87.9**	**57.0**	**41.6**	**32.7**	**16.4**	**11.5**	**9.0**
$\mathbb{E}(CRL_2)$: 4.240	CRL-CUSUM(4,30)	435.4	**156.2**	89.9	63.4	49.5	41.0	23.5	17.4	14.2
	S CRL-CUSUM(7,3,14)	435.2	184.2	99.3	64.0	46.4	36.2	17.9	12.3	9.5
	S CRL-CUSUM(7,4,36)	425.6	167.9	98.0	69.3	54.0	44.5	24.9	17.8	14.1
(γ_0,μ_0): (0.3,0.8)	Shewhart(9)	401.4	314.5	253.7	209.4	176.2	150.7	81.8	53.0	38.1
(α,ω,ρ): (0.746,1.393,0.598)	CUSUM(2,14)	400.7	287.0	214.4	165.6	131.6	107.0	48.9	29.0	19.9
zp: 0.673	CUSUM-DR(1,3,12)	404.0	294.1	223.4	175.4	141.7	117.0	57.1	35.3	24.8
μ_1^*: 2.450	CUSUM-DR(2,4,8)	403.8	301.4	233.4	186.3	152.4	127.2	63.8	39.8	28.0
μ_2^*: 3.231	CRL-CUSUM(2,6)	461.2	265.9	168.8	115.7	84.4	64.6	27.1	17.0	**12.7**
$\mathbb{E}(CRL_1)$: 3.228	CRL-CUSUM(3,25)	397.3	**201.8**	**129.4**	**94.7**	**75.0**	**62.4**	**35.8**	**26.5**	21.8
$\mathbb{E}(CRL_2)$: 3.062	S CRL-CUSUM(10,2,7)	423.4	272.7	183.3	129.0	95.0	72.9	30.0	18.5	13.5
	S CRL-CUSUM(10,3,33)	398.1	223.5	147.4	109.0	86.6	72.1	40.5	29.0	22.9
(γ_0,μ_0): (0.3,1.2)	Shewhart(12)	544.3	453.5	383.7	328.8	285.0	249.5	143.8	94.7	67.9
(α,ω,ρ): (0.727,2.034,0.587)	CUSUM(2,27)	546.3	400.5	301.9	233.3	184.4	148.8	65.2	38.1	26.2
zp: 0.625	CUSUM-DR(1,4,18)	542.4	421.0	334.6	271.5	224.2	188.1	93.5	56.8	38.9
μ_1^*: 3.198	CUSUM-DR(2,4,22)	527.0	402.9	317.1	256.0	211.1	177.3	90.3	56.7	40.0
μ_2^*: 3.808	CUSUM-DR(2,5,13)	552.2	437.4	353.8	291.3	243.7	206.6	106.0	65.0	44.6
$\mathbb{E}(CRL_1)$: 2.741	CRL-CUSUM(2,8)	672.1	**409.2**	**267.3**	**185.6**	**135.8**	**103.9**	**42.6**	**26.3**	**19.4**
$\mathbb{E}(CRL_2)$: 2.665	S CRL-CUSUM(13,2,9)	529.9	366.9	259.1	188.1	141.0	109.3	45.2	27.7	20.2
(γ_0,μ_0): (0.4,1.2)	Shewhart(14)	1289.3	1047.8	867.1	728.9	621.1	535.5	292.3	186.3	130.9
(α,ω,ρ): (0.801,1.442,0.501)	CUSUM(2,41)	1293.9	894.5	639.3	471.0	356.7	277.2	107.6	59.9	40.5
zp: 0.580	CUSUM-DR(1,3,50)	1283.0	864.6	617.7	463.2	361.4	291.2	135.5	83.8	59.4
μ_1^*: 2.854	CUSUM-DR(1,4,27)	1287.4	957.6	732.9	574.9	460.7	376.1	169.1	96.6	63.9
μ_2^*: 3.646	CUSUM-DR(2,4,33)	1275.8	913.4	679.4	522.3	413.0	334.7	152.3	90.7	62.4
$\mathbb{E}(CRL_1)$: 2.520	CRL-CUSUM(2,14)	1294.5	**660.4**	**384.3**	**249.3**	**176.4**	**133.4**	**58.4**	**38.7**	**30.0**
$\mathbb{E}(CRL_2)$: 2.378	S CRL-CUSUM(15,2,7)	1250.9	752.7	463.2	302.8	212.5	159.1	67.5	44.1	33.7
(γ_0,μ_0): (0.5,1.2)	Shewhart(12)	662.5	549.5	463.7	397.2	344.5	302.2	177.8	120.3	88.7
(α,ω,ρ): (0.813,0.976,0.385)	CUSUM(2,35)	669.3	492.1	373.3	291.0	232.3	189.5	87.4	52.8	37.0
zp: 0.534	CUSUM-DR(1,3,31)	664.5	498.7	386.7	308.4	251.8	209.9	105.4	66.4	47.5
μ_1^*: 2.576	CUSUM-DR(1,4,20)	650.6	509.4	408.7	334.9	279.4	236.7	123.0	77.3	54.4
μ_2^*: 3.515	CUSUM-DR(2,4,23)	667.1	514.8	408.6	332.1	275.5	232.6	120.8	76.8	54.8
$\mathbb{E}(CRL_1)$: 2.394	CRL-CUSUM(2,20)	699.2	**388.2**	**250.4**	**179.8**	**139.0**	**113.3**	**60.9**	**43.8**	**35.4**
$\mathbb{E}(CRL_2)$: 2.147	S CRL-CUSUM(13,2,27)	688.7	438.5	295.6	215.0	166.9	136.1	72.5	51.1	40.3

in dependence parameter induces a decrease in zero-proportion.

In Table 4.2, we provide the ATS profiles in the detection of mean increase by a shift in λ when the data follows a ZIPINAR(1) model. In this case, the change in zero-proportion is not large, so that one can easily guess that the CRL-CUSUM chart performance cannot be as good as that in Table 4.1. The result indicates that in the case of mean increase by a shift in λ, the CUSUM-DR chart is superior to the others in detecting small and moderate shifts (about $\delta \leq 0.5$ or 1.0). For $\delta \geq 1.5$, the Shewhart-type chart performs the best. For all cases, the CRL-CUSUM chart performs the worst. The combined Shewhart CRL-CUSUM chart performs better than the CRL-CUSUM chart due to the participation of the Shewhart-type chart.

In Table 4.3, we present the ATS profiles in the detection of mean increase by a down-shift in ρ when the data follows a ZIPINAR(1) model. The symbol '$*$' stands for the case that there is no $\rho \in [0, 1)$ reflecting given OoC situations. The CUSUM-DR chart with $r = 2$ performs much worse than that with $r = 1$. This phenomenon appeals to intuition because the updating frequency is relatively small when $r = 2$. Aside from this, a similar pattern to that in Table 4.1 is observed.

Tables 4.4 and 4.5 present the ATS profiles in the detection of mean increase by an up-shift in ω and down-shift in ρ when the data follows a ZIPINARCH(1) model. Table 4.4 makes a conclusion similar to that from Table 4.2. Also, the results in Table 4.5 are quite similar to those in Table 4.3. Tables 4.2 and 4.4 show that for almost all cases, the CUSUM-DR chart with $r = 1$ performs the best in detecting small to moderate shifts (about $\delta \leq 0.5$) in λ or ω. However, if considering the overall performance, including the case of large shifts, the r should be selected in range $r \leq \lceil \mu \rceil + 1$.

Our findings suggest that in monitoring count time series with serial dependence

and excessive zeros, the CUSUM-DR chart is quite useful for detecting small to moderate mean increase when the zero proportion is nearly fixed. Meanwhile, when the mean increases by a decrease of zero proportion, the CRL-CUSUM chart is highly recommendable. The combined Shewhart CRL-CUSUM chart is also recommendable if there is no prior information about the parameters of change, which is more realistic in practice.

4.5 A real data example

To illustrate the usability of the proposed CUSUM-type charts, we analyze the drug offense data series reported in the 26th police car beat in Pittsburgh. This data set is monthly observed from January 1990 to December 2001, which can be obtained from the crime data section of the forecasting principles site (http://www.forecasting principles.com). First, we use the first 60 observations, namely, from January 1990 to December 1994, as Phase I sample, and the remaining 84 values as Phase II sample. The sample path plot is illustrated in Figure 4.2, wherein the dashed line denotes December 1994. A mean increase can be seen clearly around December 1999 ($t = 120$), and henceforth, our main purpose in this example is to check whether the control charts can detect a mean increase before that time point.

The sample mean, variance, zero proportion and CRL of Phase I data are obtained as 0.9167, 1.5353, 0.5667 and 2.2308, respectively, which indicates over-dispersion and zero-inflation in the series. The ACF and PACF plots are given in Figure 4.3, indicating that the process is first-order Markovian. The sample auto-correlation is calculated as 0.2924.

We fit PINAR(1), ZIPINAR(1), PINARCH(1) and ZIPINARCH(1) models to

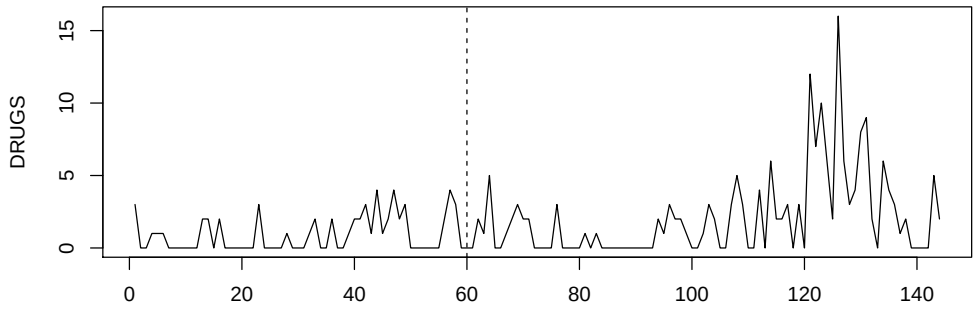

Figure 4.2: Sample path of drugs data (from January 1990 to December 2001)

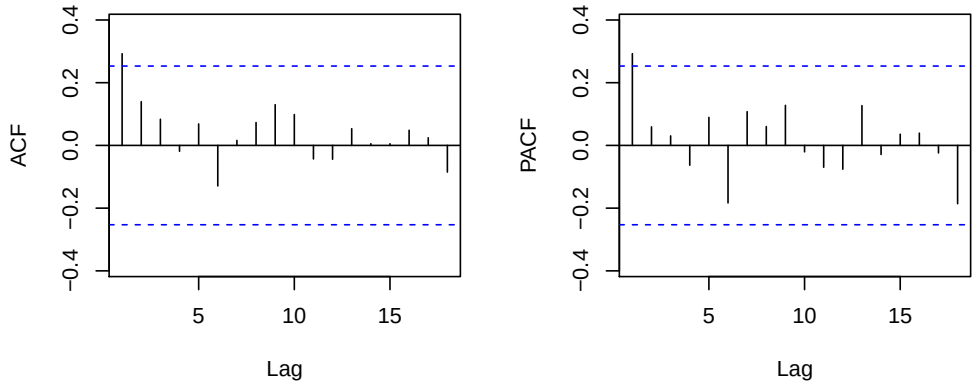

Figure 4.3: ACF and PACF plot of drugs data (January 1990 - December 1994)

Phase I sample. In addition to these models, the following models are also considered:

- i.i.d. geometric distribution.
- i.i.d. Poisson distribution.
- GINAR(1); INAR(1) model with geometric marginals (Alzaid and Al-Osh, 1988).
- NGINAR(1); negative binomial thinning based INAR(1) model with geometric

marginals (Ristić et al., 2009).

- NBINAR(1); INAR(1) model with negative binomial marginals (McKenzie, 1986; Weiß, 2008).
- INARKF(1); INAR(1) model with Katz family innovations (Kim and Lee, 2017).

For model selection, we calculate the ML estimates and Akaike information criterion (AIC) and Bayesian information criterion (BIC) values. The initial value in ML estimation is chosen based on the sample moments and the relationships in (4.2.4)-(4.2.7). Table 4.6 shows that the ZIPINARCH(1) model is the best fit. The ML estimates are obtained as $\hat{\alpha} = 0.4604$, $\hat{\omega} = 1.0586$ and $\hat{\rho} = 0.3983$. Based on these values, the corresponding $\hat{\gamma}$, $\hat{\mu}$, $\hat{\mu}_1^*$ and $\hat{\mu}_2^*$ are obtained as 0.2770, 0.8810, 1.9849 and 2.7679, respectively. Also, $\hat{\mathbb{E}}(\mathrm{CRL}_1)$ and $\hat{\mathbb{E}}(\mathrm{CRL}_2)$ are 2.4154 and 2.2531.

Below, we design the control charts with ARL_0 near 500 to detect mean increase:

- Shewhart-type chart with $u = 7$ ($\mathrm{ARL}_0 = 473.8$).
- CUSUM chart with $k = 1$ and $h = 24$ ($\mathrm{ARL}_0 = 500.7$).
- CUSUM-DR chart with $r = 2$, $k^d = 3$ and $h^d = 8$ ($\mathrm{ARL}_0 = 509.8$).

Table 4.6: ML estimates, AIC and BIC of drugs data (Phase I: January 1990 - December 1994)

Model	ML estimates	AIC	BIC
i.i.d. geometric	$\hat{\mu} = 0.9167$	161.21	163.30
i.i.d. Poisson	$\hat{\lambda} = 0.9167$	172.42	174.51
GINAR(1)	$\hat{p} = 0.5192$, $\hat{\alpha} = 0.1944$	159.42	163.61
NGINAR(1)	$\hat{\mu} = 0.9196$, $\hat{\alpha} = 0.3844$	157.69	161.88
NBINAR(1)	$\hat{n} = 1.0891$, $\hat{p} = 0.5396$, $\hat{\rho} = 0.2002$	161.39	167.68
INARKF(1)	$\hat{\theta}_1 = 0.3780$, $\hat{\theta}_2 = 0.4917$, $\hat{\alpha} = 0.1934$	162.20	168.48
PINAR(1)	$\hat{\alpha} = 0.2527$, $\hat{\lambda} = 0.6899$	167.56	171.75
ZIPINAR(1)	$\hat{\alpha} = 0.1329$, $\hat{\lambda} = 1.6395$, $\hat{\rho} = 0.5148$	156.84	163.13
PINARCH(1)	$\hat{\alpha} = 0.3981$, $\hat{\omega} = 0.5599$	164.01	168.20
ZIPINARCH(1)	$\hat{\alpha} = 0.4604$, $\hat{\omega} = 1.0586$, $\hat{\rho} = 0.3983$	**155.22**	**161.51**

- CRL-CUSUM chart with $k^c = 2$ and $h^c = 13$ ($\text{ARL}_0 = 486.5$).
- Combined Shewhart CRL-CUSUM chart with $u = 8$, $k^c = 2$ and $h^c = 15$ ($\text{ARL}_0 = 504.4$).

Figure 4.4 shows that these control charts have no false alarms in Phase I sample. Figure 4.5 provides the plots of control statistics applied to Phase II sample. The Shewhart-type, CUSUM and CUSUM-DR charts detect a mean increase at March 2000 ($t = 123$). However, this could be easily guessed without an aid of control charts. Notice that the CRL-CUSUM and combined Shewhart CRL-CUSUM charts respectively trigger an OoC signal at April 1999 ($t = 112$) and June 1999 ($t = 114$). The sample mean, autocorrelation, zero-proportion, and CRL of the data from January 1995 ($t = 61$) to March 2000 ($t = 123$) are given as 1.1587, 0.3522, 0.4603 and 1.8529, indicating that the mean increase is due to a decrease in zero-proportion.

4.6 Concluding remarks

In this study, we proposed a new CUSUM-type chart with delay rule and CRL-CUSUM charts and investigated their ATS performance when applied to detecting mean increase in counting processes with excessive zeros. For this purpose, we used the ZIPINAR(1) and ZIPINARCH(1) models and adopted the Markov chain method in the calculation of ATS values. When there is a small to moderate mean increase and zero-proportion is nearly fixed, the CUSUM-DR chart appeared to be quite effective. Meanwhile, when there is a small to moderate mean increase and also a decrease in zero-proportion, the CRL-CUSUM and combined Shewhart CRL-CUSUM charts outperformed the others. Overall, our findings confirm the validity

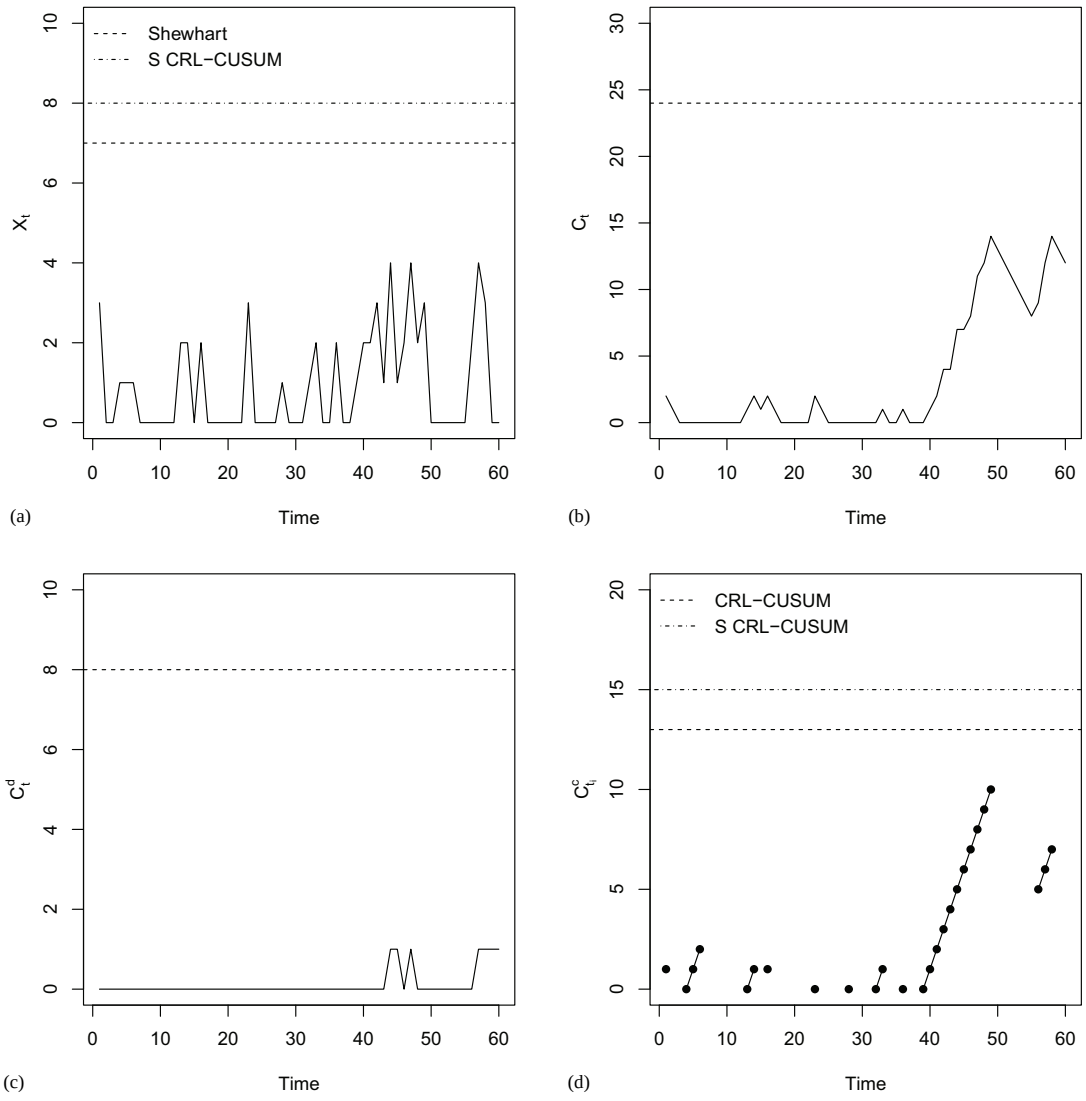

Figure 4.4: Plot of control charts (January 1990 - December 1994); (a) Shewhart-type chart; (b) CUSUM chart; (c) CUSUM-DR chart; (d) CRL-CUSUM and S CRL-CUSUM chart

of the proposed charts and show their potential as a functional SPC tool to detect mean increase in high-quality processes. Our charts are applicable to other distributions, e.g. zero-inflated negative binomial distributions, and more general models.

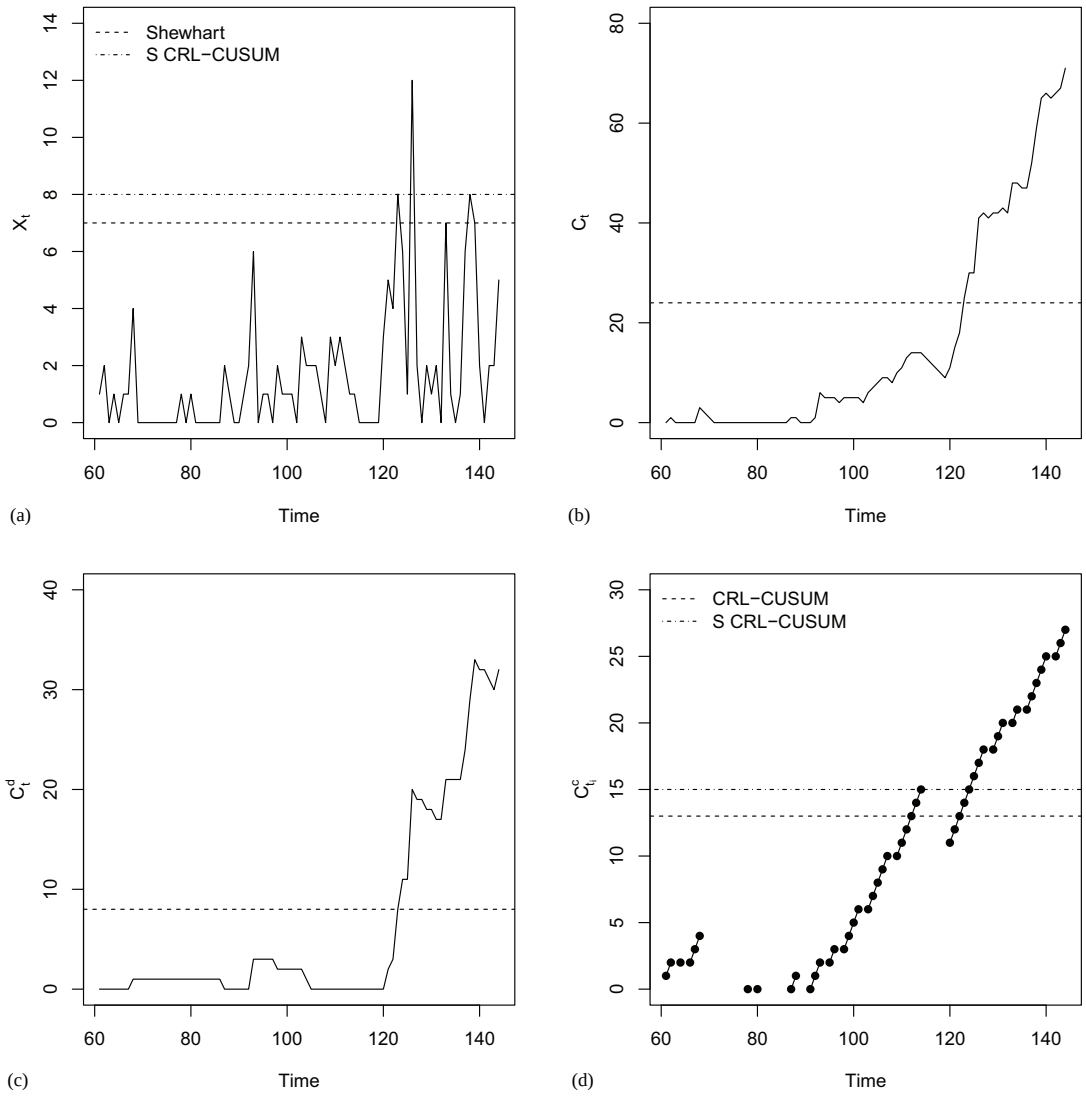

Figure 4.5: Plot of control charts (January 1995 - December 2001); (a) Shewhart-type chart; (b) CUSUM chart; (c) CUSUM-DR chart; (d) CRL-CUSUM and S CRL-CUSUM chart

The task of extension to more general and various situations is left to our future project.

4.7 Appendix A. ARL computation for CUSUM-DR chart

For calculating the ARL of CUSUM-DR charts, we take the Markov chain approach taken by Brook and Evans (1972). For an overview of the Markov chain approach for the performance evaluation of control charts, we refer to Weiss and Testik (2009) and Li et al. (2014). In Appendix 4.7 and 4.8, we suppose that $\{X_t\}_{t\in\mathbf{N}}$ follows either a stationary ZIPINAR(1) or ZIPINARCH(1) model. It is obvious that the bivariate process $\{(X_t, C_t^d)\}_{t\in\mathbf{N}}$ defined by $\{X_t\}$ and Equation (4.3.17) forms a bivariate Markov chain with transition probabilities:

$$\begin{aligned} p^d(a,b|c,d) &\equiv P(X_{t+1}=a, C_{t+1}^d=b|X_t=c, C_t^d=d) \\ &= p_{ca}\mathbb{1}(b=\mathbb{1}(a\geq r)\max(d+a-k^d,0)+\mathbb{1}(a<r)d), \end{aligned}$$

where $a,b,c,d\in\mathbf{N_0}$ and $r\in\mathbf{N}$. Moreover, the initial probabilities are given as

$$\begin{aligned} p_1^d(a,b|c) &\equiv P(X_1=a, C_1^d=b|C_0^d=c) \\ &= p_a\mathbb{1}(b=\mathbb{1}(a\geq r)\max(c+a-k^d,0)+\mathbb{1}(a<r)c), \end{aligned}$$

where $a,b,c\in\mathbf{N_0}$ and $r\in\mathbf{N}$.

Based on the predetermined design parameter (k^d,h^d), consider

$$\mathbf{Q^d} = \begin{pmatrix} p^d(0,0|0,0) & p^d(0,1|0,0) & \cdots & p^d(l_x^d, l_c^d|0,0) \\ p^d(0,0|0,1) & p^d(0,1|0,1) & \cdots & p^d(l_x^d, l_c^d|0,1) \\ \vdots & \vdots & \ddots & \vdots \\ p^d(0,0|l_x^d, l_c^d) & p^d(0,1|l_x^d, l_c^d) & \cdots & p^d(l_x^d, l_c^d|l_x^d, l_c^d) \end{pmatrix},$$

$$\boldsymbol{\mu^d} = (\mu^d_{0,0}, \mu^d_{0,1}, \ldots, \mu^d_{l_x^d, l_c^d})^\top,$$

where $l_x^d = h^d + k^d - 1$, $l_c^d = h^d - 1$ and $\boldsymbol{\mu^d}$ is the solution of the linear equation $(\mathbf{I}-\mathbf{Q})\cdot\boldsymbol{\mu^d} = \mathbf{1}$. For the vector $\boldsymbol{\mu^d}$, $\mu^d_{a,b}$, for $a \in \{0, 1, \ldots, l_x^d\}$ and $b \in \{0, 1, \ldots, l_c^d\}$ can be interpreted as the expected number of plotting before the control chart triggers an OoC signal when it starts from IC state $(X_1 = a, C_1^d = b)$. Then the ARL value with the initial state $C_0^d = c_0^d$, $\mathrm{ARL}^d(c_0^d)$, is obtained as follows:

$$\mathrm{ARL}^d(c_0^d) = 1 + \sum_{a,b} p_1^d(a,b|c_0^d) \cdot \mu^d_{a,b}$$

for $a \in \{0, 1, \ldots, l_x^d\}$ and $b \in \{0, 1, \ldots, l_c^d\}$.

4.8 Appendix B. ATS computation for CRL-CUSUM chart

Consider the bivariate process $\{(Y_i, C_i^c)\}_{i\in\mathbf{N}}$, where Y_i is the ith positive value and C_i^c is defined as the same as that in (4.3.20). Because the distribution of CRL_{i+1} is completely determined by Y_i and Y_{i+1}, we can easily see that $\{(Y_i, C_i^c)\}_{i\in\mathbf{N}}$ forms a

bivariate Markov chain with transition probabilities:

$$\begin{aligned} p^c(a,b|c,d) &\equiv P(Y_{i+1}=a, C^c_{i+1}=b|Y_i=c, C^c_i=d) \\ &= P(Y_{i+1}=a|Y_i=c)P(C^c_{i+1}=b|Y_{i+1}=a, Y_i=c, C^c_i=d) \\ &= P(Y_{i+1}=a|Y_i=c)P(b=\max(d+k^c-\mathrm{CRL}_{i+1},0)|Y_{i+1}=a, Y_i=c) \end{aligned}$$

for $a, c \in \mathbf{N}$ and $b, d \in \mathbf{N_0}$.

Note that when $b = 0$,

$$\begin{aligned} &P(b=\max(d+k^c-\mathrm{CRL}_{i+1},0)|Y_{i+1}=a, Y_i=c) \\ &\quad= P(\mathrm{CRL}_{i+1} \geq d+k^c|Y_{i+1}=a, Y_i=c) \\ &\quad= \frac{P(\mathrm{CRL}_{i+1} \geq d+k^c, Y_{i+1}=a|Y_i=c)}{P(Y_{i+1}=a|Y_i=c)} \\ &\quad= \begin{cases} 1 & \text{if } d+k^c=1 \\ \frac{p_{c0}p_{0a}p_{00}^{d+k^c-2}}{(1-p_{00})P(Y_{i+1}=a|Y_i=c)} & \text{if } d+k^c>1. \end{cases} \end{aligned}$$

Meanwhile, when $b > 0$,

$$\begin{aligned} &P(b=\max(d+k^c-\mathrm{CRL}_{i+1},0)|Y_{i+1}=a, Y_i=c) \\ &\quad= P(\mathrm{CRL}_{i+1}=d+k^c-b|Y_{i+1}=a, Y_i=c) \\ &\quad= \frac{P(\mathrm{CRL}_{i+1}=d+k^c-b, Y_{i+1}=a|Y_i=c)}{P(Y_{i+1}=a|Y_i=c)} \\ &\quad= \begin{cases} \frac{p_{ca}}{P(Y_{i+1}=a|Y_i=c)} & \text{if } b=d+k^c-1 \\ \frac{p_{c0}p_{0a}p_{00}^{d+k^c-b-2}}{P(Y_{i+1}=a|Y_i=c)} & \text{if } b<d+k^c-1 \\ 0 & \text{if } b>d+k^c-1. \end{cases} \end{aligned}$$

Since

$$\begin{aligned} P(Y_{i+1} = a|Y_i = c) &= \sum_{j=1}^{\infty} P(Y_{i+1} = a, \mathrm{CRL}_{i+1} = j|Y_i = c) \\ &= p_{ca} + \sum_{j=2}^{\infty} p_{c0} p_{00}^{j-2} p_{0a} \\ &= p_{ca} + \frac{p_{c0} p_{0a}}{1 - p_{00}}, \end{aligned}$$

$p^c(a, b|c, d)$ is explicitly given as

$$p^c(a,b|c,d) = \begin{cases} p_{ca} + \frac{p_{c0}p_{0a}}{1-p_{00}} & \text{if } b = 0 \text{ and } d + k^c = 1 \\ \frac{p_{c0}p_{0a}p_{00}^{d+k^c-2}}{1-p_{00}} & \text{if } b = 0 \text{ and } d + k^c > 1 \\ p_{ca} & \text{if } b > 0 \text{ and } b = d + k^c - 1 \\ p_{c0}p_{0a}p_{00}^{d+k^c-b-2} & \text{if } b > 0 \text{ and } b < d + k^c - 1 \\ 0 & \text{if } b > d + k^c - 1. \end{cases}$$

Similarly, we obtain the initial probabilities as

$$\begin{aligned} p_1^c(a, b|c) &\equiv P(Y_1 = a, C_1^c = b|C_0^c = c) \\ &= P(Y_1 = a)P(C_1^c = b|Y_1 = a, C_0^c = c) \\ &= \begin{cases} p_a + \frac{p_0 p_{0a}}{1-p_{00}} & \text{if } b = 0 \text{ and } c + k^c = 1 \\ \frac{p_0 p_{0a} p_{00}^{c+k^c-2}}{1-p_{00}} & \text{if } b = 0 \text{ and } c + k^c > 1 \\ p_a & \text{if } b > 0 \text{ and } b = c + k^c - 1 \\ p_0 p_{0a} p_{00}^{c+k^c-b-2} & \text{if } b > 0 \text{ and } b < c + k^c - 1 \\ 0 & \text{if } b > c + k^c - 1. \end{cases} \end{aligned}$$

Since the reachable IC values of a are unbounded, they must be replaced with

a bounded set by using a limiting condition such as $a \leq M$ for a sufficiently large $M \in \mathbf{N}$. Here we use $M = \lfloor \mu + 20\sigma \rfloor + 1$ as mentioned in Subsection 4.2.3. Despite the obtained values of ATS are only approximates, the precision level can be feasibly controlled by a proper selection of M.

Let (k^c,h^c) be the predetermined design parameter of the CRL-CUSUM chart. Similarly to the CUSUM-DR chart, we consider

$$\mathbf{Q^c} = \begin{pmatrix} p^c(1,0|1,0) & p^c(1,1|1,0) & \cdots & p^c(l_x^c, l_c^c|1,0) \\ p^c(1,0|1,1) & p^c(0,1|1,1) & \cdots & p^c(l_x^c, l_c^c|1,1) \\ \vdots & \vdots & \ddots & \vdots \\ p^c(1,0|l_x^c, l_c^c) & p^c(0,1|l_x^c, l_c^c) & \cdots & p^c(l_x^c, l_c^c|l_x^c, l_c^c) \end{pmatrix},$$

$$\boldsymbol{t^c} = (t^c_{1,0}, t^c_{1,1}, \ldots, t^c_{l_x^c, l_c^c})^\top \text{ with } t^c_{a,b} = \mathbb{E}(T|X_0 = a),$$

$$\boldsymbol{\mu^c} = (\mu^c_{1,0}, \mu^c_{1,1}, \ldots, \mu^c_{l_x^c, l_c^c})^\top,$$

where $l_x^c = \lfloor \mu + 20\sigma \rfloor + 1$, $l_c^c = h^c - 1$, $\mathbb{E}(T|X_0 = x)$'s are the ones in Equation (4.2.14) and $\boldsymbol{\mu^c}$ is the solution of the linear equation $(\mathbf{I} - \mathbf{Q}) \cdot \boldsymbol{\mu^c} = \boldsymbol{t^c}$. The $t^c_{a,b}$ in vector $\boldsymbol{t^c}$ denotes the expected next conforming run length when the current non-zero observation is given as a. It is obvious that $t^c_{a,b}$ does not depend on the value of b. Note that unlike the CUSUM-DR chart, $\mu^c_{a,b}$ in vector $\boldsymbol{\mu^c}$ stands for the expected elapsed time until the control chart triggers an OoC signal when it starts from IC state $(Y_1 = a, C_1^c = b)$ with $a \in \{1, 2, \ldots, l_x^c\}$ and $y \in \{0, 1, \ldots, l_c^c\}$. Based on those, the ATS value with initial state $C_0^c = c_0^c$, $\text{ATS}^c(c_0^c)$, is given as

$$\text{ATS}^c(c_0^c) = \mathbb{E}(\text{CRL}_1) + \sum_{a,b} p_1^c(a, b|c_0^c) \cdot \mu^c_{a,b},$$

where $a \in \{1, 2, \ldots, l_x^c\}$, $b \in \{0, 1, \ldots, l_c^c\}$ and $\mathbb{E}(\mathrm{CRL}_1)$ is the one in Equation (4.3.18).

Note that the ATS computation of the combined Shewhart CRL-CUSUM chart can be obtained by putting $l_x^c = u - 1$, where u is the control limit of the corresponding Shewhart-type chart.

Chapter 5

Monitoring Mean Shift in INAR(1)s Processes based on CLSE-CUSUM Procedure

5.1 Introduction

Bourguignon et al. (2016) recently consider the seasonal INAR(1) process with seasonal period $s \in \mathbf{N}$ (INAR(1)s) as follows:

$$X_t = \alpha \circ X_{t-s} + \epsilon_t, \qquad t \in \mathbf{Z}. \tag{5.1.1}$$

Statistical properties, such as the existence of stationary solutions, explicit form of autocorrelation function and transition probabilities can be found in Bourguignon et al. (2016).

Weiss and Testik (2009) study the upper one-sided CUSUM control charts for

Poisson INAR(1) processes and Yontay et al. (2013) consider the two-sided CUSUM control chart by combining the one-sided CUSUM charts. The two-sided CUSUM control statistic is defined as:

$$\begin{aligned} C_0^+ &= c_0^+, \\ C_t^+ &= \max\left(0, X_t - k^+ + C_{t-1}^+\right), \quad t \in \mathbf{N}, \\ C_0^- &= c_0^-, \\ C_t^- &= \max\left(0, k^- - X_t + C_{t-1}^-\right), \quad t \in \mathbf{N}, \end{aligned}$$

where c_0^+ and c_0^- are starting values, k^+ and k^- are reference values, and h^+, h^- are control limits of upper and lower one-sided CUSUM charts. When $C_t^+ \geq h^+$ or $C_t^- \geq h^-$ occurs, the process of interest is regarded as out-of-control.

In this chapter, we consider the CUSUM test based on conditional least squares estimator (CLSE) from INAR(1)s processes and apply it to monitoring the mean shift of Poisson INAR(1) processes. Based on this, we construct the one-sided control statistic and compare its performance with conventional CUSUM charts. As a relevant work, we refer to Huh et al. (2017) who use the conditional maximum likelihood (MLE)in integer-valued generalized autoregressive conditional heteroskedasticity (INGARCH) models.

This chapter is organized as follows. Section 5.2 presents the difference equations as to the moments of INAR(1)s processes. Moreover, the CLSE-CUSUM test statistic is introduced. Section 5.3 designs a new control statistic for monitoring mean shift based on the results in Section 5.2. Section 5.4 compares the proposed control procedure with the CUSUM chart based on numerical experiments using ARL, standard deviation (SD) and median. Section 5.5 illustrates a real data anal-

ysis demonstrating the superiority of our proposed procedure to the CUSUM chart. Sections 5.6 and 5.7 provide technical proofs and concluding remarks.

5.2 Higher moments and CLSE-based CUSUM test

In this section, we show the existence of a 4th moment and provide related difference equations for stationary INAR(1)s processes. These are important in the construction of the control statistic in Section 5.3.

Proposition 5.2.1. *Suppose that* $\alpha \in [0,1)$ *and* $\mathbb{E}\epsilon_t^4 < \infty$. *Then, we have* $EX^k \leq C < \infty$, $k = 1,2,3,4$, *for some* $C > 0$, *where* X *is the unique stationary limit of* X_t *in distribution.*

Difference equations for moments are obtained by using the properties of Binomial thinning operator.

Proposition 5.2.2. *Let* $\{X_t\}_{t\in\mathbf{Z}}$ *be a stationary INAR(1)s process with* $\alpha \in [0,1)$, $\mu_{\epsilon,k} = \mathbb{E}\epsilon_t^k < \infty$, $k = 1,2,3,4$, *and* $\sigma_\epsilon^2 = \mu_{\epsilon,2} - \mu_{\epsilon,1}^2$. *Then, for* $u, v, w \in \mathbf{N}$ *with* $u < v < w$,

$$(a)\ \mu_{\mathbf{x},1} := \mathbb{E}X_t = \frac{\mu_{\epsilon,1}}{1-\alpha}.$$

$$(b)\ \mu_{\mathbf{x},2} := \mathbb{E}X_t^2 = \frac{\alpha\mu_{\epsilon,1} + \sigma_\epsilon^2}{1-\alpha^2} + \frac{\mu_{\epsilon,1}^2}{(1-\alpha)^2}.$$

$$(c)\ \mu_{\mathbf{x},3} := \mathbb{E}X_t^3 = \frac{1}{1-\alpha^3}\Big[3\alpha^2(1-\alpha+\mu_{\epsilon,1})\mu_{\mathbf{x},2} + \alpha\left((1-\alpha)(1-2\alpha) + 3(1-\alpha)\mu_{\epsilon,1} + 3\mu_{\epsilon,2}\right)\mu_{\mathbf{x},1} + \mu_{\epsilon,3}\Big].$$

$$(d)\ \mu_{\mathbf{x},4} := \mathbb{E}X_t^4 = \frac{1}{1-\alpha^4}\Big[\left(6\alpha^3(1-\alpha)+4\alpha^3\mu_{\epsilon,1}\right)\mu_{\mathbf{x},3}$$
$$+\left(\alpha^2(1-\alpha)(7-11\alpha)+12\alpha^2(1-\alpha)\mu_{\epsilon,1}+6\alpha^2\mu_{\epsilon,2}\right)\mu_{\mathbf{x},2}$$
$$+\left(\alpha(1-\alpha)(1-6\alpha+6\alpha^2)+4\alpha(1-\alpha)(1-2\alpha)\mu_{\epsilon,1}+6\alpha(1-\alpha)\mu_{\epsilon,2}+4\alpha\mu_{\epsilon,3}\right)\mu_{\mathbf{x},1}$$
$$+\mu_{\epsilon,4}\Big].$$
$$(e)\ \mu_{\mathbf{x}_{(s)}}(u) := \mathbb{E}(X_tX_{t+us}) = \alpha\mu_{\mathbf{x}_{(s)}}(u-1)+\frac{\mu_{\epsilon,1}^2}{(1-\alpha)}$$
$$(f)\ \mu_{\mathbf{x}_{(s)}}(0,u) := \mathbb{E}\left(X_t^2X_{t+us}\right) = \alpha\mu_{\mathbf{x}_{(s)}}(0,u-1)+\mu_{\epsilon,1}\mu_{\mathbf{x},2}.$$
$$(g)\ \mu_{\mathbf{x}_{(s)}}(u,u) := \mathbb{E}\left(X_tX_{t+us}^2\right) = \alpha^2\mu_{\mathbf{x}_{(s)}}(u-1,u-1)$$
$$+\left(\alpha(1-\alpha)+2\alpha\mu_{\epsilon,1}\right)\mu_{\mathbf{x}_{(s)}}(u-1)+\mu_{\mathbf{x},1}\mu_{\epsilon,2}.$$
$$(h)\ \mu_{\mathbf{x}_{(s)}}(u,v) := \mathbb{E}\left(X_tX_{t+us}X_{t+vs}\right) = \alpha\mu_{\mathbf{x}_{(s)}}(u,v-1)+\mu_{\epsilon,1}\mu_{\mathbf{x}_{(s)}}(u).$$
$$(i)\ \mu_{\mathbf{x}_{(s)}}(0,0,u) := \mathbb{E}\left(X_t^3X_{t+us}\right) = \alpha\mu_{\mathbf{x}_{(s)}}(0,0,u-1)+\mu_{\epsilon,1}\mu_{\mathbf{x},3}.$$
$$(j)\ \mu_{\mathbf{x}_{(s)}}(0,u,u) := \mathbb{E}\left(X_t^2X_{t+us}^2\right) = \alpha^2\mu_{\mathbf{x}_{(s)}}(0,u-1,u-1)$$
$$+\mu_{\epsilon,2}\mu_{\mathbf{x},2}+2\alpha\mu_{\epsilon,1}\mu_{\mathbf{x},1}+\alpha(1-\alpha)\mu_{\mathbf{x}_{(s)}}(0,u-1).$$
$$(k)\ \mu_{\mathbf{x}_{(s)}}(0,u,v) := \mathbb{E}\left(X_t^2X_{t+us}X_{t+vs}\right) = \alpha\mu_{\mathbf{x}_{(s)}}(0,u,v-1)+\mu_{\epsilon,1}\mu_{\mathbf{x}_{(s)}}(0,u).$$
$$(l)\ \mu_{\mathbf{x}_{(s)}}(u,u,u) := \mathbb{E}\left(X_tX_{t+us}^3\right) = \alpha^3\mu_{\mathbf{x}_{(s)}}(u-1,u-1,u-1)$$
$$+3\alpha\left(\mu_{\epsilon,1}+\alpha(1-\alpha)\right)\mu_{\mathbf{x}_{(s)}}(u-1,u-1)$$
$$+\left(\alpha(1-3\alpha+2\alpha^2)+3\mu_{\epsilon,2}\right)\mu_{\mathbf{x}_{(s)}}(u-1)+\mu_{\epsilon,3}.$$
$$(m)\ \mu_{\mathbf{x}_{(s)}}(u,u,v) := \mathbb{E}\left(X_tX_{t+us}^2X_{t+vs}\right) = \alpha\mu_{\mathbf{x}_{(s)}}(u,u,v-1)+\mu_{\epsilon,1}\mu_{\mathbf{x}_{(s)}}(u,u).$$
$$(n)\ \mu_{\mathbf{x}_{(s)}}(u,v,v) := \mathbb{E}\left(X_tX_{t+us}X_{t+vs}^2\right) = \alpha^2\mu_{\mathbf{x}_{(s)}}(u,v-1,v-1)$$
$$+\left(\alpha(1-\alpha)+2\alpha\mu_{\epsilon,1}\right)\mu_{\mathbf{x}_{(s)}}(u,v-1)+\mu_{\epsilon,2}\mu_{\mathbf{x}_{(s)}}(u).$$
$$(o)\ \mu_{\mathbf{x}_{(s)}}(u,v,w) := \mathbb{E}\left(X_tX_{t+us}X_{t+vs}X_{t+ws}\right) = \alpha\mu_{\mathbf{x}_{(s)}}(u,v,w-1)+\mu_{\epsilon,1}\mu_{\mathbf{x}_{(s)}}(u,v).$$

Given observations $X_{-s+1}, X_{-s+2}, \ldots, X_n$ from the stationary INAR(1)s process with $\mathbb{E}\epsilon_t = \mu_\epsilon \in (0,\infty)$, $\mathrm{Var}(\epsilon_t) = \sigma_\epsilon^2 \in (0,\infty)$ and autocorrelation $\alpha \in [0,1)$, the

CLSE, $\hat{\theta}_n = (\hat{\alpha}_n, \hat{\mu}_{\epsilon n})$, of parameter $\theta = (\alpha, \mu_\epsilon)$ can be obtained by minimizing the conditional sum of squares $S_n(\theta) := \sum_{t=1}^{n} (X_t - \alpha X_{t-s} - \mu_\epsilon)^2$ over $\theta \in \{0 \leq \alpha < 1, \mu_\epsilon > 0\}$, that is,

$$\hat{\alpha}_n = \frac{n \sum_{t=1}^{n} X_t X_{t-s} - \sum_{t=1}^{n} X_{t-s} \sum_{t=1}^{n} X_t}{n \sum_{t=1}^{n} X_{t-s}^2 - (\sum_{t=1}^{n} X_{t-s})^2}, \tag{5.2.2}$$

$$\hat{\mu}_{\epsilon n} = \frac{1}{n} \left(\sum_{t=1}^{n} X_t - \hat{\alpha}_n \sum_{t=1}^{n} X_{t-s} \right), \tag{5.2.3}$$

where $\hat{\alpha}_n$ is set to be 0 if its denominator is 0. By checking the regularity conditions in Klimko and Nelson (1978), one can see that the CLSE $\hat{\theta}_n$ enjoys the property of consistency and asymptotic normality.

Since Page (1955), the change point problem has been widely appreciated as an important issue in the time series analysis context, because ignorance of parameter changes leads to a false conclusion. The CUSUM test has been popular due to the ease at its usage among researchers: see Chen and Gupta (2011) for a general review and Lee et al. (2003) for time series models. In this study, we consider to utilize the CLSE-based CUSUM test in Lee and Na (2005) and Kang and Lee (2009) for detecting the change of θ.

We set up the null and alternative hypothesis as follows:

$H_0 : \theta_0 = (\alpha_0, \mu_{\epsilon 0})$ does not changes over $X_{-s+1}, \ldots, X_n$ vs.

$H_1 :$ not H_0.

Put

$$W = \begin{pmatrix} \mathbb{E}\left(X_{t-s}^2(X_t - \alpha_0 X_{t-s} - \mu_{\epsilon 0})^2\right) & \mathbb{E}\left(X_{t-s}(X_t - \alpha_0 X_{t-s} - \mu_{\epsilon 0})^2\right) \\ \mathbb{E}\left(X_{t-s}(X_t - \alpha_0 X_{t-s} - \mu_{\epsilon 0})^2\right) & \mathbb{E}(X_t - \alpha_0 X_{t-s} - \mu_{\epsilon 0})^2 \end{pmatrix}, \quad (5.2.4)$$

$$V = \begin{pmatrix} \mathbb{E}X_t^2 & \mathbb{E}X_t \\ \mathbb{E}X_t & 1 \end{pmatrix}. \quad (5.2.5)$$

Define

$$T_n^{cls} := \max_{\nu \le k \le n} T_{n,k}^{cls} = \max_{\nu \le k \le n} \frac{k^2}{n} \left(\hat{\theta}_k - \hat{\theta}_n\right)^\top \hat{V}_n \hat{W}_n^{-1} \hat{V}_n \left(\hat{\theta}_k - \hat{\theta}_n\right),$$

where ν is a positive integer,

$$\hat{V}_n = \begin{pmatrix} \frac{1}{n}\sum_{t=1}^n X_{t-s}^2 & \frac{1}{n}\sum_{t=1}^n X_{t-s} \\ \frac{1}{n}\sum_{t=1}^n X_{t-s} & 1 \end{pmatrix}, \quad (5.2.6)$$

$$\hat{W}_n = \begin{pmatrix} \frac{1}{n}\sum_{t=1}^n X_{t-s}^2(X_t - \hat{\alpha} X_{t-s} - \hat{\mu}_\epsilon)^2 & \frac{1}{n}\sum_{t=1}^n X_{t-s}(X_t - \hat{\alpha} X_{t-s} - \hat{\mu}_\epsilon)^2 \\ \frac{1}{n}\sum_{t=1}^n X_{t-s}(X_t - \hat{\alpha} X_{t-s} - \hat{\mu}_\epsilon)^2 & \frac{1}{n}\sum_{t=1}^n (X_t - \hat{\alpha} X_{t-s} - \hat{\mu}_\epsilon)^2 \end{pmatrix}. \quad (5.2.7)$$

Following the arguments in Lee and Na (2005) and Kang and Lee (2009), we can verify the following, the proof of which is omitted for brevity:

Theorem 5.2.1. *Under H_0, as $n \longrightarrow \infty$,*

$$T_n^{cls} \xrightarrow{w} \sup_{0 \le u \le 1} \|\mathbf{B}_2^\circ(u)\|^2,$$

where $\mathbf{B}_2^\circ(u) = (B_1^\circ(u), B_2^\circ(u))^\top$ is a 2-dimensional Brownian bridge.

Tables 5.1 and 5.2 show that the performance of the CLSE-CUSUM statistics with $\lambda = \mu_{\epsilon 0} + \delta\sqrt{\mu_{\epsilon 0}}$, $\alpha = \alpha_0 + \delta$ at the nominal level of 0.05 when the innovations follow a Poisson distribution with mean λ: the corresponding critical value is 2.408 (see Lee et al. 2003). Here, we use 1,000 repetitions. When n is small ($n = 250, 500$), the sizes are somewhat over-estimated, which becomes more prominent when α is higher ($\alpha = 0.75$). However, as n increases, the size approaches the predetermined

Table 5.1: Empirical sizes and power of the CLSE-CUSUM statistic for INAR(1) process with shift in $\lambda = \mu_{\epsilon 0} + \delta\sqrt{\mu_{\epsilon 0}}$ at the level of 0.05

				δ								
s	$\mu_{\epsilon 0}$	α_0	n	-0.6	-0.45	-0.3	-0.15	0	0.15	0.3	0.45	0.6
4	5	0.25	250	0.97	0.78	0.43	0.16	0.07	0.15	0.38	0.68	0.89
			500	1.00	0.99	0.72	0.23	0.06	0.21	0.65	0.95	1.00
			1000	1.00	1.00	0.97	0.41	0.05	0.38	0.93	1.00	1.00
			1500	1.00	1.00	1.00	0.56	0.05	0.54	0.99	1.00	1.00
			2000	1.00	1.00	1.00	0.71	0.05	0.68	1.00	1.00	1.00
		0.5	250	0.96	0.77	0.44	0.18	0.10	0.17	0.36	0.59	0.83
			500	1.00	0.96	0.66	0.23	0.09	0.21	0.57	0.88	0.99
			1000	1.00	1.00	0.93	0.35	0.06	0.33	0.87	1.00	1.00
			1500	1.00	1.00	0.99	0.50	0.05	0.47	0.97	1.00	1.00
			2000	1.00	1.00	1.00	0.64	0.05	0.58	0.99	1.00	1.00
		0.75	250	0.97	0.81	0.52	0.26	0.11	0.24	0.38	0.57	0.77
			500	1.00	0.97	0.68	0.28	0.11	0.24	0.53	0.82	0.96
			1000	1.00	1.00	0.92	0.38	0.10	0.32	0.80	0.98	1.00
			1500	1.00	1.00	0.98	0.50	0.07	0.41	0.94	1.00	1.00
			2000	1.00	1.00	1.00	0.60	0.05	0.51	0.98	1.00	1.00

Table 5.2: Empirical sizes and power of the CLSE-CUSUM statistic for INAR(1) process with shift in $\alpha = \alpha_0 + \delta$ at the level of 0.05

				δ								
s	$\mu_{\epsilon 0}$	α_0	n	-0.20	-0.15	-0.10	-0.05	0.00	0.05	0.10	0.15	0.20
12	7	0.25	250	0.86	0.60	0.29	0.10	0.06	0.19	0.56	0.89	0.99
			500	1.00	0.93	0.57	0.18	0.06	0.30	0.83	1.00	1.00
			1000	1.00	1.00	0.93	0.34	0.05	0.51	0.99	1.00	1.00
			1500	1.00	1.00	0.99	0.53	0.05	0.66	1.00	1.00	1.00
			2000	1.00	1.00	1.00	0.68	0.05	0.81	1.00	1.00	1.00
		0.5	250	0.86	0.64	0.35	0.13	0.07	0.25	0.69	0.97	1.00
			500	1.00	0.95	0.64	0.19	0.07	0.39	0.94	1.00	1.00
			1000	1.00	1.00	0.96	0.39	0.05	0.62	1.00	1.00	1.00
			1500	1.00	1.00	1.00	0.59	0.05	0.80	1.00	1.00	1.00
			2000	1.00	1.00	1.00	0.73	0.05	0.89	1.00	1.00	1.00
		0.75	250	0.93	0.78	0.50	0.21	0.10	0.43	0.94	1.00	1.00
			500	1.00	0.97	0.79	0.32	0.10	0.65	1.00	1.00	1.00
			1000	1.00	1.00	0.99	0.57	0.08	0.90	1.00	1.00	1.00
			1500	1.00	1.00	1.00	0.77	0.06	0.97	1.00	1.00	1.00
			2000	1.00	1.00	1.00	0.91	0.05	1.00	1.00	1.00	1.00

level. Moreover, the power tends to increase gradually when δ and n increase. Note that when there is a shift in λ the performance in the case of $\delta < 0$ is slightly better in terms of power than in the other case. It can be also seen that for shift in α, the performance in the case of $\delta > 0$ is much better than in the other case. Overall, the results confirm the validity of the CLSE-CUSUM statistic.

5.3 Monitoring mean shift using CLSE-CUSUM scheme

In this section, we modify the CUSUM test in Theorem 5.2.1 that can detect a parameter shift more efficiently in stationary INAR(1)s processes. Given predetermined positive integer $l > (s+1)$, playing a role such as the length of virtual in-control data, we put $\nu = l - s$ and define

$$C_n(\nu) = \max_{1\le k\le n} l'_{n,k}(\nu) = \max_{1\le k\le n} \frac{(k+\nu)^2}{n+\nu} \left(\hat{\theta}'_k - \hat{\theta}'_n\right)^\top VW^{-1}V \left(\hat{\theta}'_k - \hat{\theta}'_n\right), \qquad (5.3.8)$$

where $\hat{\theta}'_k = (\hat{\alpha}'_k, \hat{\mu}_{\epsilon k}')$ with

$$\hat{\alpha}'_k = \frac{(\nu+k)\sum_{t=-\nu+1}^{k} X_t X_{t-s} - \sum_{t=-\nu+1}^{k} X_{t-s} \sum_{t=-\nu+1}^{k} X_t}{(\nu+k)\sum_{t=-\nu+1}^{k} X_{t-s}^2 - (\sum_{t=-\nu+1}^{k} X_{t-s})^2},$$
$$\hat{\mu}_{\epsilon k}' = \frac{1}{(\nu+k)} \left(\sum_{t=-\nu+1}^{k} X_t - \hat{\alpha}'_k \sum_{t=-\nu+1}^{k} X_{t-s} \right);$$

Initial sums such as $\sum_{t=-\nu+1}^{0} X_t X_{t-s}$, $\sum_{t=-\nu+1}^{0} X_{t-s}$, $\sum_{t=-\nu+1}^{0} X_t$, and $\sum_{t=-\nu+1}^{0} X_{t-s}^2$ are replaced with $\nu\mathbb{E}X_tX_{t-s}$, $\nu\mathbb{E}X_t$, $\nu\mathbb{E}X_t$, and $\nu\mathbb{E}X_t^2$, respectively; W and V are calculated using the formula in Proposition 5.2.2. The same convergence result as

in Theorem 5.2.1 also holds for $C_n(\nu)$, regardless of ν.

We evaluate the CUSUM statistic with the Poisson INAR(1) with mean λ_0 in (5.1.1). In this case, the marginal mean is $\mu_0 = \lambda_0/(1-\alpha_0)$ and W and V are obtained as:

$$V = \begin{pmatrix} \mu_0 + \mu_0^2 & \mu_0 \\ \mu_0 & 1 \end{pmatrix}, \quad W = \begin{pmatrix} \mu_0(W_{1,1} + W_{1,2} + W_{1,3}) & \mu_0(W_{2,1} + W_{2,2} + W_{2,3}) \\ \mu_0(W_{2,1} + W_{2,2} + W_{2,3}) & W_{3,1} + W_{3,2} \end{pmatrix},$$

where $W_{1,1} = (1+\mu_0)(\lambda_0^2 + \mu_0 - 2\lambda_0\mu_0 + \mu_0^2)$, $W_{1,2} = \alpha_0(1 + 2(1+\lambda_0)\mu_0 - 2(1-\lambda_0)\mu_0^2 - 2\mu_0^3)$, $W_{1,3} = -\alpha_0^2(1 + 3\mu_0 - \mu_0^3)$, $W_{2,1} = \lambda_0^2 + \mu_0 - 2\lambda_0\mu_0 + \mu_0^2$, $W_{2,2} = \alpha_0(1+2\lambda_0\mu_0 - 2\mu_0^2)$, $W_{2,3} = -\alpha_0^2(1+\mu_0-\mu_0^2)$, $W_{3,1} = \lambda_0^2 - 2\lambda_0\mu_0 + \mu_0 + 2\alpha_0\lambda_0\mu_0 + \mu_0^2$, $W_{3,2} = \alpha_0^2\mu_0(1+\mu_0) - 2\alpha_0\mu_0(\alpha_0+\mu_0)$.

Note that in the case of INAR(1) process with Poisson innovations, the elements of W can be obtained from Proposition 1 in Weiß (2012).

Tables 5.3 and 5.4 show the ARL profiles, compared with the conventional two-

Table 5.3: ARLs of the CLSE-CUSUM test statistic and conventional two-sided CUSUM chart for INAR(1) process with shift in $\lambda = \lambda_0 + \delta\sqrt{\lambda_0}$

				δ								
μ_0	α_0	ν	c	-0.2	-0.15	-0.1	-0.05	0	0.05	0.1	0.15	0.2
2.5	0.25		CUSUM (3,19,2,15):	155.7	229.4	338.8	459.5	510.7	440.8	322.1	224.8	158.3
		100	1.374	298.6	448.6	510.5	559.1	510.8	398.6	309.5	213.6	147.1
		250	1.151	149.3	227.9	355.0	505.0	510.7	387.5	263.8	177.7	127.6
		500	0.955	147.6	203.6	301.1	466.4	510.6	396.2	261.7	183.2	136.5
		750	0.828	153.9	207.0	297.3	453.5	510.8	398.3	270.3	192.1	145.0
2.5	0.5		CUSUM (3,29,2,22):	144.4	210.8	307.8	429.2	492.4	438.6	325.3	231.5	165.0
		100	1.380	390.4	509.8	573.4	530.2	492.1	403.0	305.1	217.6	159.5
		250	1.140	166.9	254.0	381.4	486.8	493.4	385.7	266.1	184.6	134.1
		500	0.942	158.5	221.9	324.2	452.1	492.6	388.8	268.0	189.6	144.6
		750	0.809	162.2	222.1	313.5	436.4	492.9	386.1	273.4	197.1	153.5
2.5	0.75		CUSUM (4,22,2,40):	143.8	202.2	296.1	413.5	497.6	477.4	386.1	292.1	216.5
		100	1.401	580.4	656.9	624.0	590.2	497.5	381.4	275.5	203.5	149.8
		250	1.146	197.5	303.8	440.0	528.4	497.6	384.7	264.6	189.5	139.5
		500	0.937	171.5	238.5	352.0	480.9	497.6	382.3	268.2	195.5	150.1
		750	0.808	173.4	235.3	334.9	467.8	497.6	389.9	277.0	204.5	159.2

sided CUSUM chart (CUSUM(k^+,h^+,k^-,h^-) with $c_0^+ = c_0^- = 0$) when the parameters change to $\lambda = \lambda_0 + \delta\sqrt{\lambda_0}$ and $\alpha = \alpha_0 + \delta$. Here, we use 30,000 repetitions. The tables show that the CLSE-CUSUM control procedure outperforms the two-sided CUSUM chart regardless of ν when there is an up-shift in λ. Overall, the ARL performance appears to be the best at $\nu = 250$ when there is an up-shift in λ. However, the performance of the proposed procedure performs poorly when there is a down-shift in λ or α which becomes clearer as ν gets smaller. When there is an up-shift in α, the performance of the two charts does not differ significantly expect $\nu = 100$. For $\nu = 100$, there are cases such that the out-of-control ARL is larger than the in-control ARL when there is a down-shift in λ or α, although this phenomenon is mitigated as ν increases. Such a case often occurs when the difference between the in-control ARLs of the two one-sided charts is large, especially when the in-control ARL of the upper one-sided chart is smaller than the lower one-sided chart: see, for example, Yontay et al. (2013). We can easily guess that for the given

Table 5.4: ARLs of the CLSE-CUSUM test statistic and conventional two-sided CUSUM chart for INAR(1) process with shift in $\alpha = \alpha_0 + \delta$

				δ								
μ_0	α_0	ν	c	-0.2	-0.15	-0.1	-0.05	0	0.05	0.1	0.15	0.2
2.5	0.25		CUSUM									
			(3,19,2,15):	108.3	171.6	292.9	489.0	512.3	263.5	119.9	63.5	38.9
		100	1.374	87.9	145.5	333.9	525.4	510.8	299.3	129.3	61.9	36.8
		250	1.151	84.1	111.3	179.0	375.3	510.7	253.9	111.1	62.3	40.5
		500	0.955	94.7	120.6	174.7	320.6	510.6	253.8	119.3	69.7	45.9
		750	0.828	102.8	129.2	181.7	313.8	510.8	260.4	126.5	75.1	49.7
2.5	0.5		CUSUM									
			(3,29,2,22):	78.7	117.2	200.2	386.2	491.9	230.0	94.9	48.9	30.0
		100	1.380	90.1	138.4	280.5	519.3	492.1	269.4	110.0	50.6	27.8
		250	1.140	84.8	109.9	167.6	355.1	493.4	222.5	93.4	50.0	30.0
		500	0.942	95.2	119.4	167.6	304.5	492.6	224.2	99.9	55.3	33.4
		750	0.809	102.6	127.2	174.1	297.2	492.9	229.7	105.7	58.8	35.5
2.5	0.75		CUSUM									
			(4,22,2,40):	65.5	86.5	134.3	279.7	500.6	185.5	57.0	25.3	15.3
		100	1.401	91.5	125.2	216.4	464.5	497.5	223.6	64.6	25.6	14.3
		250	1.146	83.4	103.4	149.0	291.2	497.6	163.8	56.6	25.9	15.0
		500	0.937	91.8	111.0	151.4	258.6	497.6	162.6	59.9	27.6	16.0
		750	0.808	98.6	118.5	159.0	261.5	497.6	167.9	62.7	28.8	16.5

control limit c, the out-of-control state signals including false alarms are mainly caused by the up-shifts of parameter. Hence, if one uses the one control limit for the two-sided monitoring, it may lead to a biased ARL performance. This problem could be avoided by using proper lower and upper one-sided control limits.

Based on these findings, we design the one-sided CLSE-CUSUM statistic-based control procedure as follows: given observations $X_{-s+1}, X_{-s+2}, \ldots, X_n$ from the stationary INAR(1)s process with $\alpha_0 \in [0,1)$, $\mathbb{E}X_t = \mu_0 > 0$ and $\mathbb{E}X_t^4 < \infty$, let $c_p(\nu, n) = \underset{1\le k\le n}{\operatorname{argmax}}\, l'_{n,k}(\nu)$, where $l'_{n,k}(\cdot)$ are in (5.3.8) and $\bar{X}_{c_p(\nu,n)} = \sum_{k=c_p(\nu,n)}^{n} X_k$ for $\nu \ge 2$. Note that $c_p(\nu, n)$ is an estimated location of change point when it exists. The upper one-sided CLSE-CUSUM control statistic is then:

$$C_n^u(\nu_u) = C_n(\nu_u) I(\bar{X}_{c_p(\nu_u,n)} > \mu_0),\ n \in \mathbf{N}, \tag{5.3.9}$$

while the lower one-sided CLSE-CUSUM control statistic is:

$$C_n^l(\nu_l) = C_n(\nu_l) I(\bar{X}_{c_p(\nu_l,n)} < \mu_0),\ n \in \mathbf{N},$$

where $C_n(\cdot)$ is the one in (5.3.8), $I(\cdot)$ is an indicator function, and $\nu_u \ge 2$ and $\nu_l \ge 2$ are predetermined positive integers. Given control limits $c_u > 0$ and $c_l > 0$, we determine that the process is out-of-control when $C_n^u(\nu_u) \ge c_u$ or $C_n^l(\nu_l) \ge c_l$ is signaled, that is, the signal of out-of-control state is triggered by a mean increase (the former case) or a mean decrease (the latter case).). The fundamental difference between the proposed and conventional methods lies in that ours uses additional information in estimation when determining the status of the process of interest.

5.4 Performance comparison

We focus on the upper one-sided control chart for detecting a mean increase, since this case receives more attention in practice. To compare with the upper one-sided CUSUM chart (CUSUM(k, h) with $c_0 = 0$), we adopt the reference value and corresponding control limit in Weiss and Testik (2009). Let $\{X_t\}_{t\in\mathbb{Z}}$ be a stationary INAR(1) process with $\alpha_0 \in [0, 1)$ and Poisson innovations with meanλ_0. In this case, the marginal mean is obtained as$\mu_0 = \lambda_0/(1 - \alpha_0)$. Numerical experiments show that the performance of our procedure and the CUSUM chart is not much affected by the values of μ and λ for fixed α, so we only take account of the case that $\mu_0 = \lambda_0/(1 - \alpha_0) = 2.5$ and $\alpha_0 \in \{0.25, 0.5, 0.75\}$. These values are assumed to change to $\mu = \lambda/(1 - \alpha)$ with $\lambda = \lambda_0 + \delta\sqrt{\lambda_0}$ and $\alpha = \alpha_0 + \delta$. Figure 5.1 shows the performance, in terms of ARL, of the CUSUM chart and our procedure with several ν. The specific values in the figures can be found in Tables 5.5 and 5.6. The ARLs, SDs and medians are obtained using $30,000$ repetitions and the same random seed is used for fairness. It is clear that the upper one-sided CLSE-CUSUM procedure with $\nu = 100$ outperforms the CUSUM chart in term of ARL, when there are small to moderate shifts in λ. For $\nu \approx 0.5$ARL, the proposed procedure has a better ARL performance when there are small shifts (about $\delta \leq 0.3$) in λ. But for some moderate shifts ($\delta = 0.35, 0.4$) in λ, the CLSE-CUSUM chart with $\nu \approx 0.5$ARL shows a slightly lower performance. This phenomenon is more apparent when $\nu \approx$ ARL,1.5ARL. Moreover, for given δ, the ARL also decreases as the ν decreases. The value of α does not have a significant impact on the ARL performance in monitoring up-shift in λ. When there is an up-shift in $\alpha = 0.25$, the CLSE-CUSUM procedure with $\nu = 100$ shows a better ARL performance. However, for other α and ν, the CLSE-CUSUM procedure shows a similar or slightly lower performance than

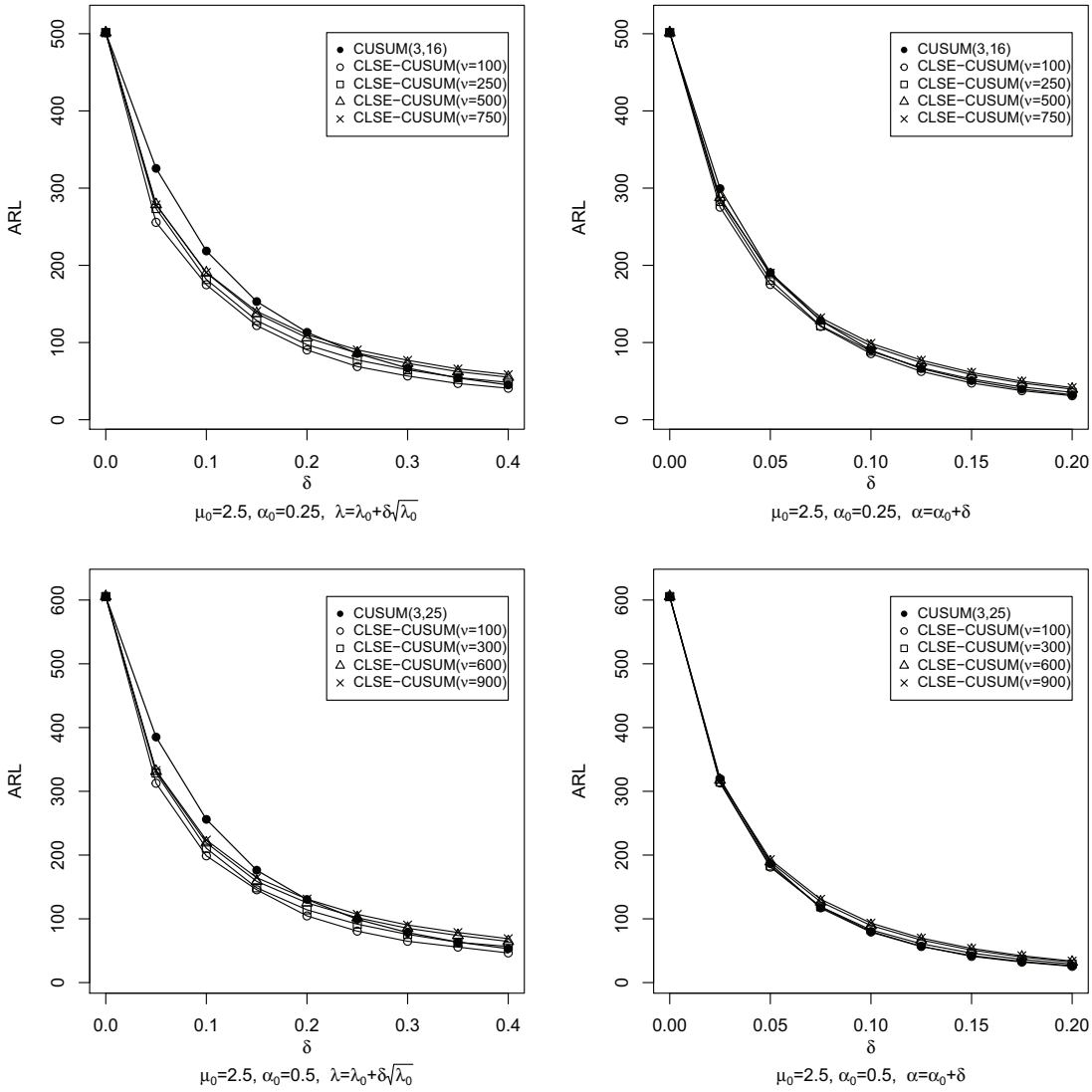

Figure 5.1: ARLs of upper one-sided CLSE-CUSUM and conventional CUSUM chart

the CUSUM chart, which becomes more significant as α gets higher. This may be due to the poor performance of the CLSE when high autocorrelations exist. Tables 5.7 and 5.8 show the results comparing the performance in terms of SD. For given

δ, the SD tends to decreases as the ν increases. For $\nu = 100$, the in-control SD and out-of-control SD performance appear to be worse than that of the CUSUM chart although the difference gets smaller as δ increases.

For $\nu \approx 0.5$ARL, the in-control SD of the CLSE-CUSUM shows a worse performance. However, the out-of-control SD shows a better performance, except for $\delta = 0.05$, when there is a shift in λ. For $\nu \approx$ ARL, 1.5ARL, the out-of-control SD

Table 5.5: ARLs of the upper one-sided CLSE-CUSUM chart and conventional CUSUM chart for INAR(1) process with shift in $\lambda = \lambda_0 + \delta\sqrt{\lambda_0}$

				δ								
μ_0	α_0	ν	c_u	0	0.05	0.1	0.15	0.2	0.25	0.3	0.35	0.4
2.5	0.25		CUSUM(3,16):	501.4	325.6	218.6	153.1	113.2	85.7	66.8	54.1	45.0
		100	1.110	501.4	255.6	174.8	122.0	90.4	68.8	56.6	46.9	40.8
		250	0.917	501.4	273.5	181.6	128.5	97.1	77.4	64.6	54.6	48.3
		500	0.719	501.4	278.7	190.2	137.5	106.1	86.3	73.1	62.3	55.1
		750	0.583	501.4	278.3	190.8	140.4	110.1	90.5	77.0	65.8	58.4
2.5	0.5		CUSUM(3,25):	605.5	385.1	256.0	176.3	130.4	99.2	78.5	63.5	53.2
		100	1.169	605.5	312.6	198.8	145.6	104.6	80.7	64.8	55.7	46.5
		300	0.931	605.5	328.6	210.6	148.7	114.1	91.6	75.6	63.2	56.7
		600	0.724	605.5	331.3	219.2	158.8	125.1	101.7	85.2	73.9	64.6
		900	0.590	604.5	332.5	223.5	164.5	131.0	107.1	90.3	78.6	68.9
2.5	0.75		CUSUM(3,39):	505.6	321.0	221.0	158.6	120.1	94.2	75.8	64.2	54.9
		100	1.149	505.6	269.4	184.6	131.5	101.0	79.9	65.9	55.7	47.7
		250	0.924	505.6	277.8	190.2	137.4	107.3	87.3	73.0	62.9	54.5
		500	0.720	505.6	289.0	199.8	147.2	116.5	96.4	81.8	70.5	61.6
		750	0.583	505.6	290.7	201.8	150.9	120.0	100.2	85.7	74.0	64.8

Table 5.6: ARLs of the upper one-sided CLSE-CUSUM chart and conventional CUSUM chart for INAR(1) process with shift in $\alpha = \alpha_0 + \delta$

				δ								
μ_0	α_0	ν	c_u	0	0.025	0.05	0.075	0.1	0.125	0.15	0.175	0.2
2.5	0.25		CUSUM(3,16):	501.4	299.5	190.6	128.4	90.0	66.2	50.6	39.6	32.3
		100	1.110	501.4	275.3	175.2	120.8	85.6	62.6	47.5	37.6	31.1
		250	0.917	501.4	282.6	180.9	121.7	88.8	67.2	52.7	42.4	35.4
		500	0.719	501.4	287.9	188.0	128.4	95.5	74.0	58.5	47.5	39.5
		750	0.583	501.4	285.8	189.9	132.1	99.0	77.1	61.2	49.8	41.6
2.5	0.5		CUSUM(3,25):	605.5	320.0	186.4	117.0	79.1	56.5	42.3	33.0	26.5
		100	1.169	605.5	313.1	181.1	118.9	80.1	57.0	41.1	32.1	25.4
		300	0.931	605.5	314.6	183.0	119.0	82.7	60.9	46.3	36.3	29.1
		600	0.724	605.5	316.5	189.4	126.6	89.5	66.7	51.0	40.1	32.1
		900	0.590	604.5	316.9	192.9	130.7	93.3	69.8	53.6	42.1	33.7
2.5	0.75		CUSUM(3,39):	505.6	221.5	115.0	68.6	45.0	32.1	24.4	19.6	16.4
		100	1.149	505.6	233.8	134.4	78.6	48.9	32.8	23.0	17.1	13.5
		250	0.924	505.6	227.8	125.5	75.2	48.1	33.3	24.0	18.0	14.3
		500	0.720	505.6	233.4	129.4	78.7	51.1	35.3	25.4	19.0	15.1
		750	0.583	505.6	233.1	131.2	80.9	52.5	36.3	26.2	19.5	15.4

in our procedure shows a better performance while the in-control SD looks reasonable for all the cases with a shift in λ. For the shift in α, a similar conclusion can be reached except for $\alpha = 0.75$. For $\alpha = 0.75$, even the out-of-control SD performance is no better than that of the CUSUM chart. Tables 5.9 and 5.10 show that when the median is used, a similar conclusion to the ARL case can be made. The median performance in our procedure tends to be smaller as the ν decreases.

Table 5.7: SDs of the upper one-sided CLSE-CUSUM chart and conventional CUSUM chart for INAR(1) process with shift in $\lambda = \lambda_0 + \delta\sqrt{\lambda_0}$

				δ								
μ_0	α_0	ν	c_u	0	0.05	0.1	0.15	0.2	0.25	0.3	0.35	0.4
2.5	0.25		CUSUM(3,16):	488.9	311.2	206.7	142.6	100.8	73.6	55.6	43.0	34.1
		100	1.110	1508.2	443.2	262.1	160.5	99.6	63.1	46.7	35.7	28.6
		250	0.917	981.8	328.9	182.5	111.2	71.9	51.3	40.0	31.9	26.5
		500	0.719	617.3	252.8	154.6	95.5	64.9	48.8	38.5	31.8	26.7
		750	0.583	560.4	228.4	138.3	88.7	62.1	47.6	38.2	31.6	27.0
2.5	0.5		CUSUM(3,25):	595.0	364.8	238.7	159.4	112.0	82.0	61.8	47.6	37.9
		100	1.169	1987.5	770.7	304.8	210.5	116.7	81.5	57.2	45.5	33.7
		300	0.931	1036.3	414.5	207.3	124.5	83.6	60.8	47.0	37.8	32.4
		600	0.724	770.9	306.6	167.1	107.9	76.5	57.6	45.3	38.2	32.0
		900	0.590	691.2	277.3	156.2	102.3	74.1	56.6	45.3	38.1	31.6
2.5	0.75		CUSUM(3,39):	482.5	302.0	198.2	136.8	98.1	74.0	56.9	45.5	37.1
		100	1.149	1638.8	585.8	279.1	168.1	111.2	73.9	56.5	43.9	35.3
		250	0.924	1240.1	323.9	187.9	117.8	85.8	60.9	47.9	39.6	33.2
		500	0.720	602.0	264.8	162.0	106.0	77.9	58.0	47.4	40.2	34.1
		750	0.583	565.4	242.3	150.2	100.3	74.2	57.6	47.5	40.5	34.8

Table 5.8: SDs of the upper one-sided CLSE-CUSUM chart and conventional CUSUM chart for INAR(1) process with shift in $\alpha = \alpha_0 + \delta$

				δ								
μ_0	α_0	ν	c_u	0	0.025	0.05	0.075	0.1	0.125	0.15	0.175	0.2
2.5	0.25		CUSUM(3,16):	488.9	287.7	177.9	117.6	79.6	56.1	41.1	30.8	23.9
		100	1.110	1508.2	580.9	277.6	166.0	102.3	59.6	41.7	30.3	23.9
		250	0.917	981.8	348.5	181.6	104.9	70.2	47.4	36.4	27.6	23.0
		500	0.719	617.3	267.1	149.9	92.4	64.3	46.0	35.5	28.2	23.3
		750	0.583	560.4	239.0	138.6	88.1	62.8	45.2	35.4	28.3	23.7
2.5	0.5		CUSUM(3,25):	595.0	302.9	169.6	101.7	64.4	43.4	30.6	22.2	16.7
		100	1.169	1987.5	602.6	310.7	187.5	88.5	53.1	34.5	24.3	18.6
		300	0.931	1036.3	374.3	173.9	97.1	60.9	41.4	30.4	23.1	18.3
		600	0.724	770.9	294.0	146.7	88.5	58.1	40.9	31.0	23.8	19.1
		900	0.590	691.2	263.5	137.6	85.0	57.3	41.1	31.4	24.3	19.5
2.5	0.75		CUSUM(3,39):	482.5	200.7	96.1	51.8	30.3	19.0	12.5	8.6	6.2
		100	1.149	1638.8	411.4	241.3	82.9	44.5	25.0	15.3	9.8	6.8
		250	0.924	1240.1	254.3	115.9	58.4	34.1	22.0	14.7	9.7	6.9
		500	0.720	602.0	206.8	99.6	55.0	33.9	22.2	15.1	9.9	7.0
		750	0.583	565.4	189.6	95.1	54.2	33.9	22.4	15.2	10.1	7.1

From these findings, we conclude that our method can be comparable with the conventional CUSUM chart if one is interested in an effective detection of the small mean increase with maintained autocorrelation, which actually attracts more attention from the researchers: see, for instance, Yontay et al. (2013) and Kim and Lee (2017). In practice, the choice of ν could be an important issue. An optimal ν in term of ARL, SD and median might be obtained based on Monte Carlo simulations.

Table 5.9: Medians of the upper one-sided CLSE-CUSUM chart and conventional CUSUM chart for INAR(1) process with shift in $\lambda = \lambda_0 + \delta\sqrt{\lambda_0}$

				δ								
μ_0	α_0	ν	c_u	0	0.05	0.1	0.15	0.2	0.25	0.3	0.35	0.4
2.5	0.25		CUSUM(3,16):	349.0	230.0	156.0	111.0	82.0	64.0	51.0	42.0	35.0
		100	1.110	189.0	136.0	101.0	76.0	62.0	51.0	44.0	38.0	34.0
		250	0.917	268.0	178.0	128.0	97.0	79.0	65.0	56.0	48.0	44.0
		500	0.719	315.0	204.0	147.0	113.0	92.0	76.0	67.0	58.0	51.0
		750	0.583	329.0	213.0	155.0	120.0	97.0	82.0	71.0	62.0	55.0
2.5	0.5		CUSUM(3,25):	425.0	272.0	180.0	130.0	96.0	75.0	61.0	50.0	43.0
		100	1.169	209.0	149.0	113.0	87.0	71.0	58.0	50.0	44.0	38.0
		300	0.931	321.0	209.0	152.0	114.0	93.0	78.0	66.0	58.0	52.0
		600	0.724	375.0	240.0	174.0	132.0	108.0	91.0	78.0	69.0	61.0
		900	0.590	392.0	252.0	184.0	141.0	116.0	98.0	84.0	74.0	66.0
2.5	0.75		CUSUM(3,39):	360.0	229.0	160.0	117.0	91.0	73.0	60.0	52.0	45.0
		100	1.149	207.0	143.0	108.0	86.0	71.0	59.0	51.0	46.0	40.0
		250	0.924	276.0	180.0	134.0	105.0	86.0	73.0	63.0	56.0	49.0
		500	0.720	320.0	208.0	154.0	123.0	100.0	86.0	75.0	65.0	58.0
		750	0.583	334.0	219.0	163.0	129.0	106.0	91.0	80.0	69.0	62.0

Table 5.10: Medians of the upper one-sided CLSE-CUSUM chart and conventional CUSUM chart for INAR(1) process with shift in $\alpha = \alpha_0 + \delta$

				δ								
μ_0	α_0	ν	c_u	0	0.025	0.05	0.075	0.1	0.125	0.15	0.175	0.2
2.5	0.25		CUSUM(3,16):	488.9	287.7	177.9	117.6	79.6	56.1	41.1	30.8	23.9
		100	1.110	1508.2	580.9	277.6	166.0	102.3	59.6	41.7	30.3	23.9
		250	0.917	981.8	348.5	181.6	104.9	70.2	47.4	36.4	27.6	23.0
		500	0.719	617.3	267.1	149.9	92.4	64.3	46.0	35.5	28.2	23.3
		750	0.583	560.4	239.0	138.6	88.1	62.8	45.2	35.4	28.3	23.7
2.5	0.5		CUSUM(3,25):	595.0	302.9	169.6	101.7	64.4	43.4	30.6	22.2	16.7
		100	1.169	1987.5	602.6	310.7	187.5	88.5	53.1	34.5	24.3	18.6
		300	0.931	1036.3	374.3	173.9	97.1	60.9	41.4	30.4	23.1	18.3
		600	0.724	770.9	294.0	146.7	88.5	58.1	40.9	31.0	23.8	19.1
		900	0.590	691.2	263.5	137.6	85.0	57.3	41.1	31.4	24.3	19.5
2.5	0.75		CUSUM(3,39):	482.5	200.7	96.1	51.8	30.3	19.0	12.5	8.6	6.2
		100	1.149	1638.8	411.4	241.3	82.9	44.5	25.0	15.3	9.8	6.8
		250	0.924	1240.1	254.3	115.9	58.4	34.1	22.0	14.7	9.7	6.9
		500	0.720	602.0	206.8	99.6	55.0	33.9	22.2	15.1	9.9	7.0
		750	0.583	565.4	189.6	95.1	54.2	33.9	22.4	15.2	10.1	7.1

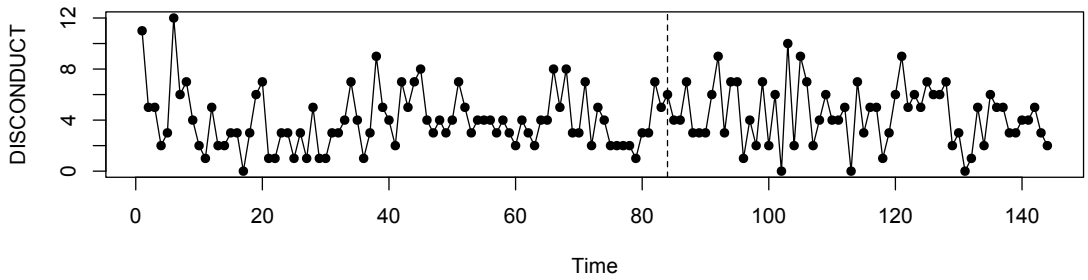

Figure 5.2: The sample path of disorderly conduct data

However, this approach is not always feasible in practice. We recommend to choose $\nu \approx 0.5\text{ARL}, \text{ARL}$ or the values between these two. Notice that if ν is smaller than 0.5ARL, the performance is poor in terms of the in-control SD. On the other hand, if the ν is much larger than ARL, the overall performance would not be satisfactory in terms of ARL. The performance does not vary much according to the type of innovations, e.g. the Katz innovation (Kim and Lee, 2017) and other parameter settings. The result is not reported here for brevity.

5.5 A real data example

In order to showcase an application of CLSE-CUSUM charts to monitoring INAR(1)s processes, we consider the monthly number of disorderly conduct reported in the 44th police car beat in Pittsburgh from 1990 to 2001 in Kim and Lee (2017). We use the data from 1990 to 1996 as an in-control sample. The CLSE-CUSUM control chart is then applied to the data from 1997 to detect whether the mean increase occurs or not.

The sample path plot is given in Figure 5.2, wherein the dashed line denotes December 1996, and the ACF and PACF plots are presented in Figure 5.3. For in-

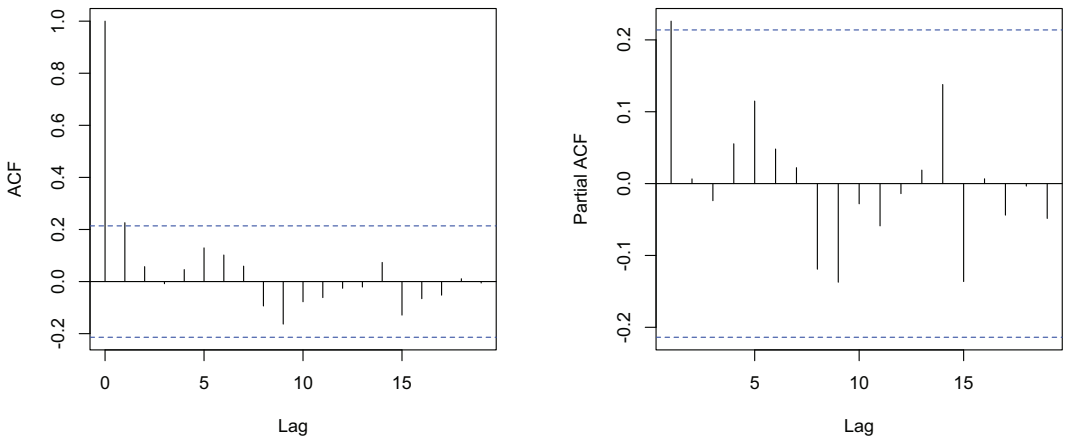

Figure 5.3: The ACF and PACF plot of disorderly conduct data (from 1990 to 1996)

control data, the sample mean, variance, and autocorrelation are given as 3.9643, 5.3602 and 0.2261, respectively. From the sample path plot, one cannot easily check whether the mean increases or not after the dashed line. Kim and Lee (2017) demonstrate that for the data from 1990 to 1996, the first order INAR(1) process with the Katz family innovation (INARKF(1)) is adequate. Based on the results from Kim and Lee (2017), assuming that in-control data follows an INARKF(1) process with $\theta_1 = 2.2080$, $\theta_2 = 0.2537$ and $\alpha = 0.2511$. Kim and Lee (2017) apply the upper one-sided CUSUM chart defined as in (2.2.4) and (2.2.5) with $k = 4$, $h = 34$ wherein the in-control ARL is computed as 205.4 and the out-of-control signal occurs in August 2000. We apply the proposed upper one-sided CLSE-CUSUM procedure in (5.3.9) to this data. Note that our procedure has the advantage of not requiring a specific distributional assumptions on the innovation process. To obtain the control limit that renders the in-control ARL near 205.4, we use $\nu = 100$ following the recommendation in Section 5.4 and replace V and W by their estimates from the in-control sample given as in (5.2.6) and (5.2.7). From numerical experiments with 30,000 repetitions,

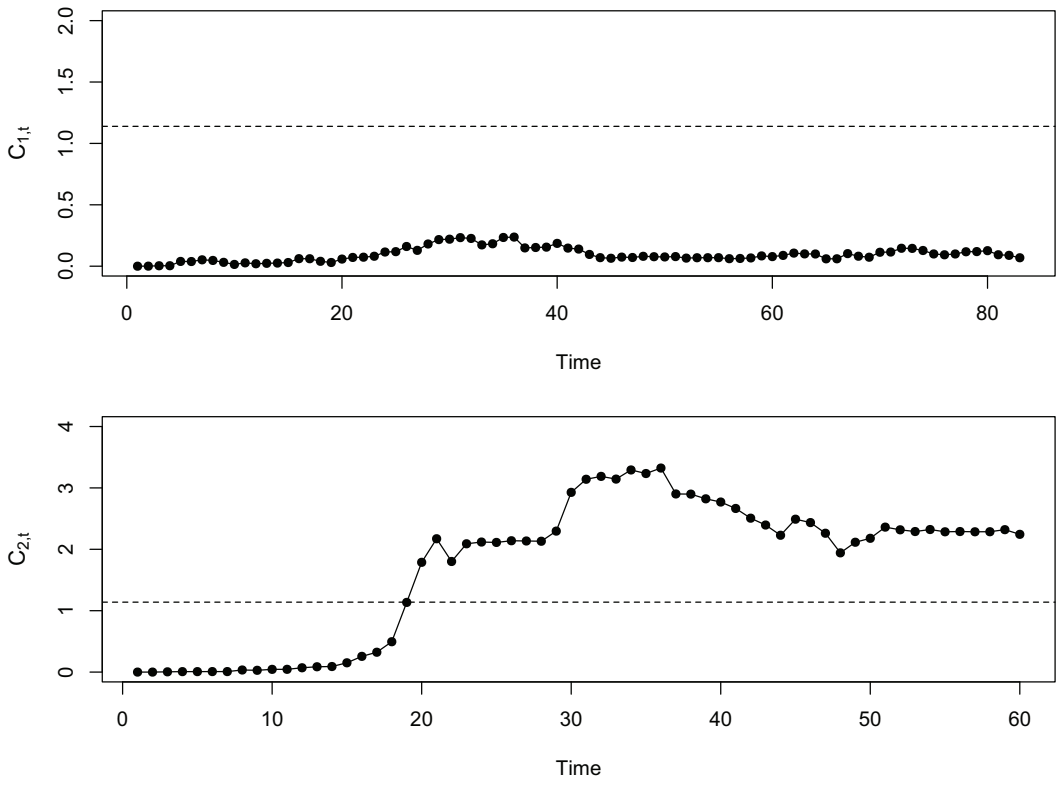

Figure 5.4: The upper one-sided CLSE-CUSUM chart of disorderly conduct data

the control limit c_u is calculated as 2.035. The plot of CLSE-CUSUM statistic is presented in Figure 5.4, wherein the dashed line denotes $c_u = 2.035$, and the $C_{1,t}$ and $C_{2,t}$ stand for the CLSE-CUSUM statistics with $\nu = 100$ of the disorderly conduct data from 1990 to 1996 and from 1997 to 2001, respectively. It can be observed that the data obtained from 1990 to 1996 is in-control because the maximum value of the statistic $C_{1,t}$ is less than 2.035. In the meantime, the plot of $C_{2,t}$ shows that the control statistic has an increasing trend and an out-of-control signal occurs at $t = 19$ (July 1998). The estimated change point appears to be $t = 8$ (August 1997),

indicating an earlier detection in comparison of the CUSUM chart. It can be also seen that the sample mean of the data from August 1997 to July 1998 appears to be 4.833, which is greater than that of the in-control data.

5.6 Proof of Proposition 5.2.1

Assume that $X_0 = 0$. For $t \in \mathbf{N}$, we can obtain the following by using the mathematical induction. Notice that $\mathbb{E}X_{ts} \leq C_k \sum_{i=0}^{t-1} \alpha^{ik}$, where

$$
\begin{aligned}
C_1 &= \mu_{\epsilon,1}, \\
C_2 &= \left(\alpha + \frac{2\alpha\mu_{\epsilon,1}}{1-\alpha}\right) C_1 + \mu_{\epsilon,2}, \\
C_3 &= 3\alpha^2 \left(1 - \alpha + \mu_\epsilon\right) \frac{C_2}{1-\alpha^2} + \alpha \left(1 - 2\alpha + 3\mu_\epsilon + \frac{3\mu_{\epsilon,2}}{1-\alpha}\right) C_1 + \mu_{\epsilon,3}, \\
C_4 &= \alpha^3 \left(6(1-\alpha) + 4\mu_{\epsilon,3}\right) \frac{C_3}{1-\alpha^3} \\
&\quad + \alpha^2 \left((1-\alpha)(7-11\alpha) + 12(1-\alpha)\mu_{\epsilon,3} + 6\mu_{\epsilon,2}\right) \frac{C_2}{1-\alpha^2} \\
&\quad + \alpha \left(1 - 6\alpha + \alpha^2 + 4\left(1 - 2\alpha + \frac{1}{1-\alpha}\right)\mu_{\epsilon,3} + 6\mu_{\epsilon,2}\right) C_1 + \mu_{\epsilon,4}.
\end{aligned}
$$

Since $\alpha \in [0, 1)$, we have $\mathbb{E}X_{ts}^k \leq C := \max\{\frac{C_k}{1-\alpha^k} : k = 1, 2, 3, 4\}$. Proposition 1 from Bourguignon et al. (2016) indicates that X_t converges in distribution to a unique stationary marginal distribution X. Thus, owing to the Portmanteau lemma (cf. Theorem 29.1 of Billingsley (1979)), we get $\mathbb{E}X^k \leq \lim_{t\to\infty} \mathbb{E}X_{ts}^k \leq C$, $k = 1, 2, 3, 4$. □

5.7 Concluding remarks

In this paper, we proposed a new control procedure based on the CLSE-CUSUM statistic. Our method outperforms the conventional CUSUM chart when there are small to moderate mean increases. Moreover, it merits to give additional information on the location of a shift and to set in-control ARLs at one's disposal. The proposed procedure can be applied to other distributions and probabilistic structures without serious difficulties.

Chapter 6

On Residual CUSUM Statistic for PINAR(1) Model in Statistical Design and Diagnostic of Control Chart

6.1 Introduction

During the past three decades, count time series models have been extensively studied in various fields such as production, medicine, communication, insurance and bioscience. Since Al-Osh and Alzaid (1987), the first-order integer-valued autoregressive (INAR(1)) model has been popular among researchers. For example, Jin-Guan and Yuan (1991) proposed an extension to higher order and studied related statistical properties. Franke and Seligmann (1993) studied the conditional maximum likelihood (CML) estimator and Park and Oh (1997) studied asymptotic properties

of parameter estimators. The random coefficient INAR(1) (RCINAR(1)) model was studied by Zheng et al. (2007). Further, Bourguignon et al. (2015) considered the INAR(1) model with power series innovations and Bourguignon and Vasconcellos (2015) considered an improved estimator of the squared difference (SD) estimator originally proposed by Weiß (2012).

The change point problem has been extensively studied in time series analysis since parameter change in underlying time series models is frequently observed in practice, e.g. owing to the change of governmental policy, health care quality, and machine performance in manufacturing process. It is well known that inferences ignoring a parameter change can lead to incorrect conclusions. For retrospective change point analysis, see Csörgö and Horváth (1997), Lee et al. (2003), Hušková et al. (2007), Franke et al. (2012), Pap and Szabó (2013), Kang and Lee (2014), Lee et al. (2016) and Huh et al. (2017).

Many authors also have considered statistical process control (SPC) for monitoring abnormal changes in count time series. The existence of autocorrelation in process is common due to technological advances such as production automation. The SPC for autocorrelated data has received considerable attention in recent years. For instance, Weiß (2007) considered several control charts to monitor the Poisson INAR(1) (PINAR(1)) model and Weiss and Testik (2009) applied the cumulative sum (CUSUM) chart to PINAR(1) model. Recently, Kim and Lee (2017) considered the INAR(1) model with Katz family innovations for modeling the process featuring under-, equi- and over-dispersion and investigated the performance of the CUSUM chart.

In this study, we consider the residual-based CUSUM test statistic using SD estimator in PINAR(1) models and its application to the diagnostic of control chart

design. Also, we propose an upper one-sided CUSUM-type chart for an effective detection and accurate change point estimation, which is very important in practice because it can reduce the time and cost required to diagnose an abnormal signal.

This paper is organized as follows. Section 6.2 reviews the PINAR(1) model and its statistical properties such as transition probabilities, stationarity, conditional moments and estimation. Section 6.3 considers some asymptotic properties of the residual-based CUSUM test statistic with SD estimator and considers an application to the retrospective phase (Phase I) analysis of CUSUM charts including a real data example. Section 6.4 investigates an upper one-sided CUSUM procedure, carries out performance comparison using numerical experiments in a monitoring phase (Phase II), and presents a real data example. Concluding remarks are presented in Section 6.6. The proofs of the theorems are provided in Section 6.5.

6.2 PINAR(1) process

Steutel and van Harn (1979) designated the binomial thinning operator $\circ$ using independent and identically distributed (i.i.d.) Bernoulli random variables as follows:

$$\alpha \circ X = \sum_{i=1}^{X} B_i(\alpha), \tag{6.2.1}$$

where X is a non-negative integer-valued random variable, $B_i(\alpha)$'s, $i = 1, \ldots, X$, are i.i.d. random variables with $P(B_i(\alpha) = 1) = \alpha \in [0, 1]$, independent of X. Based on this operator, Al-Osh and Alzaid (1987) introduced the PINAR(1) model with

parameter vector $\theta^\top = (\alpha, \lambda) \in [0,1] \times (0,\infty)$ as follows:

$$X_t = \alpha \circ X_{t-1} + \epsilon_t, \qquad t \in \mathbf{Z}, \tag{6.2.2}$$

where ϵ_t's are i.i.d. Poisson random variables with mean parameter $\lambda > 0$, independent of X_s, $s \leq t-1$. It is well known that when $\alpha \in [0,1)$, $\{X_t\}_{t\in\mathbf{Z}}$ forms an ergodic Markov chain, see Jin-Guan and Yuan (1991), and is strictly stationary, satisfying Equation (6.2.2). The stationary PINAR(1) process with $\theta^\top = (\alpha, \lambda) \in [0,1)\times(0,\infty)$ has a marginal density following a Poisson distribution with mean $\mu = \frac{\lambda}{1-\alpha}$, and transition probabilities are given as

$$\begin{aligned} P\left(X_t = j | X_{t-1} = i\right) &= \sum_{k=0}^{\min(i,j)} P\left(\alpha \circ X_{t-1} = k | X_{t-1} = i\right) P\left(\epsilon_t = j-k\right) \\ &= \mathrm{e}^{-\lambda} \sum_{k=0}^{\min(i,j)} \binom{i}{k} \alpha^k (1-\alpha)^{i-k} \frac{\lambda^{j-k}}{(j-k)!}, \qquad i,j \in \mathbf{N_0}. \end{aligned}$$

Also, the h-step conditional mean and variance are calculated as

$$\begin{aligned} \mathbb{E}\left(X_{t+h}|X_t\right) &= \alpha^h (X_t - \mu) + \mu, \\ \mathrm{Var}\left(X_{t+h}|X_t\right) &= \alpha^h(1-\alpha^h)X_t + (1-\alpha^h)\mu, \qquad h \in \mathbf{N}, \end{aligned}$$

where $\mu = \frac{\lambda}{1-\alpha}$, see Kim and Lee (2017). For additional properties including higher moments, we refer to Eduarda Da Silva and Oliveira (2004) and Bourguignon and Vasconcellos (2015).

Let $u_t = X_t - \alpha X_{t-1} - \lambda$, $t \geq 1$, be the residual process. Then, using Proposition 1 of Weiß (2012) and Theorem 14.0.1 of Meyn and Tweedie (2012), we can see that $\lim_{t\to\infty} \mathbb{E}u_t = 0$ and $\lim_{t\to\infty} \mathrm{Var}(u_t) = \lambda(1+\alpha)$. Moreover, we obtain the following.

Lemma 6.2.1. *Suppose that* $\{X_t\}_{t\geq 0}$ *is PINAR(1) with parameter vector* $\theta^\top = (\alpha, \lambda) \in (0,1)\times(0,\infty)$ *and* $\mathbb{E}X_0^4 \in (0,\infty)$*. Then, there exists a stationary PINAR(1) process* $\{Y_t\}_{t\geq 0}$ *with parameter vector* $\theta^\top = (\alpha, \lambda) \in (0,1) \times (0,\infty)$*, such that for* $k = 1, 2, 3, 4,$ *and* $1 \leq i < j$*,*

$(a)\ |\mathbb{E}X_t^k - \mathbb{E}Y_0^k| = O(\alpha^t),$

$(b)\ |\mathrm{Cov}(X_i, X_j) - \mathrm{Cov}(Y_i, Y_j)| = O(\alpha^{j-i}),$

$(c)\ |\mathrm{Cov}(D_{X,i}^2, D_{X,j}^2) - \mathrm{Cov}(D_{Y,i}^2, D_{Y,j}^2)| = O(\alpha^{j-i}),$

where $D_{X,i} = \frac{X_i - X_{i-1}}{2}$ *and* $D_{Y,i} = \frac{Y_i - Y_{i-1}}{2}$.

Conventionally, PINAR(1) parameters are estimated with the Yule-Walker (YW), conditional least squares (CLS), and CML estimators. The CML estimator has the best performance in terms of bias and mean squared error (MSE), see Al-Osh and Alzaid (1987). Weiß (2012) considered the SD estimator from $X_0, \ldots, X_n$, based on an unbiased estimator of λ and the fact that $\mu = \frac{\lambda}{1-\alpha}$, as follows:

$$\hat{\theta}^{sd} = \begin{pmatrix} \hat{\alpha}^{sd} \\ \hat{\lambda}^{sd} \end{pmatrix} = \begin{pmatrix} 1 - \frac{\hat{\lambda}^{sd}}{\bar{X}_n} \\ \frac{\sum_{t=1}^n (X_t - X_{t-1})^2}{2n} \end{pmatrix}, \tag{6.2.3}$$

where $\bar{X}_n = \frac{\sum_{t=0}^n X_t}{n+1}$. Bourguignon and Vasconcellos (2015) show that when $\{X_t\}_{t\geq 0}$ is stationary, $\sqrt{n}(\hat{\theta}^{sd} - \theta)$ is asymptotically normal with mean 0 and covariance matrix

$$\Sigma = \begin{pmatrix} \frac{\alpha(1-\alpha^2)}{\lambda} + (1-\alpha)^2 \frac{3+\alpha}{1+\alpha} & -\lambda(1-\alpha)\frac{3+\alpha}{1+\alpha} \\ -\lambda(1-\alpha)\frac{3+\alpha}{1+\alpha} & \lambda\left(1 + \lambda\frac{3+\alpha}{1+\alpha}\right) \end{pmatrix}.$$

Weiß (2012) and Bourguignon and Vasconcellos (2015) demonstrated that the SD estimator can be a good alternative to the CML estimator. In the next section, we study the asymptotic properties of the residual-based CUSUM test with SD estimates in Equation (6.2.3) and applications to statistical design and diagnostic in SPC.

6.3 Change point test based on SD estimator

Let $\{X_t\}_{t\geq 0}$ be a stationary PINAR(1) process with parameter vector $\theta^\top = (\alpha, \lambda) \in (0,1) \times (0,\infty)$. For a parameter change test, we set up the null and alternative hypotheses as follows:

$$H_0 : \theta^\top = (\alpha, \lambda) \text{ does not change over } X_0, \ldots, X_n,$$
$$H_1 : \text{not } H_0.$$

As mentioned in Lee et al. (2004), in general, the residual-based test merits to make a more stable test than the estimate-based test, see also Kang and Lee (2014). Thus, in this section, we consider the residual-based CUSUM statistic:

$$\frac{1}{\sqrt{n}\sigma_u}\left(\sum_{t=1}^{\lfloor ns \rfloor} u_t - \frac{\lfloor ns \rfloor}{n}\sum_{t=1}^{n} u_t\right), \qquad s \in [0,1],$$

where $\sigma_u^2 = \lambda(1+\alpha)$. Since $\{u_t = X_t - \alpha X_{t-1} - \lambda\}_{t\geq 1}$ forms a sequence of stationary martingale differences, it follows from Donsker's invariance principle that

$$\frac{1}{\sqrt{n}\sigma_u}\left(\sum_{t=1}^{\lfloor ns\rfloor} u_t - \frac{\lfloor ns\rfloor}{n}\sum_{t=1}^{n} u_t\right) \xrightarrow[n\to\infty]{w} \mathbf{B}_1^{\circ}(s), \tag{6.3.4}$$

where $\mathbf{B}_1^{\circ}(\cdot)$ denotes a Brownian bridge. Using estimator $\hat{\theta}_n^{\top} = (\hat{\alpha}_n, \hat{\lambda}_n)$ of $\theta^{\top} = (\alpha, \lambda)$, based on $X_0, \ldots, X_n$ with $\sqrt{n}(\hat{\theta}_n - \theta) = O_p(1)$, we consider $\hat{u}_t = X_t - \hat{\alpha}_n X_{t-1} - \hat{\lambda}_n$ and $\hat{\sigma}_{u,n}^2 = \widehat{\mathrm{Var}}(u_t) = \frac{1}{n}\sum_{t=1}^{n}\hat{u}_t^2$. It can be easily checked that for $s \in [0,1]$,

$$\frac{1}{\sqrt{n}}\left(\sum_{t=1}^{\lfloor ns\rfloor}(\hat{u}_t - u_t) - \frac{\lfloor ns\rfloor}{n}\sum_{t=1}^{n}(\hat{u}_t - u_t)\right) = o_p(1)$$

and $\hat{\sigma}_{u,n}^2 \xrightarrow[n\to\infty]{p} \sigma_u^2$. Hence, we obtain the following.

Theorem 6.3.1. *Let $\{X_t\}_{t\geq 0}$ be a stationary PINAR(1) process with parameter vector $\theta^{\top} = (\alpha, \lambda) \in (0,1)\times(0,\infty)$, consider an estimator $\hat{\theta}_n$ of θ such that $\sqrt{n}(\hat{\theta}_n - \theta) = O_p(1)$. For $s \in [0,1]$, define*

$$T_n(s) = \frac{1}{\sqrt{n}\hat{\sigma}_{u,n}}\left(\sum_{t=1}^{\lfloor ns\rfloor}\hat{u}_t - \frac{\lfloor ns\rfloor}{n}\sum_{t=1}^{n}\hat{u}_t\right). \tag{6.3.5}$$

Then, under H_0,

$$T_n(s) \xrightarrow[n\to\infty]{w} \mathbf{B}_1^{\circ}(s).$$

From Theorem 6.3.1 and the continuous mapping theorem, we get the following

result.

Corollary 6.3.1. *Under the assumptions in Theorem 6.3.1 and H_0, we have*

$$\sup_{0\le s\le 1} T_n(s) \xrightarrow[n\to\infty]{w} \sup_{0\le s\le 1} \mathbf{B}_1^{\circ}(s),$$
$$\inf_{0\le s\le 1} T_n(s) \xrightarrow[n\to\infty]{w} \inf_{0\le s\le 1} \mathbf{B}_1^{\circ}(s),$$
$$\sup_{0\le s\le 1} |T_n(s)| \xrightarrow[n\to\infty]{w} \sup_{0\le s\le 1} |\mathbf{B}_1^{\circ}(s)|.$$

In the remainder of this section, we investigate the asymptotic properties of the change point estimator when a change exists:

(A1) Given $\rho \in (0,1)$, $\{X_t\}_{0\le t\le \lfloor n\rho\rfloor}$ and $\{X_t\}_{(\lfloor n\rho\rfloor+1)\le t\le n}$ follow PINAR(1) models with parameter vectors $\dot{\theta}^\top = (\dot{\alpha},\dot{\lambda}) \in (0,1)\times(0,\infty)$ and $\ddot{\theta}^\top = (\ddot{\alpha},\ddot{\lambda}) \in (0,1)\times(0,\infty)$, respectively, with $\mathbb{E}X_0^4 \in (0,\infty)$.

Suppose that $\{\dot{Y}_t\}_{t\ge 0}$ and $\{\ddot{Y}_t\}_{t\ge 0}$ are stationary with parameter vectors $\dot{\theta}$ and $\ddot{\theta}$, respectively. As seen in Pap and Szabó (2013), it follows from the ergodic theorem and Theorem 13.1.2 of Meyn and Tweedie (2012) that

$$\frac{1}{n-\lfloor n\rho\rfloor}\sum_{t=\lfloor n\rho\rfloor+1}^{n} f(X_t, X_{t-1}) \xrightarrow[n\to\infty]{p} \mathbb{E} f(\ddot{Y}_1, \ddot{Y}_0), \qquad \rho\in(0,1), \tag{6.3.6}$$

where $f : \mathbf{N_0}\times\mathbf{N_0} \to \mathbf{R}$ with $\mathbb{E}|f(\ddot{Y}_1,\ddot{Y}_0)| < \infty$. Using this, we can easily check the following, the proof of which is omitted for brevity:

Lemma 6.3.1. *Suppose that $\{X_t\}_{t\ge 0}$ satisfies (A1) and let $\hat{\theta}_n^\top = (\hat{\alpha}_n, \hat{\lambda}_n)$ be the SD estimator in Equation (6.2.3). Then, for $\rho\in(0,1)$, we obtain*

$$\sqrt{n}(\hat{\theta}_n - \tilde{\theta}) = O_p(1),$$

where $\tilde{\theta}^\top = (\tilde{\alpha}, \tilde{\lambda})$, $\tilde{\alpha} = \tilde{\mu}^{-1}(\rho\dot{\alpha}\dot{\mu}+(1-\rho)\ddot{\alpha}\ddot{\mu})$, $\tilde{\lambda} = \rho\dot{\lambda}+(1-\rho)\ddot{\lambda}$ *and* $\tilde{\mu} = \rho\dot{\mu}+(1-\rho)\ddot{\mu}$ *with* $\dot{\mu} = \frac{\dot{\lambda}}{1-\dot{\alpha}}$ *and* $\ddot{\mu} = \frac{\ddot{\lambda}}{1-\ddot{\alpha}}$.

Lemma 6.3.2. *Suppose that* $\{X_t\}_{t\geq 0}$ *satisfies (A1) and let* $\hat{\theta}_n^\top = (\hat{\alpha}_n, \hat{\lambda}_n)$ *be the SD estimator in Equation (6.2.3). Then, we obtain*

$$(a)\ \frac{1}{n}\sum_{t=1}^{n} \breve{u}_t \xrightarrow[n\to\infty]{p} 0,$$

$$(b)\ \frac{1}{n}\sum_{t=1}^{n} \hat{u}_t \xrightarrow[n\to\infty]{p} 0,$$

$$(c)\ \frac{1}{n}\sum_{t=1}^{n} \hat{u}_t^2 \xrightarrow[n\to\infty]{p} \tilde{\sigma}_u^2,$$

where $\breve{u}_t = X_t - \breve{\alpha}_t X_{t-1} - \breve{\lambda}_t$, $\breve{\alpha}_t = \dot{\alpha} I(t \leq \lfloor n\rho \rfloor) + \ddot{\alpha} I(t > \lfloor n\rho \rfloor)$, $\breve{\lambda}_t = \dot{\lambda} I(t \leq \lfloor n\rho \rfloor) + \ddot{\lambda} I(t > \lfloor n\rho \rfloor)$ *and* $\tilde{\sigma}_u^2 = \rho\dot{\lambda}(1+\dot{\alpha}) + (1-\rho)\ddot{\lambda}(1+\ddot{\alpha})$.

Using these lemmas, we can have the following, the proof of which is given in Section 6.5.

Theorem 6.3.2. *Suppose that* $\{X_t\}_{t\geq 0}$ *satisfies (A1) and let* $T_n(s)$ *be the one in Equation (6.3.5) with SD estimators in Equation (6.2.3). Let* $\gamma = \tilde{\sigma}_u^{-1}\rho(1-\rho)(\tilde{\mu}^{-1}\dot{\mu}(\dot{\alpha}-\ddot{\alpha})\ddot{\mu} + \dot{\lambda} - \ddot{\lambda})$, $\tilde{\sigma}_u^2 = \rho\dot{\lambda}(1+\dot{\alpha}) + (1-\rho)\ddot{\lambda}(1+\ddot{\alpha})$ *and* $\tilde{\mu} = \rho\dot{\mu} + (1-\rho)\ddot{\mu}$ *with* $\dot{\mu} = \frac{\dot{\lambda}}{1-\dot{\alpha}}$ *and* $\ddot{\mu} = \frac{\ddot{\lambda}}{1-\ddot{\alpha}}$. *Then, we have*

$$(a)\ \textit{If } \gamma > 0, \frac{1}{\sqrt{n}} \sup_{0\leq s\leq 1} T_n(s) = \gamma + o_p(1),$$

$$(b)\ \textit{If } \gamma < 0, \frac{1}{\sqrt{n}} \inf_{0\leq s\leq 1} T_n(s) = \gamma + o_p(1).$$

Based on the results from Corollary 6.3.1 and Theorem 6.3.2, we consider the CUSUM test and the change point estimate based on $T_{n,k} = T_n\left(\frac{k}{n}\right)$, defined in

Equation (6.3.5) that uses the SD estimator in Equation (6.2.3), as follows:

(a) $\max\limits_{1\le k\le n} T_{n,k}$ and $\operatorname{argmax}\limits_{1\le k\le n} T_{n,k}$ to test whether there is a downward parameter change.

(b) $\max\limits_{1\le k\le n} -T_{n,k}$ and $\operatorname{argmax}\limits_{1\le k\le n} -T_{n,k}$ to test whether there is an upward parameter change.

(c) $\max\limits_{1\le k\le n} |T_{n,k}|$ and $\operatorname{argmax}\limits_{1\le k\le n} |T_{n,k}|$ for a two-sided test.

Then, we obtain the following, the proof of which is deferred to Section 6.5.

Theorem 6.3.3. *Suppose that* $\{X_t\}_{t\ge 0}$ *satisfies (A1). Let*

$$\hat{\tau}_n = \begin{cases} \max_{1\le k\le n} T_{n,k} & \text{if } \gamma > 0 \\ \max_{1\le k\le n} -T_{n,k} & \text{if } \gamma < 0, \end{cases}$$

and $\hat{\rho}_n = \frac{\hat{\tau}_n}{n}$. *Then, we have*

(*a*) $\hat{\tau}_n - \lfloor n\rho \rfloor = O_p(1)$,

(*b*) $\hat{\rho}_n - \rho = O_p(n^{-1})$.

Tables 6.1 and 6.2 present the performance of the statistic $\max_{1\le k\le n} |T_{n,k}|$ with $\rho = 1/2$. The empirical sizes and powers are calculated at the nominal level of 0.5: the corresponding critical value is 1.353, see Kang and Lee (2014). Figure 6.1 displays the histograms of simulated 100,000 sample of $\hat{\rho}_n - \rho$ when $\max_{1\le k\le n} |T_{n,k}| \ge 1.353$ with $(\dot{\alpha}, \dot{\lambda}) = (0.6, 5)$, $(\ddot{\alpha}, \ddot{\lambda}) = (\dot{\alpha} + \delta/2, \dot{\lambda} + 2\delta\sqrt{\dot{\lambda}})$, $\delta = 0.1$ and $\rho = 1/2$. In each experiment, the replication number is 10,000. The results show that the performance gets better in power and MSE as n increases and is irrespective of δ eventually.

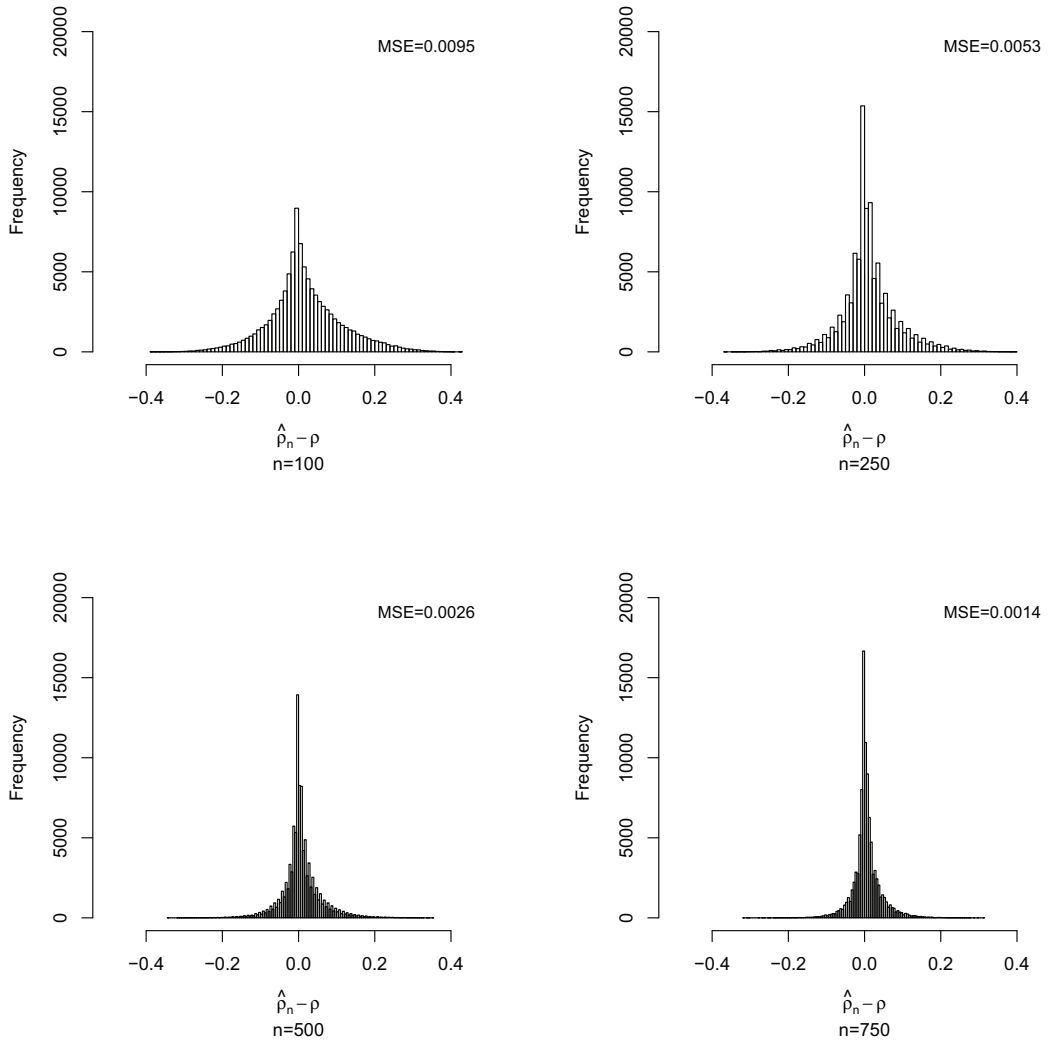

Figure 6.1: Histogram of $\hat{\rho}_n - \rho$ with $(\dot{\alpha}, \dot{\lambda}) = (0.6, 5)$, $(\ddot{\alpha}, \ddot{\lambda}) = (\dot{\alpha} + \delta/2, \dot{\lambda} + 2\delta\sqrt{\dot{\lambda}})$, $\delta = 0.1$ and $\rho = 1/2$

To illustrate a real example, we analyze the IP data studied by Weiß (2007) and Weiss and Testik (2009). This data set consists of the numbers of different IP addresses accessing to the server page of Department of Statistics at University of

Würzburg within 2-min period. We use the outliers-corrected IP data collected from 10 a.m. to 6 p.m. on November 29, 2005, see Weiß (2007) for the outliers correction. The sample path, autocorrelation function (ACF) and partial ACF (PACF) plots are provided in Figure 6.2. Because the sample mean and variance are 1.29 and 1.21, the data does not indicate over-dispersion. Weiss and Testik (2009) fitted a PINAR(1) model with $\alpha = 0.29$ and $\lambda = 0.91$ to this data, and used the conventional CUSUM chart for detecting parameter changes. We here apply the two-sided residual-based CUSUM test at the nominal level of 0.05, see Figure 6.3, which demonstrates the validity of the method in Weiss and Testik (2009).

Table 6.1: Empirical sizes and power of $\max_{1\leq k\leq n}|T_{n,k}|$ with $\rho = 1/2$ and shift in $\dot{\alpha}$ at the level of 0.05

			δ										
$(\dot{\alpha},\dot{\lambda})$	$(\ddot{\alpha},\ddot{\lambda})$	n	-0.25	-0.2	-0.15	-0.1	-0.05	0	0.05	0.1	0.15	0.2	0.25
(0.3,2.5)	$(\dot{\alpha}+\delta,\dot{\lambda})$	100	0.46	0.33	0.21	0.11	0.06	0.04	0.06	0.13	0.26	0.46	0.70
		250	0.87	0.71	0.47	0.25	0.10	0.05	0.10	0.28	0.61	0.89	0.98
		500	0.99	0.95	0.79	0.45	0.15	0.05	0.16	0.54	0.91	1.00	1.00
		750	1.00	0.99	0.93	0.63	0.20	0.05	0.22	0.72	0.98	1.00	1.00
(0.3,3.75)		100	0.63	0.47	0.29	0.15	0.07	0.04	0.07	0.18	0.37	0.64	0.87
		250	0.97	0.87	0.65	0.36	0.12	0.05	0.13	0.41	0.79	0.97	1.00
		500	1.00	1.00	0.92	0.64	0.20	0.05	0.23	0.73	0.98	1.00	1.00
		750	1.00	1.00	0.99	0.82	0.29	0.05	0.32	0.89	1.00	1.00	1.00
(0.3,5)		100	0.76	0.58	0.38	0.19	0.08	0.05	0.09	0.23	0.49	0.77	0.94
		250	0.99	0.95	0.77	0.45	0.15	0.05	0.16	0.53	0.90	0.99	1.00
		500	1.00	1.00	0.98	0.76	0.26	0.05	0.29	0.84	1.00	1.00	1.00
		750	1.00	1.00	1.00	0.91	0.37	0.05	0.41	0.96	1.00	1.00	1.00
(0.6,2.5)		100	0.77	0.60	0.39	0.21	0.08	0.04	0.09	0.29	0.68	0.95	1.00
		250	0.99	0.96	0.81	0.49	0.17	0.04	0.19	0.68	0.98	1.00	1.00
		500	1.00	1.00	0.99	0.80	0.30	0.05	0.37	0.95	1.00	1.00	1.00
		750	1.00	1.00	1.00	0.94	0.42	0.05	0.51	0.99	1.00	1.00	1.00
(0.6,3.75)		100	0.92	0.79	0.56	0.30	0.11	0.04	0.12	0.43	0.86	0.99	1.00
		250	1.00	1.00	0.95	0.67	0.22	0.04	0.27	0.86	1.00	1.00	1.00
		500	1.00	1.00	1.00	0.94	0.43	0.04	0.50	0.99	1.00	1.00	1.00
		750	1.00	1.00	1.00	0.99	0.60	0.05	0.69	1.00	1.00	1.00	1.00
(0.6,5)		100	0.98	0.89	0.69	0.39	0.13	0.04	0.15	0.57	0.94	1.00	1.00
		250	1.00	1.00	0.98	0.80	0.29	0.04	0.35	0.94	1.00	1.00	1.00
		500	1.00	1.00	1.00	0.98	0.54	0.04	0.64	1.00	1.00	1.00	1.00
		750	1.00	1.00	1.00	1.00	0.72	0.05	0.82	1.00	1.00	1.00	1.00

6.4 Anomaly detection and post-signal diagnostic

Since Page (1954) introduced the CUSUM control scheme, the CUSUM method has been an important tool in SPC. The CUSUM chart is well known to outperform the Shewhart-type chart in detecting small to moderate changes, see Montgomery (2012) for a general review of standard control charts. In this section, we focus on the upper one-sided process monitoring in PINAR(1) models to detect a mean increase. This problem has been regarded important in the SPC context on count processes because mean increase is mainly due to critical process deterioration in practice, see Weiss and Testik (2009), Kim and Lee (2017) and Rakitzis et al. (2017). In what follows, in-control (IC) parameter vector $\dot{\theta}^\top = (\dot{\alpha}, \dot{\lambda}) \in (0,1) \times (0,\infty)$ is assumed to be either known or estimable from IC sample.

Table 6.2: Empirical sizes and power of $\max_{1\leq k\leq n} |T_{n,k}|$ with $\rho = 1/2$ and shift in $\dot{\lambda}$ at the level of 0.05

			δ										
$(\dot{\alpha}, \dot{\lambda})$	$(\ddot{\alpha}, \ddot{\lambda})$	n	-1.0	-0.8	-0.6	-0.4	-0.2	0	0.2	0.4	0.6	0.8	1.0
(0.3,2.5)	$(\dot{\alpha}, \dot{\lambda} + \delta\sqrt{\dot{\lambda}})$	100	1.00	0.95	0.72	0.35	0.12	0.04	0.10	0.28	0.53	0.78	0.92
		250	1.00	1.00	0.99	0.74	0.24	0.05	0.20	0.63	0.93	0.99	1.00
		500	1.00	1.00	1.00	0.97	0.44	0.05	0.39	0.92	1.00	1.00	1.00
		750	1.00	1.00	1.00	1.00	0.60	0.05	0.54	0.99	1.00	1.00	1.00
(0.3,3.75)		100	1.00	0.94	0.69	0.34	0.11	0.04	0.10	0.29	0.54	0.78	0.93
		250	1.00	1.00	0.98	0.73	0.23	0.04	0.21	0.63	0.93	1.00	1.00
		500	1.00	1.00	1.00	0.96	0.43	0.05	0.38	0.92	1.00	1.00	1.00
		750	1.00	1.00	1.00	1.00	0.59	0.05	0.56	0.99	1.00	1.00	1.00
(0.3,5)		100	0.99	0.92	0.69	0.34	0.12	0.05	0.11	0.29	0.55	0.80	0.93
		250	1.00	1.00	0.98	0.73	0.22	0.05	0.21	0.64	0.94	1.00	1.00
		500	1.00	1.00	1.00	0.96	0.42	0.05	0.39	0.93	1.00	1.00	1.00
		750	1.00	1.00	1.00	1.00	0.59	0.05	0.54	0.99	1.00	1.00	1.00
(0.6,2.5)		100	0.99	0.90	0.62	0.29	0.10	0.04	0.08	0.22	0.44	0.69	0.86
		250	1.00	1.00	0.97	0.67	0.19	0.05	0.17	0.53	0.86	0.98	1.00
		500	1.00	1.00	1.00	0.93	0.36	0.05	0.31	0.85	0.99	1.00	1.00
		750	1.00	1.00	1.00	0.99	0.52	0.05	0.46	0.96	1.00	1.00	1.00
(0.6,3.75)		100	0.99	0.88	0.61	0.29	0.10	0.04	0.09	0.22	0.46	0.71	0.87
		250	1.00	1.00	0.95	0.65	0.19	0.05	0.17	0.53	0.88	0.98	1.00
		500	1.00	1.00	1.00	0.92	0.36	0.05	0.31	0.86	0.99	1.00	1.00
		750	1.00	1.00	1.00	0.99	0.50	0.05	0.46	0.96	1.00	1.00	1.00
(0.6,5)		100	0.98	0.87	0.60	0.28	0.10	0.04	0.09	0.23	0.48	0.71	0.88
		250	1.00	1.00	0.95	0.63	0.19	0.04	0.18	0.55	0.88	0.99	1.00
		500	1.00	1.00	1.00	0.92	0.36	0.04	0.32	0.86	1.00	1.00	1.00
		750	1.00	1.00	1.00	0.98	0.50	0.05	0.46	0.97	1.00	1.00	1.00

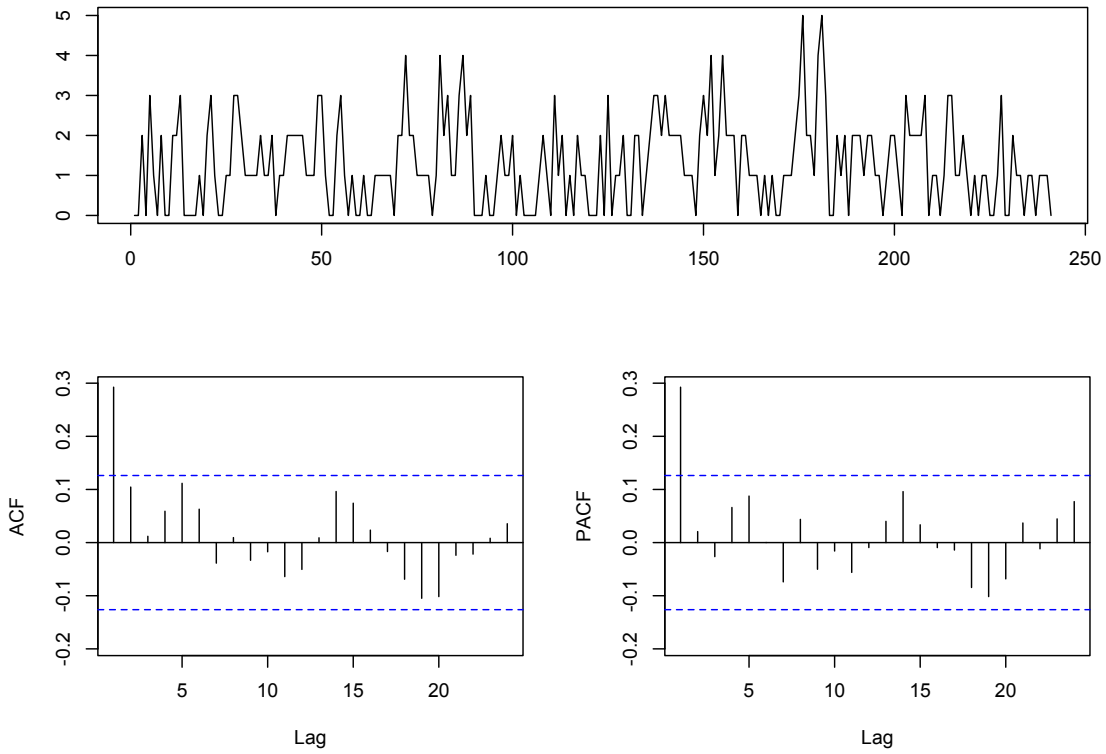

Figure 6.2: Sample path, ACF and PACF of IP data (29 November 2005)

The upper one-sided CUSUM control chart with design parameter (k, h, c_0^c) is expressed as a plot of CUSUM statistics as follows:

$$C_0^c = c_0^c,$$
$$C_t^c = \max\left(0, C_{t-1}^c + X_t - k\right), \quad t \in \mathbf{N},$$

where $c_0^c \geq 0$ is an initial value, usually set to 0, and $k \geq \dot{\mu}$ is a reference value which affects the sensitivity of charts and prevents the statistics from absorbing

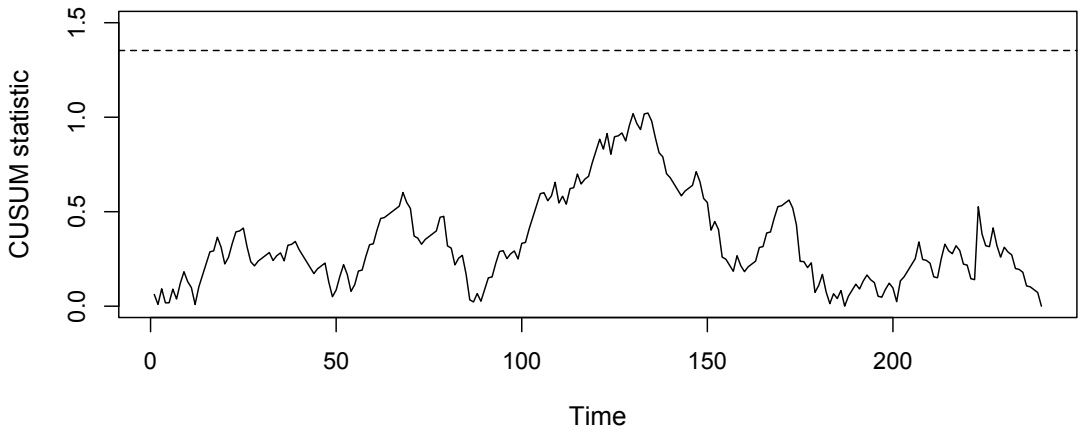

Figure 6.3: Two-sided residual-based CUSUM statistic with SD estimator of IP data (29 November 2005)

into out-of-control (OoC) region. For integer-valued count time series, $k = \lfloor \dot{\mu} \rfloor + 1$ or $\lfloor \dot{\mu} \rfloor + 2$ is recommended, see Weiss and Testik (2009), Yontay et al. (2013) and Kim and Lee (2017). The h indicates a predetermined control limit and the process is regarded OoC when $C_t^c \geq h$ occurs. Provided $C_t^c \geq h$ at time n, the conventional change point estimate is defined as follows:

$$\hat{\tau}_n^c = \max\{1 \leq t \leq n : C_t^c = 0\}.$$

As a counterpart to the conventional CUSUM chart, we consider a modified residual-based CUSUM statistic:

$$T_{n,k}^{\nu} = \frac{1}{\sqrt{n+\nu}} \frac{1}{\dot{\sigma}_u} \left(\sum_{t=-\nu+1}^{k} u_t^{\nu} - \frac{k+\nu}{n+\nu} \sum_{t=-\nu+1}^{n} u_t^{\nu} \right), \quad k = 1, 2, \ldots, n, \tag{6.4.7}$$

where ν is a predetermined nonnegative integer value which plays a role as the

number of virtual residuals, $u_t^\nu = (X_t - \dot{\alpha}X_t - \dot{\lambda})I(t \geq 1)$ with $X_0 = \dot{\mu}$, and $\dot{\sigma}_u^2 = \dot{\lambda}(1+\dot{\alpha})$. Then we get the following result similarly to Theorem 6.3.2, the proof of which is omitted for brevity.

Theorem 6.4.1. *Suppose that given $\rho \in (0,1)$, $\{X_t\}_{1\leq t\leq \lfloor n\rho \rfloor}$ follows a stationary PINAR(1) model with $\dot{\theta}^\top = (\dot{\alpha}, \dot{\lambda}) \in (0,1)\times(0,\infty)$ and $\{X_t\}_{(\lfloor n\rho\rfloor+1)\leq t\leq n}$ follows a stationary PINAR(1) model with $\ddot{\theta}^\top = (\ddot{\alpha}, \ddot{\lambda}) \in (0,1)\times(0,\infty)$. Let $T_{n,k}^\nu$ be the one in Equation (6.4.7), $\dot{\gamma} = \dot{\sigma}_u^{-1}\rho(1-\rho)(\tilde{\mu}^{-1}\dot{\mu}(\dot{\alpha}-\ddot{\alpha})\ddot{\mu} + \dot{\lambda} - \ddot{\lambda})$ and $\tilde{\mu} = \rho\dot{\mu} + (1-\rho)\ddot{\mu}$ with $\dot{\mu} = \frac{\dot{\lambda}}{1-\dot{\alpha}}$ and $\ddot{\mu} = \frac{\ddot{\lambda}}{1-\ddot{\alpha}}$. Then, we have*

(a) If $\dot{\gamma} > 0$, then $\dfrac{1}{\sqrt{n}} \max\limits_{1\leq k\leq n} T_{n,k}^\nu = \dot{\gamma} + o_p(1)$,

(b) If $\dot{\gamma} < 0$, then $\dfrac{1}{\sqrt{n}} \min\limits_{1\leq k\leq n} T_{n,k}^\nu = \dot{\gamma} + o_p(1)$.

Using the above, as in Section 6.3 we consider the residual-based CUSUM statistic with a virtual IC sample (RCUSUMV) with $T_{n,k}^\nu$ in Equation (6.4.7) as follows:

(a) $\max\limits_{1\leq k\leq n} T_{n,k}^\nu$ for a lower one-sided monitoring.

(b) $\max\limits_{1\leq k\leq n} -T_{n,k}^\nu$ for an upper one-sided monitoring.

(c) $\max\limits_{1\leq k\leq n} |T_{n,k}^\nu|$ for a two-sided monitoring.

Then, we obtain the following similarly to Theorem 6.3.3.

Theorem 6.4.2. *Let*

$$\hat{\tau}_n^\nu = \begin{cases} \max_{1\leq k\leq n} T_{n,k}^\nu & \text{if } \dot{\gamma} > 0 \\ \max_{1\leq k\leq n} -T_{n,k}^\nu & \text{if } \dot{\gamma} < 0, \end{cases}$$

and $\hat{\rho}_n^\nu = \frac{\hat{\tau}_n^\nu}{n}$. *Then, under the assumptions in Theorem 6.4.1, we obtain*

$(a)\ \hat{\tau}_n^\nu - \lfloor n\rho \rfloor = O_p(1)$,

$(b)\ \hat{\rho}_n^\nu - \rho = O_p(n^{-1})$.

As mentioned earlier, we focus on the upper one-sided monitoring. The upper one-sided RCUSUMV chart with design parameter (ν, c_ν) and its corresponding change point estimate is defined as follows:

$$C_t^\nu = \max_{1\le k\le t} -T_{t,k}^\nu, \qquad t \in \mathbf{N},$$

$$\hat{\tau}_n^\nu = \operatorname*{argmax}_{1\le k\le n} -T_{n,k}^0 \quad \text{if } C_t^\nu \ge c_\nu \text{ occurs at time } n,$$

where $T_{n,k}^\nu$ is the one in Equation (6.4.7) and c_ν is a predetermined control limit.

Remark 5. One can consider a change point estimate such as $\operatorname*{argmax}_{1\le k\le n} -T_{n,k}^m$ with $m = \nu$ or $m \neq 0$ instead of $m = 0$. But our numerical experiments indicate, although not provided here, that $\operatorname*{argmax}_{1\le k\le n} -T_{n,k}^0$ is recommendable in terms of bias and MSE.

Control charts are usually evaluated with average run length (ARL), defined as the average number of points plotted within the IC region of chart till an OoC signal is triggered. In-control ARL (ARL_0) is the ARL until a false alarm occurs when the process is still IC, while OoC ARL (ARL_1) is the ARL until a correct signal indicating an abnormal change occurs. Besides the ARL, one can also use the standard deviation of run length (SDRL) as a performance measure. The SDRL is an important measure because low SDRL indicates an efficient detection of abnormal changes.

In general, the process is not always OoC at starting point, and thereby, the

ARL_1 does not represent typical OoC behavior. In practice, we do not know when the process will go OoC, and thus, consider a more realistic performance measure such as the expected conditional delay:

$$\text{ARL}^{(\tau)} = \mathbb{E}(L - \tau | L > \tau), \qquad \tau \in \mathbf{N_0},$$

where L is the random variable denoting the number of points plotted on the chart till an OoC signal is triggered and τ is unknown change point. In this study, we put 100 as a representative.

Since mean change is caused only by a change in λ when other features, e.g. dispersion and autocorrelation, are fixed, we also focus on the change in λ, which is common in existing literatures, see Yontay et al. (2013), Kim and Lee (2017) and Rakitzis et al. (2017). To evaluate the upper one-sided RCUSUMV chart, we carry out numerical experiments for $(\dot{\alpha}, \dot{\lambda}) = (0.25, 1.875), (0.25, 3.75), (0.25, 7.5), (0.5, 1.25), (0.5,2.5), (0.5, 5)$, where $(\dot{\alpha}, \dot{\lambda})$ is assumed to change to $(\dot{\alpha}, \dot{\lambda} + \delta\sqrt{\dot{\lambda}})$. We design the CUSUM charts to get $\text{ARL}_0 \approx 500$, see Weiss and Testik (2009) concerning the determination of design parameters in CUSUM charts.

Figure 6.4 shows that the SDRL when the process is IC decreases as ν increases. For efficient statistical design and comparison, we choose ν to get the IC SDRL (SDRL_0) close to that of the CUSUM chart. For convenience, we restrict the range of ν to $\{50n : n \in \mathbf{N}\}$. Figure 6.4 shows that SDRL_0 does not vary much according as ν varies.

Table 6.3 displays the result when the process goes OoC at starting point. This situation occurs, for example, when the process is restarted just after taking an appropriate action. Table 6.3 reveals that the RCUSUMV chart has a better performance in ARL for the detection of small shifts (about $\delta \leq 0.25$). Moreover, for

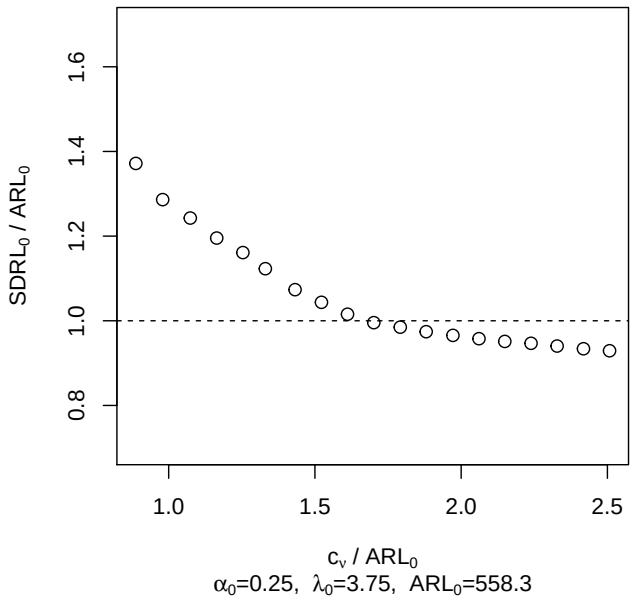

Figure 6.4: Ratio of $SDRL_0$ to ARL_0 profiles

almost all cases, the RCUSUMV chart shows a better SDRL performance. Table 6.4 provides conditional ARL and SDRL when the true change point is 100. The table also presents the performance of the change point estimates, evaluated with bias and root mean squared error (RMSE). The RCUSUMV chart outperforms the CUSUM chart in ARL when there are small to moderate shifts (about $\delta \leq 0.4$). The RCUSUMV chart appears to perform better in SDRL than that of the CUSUM chart for $\delta \leq 0.6$. Moreover, the RCUSUMV chart performance in bias and RMSE is better in change point estimation than that of the CUSUM chart when there are small to moderate shifts (about $\delta \leq 0.4$). Notice that the range of δ to yield more efficient RCUSUMV chart is similar to that in change point estimation. For $\delta > 0.3$, the change point estimate of the RCUSUMV chart tends to be left-biased. In con-

trast, that of the CUSUM chart tends to be right-biased up to $\delta = 0.6$. When there is a large shift (about $\delta \geq 0.6$), the CUSUM chart outperforms the RCUSUMV chart in change point estimation. In the meanwhile, the RCUSUMV chart performance in RMSE does not decline significantly while $\delta \geq 0.6$. Although not reported here, a similar conclusion can be reached for other τ's.

Thus far, we have seen that the RCUSUMV chart performs adequately in detecting small mean increase. The ν must be chosen numerically, which, however, is not an easy task in practice. According to our experiments, the SDRL_0 of the RCUSUMV chart is similar to that of the CUSUM chart when the ν is selected in between 2ARL_0 and 2.3ARL_0.

Table 6.3: Performance of RCUSUMV and CUSUM chart when the process go OoC at start-up with shift in $\dot{\lambda}$

$(\dot{\alpha}, \dot{\lambda})$	Design		δ													
	RCUSUMV(ν,c_ν)															
	CUSUM(k,h)		0	0.05	0.1	0.15	0.2	0.25	0.3	0.35	0.4	0.45	0.5	0.6	0.8	1.0
(0.25,1.875)	RCUSUMV	ARL	501.4	278.8	179.4	129.5	100.3	81.7	66.6	59.3	52.1	46.5	42.3	35.3	26.9	21.8
	(1000,0.5468)	SDRL	492.5	234.0	130.8	82.6	58.0	43.4	33.8	27.1	22.6	19.3	16.7	13.0	8.9	6.6
	CUSUM	ARL	501.3	324.6	220.9	154.8	112.1	85.9	67.5	54.1	44.8	37.7	32.9	25.4	17.5	13.3
	(3,16)	SDRL	491.4	310.2	209.2	142.1	98.8	73.1	56.1	42.3	33.6	27.2	22.5	16.1	9.6	6.6
(0.25,3.75)	RCUSUMV	ARL	558.2	299.2	191.8	136.6	106.8	85.9	72.0	62.3	55.0	49.0	44.4	37.1	28.3	22.9
	(1150,0.5396)	SDRL	549.8	246.5	135.7	85.2	59.1	43.3	33.4	27.2	22.7	19.1	16.5	12.8	8.6	6.5
	CUSUM	ARL	558.3	376.6	258.7	183.4	136.5	102.4	78.2	62.2	50.6	41.6	35.4	26.3	17.1	12.6
	(6,18)	SDRL	549.8	368.3	249.3	174.9	127.4	94.1	69.0	53.7	42.1	33.2	27.1	18.5	10.5	6.9
(0.25,7.5)	RCUSUMV	ARL	565.6	306.0	195.0	139.1	107.2	87.5	73.7	63.2	55.5	49.6	44.8	37.8	28.6	23.1
	(1200,0.5366)	SDRL	553.1	253.2	136.7	84.2	58.2	43.2	33.7	26.8	22.1	18.8	16.0	12.5	8.3	6.1
	CUSUM	ARL	565.7	361.5	239.1	165.7	118.2	88.7	69.3	54.8	45.0	37.8	32.5	25.3	17.1	13.0
	(11,31)	SDRL	552.6	348.4	224.8	152.4	104.8	75.2	56.3	42.4	33.0	26.3	21.5	15.1	8.7	5.9
(0.5,1.25)	RCUSUMV	ARL	605.5	332.1	215.9	154.5	120.0	98.3	82.9	71.6	62.9	56.3	50.8	42.6	32.3	26.3
	(1350,0.5271)	SDRL	595.1	277.7	157.5	99.0	70.2	52.6	41.0	33.5	28.0	23.8	20.6	16.2	11.0	8.4
	CUSUM	ARL	605.5	383.2	252.6	176.6	129.8	99.2	78.3	64.0	53.3	45.8	39.6	31.2	22.0	17.0
	(3,25)	SDRL	590.2	365.5	234.5	159.4	112.8	81.5	61.2	48.2	38.1	31.1	25.7	18.7	11.3	8.0
(0.5,2.5)	RCUSUMV	ARL	513.3	297.5	195.5	142.9	111.2	91.2	76.3	66.0	58.3	52.1	47.1	39.5	30.0	24.3
	(1150,0.5256)	SDRL	499.8	250.5	143.1	93.1	65.1	49.1	38.1	30.9	25.8	22.0	18.9	14.8	10.0	7.5
	CUSUM	ARL	513.3	344.1	240.2	172.5	128.9	99.0	76.7	62.1	51.7	43.4	37.4	28.8	19.5	14.7
	(6,26)	SDRL	502.1	332.4	228.9	159.9	117.0	87.9	65.0	51.2	40.9	32.8	27.4	19.3	11.4	7.6
(0.5,5)	RCUSUMV	ARL	566.8	319.7	208.1	151.0	116.6	93.3	80.0	69.1	60.9	54.5	49.1	41.2	31.3	25.4
	(1250,0.5280)	SDRL	554.6	269.5	151.0	95.9	66.2	49.0	38.1	30.9	25.5	21.9	18.7	14.5	9.8	7.2
	CUSUM	ARL	566.7	363.2	240.2	168.6	122.2	93.6	73.5	59.7	49.9	42.7	37.0	29.0	20.4	15.8
	(11,46)	SDRL	551.6	348.3	222.6	151.7	104.7	76.3	56.6	43.9	34.5	28.1	23.1	16.4	9.9	6.8

Table 6.4: Performance of RCUSUMV and CUSUM chart except false alarms with shift in $\dot{\lambda}$ and $\tau = 100$

$(\dot{\alpha}, \dot{\lambda})$	Design		δ												
	RCUSUMV(ν,c_ν)														
	CUSUM(k,h)		0.05	0.1	0.15	0.2	0.25	0.3	0.35	0.4	0.45	0.5	0.6	0.8	1.0
(0.25,1.875)	RCUSUMV	ARL	237.3	146.3	102.5	78.0	62.6	52.2	44.7	39.2	34.8	31.1	25.9	19.5	15.6
	(1000,0.5468)	SDRL	235.5	128.2	82.0	57.8	42.9	34.0	28.0	23.6	20.2	17.6	14.0	9.9	7.6
		Bias($\hat{\tau}_n$)	129.4	59.5	28.2	11.6	2.3	-3.0	-6.3	-8.4	-9.9	-10.9	-12.0	-13.0	-13.4
		RMSE($\hat{\tau}_n$)	233.6	121.3	74.1	50.1	37.5	31.2	27.6	25.6	24.6	23.9	23.1	22.8	22.4
	CUSUM	ARL	316.9	210.4	147.3	106.7	81.1	63.0	50.9	41.6	35.0	29.9	23.3	15.8	11.9
	(3,16)	SDRL	314.6	206.5	141.5	99.8	73.8	55.5	43.3	33.7	27.4	22.5	16.1	9.7	6.7
		Bias($\hat{\tau}_n$)	298.1	190.3	126.0	84.5	58.2	39.8	27.7	18.7	12.6	8.5	3.4	-1.0	-2.7
		RMSE($\hat{\tau}_n$)	433.5	280.8	189.3	130.6	93.6	67.4	50.3	37.4	28.9	22.7	15.4	10.5	9.6
(0.25,3.75)	RCUSUMV	ARL	254.4	155.1	108.4	82.0	65.6	54.8	46.8	40.9	36.3	32.7	27.1	20.4	16.3
	(1150,0.5396)	SDRL	248.9	132.4	84.7	58.4	43.6	34.6	28.1	23.5	20.2	17.7	14.0	9.9	7.5
		Bias($\hat{\tau}_n$)	137.8	62.7	28.8	11.7	2.0	-3.1	-6.6	-8.8	-10.2	-11.1	-12.4	-13.3	-13.6
		RMSE($\hat{\tau}_n$)	245.0	125.6	75.8	50.6	37.9	31.4	27.7	25.7	24.7	24.0	23.3	23.0	22.7
	CUSUM	ARL	372.4	253.6	178.2	130.4	97.8	75.3	59.6	48.2	39.5	33.3	24.9	16.0	11.5
	(6,18)	SDRL	372.9	251.7	173.6	125.6	92.4	69.4	53.4	41.9	33.7	26.9	18.9	10.6	6.8
		Bias($\hat{\tau}_n$)	359.9	240.3	164.1	115.8	82.5	59.5	43.3	31.7	23.0	17.0	9.3	2.4	-0.1
		RMSE($\hat{\tau}_n$)	518.3	348.1	238.9	170.7	123.7	91.1	68.4	52.0	40.0	30.9	19.8	9.7	6.7
(0.25,7.5)	RCUSUMV	ARL	258.7	156.9	108.8	82.2	66.1	55.3	47.1	41.3	36.6	33.0	27.4	20.5	16.5
	(1200,0.5366)	SDRL	250.2	134.7	83.7	57.6	43.3	34.0	27.8	23.4	20.1	17.5	13.8	9.7	7.4
		Bias($\hat{\tau}_n$)	139.5	62.4	27.8	11.0	1.6	-3.8	-7.3	-9.3	-10.7	-11.7	-12.6	-13.4	-13.7
		RMSE($\hat{\tau}_n$)	248.3	127.8	75.1	50.1	37.8	31.1	27.7	25.8	24.8	24.2	23.6	23.0	22.7
	CUSUM	ARL	352.4	229.6	158.9	112.6	83.4	64.4	50.8	41.8	35.0	29.8	22.9	15.4	11.5
	(11,31)	SDRL	346.5	224.4	151.8	105.1	75.2	56.1	42.5	33.1	26.6	21.6	15.3	9.0	6.0
		Bias($\hat{\tau}_n$)	331.8	207.5	135.4	88.0	58.2	38.6	25.4	16.7	10.7	6.5	1.5	-2.3	-3.7
		RMSE($\hat{\tau}_n$)	479.8	305.6	203.3	136.9	94.6	67.3	48.4	35.7	27.2	21.1	14.7	10.6	10.2
(0.5,1.25)	RCUSUMV	ARL	283.6	178.1	124.9	95.1	76.5	63.8	54.6	47.8	42.5	38.2	31.9	23.9	19.2
	(1350,0.5271)	SDRL	273.9	154.5	98.6	68.9	52.4	41.4	33.8	28.7	24.6	21.7	17.2	12.2	9.3
		Bias($\hat{\tau}_n$)	161.0	80.3	41.1	21.0	9.3	2.3	-2.3	-5.2	-7.0	-8.4	-10.0	-11.3	-12.1
		RMSE($\hat{\tau}_n$)	276.4	149.8	91.6	61.3	45.3	35.7	30.2	27.4	25.2	24.1	22.9	21.6	21.6
	CUSUM	ARL	370.5	242.8	169.6	123.3	93.0	72.8	59.0	49.0	41.6	36.1	28.4	19.8	15.2
	(3,25)	SDRL	366.3	237.6	159.7	113.3	82.3	62.5	47.8	38.5	31.1	25.8	18.9	11.7	8.1
		Bias($\hat{\tau}_n$)	341.6	211.9	136.7	88.9	58.0	38.0	24.6	15.6	9.7	5.3	0.3	-3.7	-5.4
		RMSE($\hat{\tau}_n$)	501.0	318.4	210.0	143.5	99.8	71.8	51.9	39.5	31.1	25.2	19.0	15.6	15.0
(0.5,2.5)	RCUSUMV	ARL	253.1	160.3	113.0	86.4	69.8	58.0	50.1	43.7	39.0	35.1	29.1	21.7	17.5
	(1150,0.5256)	SDRL	248.0	141.7	90.5	64.3	49.0	38.6	31.5	26.6	23.0	19.9	15.9	11.0	8.5
		Bias($\hat{\tau}_n$)	140.7	69.0	34.1	15.8	5.6	-0.7	-4.6	-7.2	-8.8	-10.0	-11.7	-13.0	-13.2
		RMSE($\hat{\tau}_n$)	247.9	135.5	82.9	55.8	42.3	34.2	29.4	27.0	25.5	24.4	23.7	23.0	22.5
	CUSUM	ARL	339.0	233.5	167.3	122.5	93.5	73.6	59.2	49.1	40.8	34.9	26.9	18.0	13.6
	(6,26)	SDRL	335.1	228.7	160.2	115.2	87.5	66.3	51.9	41.3	32.9	26.9	19.6	11.4	7.8
		Bias($\hat{\tau}_n$)	321.1	214.6	147.2	101.7	71.9	51.6	37.1	26.8	18.9	13.5	6.7	0.8	-1.5
		RMSE($\hat{\tau}_n$)	464.2	313.6	217.5	153.6	113.0	83.5	63.1	48.1	36.8	28.7	19.2	11.2	9.3
(0.5,5)	RCUSUMV	ARL	271.4	167.3	119.1	90.5	73.0	60.6	51.8	44.8	39.6	36.4	30.3	22.5	18.1
	(1250,0.5280)	SDRL	265.6	144.8	93.3	65.5	49.5	38.9	31.7	26.8	23.1	19.9	15.8	11.0	8.5
		Bias($\hat{\tau}_n$)	150.8	70.8	35.4	16.4	5.6	-0.9	-5.0	-7.4	-9.1	-10.2	-11.7	-13.0	-13.6
		RMSE($\hat{\tau}_n$)	265.4	138.5	84.9	57.4	42.6	34.4	29.6	27.0	25.7	24.4	23.5	22.9	22.9
	CUSUM	ARL	350.5	228.8	159.3	115.0	87.0	68.3	54.9	45.5	38.5	33.4	26.2	18.2	13.9
	(11,46)	SDRL	348.9	220.9	150.9	104.8	76.6	57.5	43.9	35.0	28.0	23.1	16.7	10.2	7.0
		Bias($\hat{\tau}_n$)	320.9	197.1	125.8	80.1	51.7	33.0	20.5	12.2	6.5	3.2	-1.4	-5.0	-6.4
		RMSE($\hat{\tau}_n$)	474.1	296.0	196.3	131.4	91.4	65.1	46.9	35.6	27.6	22.5	17.8	15.5	15.3

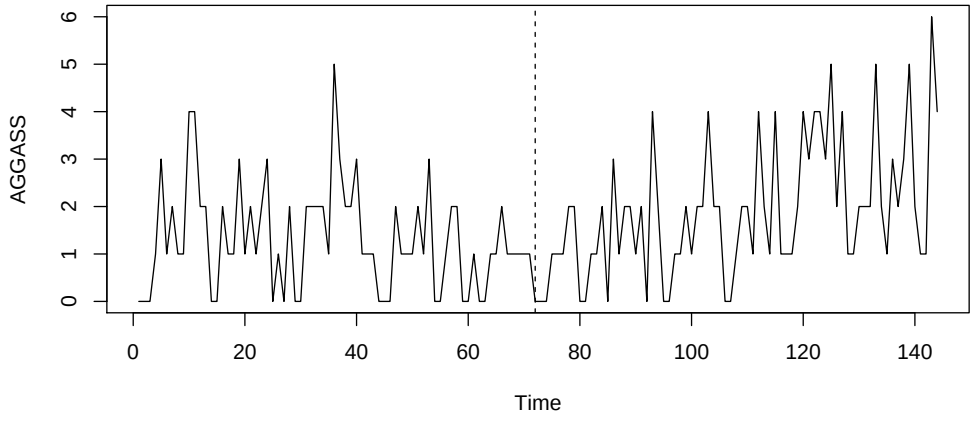

Figure 6.5: Sample path for aggravated assaults data (January 1990 - December 2001)

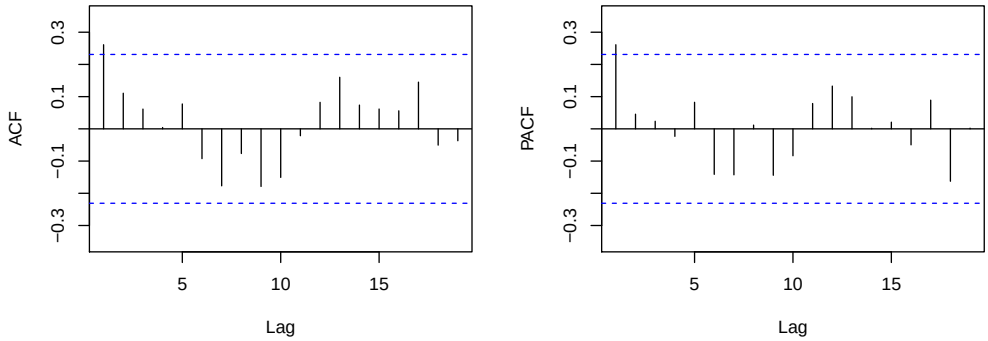

Figure 6.6: The ACF and PACF plot of aggravated assaults data (January 1990 - December 1995)

Next, we apply the RCUSUMV chart to aggravated assaults data of length 144, observed monthly from January 1990 to December 2001 by the 31th police car beats in Pittsburgh: see the forecasting principles site (http://www.forecastingprinciples.com). Figure 6.5 provides the sample path plot of the data, wherein the dashed line indicates December 1995 ($t = 72$). We use the first 72 observations as Phase I data and the remaining 84 values as Phase II data. The ACF and PACF plots of Phase

I data are provided in Figure 6.6, indicating that the data has the characteristics of first-order autoregression. The sample autocorrelation is obtained as 0.2611, and the sample mean and variance are obtained as 1.2917 and 1.2518, which indicates equi-dispersion. We fit the PINAR(1) model and the following models to Phase I data:

- i.i.d. geometric distribution.
- i.i.d. Poisson distribution.
- GINAR(1); INAR(1) model with geometric marginals (Alzaid and Al-Osh, 1988).
- NGINAR(1); negative binomial thinning based INAR(1) model with geometric marginals (Ristić et al., 2009).
- NBINAR(1); INAR(1) model with negative binomial marginals (McKenzie, 1986; Weiß, 2008).
- INARKF(1); INAR(1) model with Katz family innovations (Kim and Lee, 2017).
- ZIPINAR(1); INAR(1) model with zero-inflated Poisson innovations (Jazi et al., 2012a).

The results on ML estimates, Akaike information criterion (AIC) and Bayesian information criterion (BIC) are reported in Table 6.5, indicating that the PINAR(1) model is the best fit. The ML estimates are $\hat{\alpha} = 0.3036$ and $\hat{\lambda} = 0.8890$. The residual-based CUSUM test in Section 6.3 is provided in Figure 6.7, where the SD estimates of λ and α are obtained as 0.9014 and 0.3021. No parameter changes are detected at the level of 0.05.

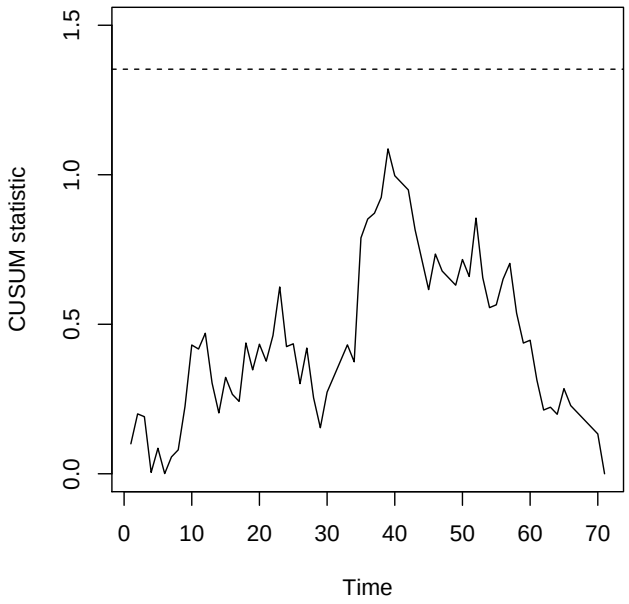

Figure 6.7: Two-sided residual-based CUSUM statistic with SD estimator of aggravated assaults data (January 1990 - December 1995)

Below, we consider the CUSUM chart with reference value $k = 2$, control limit $h = 7$ and initial value $c_0^c = 0$. Here, the corresponding ARL_0 and SDRL_0 are obtained as 260.1 and 255.9. Based on these, we design the RCUSUMV chart with $\nu = 600$ and $c^\nu = 0.5088$, wherein the ARL_0 and SDRL_0 are obtained as 260.1 and

Table 6.5: ML estimates, AIC and BIC of aggravated assaults data (January 1990 - December 1995)

Model	ML estimates	AIC	BIC
i.i.d. geometric	$\hat{\mu} = 1.2917$	228.06	230.34
i.i.d. Poisson	$\hat{\lambda} = 1.2917$	209.14	211.41
GINAR(1)	$\hat{p} = 0.4897$, $\hat{\alpha} = 0.4051$	218.44	222.99
NGINAR(1)	$\hat{\mu} = 1.2479$, $\hat{\alpha} = 0.5551$	217.52	222.07
NBINAR(1)	$\hat{n} = 42.6904$, $\hat{p} = 0.9710$, $\hat{\rho} = 0.3133$	207.47	214.30
INARKF(1)	$\hat{\theta}_1 = 0.8426$, $\hat{\theta}_2 = 0.0378$, $\hat{\alpha} = 0.3134$	207.47	214.30
ZIPINAR(1)	$\hat{\alpha} = 0.3117$, $\hat{\lambda} = 0.9048$, $\hat{\rho} = 0.0297$	207.49	214.32
PINAR(1)	$\hat{\alpha} = 0.3036$, $\hat{\lambda} = 0.8890$	**205.50**	**210.06**

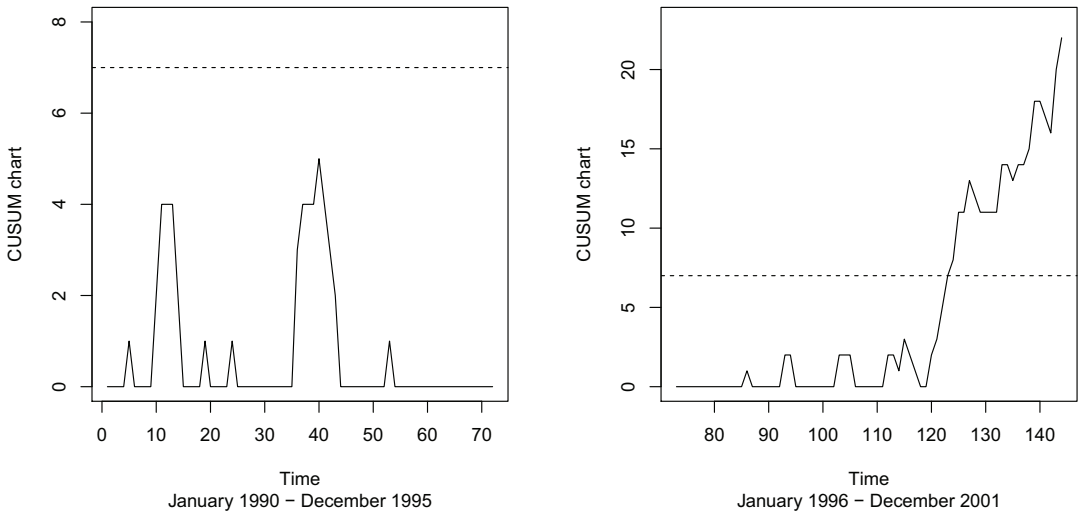

Figure 6.8: CUSUM charts for aggravated assaults data

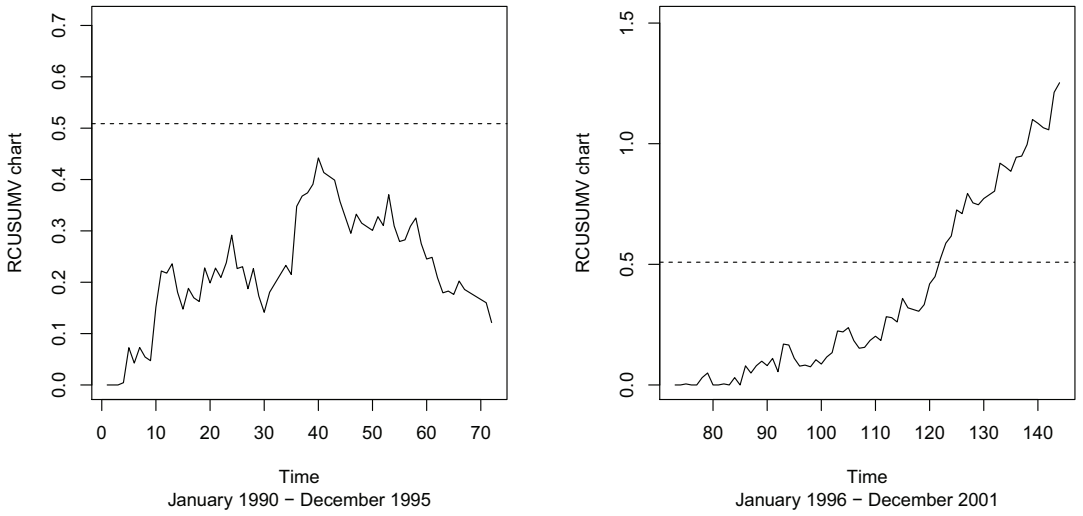

Figure 6.9: RCUSUMV charts for aggravated assaults data

253.8.

Figure 6.8 displays the CUSUM chart of the aggravated assaults data, triggering

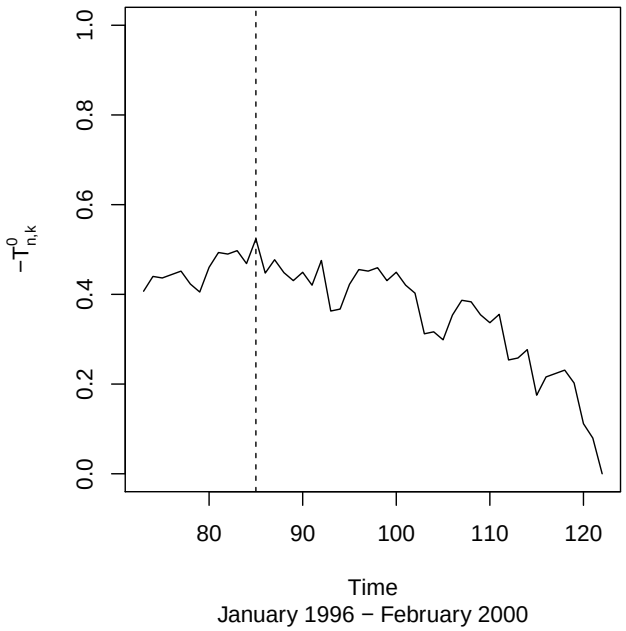

Figure 6.10: Change point estimates from RCUSUMV chart

a mean increase at March 2000 ($t = 123$). The change point is estimated as November 1999 ($t = 119$), which is too close to the point $t = 123$. On the other hand, Figure 6.9 shows that the RCUSUMV chart indicates a mean increase at February 2000 ($t = 122$), a little earlier than that obtained from the CUSUM chart. In this case, however, the change point is much earlier estimated as January 1997 ($t = 85$), see Figure 6.10. The sample means in January 1990 to January 1997 and February 1997 to February 2000 are respectively 1.2235 and 1.8110, which vividly shows a significant mean increase. In fact, the estimated change point coincides with that obtained through the SD residual-based CUSUM test when applied to the observations from January 1990 to February 2000, see Figure 6.11. Overall, our findings demonstrate the superiority of the RCUSUMV chart to the CUSUM chart.

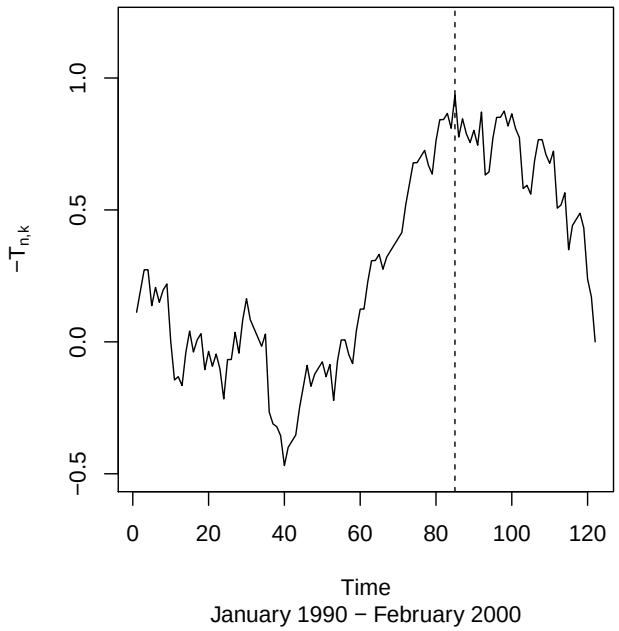

Figure 6.11: Change point estimates from residual-based CUSUM test with SD estimator

6.5 Proofs

Proof of Theorem 6.3.2. For the proof, we adopt the idea from Hušková et al. (2007) and Pap and Szabó (2013). Observe that

$$\begin{aligned}\frac{1}{\sqrt{n}}T_n(s) &= \frac{1}{n}\frac{1}{\hat{\sigma}_{u,n}}\left(\sum_{t=1}^{\lfloor ns\rfloor}\hat{u}_t - \frac{\lfloor ns\rfloor}{n}\sum_{t=1}^{n}\hat{u}_t\right)\\ &= \frac{1}{\tilde{\sigma}_u}\frac{1}{n}\left(\sum_{t=1}^{\lfloor ns\rfloor}\hat{u}_t - \frac{\lfloor ns\rfloor}{n}\sum_{t=1}^{n}\hat{u}_t\right) + \left(\frac{1}{\hat{\sigma}_{u,n}} - \frac{1}{\tilde{\sigma}_u}\right)\frac{1}{n}\left(\sum_{t=1}^{\lfloor ns\rfloor}\hat{u}_t - \frac{\lfloor ns\rfloor}{n}\sum_{t=1}^{n}\hat{u}_t\right).\end{aligned}$$

From Lemma 6.3.2, we can readily check that

$$\sup_{0\leq s\leq 1}\left|\left(\frac{1}{\hat{\sigma}_{u,n}}-\frac{1}{\tilde{\sigma}_u}\right)\frac{1}{n}\left(\sum_{t=1}^{\lfloor ns\rfloor}\hat{u}_t-\frac{\lfloor ns\rfloor}{n}\sum_{t=1}^{n}\hat{u}_t\right)\right|\xrightarrow[n\to\infty]{p}0.$$

Write

$$\sum_{t=1}^{\lfloor ns\rfloor}\hat{u}_t=\sum_{t=1}^{\lfloor ns\rfloor}\breve{u}_t+\sum_{t=1}^{\lfloor ns\rfloor}(\breve{\alpha}_t-\hat{\alpha}_n)X_{t-1}+\sum_{t=1}^{\lfloor ns\rfloor}(\breve{\lambda}_t-\hat{\lambda}_n),$$

where $\breve{u}_t$, $\breve{\alpha}_t$ and $\breve{\lambda}_t$ are the ones in Lemma 6.3.2. Using Lemma 6.3.1 and the ergodic theorem, we can see that

$$\begin{aligned}\sum_{t=1}^{\lfloor ns\rfloor}(\breve{\alpha}_t-\hat{\alpha}_n)X_{t-1}&=(\dot{\alpha}-\tilde{\alpha})\left(\sum_{t=1}^{\min(\lfloor ns\rfloor,\lfloor n\rho\rfloor)}X_{t-1}\right)+(\ddot{\alpha}-\tilde{\alpha})\left(\sum_{t=\min(\lfloor ns\rfloor,\lfloor n\rho\rfloor)+1}^{\lfloor ns\rfloor}X_{t-1}\right)+o_p(n)\\&:=I_n+II_n+o_p(n).\end{aligned}$$

Moreover, by Lemma 6.2.1 and Lemma 7.5 of Pap and Szabó (2013), we can write

$$\begin{aligned}I_n&=\min(\lfloor ns\rfloor,\lfloor n\rho\rfloor)\tilde{\mu}^{-1}(1-\rho)\dot{\mu}(\dot{\alpha}-\ddot{\alpha})\ddot{\mu}+o_p(n),\\II_n&=-\min(\lfloor ns\rfloor-\lfloor n\rho\rfloor,0)\tilde{\mu}^{-1}\rho\dot{\mu}(\dot{\alpha}-\ddot{\alpha})\ddot{\mu}+o_p(n),\end{aligned}$$

where $\tilde{\mu}$ is the one in Lemma 6.3.1. Hence,

$$\begin{aligned}\sum_{t=1}^{\lfloor ns\rfloor}(\breve{\alpha}_t-\hat{\alpha}_n)X_{t-1}&=\min(\lfloor ns\rfloor,\lfloor n\rho\rfloor)\tilde{\mu}^{-1}(1-\rho)\dot{\mu}(\dot{\alpha}-\ddot{\alpha})\ddot{\mu}\\&\quad-\min(\lfloor ns\rfloor-\lfloor n\rho\rfloor,0)\tilde{\mu}^{-1}\rho\dot{\mu}(\dot{\alpha}-\ddot{\alpha})\ddot{\mu}+o_p(n).\end{aligned}$$

Similarly,

$$\sum_{t=1}^{\lfloor ns \rfloor} (\breve{\lambda}_t - \hat{\lambda}_n) = \min(\lfloor ns \rfloor, \lfloor n\rho \rfloor)(1-\rho)(\dot{\lambda} - \ddot{\lambda}) - \min(\lfloor ns \rfloor - \lfloor n\rho \rfloor, 0)\rho(\dot{\lambda} - \ddot{\lambda}) + o_p(n).$$

Then combing these and the fact that $\sum_{t=1}^{\lfloor ns \rfloor} \breve{u}_t = o_p(n)$, owing to Lemma 6.3.2, we have that for $\gamma > 0$,

$$\begin{aligned}
&\left| \frac{1}{\tilde{\sigma}_u} \frac{1}{n} \sup_{0 \le s \le 1} \left(\sum_{t=1}^{\lfloor ns \rfloor} \hat{u}_t - \frac{\lfloor ns \rfloor}{n} \sum_{t=1}^{n} \hat{u}_t \right) - \gamma \right| \le \left| \frac{1}{\tilde{\sigma}_u} \frac{1}{n} \sup_{0 \le s \le 1} \left(\sum_{t=1}^{\lfloor ns \rfloor} \hat{u}_t \right) - \gamma \right| + o_p(1) \\
&\le \left| \sup_{0 \le s \le 1} \left(\frac{\min(\lfloor ns \rfloor, \lfloor n\rho \rfloor)}{n\rho} - \frac{\min(\lfloor ns \rfloor - \lfloor n\rho \rfloor, 0)}{n(1-\rho)} - 1 \right) \gamma \right| + o_p(1) \\
&\le \gamma \left(1 - \frac{\lfloor n\rho \rfloor}{n\rho} \right) + o_p(1) \\
&= o_p(1).
\end{aligned}$$

Hence, since $\hat{\sigma}_{u,n} \xrightarrow[n\to\infty]{p} \tilde{\sigma}_u$ by Lemma 6.3.2, $\frac{1}{\sqrt{n}} \sup_{0 \le s \le 1} T_n(s) - \gamma = o_p(1)$. Similarly, $\frac{1}{\sqrt{n}} \inf_{0 \le s \le 1} T_n(s) - \gamma = o_p(1)$ when $\gamma < 0$. This validates the theorem. □

Proof of Theorem 6.3.3. We only provide the proof for the case of $\gamma > 0$ since the other case can be handled similarly. Let $\hat{\tau}_n = \underset{1 \le k \le n}{\operatorname{argmax}} T_{n,k}$. Since $\hat{\tau}_n - \lfloor n\rho \rfloor = O_p(1)$ can be written as

$$\lim_{M \to \infty} \limsup_{n \to \infty} P(|\hat{\tau}_n - \lfloor n\rho \rfloor| \ge M) = 0,$$

it suffice to show that

$$\lim_{M\to\infty}\limsup_{n\to\infty} P\left(\max_{\lfloor n\rho\rfloor-M<k<\lfloor n\rho\rfloor+M} T_{n,k} \leq \max_{1\leq k\leq\lfloor n\rho\rfloor-M} T_{n,k}\right) = 0$$

and

$$\lim_{M\to\infty}\limsup_{n\to\infty} P\left(\max_{\lfloor n\rho\rfloor-M<k<\lfloor n\rho\rfloor+M} T_{n,k} \leq \max_{\lfloor n\rho\rfloor+M\leq k\leq n} T_{n,k}\right) = 0.$$

For $M \in \{0, 1, \ldots, \lfloor n\rho\rfloor\}$, we have

$$\begin{aligned}
&P\left(\max_{\lfloor n\rho\rfloor-M<k<\lfloor n\rho\rfloor+M} T_{n,k} \leq \max_{1\leq k\leq\lfloor n\rho\rfloor-M} T_{n,k}\right) \leq P\left(T_n(\rho) \leq \max_{1\leq k\leq\lfloor n\rho\rfloor-M} T_{n,k}\right)\\
&= P\left(\frac{1}{\sqrt{n}}\frac{1}{\hat{\sigma}_{u,n}} \min_{M\leq i\leq\lfloor n\rho\rfloor-1}\left(\sum_{t=\lfloor n\rho\rfloor-i+1}^{\lfloor n\rho\rfloor}\hat{u}_t - \frac{i}{n}\sum_{t=1}^{n}\hat{u}_t\right) \leq 0\right)\\
&= P\left(\frac{1}{\hat{\sigma}_{u,n}} \min_{M\leq i\leq\lfloor n\rho\rfloor-1}\left(\frac{1}{i}\sum_{t=\lfloor n\rho\rfloor-i+1}^{\lfloor n\rho\rfloor}\hat{u}_t\right) - \frac{1}{\hat{\sigma}_{u,n}}\frac{1}{n}\sum_{t=1}^{n}\hat{u}_t \leq 0\right)\\
&\leq P\left(\frac{1}{\hat{\sigma}_{u,n}} \min_{M\leq i\leq\lfloor n\rho\rfloor-1}\left(\frac{1}{i}\sum_{t=\lfloor n\rho\rfloor-i+1}^{\lfloor n\rho\rfloor}\hat{u}_t\right) \leq \frac{\gamma}{4}\right) + P\left(\left|\frac{1}{\hat{\sigma}_{u,n}}\frac{1}{n}\sum_{t=1}^{n}\hat{u}_t\right| > \frac{\gamma}{4}\right).
\end{aligned}$$

Note that owing to Lemma 6.3.2,

$$P\left(\left|\frac{1}{\hat{\sigma}_{u,n}}\frac{1}{n}\sum_{t=1}^{n}\hat{u}_t\right| > \frac{\gamma}{4}\right) \underset{n\to\infty}{\longrightarrow} 0.$$

Moreover,

$$
\begin{aligned}
&P\left(\frac{1}{\hat{\sigma}_{u,n}}\min_{M\le i\le\lfloor n\rho\rfloor-1}\left(\frac{1}{i}\sum_{t=\lfloor n\rho\rfloor-i+1}^{\lfloor n\rho\rfloor}\hat{u}_t\right)\le\frac{\gamma}{4}\right)\\
&\le P\left(\frac{1}{\sigma_u}\min_{M\le i\le\lfloor n\rho\rfloor-1}\left(\frac{1}{i}\sum_{t=\lfloor n\rho\rfloor-i+1}^{\lfloor n\rho\rfloor}\hat{u}_t\right)+\left(\frac{1}{\hat{\sigma}_{u,n}}-\frac{1}{\sigma_u}\right)\min_{M\le i\le\lfloor n\rho\rfloor-1}\left(\frac{1}{i}\sum_{t=\lfloor n\rho\rfloor-i+1}^{\lfloor n\rho\rfloor}\hat{u}_t\right)\le\frac{\gamma}{4}\right)\\
&\le P\left(\frac{1}{\sigma_u}\min_{M\le i\le\lfloor n\rho\rfloor-1}\left(\frac{1}{i}\sum_{t=\lfloor n\rho\rfloor-i+1}^{\lfloor n\rho\rfloor}(1-\rho)(\tilde{\mu}^{-1}(\dot{\alpha}-\ddot{\alpha})\ddot{\mu}\mathbb{E}X_{t-1}+\dot{\lambda}-\ddot{\lambda})\right)\le\frac{\gamma}{2}\right)\\
&\quad+P\left(\frac{1}{\sigma_u}\max_{M\le i\le\lfloor n\rho\rfloor-1}\left|\frac{1}{i}\sum_{t=\lfloor n\rho\rfloor-i+1}^{\lfloor n\rho\rfloor}\breve{u}_t\right|>\frac{\gamma}{16}\right)\\
&\quad+P\left(\frac{1}{\sigma_u}\max_{M\le i\le\lfloor n\rho\rfloor-1}\left|\frac{1}{i}(\dot{\alpha}-\hat{\alpha}_n)\sum_{t=\lfloor n\rho\rfloor-i+1}^{\lfloor n\rho\rfloor}(X_{t-1}-\mathbb{E}X_{t-1})\right|>\frac{\gamma}{16}\right)\\
&\quad+P\left(\frac{1}{\sigma_u}\max_{M\le i\le\lfloor n\rho\rfloor-1}\left|\frac{1}{i}(\tilde{\alpha}-\hat{\alpha}_n)\left(\sum_{t=\lfloor n\rho\rfloor-i+1}^{\lfloor n\rho\rfloor}\mathbb{E}X_{t-1}\right)+\tilde{\lambda}-\hat{\lambda}_n\right|>\frac{\gamma}{16}\right)\\
&\quad+P\left(\max_{M\le i\le\lfloor n\rho\rfloor-1}\left|\left(\frac{1}{\hat{\sigma}_{u,n}}-\frac{1}{\hat{\sigma_u}}\right)\frac{1}{i}\sum_{t=\lfloor n\rho\rfloor-i+1}^{\lfloor n\rho\rfloor}\hat{u}_t\right|>\frac{\gamma}{16}\right)\\
&:=A_{1,n,M}+A_{2,n,M}+A_{3,n,M}+A_{4,n,M}+A_{5,n,M},
\end{aligned}
$$

where $\tilde{\alpha}$, $\tilde{\lambda}$ and $\tilde{\mu}$ are the ones in Lemma 6.3.1 and $\breve{u}_t$ is the one in Lemma 6.3.2.

First, using Theorem 14.0.1 of Meyn and Tweedie (2012) and Lemma 7.7 of Pap and Szabó (2013), we can get

$$
\frac{1}{\sigma_u}\min_{M\le i\le\lfloor n\rho\rfloor-1}\left(\frac{1}{i}\sum_{t=\lfloor n\rho\rfloor-i+1}^{\lfloor n\rho\rfloor}(1-\rho)(\tilde{\mu}^{-1}(\dot{\alpha}-\ddot{\alpha})\ddot{\mu}\mathbb{E}X_{t-1}+\dot{\lambda}-\ddot{\lambda})\right)\underset{n\to\infty}{\longrightarrow}\frac{\gamma}{\rho},
$$

which yields $A_{1,n,M}\underset{n\to\infty}{\longrightarrow}0$ regardless of M.

Next, applying Lemma 6.3.1, Lemma 6.3.2 and Lemma 7.8 of Pap and Szabó

(2013), we have

$$\lim_{M\to\infty} \limsup_{n\to\infty} A_{m,n,M} = 0, \qquad m = 2, 3, 4.$$

Finally, since $\hat{\sigma}_{u,n} \xrightarrow[n\to\infty]{p} \sigma_u$ due to Lemma 6.3.2 and the continuous mapping theorem, we have

$$\lim_{M\to\infty} \limsup_{n\to\infty} A_{5,n,M} = 0.$$

Combining all these, we have

$$\lim_{M\to\infty} \limsup_{n\to\infty} P\left(\max_{\lfloor n\rho\rfloor - M < k < \lfloor n\rho\rfloor + M} T_{n,k} \leq \max_{1\leq k\leq \lfloor n\rho\rfloor - M} T_{n,k} \right) = 0.$$

Now that similarly, we can verify

$$\lim_{M\to\infty} \limsup_{n\to\infty} P\left(\max_{\lfloor n\rho\rfloor - M < k < \lfloor n\rho\rfloor + M} T_{n,k} \leq \max_{\lfloor n\rho\rfloor + M\leq k\leq n} T_{n,k} \right) = 0,$$

$\hat{\tau}_n - \lfloor n\rho\rfloor = O_p(1)$, and thus, $\hat{\rho}_n - \rho = O_p(n^{-1})$. This completes the proof. □

6.6 Concluding remarks

In this paper, we investigated the asymptotic properties of the residual-based CUSUM test statistic for PINAR(1) models with the SD estimator. we also proposed a residual-based CUSUM-type procedure to monitor abnormal changes in PINAR(1) models. Our proposed procedure efficiently detects abnormal changes and estimates change points better than the conventional CUSUM chart when there are small shifts. It has a high potential to apply to diverse models such as the NGINAR

model and the integer-valued autoregressive conditional heteroskedastic (INARCH) model. We leave this issue as our future work.

Chapter 7

On the VSI CUSUM Chart for Count Processes and its Implementation with R Package attrCUSUM

7.1 Introduction

When dealing with the rare events such as the infection rate of rare diseases or the number of non-conforming units in a high-quality manufacturing process, traditional control charts for attribute often lose their efficiency owing to the excessive number of zeros in count data. Those zeros cause an over-dispersion for the data, and thereby, underestimating the target values in the monitoring process: see Woodall (2006). In order to overcome this defect, several authors considered control charts adopting zero-inflated models for count data. Sim and Lim (2008) considered Shewhart-type

control charts for zero-inflated Poisson (ZIP) and binomial (ZIB) distributions based on the Jeffrey's prior intervals and Blyth-Still intervals. Wang (2009) introduced an improved control chart using adjusted confidence intervals to cope with the case of small non-conforming rates. He et al. (2012) and Rakitzis et al. (2016) recently studied the CUSUM control chart for zero-inflated Poisson and binomial distributions. Conventionally, the detection of an increase, rather than a decrease, in model parameters has been a core issue, because the increase is mainly due to the process deterioration induced by an assignable cause.

In this chapter, we consider the VSI CUSUM control chart considered by Reynolds et al. (1990), focusing on the ZIB distribution proposed by Hall (2000). We particularly deal with the task of monitoring an increase of the propor-tion parameter in ZIB processes using the VSI CUSUM chart and compare its performance with that of the FSI CUSUM chart considered by Rakitzis et al. (2016) via measuring their ATS triggering an out-of-control condition. Moreover, we put our efforts to develop an R package, attrCUSUM, for an easy implementation of the attribute VSI CUSUM control chart, which is available from the comprehensive R archive network (CRAN).

This chapter is organized as follows. Section 7.2 introduces zero-inflated count models and summarizes their probabilistic properties. Section 7.3 presents the FSI and VSI CUSUM control charts in ZIB processes. Section 7.4 demonstrates the effects of the VSI CUSUM chart in ZIB processes through numerical experiments. Section 7.5 describes the R package attrCUSUM by illustrating some examples using ZIB, Poisson and negative binomial distributions. Section 7.6 provides concluding remarks.

7.2 The zero-inflated model for count data

The zero-inflated model for count data has been popular in analyzing excessive number of zeros in observations: see, for example, Lambert (1992), Hall (2000) and Vieira et al. (2000). Let X be a random variable (r.v.) for zero-inflated count data. Then, the probability mass function (pmf) of X is expressed as follows (Agarwal et al., 2002):

$$p_x(x;\rho,\theta) = \rho\mathbb{1}(x=0) + +(1-\rho)p_w(x;\theta), \quad x = 0,1,\ldots, \tag{7.2.1}$$

where $\mathbb{1}(x=0)$ denotes the Dirac distribution on $x=0$, W is a nonnegative r.v. with pmf $p_w(x;\theta)$, $x=0,1,2,\ldots$, with parameter vector θ, and the $\rho \in [0,1]$ is the zero-inflation parameter. When $\rho = 0$, the distribution of X coincides with that of W, whereas when $\rho = 1$, the distribution of X reduces to the Dirac distribution on $x=0$. From Equation (7.2.1), the cumulative distribution function (cdf) of X is obtained as:

$$F_X(x;\rho,\theta) = \rho + (1-\rho)F_W(x;\theta), \quad x = 0,1,\ldots,$$

where $F_W(x;\theta)$ is the cdf of X with parameter vector θ. Further, it can be easily seen that the k-th moments and the variance of X are given as:

$$\mathbb{E}X^k = (1-\rho)\mathbb{E}W^k, \quad x = 0,1,\ldots,$$
$$\mathrm{Var}(X) = (1-\rho)(\mathbb{E}W^2 - (1-\rho)\mathbb{E}^2W).$$

Thus, the dispersion of X is given as:

$$\begin{aligned} D_X := \frac{\mathrm{Var}(X)}{\mathbb{E}X} &= \frac{(1-\rho)(\mathbb{E}W^2 - (1-\rho)\mathbb{E}^2 W)}{(1-\rho)\mathbb{E}W} \\ &= D_W + \rho\mathbb{E}W \geq D_W, \end{aligned}$$

where $D_W = \mathrm{Var}(W)/\mathbb{E}W$ denotes the dispersion of W. This particularly shows that the existence of frequent zeros causes the over-dispersion. The maximum likelihood (ML) estimator $(\hat{\rho}^{ml}, \hat{\theta}^{ml})$ of parameters (ρ, θ), given $x_1, \ldots, x_m$, is obtained as the maximizer of the log-likelihood function:

$$l(\rho, \theta) := \log \prod_{t=1}^{m} p_X(x_t; \rho, \theta) = \sum_{t=1}^{m} \log p_X(x_t; \rho, \theta).$$

The ML estimator can be calculated using a numerical maximization procedure easily accessible from statistical programming languages such as R (R Core Team, 2017). Since we here focus on Phase II control chart, we assume that the parameter values of (ρ, θ) are known or have been estimated precisely from a precedent large Phase I sample. In this study, we consider the VSI CUSUM control chart based on the ZIB distribution. We do this because the ZIB process is the most appropriate when we deal with count data with an excessive number of zeros and the sampled data is viewed as a group of size $n > 1$ (Noorossana et al., 2011). Assume that X follows a ZIB distribution with parameters (ρ, n, p). Then, its pmf $p_x(x; \rho, n, p)$ is given as (Hall, 2000):

$$p_X(x; \rho, n, p) = \rho\mathbb{1}(x = 0) + (1-\rho)\binom{n}{x} p^x (1-p)^{n-x}, \quad x = 0, 1, \ldots, n,$$

where $(n, p) \in (\mathbf{N}, [0, 1])$ is the parameters of a standard binomial distribution. The mean, variance and dispersion of X are given by:

$$\begin{aligned}
\mu_X &= (1-\rho)np, \\
\sigma_X^2 &= (1-\rho)np(1-p+\rho np), \\
D_X &= (1-p)+\rho np.
\end{aligned}$$

Given observations $x_1, \ldots, x_m$ from a ZIB process with parameters (ρ, n, p), where n is assumed to be known, the ML estimator $(\hat{\rho}^{ml}, \hat{p}^{ml})$ of the parameters (ρ, p) is obtained by solving the nonlinear equations (Vieira et al., 2000):

$$\begin{cases}
\hat{\rho}^{ml} &= 1 - \frac{\bar{x}}{n\hat{p}^{ml}} \\
\hat{p}^{ml} &= \frac{\bar{x}^{+}(1-(1-\hat{p}^{ml})^n)}{n},
\end{cases}$$

where $\bar{x}$ is the sample mean and $\bar{x}^{+} = \sum_{t=1}^{m} x_t \mathbb{1}(x_t > 0) / \sum_{t=1}^{m} \mathbb{1}(x_t > 0)$ is the mean of the positive values of the observations. Since the ML estimator $(\hat{\rho}^{ml}, \hat{p}^{ml})$ has no closed form, a numerical optimization procedure should be hired in its calculation.

7.3 FSI and VSI control scheme for ZIB process

In this section, we describe the FSI and VSI CUSUM control charts with ZIB processes, including the Markov chain approach proposed by Brook and Evans (1972).

7.3.1 CUSUM control statistic for ZIB process

We consider the monitoring process for the proportion p of non-conforming units of ZIB processes with parameters (ρ, n, p), where the ρ is assumed to be known and

to remain unchanged and the sample size n is fixed as in Rakitzis et al. (2016), Noorossana et al. (2011) and Sim and Lim (2008). We assume that X_i, $i = 1, 2, \ldots$, are independent and identically distributed ZIB$(\rho, n, \delta p_0)$ r.v.s, where $\delta > 0$ is a positive constant that determines the magnitude of a shift in p_0. Notice that when $\delta = 1$, the process is regarded as in-control, whereas it is regarded as out-of-control when $\delta \neq 1$. As mentioned by Rakitzis et al. (2016), when $\delta > 1$, the out-of-control condition is attributed to an increase in the proportion of non-conforming units, mainly caused by a deterioration in the process performance. Meanwhile, $\delta < 1$ implies that there is an improvement in the process, which can be used to set up a potential future direction for process adjustment.

In this study, we design the one-sided VSI CUSUM control chart for monitoring the proportion increase in ZIB processes, based on their corresponding FSI CUSUM charts. Traditional one-sided FSI CUSUM control charts for detecting a mean increase are expressed as the plot of CUSUM statistic:

$$\tilde{C}_0 = \tilde{c}_0, \quad \tilde{C}_t = \max(0, \tilde{C}_{t-1} + X_t - k), \quad t \in \mathbf{N}, \tag{7.3.2}$$

where $\tilde{c}_0 \in [0, h)$ is a starting value, usually set to be 0, $k \geq \mu_X$ is a reference value, which has a roll to inhibit the CUSUM statistic from drifting toward the control limit h. CUSUM charts get less sensitive to small shifts but more sensitive to larger shifts as k increases. Other starting values are sometimes used, for instance, when considering a fast initial response (FIR) feature (Lucas and Crosier, 1982). The process is regarded as out-of-control when the signal, $\tilde{C}_t \geq h$ is triggered.

In the VSI CUSUM control scheme, a modified statistic is usually used. The VSI upper one-sided CUSUM control statistic for detecting a mean increase is expressed

as follows (Reynolds et al., 1990):

$$C_0 = c_0, \quad C_t = \max(0, C_{t-1}) + X_t - k, \quad t \in \mathbf{N}, \tag{7.3.3}$$

where $c_0 \in [-k, h)$ is a starting value. As mentioned by Reynolds et al. (1990), a remarkable difference between $\tilde{C}_t$ in (7.3.2) and C_t in (7.3.3) lies in whether or not they record the negative CUSUM values: $\tilde{C}_t$ resets any negative CUSUM values to zero, whereas C_t records negative CUSUM values and proceeds its accumulation from zero for the next sample. Like the conventional FSI CUSUM chart, the VSI CUSUM chart signals a mean increase whenever $C_t \geq h$. It can be easily seen that $C_t \geq h$ is equivalent to $\tilde{C}_t \geq h$. For this reason, we employ the modified CUSUM statistic for both FSI and VSI CUSUM charts.

The VSI CUSUM chart is operated with two sampling intervals $0 < d_s \leq d_l$, where d_s denotes a shorter sampling interval, required to be as short as possible, and d_l is a longer one which should be properly chosen for the process to run without sampling. Given a warning limit $w \in (-k, h)$, the sampling interval is determined by the current value of the CUSUM statistic. When the process is seemingly close to out-of-control state, namely $w \leq C_t < h$, the next sample is taken after a relatively shorter time, d_s, for reducing the delay time until an assignable cause is detected; otherwise, namely if $C_t < w$, the next sample is taken after a relatively longer time, d_l, for preserving the predetermined average sampling frequency (see Figure 7.1). When $d_s = d_l$, the VSI scheme can be regarded as a FSI scheme. For convenience, it is assumed that $d_s = d_l = 1$ when considering the FSI scheme in this study. The condition $d_s = d_l = 1$ implies that the ATS is the same as the average number of sample to signal (ANSS)s. The VSI CUSUM statistic C_t, which uses negative values, provides more warning limits than the conventional FSI CUSUM statistic $\tilde{C}_t$. Thus,

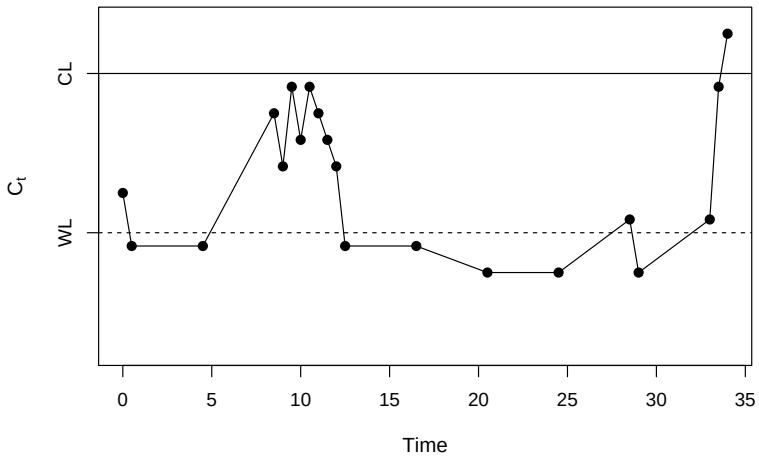

Figure 7.1: An example of plot of VSI CUSUM statistic

it provides more diverse design parameter candidates and yields a better parameter design. This is the main reason to use the modified statistic C_t instead of $\tilde{C}_t$.

Assume that one is interested in the quick detection of a shift $\delta > 1$ in p_0. The performance of the FSI CUSUM chart is usually measured by the ANSS in an out-of-control condition. Let $\text{ANSS}(\rho, n, \delta p_0, c_0, k, h)$ denote the ANSS for the case of the starting value, reference value, and control limit (c_0, k, h) in ZIB processes with parameters $(\rho, n, \delta p_0)$. Then, the optimal pair (k^*, h^*) is obtained by solving the optimization problem stated below:

$$(k^*, h^*) = \underset{(k,h)}{\text{argmin}}\ \text{ANSS}(\rho, n, \delta p_0, c_0, k, h), \tag{7.3.4}$$

where $\text{ANSS}(\rho, n, \delta p_0, c_0, k, h) = \text{ANSS}_0$. Here, the ANSS_0 denotes a predetermined in-control ANSS. Given ANSS_0, the procedure of finding an optimal pair (k^*, h^*) consists of the following two steps (Rakitzis et al., 2016): i) finding all possible pairs

satisfying the condition ii) selecting the one satisfying (7.3.4) among such pairs. Let Ψ_s, Ψ_l be the average number of samples before the occurrence of an out-of-control signal, except the initial state, that use d_s and d_l, respectively, and let ρ_s be the long-run proportion of shorter sampling intervals d_s. Then, the following relations hold (Reynolds et al., 1990):

$$\begin{aligned}
\text{ANSS} &= 1 + \Psi_l s + \Psi_l l, \\
\rho_s &= \begin{cases} (1 + \Psi_l s)/\text{ANSS}, & \text{if } c_0 \geq w \\ \Psi_s/\text{ANSS}, & \text{if } c_0 < w, \end{cases} \qquad (7.3.5) \\
\text{ATS} &= \begin{cases} d_s(1 + \Psi_s) + d_l \Psi_l, & \text{if } c_0 \geq w \\ d_s \Psi_s + d_l(1 + \Psi_l), & \text{if } c_0 < w. \end{cases} \qquad (7.3.6)
\end{aligned}$$

From the above, we see that $\text{ATS} = \bar{d} \cdot \text{ANSS}$, where $\bar{d} = d_s\rho_s + d_l(1 - \rho_s)$. Note that $\bar{d}$ is regarded as the average sampling interval.

Similarly to the FSI CUSUM chart, we define $\text{ATS}(\rho, n, \delta p_0, c_0, k, h, w, d_s, d_l)$ to be the ATS for the case of the warning limit, shorter interval and longer sampling interval w, d_s, d_l: the others are the same as in the FSI CUSUM chart. Then, given d_s, the optimal pair (k^*, h^*, w^*) is obtained by solving the optimization problem given below:

$$(k^*, h^*, w^*) = \underset{(k,h,w)}{\text{argmin}}\ \text{ATS}(\rho, n, \delta p_0, c_0, k, h, w, d_s, d_l), \qquad (7.3.7)$$

where $\text{ATS}_0 := \text{ATS}(\rho, n, \delta p_0, c_0, k^*, h^*, w^*, d_s, d_l) = \text{ANSS}_0$.

In this study, the procedure of finding an optimal (k^*, h^*, w^*) is based on the optimal pair (k^*, h^*) found in the FSI CUSUM scheme for procedural efficiency and practicality, which implies that both FSI and VSI chart have the same ANSS

function (Reynolds et al., 1988). Given ANSS_0, d_s and (k^*, h^*) in the FSI CUSUM scheme, the procedure of finding an optimal warning limit w^* consists of the two steps: i) for all possible warning limits, calculate d_l such that $\text{ATS}_0 = \text{ANSS}_0$ ii) for all pairs (w, d_l), select the one satisfying (7.3.7). The details on the calculations of ANSS and ATS and obtaining d_l values based on the Markov chain approach are described in Subsection 7.3.2.

7.3.2 The Markov chain approach for CUSUM control chart

The optimization problems in (7.3.4) and (7.3.7) can be solved approximately based on the discretization of state space and the Markov chain approach proposed by Brook and Evans (1972). For details on the Markov chain approach in the VSI CUSUM scheme, we also refer to Reynolds et al. (1990). For describing the procedure of discretization and the Markov chain approach in this study, we first consider an interval $[-L, H)$ with $L, H > 0$. This interval is then divided into $(H/d) + (L/d)$ subintervals with length $0 < d < H$, satisfying $H/d \in \mathbf{N}$, $L/d \in \mathbf{N}$, such as:

$$[-L, -L + d), [-L + d, -L + 2d), \ldots, [H - d, H).$$

Suppose that there is a discrete-time Markov chain consisting of states $-L, -L + d, \ldots, H - d, H$ with $0 < d < H$, $H/d \in \mathbf{N}$ and $L/d \in \mathbf{N}$, where $-L, -L+d, \ldots, H-d$ denote transient states and H denotes an absorbing state. The corresponding transition probability matrix $\mathbf{P}$ and the transient probability matrix $\mathbf{Q}$ of size $(H/d) +$

$(L/d), (H/d) + (L/d)$ are given as follows:

$$\mathbf{P} = \begin{pmatrix} \mathbf{Q} & 1 - \mathbf{Q} \cdot 1 \\ 0^\top & 1 \end{pmatrix},$$

$$\mathbf{Q} = \begin{pmatrix} q_{-L,-L} & q_{-L,-L+d} & \cdots & q_{-L,(H-d)} \\ q_{-L+d,-L} & q_{-L+d,-L+d} & \cdots & q_{-L+d,(H-d)} \\ \vdots & \vdots & \ddots & \vdots \\ q_{(H-d),0} & q_{(H-d),d} & \cdots & q_{(H-d),(H-d)} \end{pmatrix},$$

where $q_{i,j} = P(C_t = j | C_{t-1} = i)$, $i, j = -L, -L + d, \ldots, H - d$, $0 = (0, 0, \ldots, 0)^\top$ and $1 = (1, 1, \ldots, 1)^\top$. Note that each $q_{i,j}$ can be approximated as stated below:

$$\begin{aligned} q_{i,j} &= P(C_t = j | C_{t-1} = i) \\ &\approx P(C_t \in [j, j + d) | C_{t-1} = i) \\ &= P((\max(0, i) + X_t - k) \in [j, j + d)) \end{aligned}$$

Define the initial probability vector α for transient state with $C_0 = c_0$ as follows:

$$\begin{aligned} \alpha &= (\alpha_{-L}, \alpha_{-L+d}, \ldots, \alpha_{H-d})^\top, \\ \alpha_j &= P(C_1 = j | C_0 = c_0), \quad j = -L, -L + d, \ldots, H - d, \end{aligned}$$

where $0 < d < H, H/d \in \mathbf{N}$ and $L/d \in \mathbf{N}$. Similarly, each α_j is calculated approxi-

mately by:

$$\begin{aligned}\alpha_j &= P(C_1 = j | C_0 = c_0) \\ &\approx P(C_1 \in [j, j+d) | C_0 = c_0) \\ &= P((\max(0, c_0) + X_t - k) \in [j, j+d))\end{aligned}$$

Let $\mu = (\mu_{-L}, \mu_{-L+d}, \ldots, \mu_{H-d})^\top$ be the solution of the linear equation $(\mathbf{I} - \mathbf{Q}) \cdot \mu = 1$ where $\mathbf{I}$ denotes the identity matrix and $1 = (1, 1, \ldots, 1)^\top$. Each μ_i, $i = -L, -L+d, \ldots, H-d$, is interpreted as the average number of steps before the Markov chain is absorbed when it starts from transient state i. Then, the ANSS$(\rho, n, \delta p_0, c_0, k, h)$is computed by:

$$\text{ANSS}(\rho, n, \delta p_0, c_0, k, h) = 1 + \alpha^\top \mu. \tag{7.3.8}$$

Let μ_s be the solution of the linear equation $(\mathbf{I}-\mathbf{Q}) \cdot \mu_\mathbf{s} = \mathbf{v_s}$ where $\mathbf{v_s}=(v_{s,-L}, v_{s,-L+d}, \ldots, v_{s,H-d})^\top$ with

$$v_{s,j} = \begin{cases} 1, & \text{if } j \geq w \\ 0, & \text{if } j < w, \end{cases}$$

Then, it can be easily seen that Ψ_s is obtained by $\Psi_s = \alpha^\top \mu_\mathbf{s}$, and the d_l satisfying $\text{ATS}_0 = \text{ANSS}_0$ can be obtained using equation (7.3.5) and the equation: $1 = d_s \rho_s + d_l(1 - \rho_s)$ with $\delta = 1$. Therefore, the ATS is obtained by equation (7.3.6). In the evaluation of ANSS and ATS, we keep an accuracy to two decimal places as in

Rakitzis et al. (2016). To be more specific, we use the settings as follows:

$$
\begin{aligned}
k &\in \{0.01, 0.02, \ldots, n - 0.01\}, \\
h &\in \{0.01, 0.02, \ldots\}, \\
w &\in \{-k + 0.01, -k + 0.02, \ldots, h - 0.01\}, \\
d &= 0.01, \\
L &= k, \\
H &= h.
\end{aligned}
$$

Notice that a better approximation result can be obtained as mentioned by Rakitzis et al. (2016), but such a setting can induce the dimension of the transient matrix $\mathbf{Q}$ to increase geometrically, giving rise to some cumbersome issues as to memory allocation, computation time, and the validity of related matrices.

7.4 Effects of the VSI CUSUM control scheme in ZIB process

In this section, we illustrate an example of the VSI CUSUM control scheme in ZIB processes. The performance of the FSI CUSUM and VSI CUSUM charts is compared by their ATS values. For the design of the FSI ZIB-CUSUM chart, we refer to Rakitzis et al. (2016). They provide optimal parameters in the quick detection of shift 1.2 in p_0 by conducting considerably many numerical experiments for several cases with starting value $c_0 = 0$ and $\text{ANSS}_0 = 370.4$. Using the $\text{ANSS}_0 = 370.4$ of the FSI CUSUM chart, we compute the ATS values of FSI and VSI CUSUM

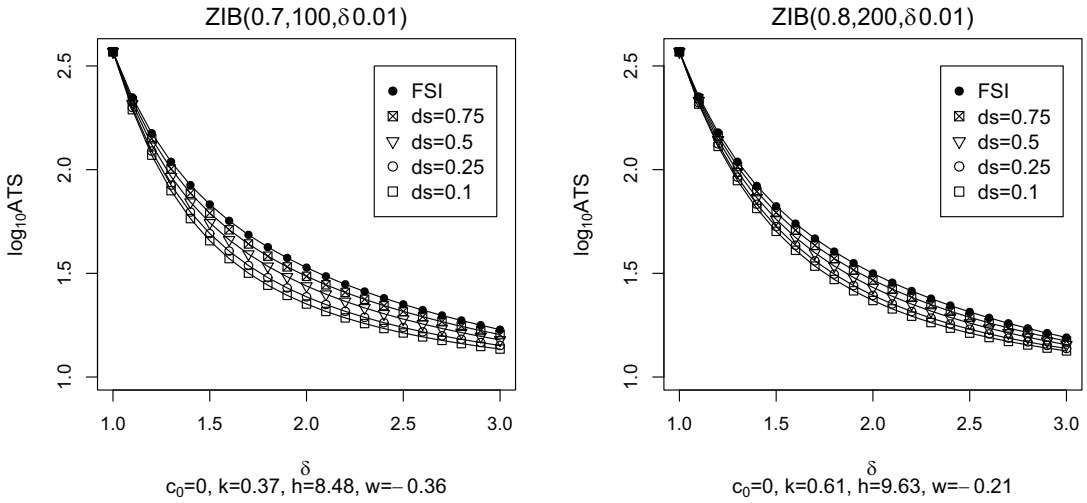

Figure 7.2: ATS profiles of VSI upper one-sided CUSUM(k,h) chart with $c_0 = 0$, when the data is ZIB($\rho, n, \delta p_0$)

charts with $\text{ATS}_0 = \text{ANSS}_0$, corresponding to the optimal warning limit in the quick detection of a shift 1.2 in p_0, when $c_0 = 0$ and $d_s = 0.1, 0.25, 0.5$. The ATS value in the FSI CUSUM chart is regarded as the ANSS value. The average sampling frequency (ASF) values, that is the ratio of the ANSS to the ATS, are also presented for comparison. The results are provided in Figure 7.2 and Tables 7.1-7.3, wherein $\rho_{s,0}$ denotes the long-run proportion of shorter sampling intervals when the process is in-control. From these results, we can see that i) In the detection of the shift 1.2 in p_0 (which is the most interesting case), for all cases, there is a reduction in ATS when adopting the VSI control scheme. Moreover, smaller values of d_s imply smaller ATS values when all other parameters are fixed (see also Figure 7.2). ii) There is no guarantee that for all possible shifts, the optimal warning limit w yields smaller ATS values than the ANSS of the FSI chart. When w is large (i.e. the large shift in p_0 for some cases, such as ZIB$(0.9, 100, \delta \cdot 0.02)$ and $\delta = 3$, the ATS

Table 7.1: ATS and ASF (in parentheses) values when the data is ZIB$(\rho, n, \delta p_0)$ with $n = 100$

(ρ, n, p_0, c_0)	Optimal design	$\rho_{s,0}$	ATS and ASF (in parentheses) values						
	FSI CUSUM(k, h)		δ						
	VSI CUSUM(k, h, w, d_s, d_l)		1.0	1.1	1.2	1.3	1.5	2.0	3.0
(0.9,100,0.02,0)	FSI (0.24,10.33)		370.42	252.67	186.30	145.33	99.20	54.59	29.57
	VSI (0.24,10.33,0.81,0.50,1.703)	0.585	370.42	243.03	174.37	133.61	89.71	50.13	29.93
			(1.00)	(1.04)	(1.07)	(1.09)	(1.11)	(1.09)	(0.99)
	VSI (0.24,10.33,0.81,0.25,2.055)	0.585	370.42	238.21	168.41	127.75	84.97	47.90	30.12
			(1.00)	(1.06)	(1.11)	(1.14)	(1.17)	(1.14)	(0.98)
	VSI (0.24,10.33,0.81,0.10,2.266)	0.585	370.42	235.32	164.84	124.23	82.12	46.56	30.23
			(1.00)	(1.07)	(1.13)	(1.17)	(1.21)	(1.17)	(0.98)
(0.8,100,0.01,0)	FSI (0.22, 8.96)		368.60	240.12	171.84	131.49	87.86	47.41	25.13
	VSI (0.22,8.96,-0.01,0.50,2.743)	0.777	368.60	225.49	154.78	115.41	75.46	41.45	24.31
			(1.00)	(1.06)	(1.11)	(1.14)	(1.16)	(1.14)	(1.03)
	VSI (0.22,8.96,-0.01,0.25,3.615)	0.777	368.60	218.18	146.25	107.37	69.26	38.47	23.90
			(1.00)	(1.10)	(1.18)	(1.22)	(1.27)	(1.23)	(1.05)
	VSI (0.22,8.96,-0.01,0.10,4.138)	0.777	368.60	213.79	141.13	102.55	65.54	36.68	23.65
			(1.00)	(1.12)	(1.22)	(1.28)	(1.34)	(1.29)	(1.06)
(0.7,100,0.01,0)	FSI (0.37,8.48)		370.35	223.22	149.94	109.12	67.96	33.70	16.92
	VSI (0.37,8.48,-0.36,0.50,2.641)	0.766	370.35	207.32	131.91	92.48	55.43	27.47	15.10
			(1.00)	(1.08)	(1.14)	(1.18)	(1.23)	(1.23)	(1.12)
	VSI (0.37,8.48,-0.36,0.25,3.461)	0.766	370.35	199.37	122.90	84.17	49.17	24.36	14.19
			(1.00)	(1.12)	(1.22)	(1.30)	(1.38)	(1.38)	(1.19)
	VSI (0.37,8.48,-0.36,0.10,3.954)	0.766	370.35	194.60	117.49	79.18	45.41	22.50	13.64
			(1.00)	(1.15)	(1.28)	(1.38)	(1.50)	(1.50)	(1.24)

Table 7.2: ATS and ASF (in parentheses) values when the data is ZIB$(\rho, n, \delta p_0)$ with $n = 200$

(ρ, n, p_0, c_0)	Optimal design	$\rho_{s,0}$	ATS and ASF (in parentheses) values						
	FSI CUSUM(k, h)		δ						
	VSI CUSUM(k, h, w, d_s, d_l)		1.0	1.1	1.2	1.3	1.5	2.0	3.0
(0.9,200,0.02,0)	FSI (0.79,11.92)		370.40	236.11	164.01	121.52	76.48	37.35	17.82
	VSI (0.79,11.92,1.43,0.50,1.363)	0.319	370.40	230.83	157.50	115.14	71.35	35.01	18.30
			(1.00)	(1.02)	(1.04)	(1.06)	(1.07)	(1.07)	(0.97)
	VSI (0.79,11.92,1.43,0.25,1.351)	0.319	370.40	228.19	154.24	111.95	68.79	33.83	18.54
			(1.00)	(1.03)	(1.06)	(1.09)	(1.11)	(1.10)	(0.96)
	VSI (0.79,11.92,1.43,0.10,1.363)	0.319	370.40	226.60	152.29	110.04	67.25	33.13	18.68
			(1.00)	(1.04)	(1.08)	(1.10)	(1.14)	(1.13)	(0.95)
(0.8,200,0.01,0)	FSI (0.61,9.63)		370.43	225.30	151.16	109.21	66.60	31.60	15.51
	VSI (0.61,9.63,-0.21,0.50,1.711)	0.587	370.43	215.14	139.13	97.75	57.61	27.04	14.32
			(1.00)	(1.05)	(1.09)	(1.12)	(1.16)	(1.17)	(1.08)
	VSI (0.61,9.63,-0.21,0.25,2.066)	0.587	370.43	210.06	133.12	92.02	53.12	24.76	13.72
			(1.00)	(1.07)	(1.14)	(1.19)	(1.25)	(1.28)	(1.13)
	VSI (0.61,9.63,-0.21,0.10,2.279)	0.587	370.43	207.02	129.51	88.58	50.42	23.39	13.36
			(1.00)	(1.09)	(1.17)	(1.23)	(1.32)	(1.35)	(1.16)
(0.7,200,0.01,0)	FSI (0.86,10.67)		370.45	205.80	129.72	89.83	52.18	23.82	11.49
	VSI (0.86,10.67,-0.57,0.50,1.990)	0.664	370.45	193.37	116.04	77.47	43.13	19.47	10.26
			(1.00)	(1.06)	(1.12)	(1.16)	(1.21)	(1.22)	(1.12)
	VSI (0.86,10.67,-0.57,0.25,2.485)	0.664	370.45	187.15	109.19	71.29	38.61	17.30	9.64
			(1.00)	(1.10)	(1.19)	(1.26)	(1.35)	(1.38)	(1.19)
	VSI (0.86,10.67,-0.57,0.10,2.782)	0.664	370.45	183.42	105.09	67.59	35.89	15.99	9.27
			(1.00)	(1.12)	(1.23)	(1.33)	(1.45)	(1.49)	(1.24)

Table 7.3: ATS and ASF (in parentheses) values when the data is ZIB$(\rho, n, \delta p_0)$ with $n = 500$

(ρ, n, p_0, c_0)	Optimal design	$\rho_{s,0}$	ATS and ASF (in parentheses) values						
	FSI CUSUM(k, h)		δ						
	VSI CUSUM(k, h, w, d_s, d_l)		1.0	1.1	1.2	1.3	1.5	2.0	3.0
(0.9,500,0.02,0)	FSI (7.74,9.30)		370.35	185.29	106.68	68.10	34.52	13.95	10.06
	VSI (7.74,9.30,-0.73,0.50,1.047)	0.086	370.35	184.15	105.47	67.06	33.83	13.72	9.98
			(1.00)	(1.01)	(1.01)	(1.02)	(1.02)	(1.02)	(1.01)
	VSI (7.74,9.30,-0.73,0.25,1.071)	0.086	370.35	183.57	104.87	66.54	33.48	13.60	9.94
			(1.00)	(1.01)	(1.02)	(1.02)	(1.03)	(1.03)	(1.01)
	VSI (7.74,9.30,-0.73,0.10,1.085)	0.086	370.35	183.23	104.51	66.23	33.28	13.53	9.92
			(1.00)	(1.01)	(1.02)	(1.03)	(1.04)	(1.03)	(1.01)
(0.8,500,0.01,0)	FSI (3.79,8.26)		370.29	197.72	118.89	78.35	41.41	15.80	6.60
	VSI (3.79,8.26,-0.78,0.50,1.126)	0.202	370.29	194.61	115.39	75.14	39.02	14.68	6.38
			(1.00)	(1.02)	(1.03)	(1.04)	(1.06)	(1.08)	(1.03)
	VSI (3.79,8.26,-0.78,0.25,1.190)	0.202	370.29	193.05	113.64	73.53	37.82	14.12	6.27
			(1.00)	(1.02)	(1.05)	(1.07)	(1.09)	(1.12)	(1.05)
	VSI (3.79,8.26,-0.78,0.10,1.228)	0.202	370.29	192.11	112.59	72.57	37.11	13.79	6.21
			(1.00)	(1.03)	(1.06)	(1.08)	(1.12)	(1.15)	(1.06)
(0.7,500,0.01,0)	FSI (3.99,9.07)		370.17	178.69	100.27	63.05	31.66	11.79	4.84
	VSI (3.99,9.07,-0.98,0.50,1.227)	0.312	370.17	173.78	95.17	58.65	28.61	10.45	4.55
			(1.00)	(1.03)	(1.05)	(1.08)	(1.11)	(1.13)	(1.06)
	VSI (3.99,9.07,-0.98,0.25,1.341)	0.312	370.17	171.33	92.63	56.45	27.09	9.77	4.40
			(1.00)	(1.04)	(1.08)	(1.12)	(1.17)	(1.21)	(1.10)
	VSI (3.99,9.07,-0.98,0.10,1.409)	0.312	370.17	169.85	91.10	55.13	26.18	9.37	4.32
			(1.00)	(1.05)	(1.10)	(1.14)	(1.21)	(1.26)	(1.12)

value of the VSI ZIB-CUSUM chart becomes larger than the ANSS of the FSI ZIB-CUSUM chart, which might be due to the longer sampling interval. However, this is not an important case because the the CUSUM control chart is mainly designed for monitoring small to moderate shifts. In fact, one may raise a question as to an optimal d_s since the smaller d_s is, the smaller out-of-control ATS becomes, which is a common phenomenon in VSI CUSUM charts. Although the shortest possible d_s is required, it must be at least greater than or equal to the minimum time required for taking a sample and the corresponding longer sampling time d_l must be admissible to allow the process of interest to run without taking a sample. For a more detailed discussion, we refer to Reynolds et al. (1990).

Although we mainly illustrate the ZIB case, the VSI control chart also works properly and efficiently in detecting assignable causes for count processes: see Sub-

section 7.5.2 for example. The VSI CUSUM control scheme is somewhat cumbersome in application compared to the FSI control chart, but it provides attractive opportunities to practitioners. The attribute VSI CUSUM chart is easily implemented by the R package attrCUSUM described in Section 7.5.

7.5 Software

In this section, we develop the R package attrCUSUM for an easy use of the VSI CUSUM chart for count data in practice. The attrCUSUM deals with the Markov chain approach for control charts, which is available from the CRAN. The latest version of the package is available from the authors upon request. This package utilizes the Markov chain approach by Brook and Evans (1972) (see also Reynolds et al. (1990) for details). The core computational algorithms use the R package RcppArmadillo by Eddelbuettel and Sanderson (2014), which is for the use of the Armadillo C++ library by Sanderson (2010). The Armadillo is a C++ template library for high quality linear algebras, aiming at good balance between usability and computation speed. The attrCUSUM provides useful information in the design of VSI CUSUM control charts for (zero inflated) binomial/Poisson processes, and has merit of easy extension to other count processes.

7.5.1 Examples of usage with zero inflated binomial process

The function `getAve_zibinom` in the attrCUSUM provides useful information on the design of the upper one-sided CUSUM control chart for ZIB processes. In fact, it is a wrapper function of `getAve` and can be easily extended to any count processes. It also gives an object of list including ANSS, ATS and transition probability matrices, and,

further, provides the function `getContl_zibinom`, a wrapper function of `getContl`, which returns the most suitable control limits h for a given ANSS_0 value. Below, we provide some example: First of all, the following package should be installed and attached:

```
> install.packages("attrCUSUM")
> library(attrCUSUM)
```

Here, we only illustrate the case of $\text{ZIB}(0.9, 200, 0.01)$ with $c_0 = 0$, $w = 0$ and $k = 0.47$. Assume that X_i is a ZIB process with parameters $(0.9, 200, \delta \cdot 0.01)$. For reproducing the result from Rakitzis et al. (2016) and applying the VSI control scheme, we find a suitable control limit h with the in-control ANSS being near 370.4 as stated below:

```
> getContl_zibinom(rho = 0.9,
+                  size = 200,
+                  prob = 0.01,
+                  anss.target = 370.4,
+                  refv = 0.47,
+                  c.zero = 0)
$refv.act
[1] 0.47
$c.zero.act
[1] 0

$sol1
contl1 ANSS1
```

```
6.5300 370.3765


$sol2
contl2 ANSS2
6.5400 389.5988
```

We find that the suitable control limit h is given as 6.53 (notice that in Rakitzis et al. (2016), the CUSUM statis-tic signals the out-of-control condition when $\tilde{C}_t > h$ but not $\tilde{C}_t \geq h$).

We compute d_l of the CUSUM control chart when $k = 0.47$, $h = 6.53$, $c_0 = 0$, $w = 0$ and $d_s = 0.1$ as stated below:

```
> res0 <- getAve_zibinom(rho = 0.9,
+                        size = 200,
+                        prob = 0.01,
+      refv = 0.47,
+      contl = 6.53,
+      c.zero = 0,
+      warnl = 0,
+      ds = 0.1)
> res0$ANSS
[1] 370.3765
> res0$dl
[1] 1.516956
```

The out-of control ANSS and ATS of ZIB process with $(0.9, 200, 0.01(1.2))$ and $w = 0$ are obtained as follows:

```
> res1 <- getAve_zibinom(rho = 0.9,
+                        size = 200,
+                        prob = 0.01 * 1.2,
+                        refv = 0.47,
+                        contl = 6.53,
+                        c.zero = 0,
+                        warnl = 0,
+                        ds = 0.1,
+                        dl = res0$dl)
> res1$ANSS
[1] 183.0429
> res1$ATS
[1] 172.8257
```

Note that invalid arguments will end up with an error message:

```
> res0 <- getAve_zibinom(rho = -1,
+                        size = -1,
+                        prob = 0.01,
+                        refv = 0.47,
+                        contl = 6.53,
+                        c.zero = 0,
+                        warnl = 0,
+                        ds = 0.1)
Error:
CheckArgs_dzibinom(x, rho, size, prob, log)
1: Argument ‘rho’ must be a numeric value in [0,1)
```

```
2: Argument 'size' must be a positive integer value
```

7.5.2 Other count models

It is well known that a great number of nonconformities per sample situations can be modeled by a Poisson distribution, so that the Poisson CUSUM chart for nonconformities becomes an unquestionably popular procedure: see, for example, Lucas (1985), White et al. (1997). Let X_i, $i = 1, 2, \ldots$, be the number of nonconformities observed in consecutive random samples of constant size from a production process of interest. We assume that X_i's are independent and identically distributed Poisson r.v.s with mean $\lambda + \delta\sqrt{\lambda}$. In this case, the VSI CUSUM control chart can be well designed by using the function `getAve_pois` and `getContl_pois` similarly to the case of ZIB processes.

Suppose that one is interested in detecting the shift of 0.2 from the mean in units of standard deviation, that is $\delta = 0.2$. An example of the ATS and ASF values of the VSI CUSUM chart with $\text{ATS}_0 = \text{ANSS}_0 = 370.4$, when the data is Poisson with mean $4 + \delta 2$, can be found in Figure 7.3 and Table 7.4. Notice that the optimal (k^*, h^*) is obtained through considerable amount of numerical experiments as stated in Subsection 7.3.1. Although the optimal warning limit, in the view of the ATS value, is found to be -4.20, we also consider other warning limits because in case the longer sampling intervals d_l corresponding to the optimal warning value, are too long, it might not be acceptable for practitioners. The results in Table 7.4 reveal that there are desirable reductions in terms of ATS, confirming the validity of the VSI CUSUM control scheme.

Note that the function `getAve` and `getContl` can be easily extended to other count models. For instance, assume that one wishes to compute the ANSS when

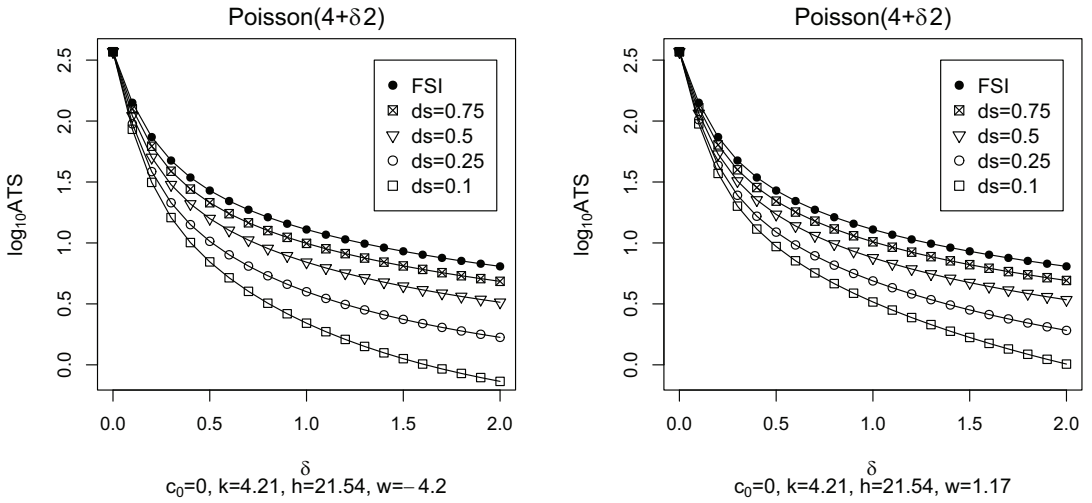

Figure 7.3: ATS profiles of VSI upper one-sided CUSUM(k,h) chart with $c_0 = 0$, when the data is Poisson(4)

Table 7.4: ATS and ASF (in parentheses) values when the data is Poisson(4)

(λ, c_0)	Optimal design	$\rho_{s,0}$	ATS and ASF (in parentheses) values						
	FSI CUSUM(k,h)		δ						
	VSI CUSUM(k,h,w,d_s,d_l)		0.0	0.1	0.2	0.3	0.5	1.0	2.0
(4,0)	FSI (4.21,21.54)		370.44	141.40	73.92	47.44	26.91	12.89	6.42
	VSI (4.21,21.54,-4.20,0.50,132.555)	0.996	370.44	110.39	50.29	30.06	15.84	6.95	3.26
			(1.00)	(1.28)	(1.47)	(1.58)	(1.70)	(1.85)	(1.97)
	VSI (4.21,21.54,-4.20,0.25,198.332)	0.996	370.44	94.89	38.48	21.36	10.31	3.98	1.68
			(1.00)	(1.49)	(1.92)	(2.22)	(2.61)	(3.24)	(3.82)
	VSI (4.21,21.54,-4.20,0.10,237.799)	0.996	370.44	85.58	31.39	16.15	6.99	2.20	0.73
			(1.00)	(1.65)	(2.35)	(2.94)	(3.85)	(5.87)	(8.78)
	VSI (4.21,21.54,1.17,0.50,2.144)	0.696	370.44	120.46	57.35	35.32	19.65	9.63	5.25
			(1.00)	(1.17)	(1.29)	(1.34)	(1.37)	(1.34)	(1.22)
	VSI (4.21,21.54,1.17,0.25,2.716)	0.696	370.44	110.00	49.06	29.25	16.02	8.01	4.66
			(1.00)	(1.29)	(1.51)	(1.62)	(1.68)	(1.61)	(1.38)
	VSI (4.21,21.54,1.17,0.10,3.059)	0.696	370.44	103.72	44.09	25.61	13.84	7.03	4.30
			(1.00)	(1.36)	(1.68)	(1.85)	(1.94)	(1.83)	(1.49)
	VSI (4.21,21.54,5.07,0.50,1.327)	0.396	370.44	125.91	60.69	37.28	20.46	9.71	4.95
			(1.00)	(1.12)	(1.22)	(1.27)	(1.32)	(1.33)	(1.30)
	VSI (4.21,21.54,5.07,0.25,1.491)	0.396	370.44	118.17	54.08	32.19	17.24	8.13	4.21
			(1.00)	(1.20)	(1.37)	(1.47)	(1.56)	(1.59)	(1.52)
	VSI (4.21,21.54,5.07,0.10,1.589)	0.396	370.44	113.53	50.12	29.14	15.30	7.17	3.77
			(1.00)	(1.25)	(1.47)	(1.63)	(1.76)	(1.80)	(1.70)

the data is obtained from a negative binomial distribution of size 2 and success probability 0.5. For $k = 4.5$ and $c_0 = 0$, a suitable control limit h, allowing the

in-control ANSS value to be around 400, can be obtained as stated below:

```
> getContl(anss.target = 400,
+          refv = 4.5,
+          c.zero = 0,
+          process = function(x) {
+            dnbinom(x, size = 2, prob = 0.5)
+          })
$refv.act
[1] 4.5


$c.zero.act
[1] 0


$sol1
contl1 ANSS1
7.0000 344.3132


$sol2
contl2 ANSS2
7.1000 406.2175
```

Then, the corresponding longer sampling interval d_l for (k, h) =(4.5,7.1), $c_0 = 0$. $d_s = 0.1$ and $w = -2$ is given as follows:

```
> res0 <- getAve(refv = 4.5,
+                contl = 7.1,
```

```
+                 c.zero = 0,
+                 process = function(x) {
+                 dnbinom(x,
+                 size = 2,
+                 prob = 0.5)
+                 },
+                 warnl = -2,
+                 ds = 0.1)
> res0$dl
[1] 1.522315
```

The out-of control ANSS and ATS values when the size is equal 2.5 are also obtained as follows:

```
> res1 <- getAve(refv = 4.5,
+                 contl = 7.1,
+                 zero = 0,
+                 process = function(x) {
+                 dnbinom(x,
+                 size = 2.5,
+                 prob = 0.5)
+                 },
+                 warnl = -2,
+                 ds = 0.1,
+                 dl = res0$dl)
> res1$ANSS
[1] 164.7614
```

```
> res1$ATS
[1] 135.5315
```

7.6 Concluding remarks

In this study, we considered the VSI CUSUM chart proposed by Reynolds et al. (1990), particularly focusing on its application to the monitoring a small to moderate increase of the proportion parameter in ZIB distributions proposed by Hall (2000). We employed the Markov chain approach taken by Brook and Evans (1972) for the calculation of ATS values and compared its performance with that of the FSI CUSUM chart studied by Rakitzis et al. (2016). Our findings in numerical experiments show that the VSI CUSUM chart is superior to the FSI CUSUM chart when monitoring an increase of the proportion parameter in ZIB processes in terms of ATS. We also developed an R package attrCUSUM to implement the VSI CUSUM chart more efficiently, which has merit of an easy extension to other count processes of interest. The method proposed in this study can be extended to more sophisticated CUSUM charts such as the two-sided VSI CUSUM chart.

Bibliography

Agarwal, D. K., Gelfand, A. E., and Citron-Pousty, S. (2002). Zero-inflated models with application to spatial count data. *Environmental and Ecological Statistics*, 9(4):341–355.

Al-Osh, M. A. and Aly, E.-E. A. (1992). First order autoregressive time series with negative binomial and geometric marginals. *Communications in Statistics - Theory and Methods*, 21(9):2483–2492.

Al-Osh, M. A. and Alzaid, A. A. (1987). First-order integer-valued autoregressive (INAR(1)) process. *Journal of Time Series Analysis*, 8(3):261–275.

Alzaid, A. and Al-Osh, M. (1988). First-order integer-valued autoregressive (INAR(1)) process: Distributional and regression properties. *Statistica Neerlandica*, 42(1):53–61.

Alzaid, A. and Al-Osh, M. (1990). An integer-valued pth-order autoregressive structure (INAR(p)) process. *Journal of Applied Probability*, 27(2):314–324.

Alzaid, A. A. and Al-Osh, M. A. (1993). Some autoregressive moving average processes with generalized Poisson marginal distributions. *Annals of the Institute of Statistical Mathematics*, 45(2):223–232.

Billingsley, P. (1979). *Probability and measure*. John Wiley & Sons.

Bourguignon, M. and Vasconcellos, K. (2015). Improved estimation for poisson INAR(1) models. *Journal of Statistical Computation and Simulation*, 85(12):2425–2441.

Bourguignon, M., Vasconcellos, K. L., et al. (2015). First order non-negative integer valued autoregressive processes with power series innovations. *Brazilian Journal of Probability and Statistics*, 29(1):71–93.

Bourguignon, M., Vasconcellos, K. L., Reisen, V. A., and Ispány, M. (2016). A Poisson INAR(1) process with a seasonal structure. *Journal of Statistical Computation and Simulation*, 86(2):373–387.

Brook, D. and Evans, D. A. (1972). An approach to the probability distribution of CUSUM run length. *Biometrika*, 59(3):539–549.

Chao-Wen, L. and Reynolds Jr, M. R. (2001). Cusum charts for monitoring an autocorrelated process. *Journal of Quality Technology*, 33(3):316.

Chen, J. and Gupta, A. K. (2011). *Parametric statistical change point analysis: with applications to genetics, medicine, and finance*. Springer Science & Business Media.

Csörgö, M. and Horváth, L. (1997). *Limit theorems in change-point analysis*. John Wiley & Sons, New York; Chichester.

Eddelbuettel, D. and Sanderson, C. (2014). RcppArmadillo: Accelerating R with high-performance C++ linear algebra. *Computational Statistics and Data Analysis*, 71:1054–1063.

Eduarda Da Silva, M. and Oliveira, V. L. (2004). Difference equations for the higher-order moments and cumulants of the INAR(1) model. *Journal of Time Series Analysis*, 25(3):317–333.

Epprecht, E. K., Simões, B. F. T., and Mendes, F. C. T. (2010). A variable sampling interval EWMA chart for attributes. *The International Journal of Advanced Manufacturing Technology*, 49(1):281–292.

Fang, Y. (2003). C-chart, X-chart, and the Katz family of distributions. *Journal of Quality Technology*, 35(1):104–114.

Ferland, R., Latour, A., and Oraichi, D. (2006). Integer-valued GARCH process. *Journal of Time Series Analysis*, 27(6):923–942.

Franke, J., Kirch, C., and Kamgaing, J. T. (2012). Changepoints in times series of counts. *Journal of Time Series Analysis*, 33(5):757–770.

Franke, J. and Seligmann, T. (1993). Conditional maximum likelihood estimates for INAR(1) processes and their application to modelling epileptic seizure counts. In Rao, T. S., editor, *Developments in time series analysis*, pages 310–330. Chapman & Hall, London.

Goh, T. N. (1987). A control chart for very high yield processes. *Quality Assurance*, 13(1):18–22.

Hall, D. B. (2000). Zero-inflated poisson and binomial regression with random effects: A case study. *Biometrics*, 56(4):1030–1039.

He, S., Huang, W., and Woodall, W. H. (2012). CUSUM charts for monitoring a

zero-inflated poisson process. *Quality and Reliability Engineering International*, 28(2):181–192.

He, S., Li, S., and He, Z. (2014). A combination of cusum charts for monitoring a zero-inflated poisson process. *Communications in Statistics-Simulation and Computation*, 43(10):2482–2497.

Huh, J., Kim, H., and Lee, S. (2017). Monitoring parameter shift with poisson integer-valued GARCH models. *Journal of Statistical Computation and Simulation*, 87(9):1754–1766.

Hušková, M., Prášková, Z., and Steinebach, J. (2007). On the detection of changes in autoregressive time series I. Asymptotics. *Journal of Statistical Planning and Inference*, 137(4):1243–1259.

Jazi, M. A., Jones, G., and Lai, C.-D. (2012a). First-order integer valued AR processes with zero inflated Poisson innovations. *Journal of Time Series Analysis*, 33(6):954–963.

Jazi, M. A., Jones, G., and Lai, C.-D. (2012b). Integer valued AR(1) with geometric innovations. *Journal of Iranian Statistical Society*, 11(2):173–190.

Jin-Guan, D. and Yuan, L. (1991). The integer-valued autoregressive (INAR(p)) model. *Journal of Time Series Analysis*, 12(2):129–142.

Johnson, N. L., Kemp, A. W., and Kotz, S. (1992). *Univariate discrete distributions*. John Wiley & Sons, 2nd edition.

Kang, J. and Lee, S. (2009). Parameter change test for random coefficient integer-

valued autoregressive processes with application to polio data analysis. *Journal of Time Series Analysis*, 30(2):239–258.

Kang, J. and Lee, S. (2014). Parameter change test for poisson autoregressive models. *Scandinavian Journal of Statistics*, 41(4):1136–1152.

Katz, L. (1965). Unified treatment of a broad class of discrete probability distributions. In Patil, G. P., editor, *Classical and Contagious Discrete Distributions. Proceedings of the international symposium held at McGill University. Montreal, Canada. August 15–August 20, 1963*, pages 175–182. Pergamon Press, Oxford.

Kim, H. and Lee, S. (2017). On first-order integer-valued autoregressive process with Katz family innovations. *Journal of Statistical Computation and Simulation*, 87(3):546–562.

Klimko, L. A. and Nelson, P. I. (1978). On conditional least squares estimation for stochastic processes. *The Annals of Statistics*, 6(3):629–642.

Lambert, D. (1992). Zero-inflated poisson regression, with an application to defects in manufacturing. *Technometrics*, 34(1):1–14.

Lee, S., Ha, J., Na, O., and Na, S. (2003). The cusum test for parameter change in time series models. *Scandinavian Journal of Statistics*, 30(4):781–796.

Lee, S., Lee, Y., and Chen, C. W. (2016). Parameter change test for zero-inflated generalized Poisson autoregressive models. *Statistics*, 50(3):540–557.

Lee, S. and Na, O. (2005). Test for parameter change in stochastic processes based on conditional least-squares estimator. *Journal of Multivariate Analysis*, 93(2):375 – 393.

Lee, S., Tokutsu, Y., and Maekawa, K. (2004). The CUSUM test for parameter change in regression models with ARCH errors. *Journal of the Japan Statistical Society*, 34(2):173–188.

Li, C., Wang, D., and Zhang, H. (2015). First-order mixed integer-valued autoregressive processes with zero-inflated generalized power series innovations. *Journal of the Korean Statistical Society*, 44(2):232–246.

Li, C., Wang, D., and Zhu, F. (2016). Effective control charts for monitoring the NG-INAR(1) process. *Quality and Reliability Engineering International*, 32(3):877–888.

Li, Z., Zou, C., Gong, Z., and Wang, Z. (2014). The computation of average run length and average time to signal: an overview. *Journal of Statistical Computation and Simulation*, 84(8):1779–1802.

Lucas, J. M. (1985). Counted data CUSUM's. *Technometrics*, 27(2):129–144.

McKenzie, E. (1985). Some simple models for discrete variate time series. *JAWRA Journal of the American Water Resources Association*, 21(4):645–650.

McKenzie, E. (1986). Autoregressive moving-average processes with negative-binomial and geometric marginal distributions. *Advances in Applied Probability*, 18(3):679–705.

McKenzie, E. (1988). Some ARMA models for dependent sequences of Poisson counts. *Advances in Applied Probability*, 20(4):822–835.

Meyn, S. P. and Tweedie, R. L. (2012). *Markov chains and stochastic stability*. Springer Science & Business Media, 2nd edition.

Montgomery, D. C. (2009). *Introduction to Statistical Quality Control*. John Wiley & Sons, Inc., New York, USA, 6th edition.

Montgomery, D. C. (2012). *Statistical Quality Control: A Modern Introduction*. John Wiley & Sons, 7th edition.

Noorossana, R., Fatahi, A. A., Dokouhaki, P., and Babakhani, M. (2011). ZIB-EWMA control chart for monitoring rare health events. *Journal of Mechanics in Medicine and Biology*, 11(04):881–895.

Ohta, H., Kusukawa, E., and Rahim, A. (2001). A ccc-r chart for high-yield processes. *Quality and Reliability Engineering International*, 17(6):439–446.

Page, E. S. (1954). Continuous inspection schemes. *Biometrika*, 41(1-2):100–115.

Page, E. S. (1955). A test for a change in a parameter occurring at an unknown point. *Biometrika*, 42(3/4):523–527.

Pap, G. and Szabó, T. T. (2013). Change detection in INAR(p) processes against various alternative hypotheses. *Communications in Statistics - Theory and Methods*, 42(7):1386–1405.

Park, Y. and Oh, C. W. (1997). Some asymptotic properties in INAR(1) processes with Poisson marginals. *Statistical Papers*, 38(3):287–302.

R Core Team (2017). *R: A Language and Environment for Statistical Computing*. R Foundation for Statistical Computing, Vienna, Austria.

Rakitzis, A. C., Maravelakis, P. E., and Castagliola, P. (2016). CUSUM control charts for the monitoring of zero-inflated binomial processes. *Quality and Reliability Engineering International*, 32(2):465–483.

Rakitzis, A. C., Weiß, C. H., and Castagliola, P. (2017). Control charts for monitoring correlated poisson counts with an excessive number of zeros. *Quality and Reliability Engineering International*, 33(2):413–430. qre.2017.

Reynolds, M. R., Amin, R. W., and Arnold, J. C. (1990). CUSUM charts with variable sampling intervals. *Technometrics*, 32(4):371–384.

Reynolds, M. R., Amin, R. W., Arnold, J. C., and Nachlas, J. A. (1988). $\bar{X}$ charts with variable sampling intervals. *Technometrics*, 30(2):181–192.

Ristić, M. M., Bakouch, H. S., and Nastić, A. S. (2009). A new geometric first-order integer-valued autoregressive (NGINAR(1)) process. *Journal of Statistical Planning and Inference*, 139(7):2218–2226.

Ristić, M. M., Nastić, A. S., and Miletić Ilić, A. V. (2013). A geometric time series model with dependent bernoulli counting series. *Journal of Time Series Analysis*, 34(4):466–476.

Ross, S. M. (1996). *Stochastic processes*. John Wiley & Sons, New York, 2nd edition.

Saccucci, M. S., Amin, R. W., and Lucas, J. M. (1992). Exponentially weighted moving average control schemes with variable sampling intervals. *Communications in Statistics - Simulation and Computation*, 21(3):627–657.

Sanderson, C. (2010). Armadillo: An open source C++ linear algebra library for fast prototyping and computationally intensive experiments. Technical report, NICTA, Australia.

Scotto, M. G., Weiß, C. H., and Gouveia, S. (2015). Thinning-based models in the

analysis of integer-valued time series: a review. *Statistical Modelling*, 15(6):590–618.

Shewhart, W. A. (1924). Some applications of statistical methods to the analysis of physical and engineering data. *Bell System Technical Journal*, 3(1):43–87.

Sim, C. H. and Lim, M. H. (2008). Attribute charts for zero-inflated processes. *Communications in Statistics - Simulation and Computation*, 37(7):1440–1452.

Steutel, F. W. and van Harn, K. (1979). Discrete analogues of self-decomposability and stability. *The Annals of Probability*, 7(5):893–899.

Vieira, A. M. C., Hinde, J. P., and Demetrio, C. G. B. (2000). Zero-inflated proportion data models applied to a biological control assay. *Journal of Applied Statistics*, 27(3):373–389.

Wang, H. (2009). Comparison of p control charts for low defective rate. *Computational Statistics & Data Analysis*, 53(12):4210–4220.

Weiß, C. H. (2007). Controlling correlated processes of Poisson counts. *Quality and reliability engineering international*, 23(6):741–754.

Weiß, C. H. (2008). Thinning operations for modeling time series of counts—a survey. *AStA Advances in Statistical Analysis*, 92(3):319–341.

Weiß, C. H. (2010). The INARCH(1) model for overdispersed time series of counts. *Communications in Statistics - Simulation and Computation*, 39(6):1269–1291.

Weiß, C. H. (2012). Process capability analysis for serially dependent processes of Poisson counts. *Journal of Statistical Computation and Simulation*, 82(3):383–404.

Weiss, C. H. and Testik, M. C. (2009). CUSUM monitoring of first-order integer-valued autoregressive processes of Poisson counts. *Journal of quality technology*, 41(4):389–400.

Weiß, C. H. and Testik, M. C. (2012). Detection of abrupt changes in count data time series: Cumulative sum derivations for INARCH(1) models. *Journal of Quality Technology*, 44(3):249–264.

White, C. H., Keats, J. B., and Stanley, J. (1997). Poisson CUSUM versus c chart for defect data. *Quality Engineering*, 9(4):673–679.

Woodall, W. H. (2006). The use of control charts in health-care and public-health surveillance. *Journal of Quality Technology*, 38(2):89–104.

Wu, Z., Yeo, S. H., and Fan, H. (2000). A comparative study of the CRL-type control charts. *Quality and Reliability Engineering International*, 16(4):269–279.

Wu, Z., Zhang, X., and Yeo, S. H. (2001). Design of the sum-of-conforming-run-length control charts. *European Journal of Operational Research*, 132(1):187–196.

Xie, M. and Goh, T. N. (1993). SPC of a near zero-defect process subject to random shocks. *Quality and Reliability Engineering International*, 9(2):89–93.

Yontay, P., Weiß, C. H., Testik, M. C., and Pelin Bayindir, Z. (2013). A two-sided cumulative sum chart for first-order integer-valued autoregressive processes of poisson counts. *Quality and Reliability Engineering International*, 29(1):33–42.

Zhang, H. and Wang, D. (2015). Inference for random coefficient INAR(1) process based on frequency domain analysis. *Communications in Statistics - Simulation and Computation*, 44(4):1078–1100.

Zheng, H., Basawa, I. V., and Datta, S. (2007). First-order random coefficient integer-valued autoregressive processes. *Journal of Statistical Planning and Inference*, 137(1):212–229.

Zhu, F. (2012). Zero-inflated Poisson and negative binomial integer-valued GARCH models. *Journal of Statistical Planning and Inference*, 142(4):826–839.

국문초록

본 논문에서는 계수 시계열 모형에서 CUSUM 관리도를 기반으로 한 통계적 공정 관리를 연구 하였다. 먼저, 기존 INAR(1) 모형의 균등산포 성질을 극복하기 위하여 Katz 분포족을 이용하여 균등, 과대, 과소산포를 모두 설명할 수 있는 INARKF(1) 모형을 제안하고, 이와 관련된 통계적 성질들을 규명한 뒤 CUSUM 관리도를 적용하여 모수 변화 탐지에 있어 그 우수성을 규명하였다. 또한, 기존 INAR(1) 모형에 대한 조건부 최소 제곱 및 squared difference 추정량을 이용한 CUSUM 변화점 검정에 대해 탐구하고 이를 기반으로 효과적인 조기 탐지 및 이상점의 추정을 위한 CUSUM 방법론을 제안하였다. 더불어, 자기상관과 영과잉 특성을 갖는 고품질 프로세스에서 효과적인 모니터링을 위하여 지연 규칙이 있는 CUSUM 관리도, conforming run length 기반의 CUSUM 관리도를 제안하고 그 특성을 탐구하였다. 마지막으로, 기존 고정 샘플링 간격 관리도의 효율을 극대화 하기 위한 가변 샘플링 간격 CUSUM 관리도를 구현하였고, 현장에서의 쉬운 적용을 위하여 R 패키지 attrCUSUM 으로 구현하였다.

주요어: INAR 모형, CUSUM 관리도, 통계적 공정 관리, R, 소프트웨어.

학번: 2010-20220